**AALBORG UNIVERSITET**

# MASTER'S THESIS

# SYNTHESIS OF ANTICANCER PRODRUGS FOR ENHANCED COMPLEXATION WITH CYCLODEXTRIN

**Written by: Maria Fritz Berentzen**

**Supervisor: Associate Professor Thorbjørn Terndrup Nielsen**

**Submitted: 09/06-2017**

# Table of content

3

## Preface

The experimental part of the project was carried out from September 2016 to May 2017 at Aalborg University, Department of Chemistry and Bioscience, section of chemistry in the group of supramolecular chemistry. I would like to thank staff member Lars Wagner Städe for helping with LC-MS and ITC measurements. I would like to express my gratitude to my family, in-laws and friends, who have supported me throughout the entire process and kept me balanced. Lastly, I would like to thank my boyfriend, Mads Winther, for all his support, for making me laugh along the way and helping me putting the pieces together. I will be forever grateful for your love.

## Abstract

Cancer was responsible for an estimated 13% of all deaths worldwide in 2012. The main treatment for cancer remains chemotherapy; however, it faces problems due to low specificity and systemic toxicity. A way to improve chemotherapy is to use nanocarriers such as cyclodextrins. This study concerns the synthesis of prodrugs from known anticancer drugs to enhance their complexation with cyclodextrins. The focus has been on the synthesis of Doxorubicin and Gemcitabine prodrugs in order to improve their complexation with cyclodextrin and thereby minimize the side effects and improve their affinity.
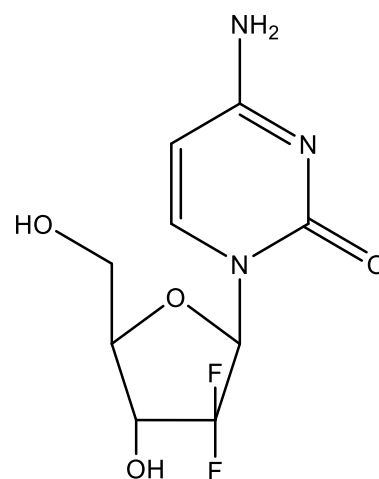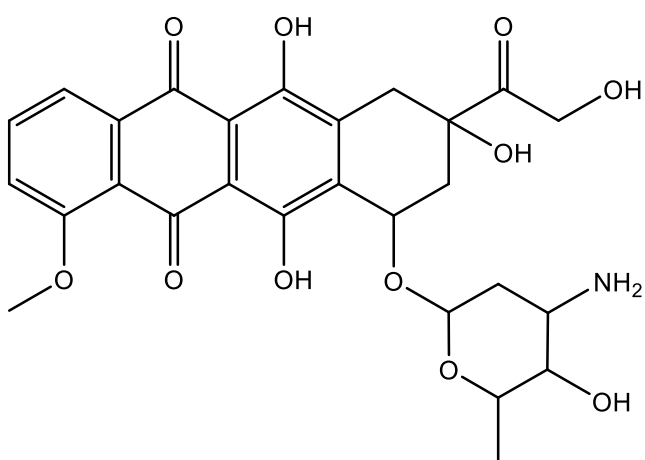
Assessments of each molecule were made and four different prodrugs (two of each) were designed and synthesized. The final four products were isolated in ~10-20 mg. The complex formation of the synthesized prodrugs was analyzed by ITC. Five different β-cyclodextrins derivatives were chosen and obtained $K_A$ values were compared.

## Resumé

Kræft anslås at være ansvarlig for 13 % af alle dødsfald på verdensplan i 2012. Den primære behandling for kræft er fortsat kemoterapi, men behandlingen er langt fra perfekt. Kemoterapi kæmper blandt andet med problemer som lav specificitet og systemisk toksicitet. En måde at forbedre kemoterapi er ved hjælp af såkaldte nanocarriers, så som cyclodextriner. Dette studie beskæftiger sig med syntesen af prodrugs fra kendte anti-kræft medicin for at øge deres kompleksdannelse med cyclodextriner. Fokus har været på syntesen af Doxorubicin og Gemcitabin prodrugs for at minimere bivirkningerne og forbedre deres affinitet.
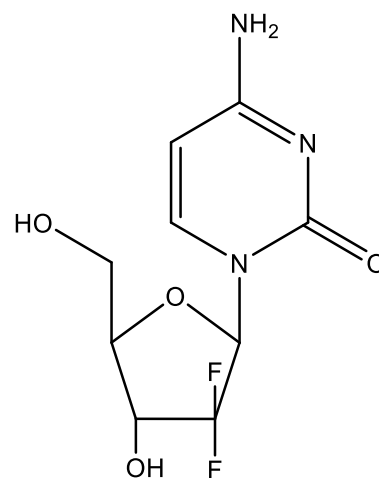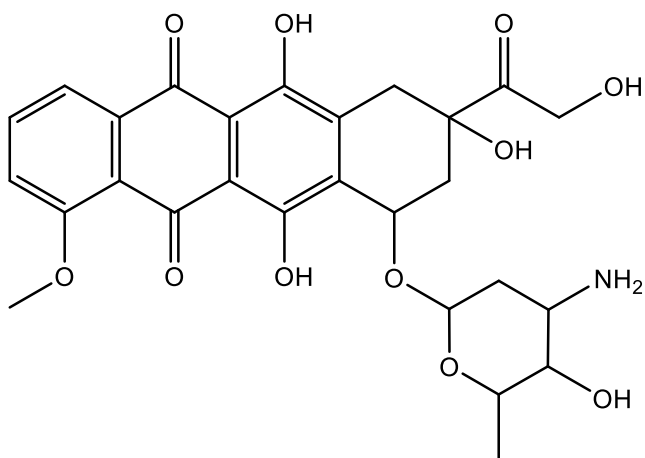
Det blev vurderet hvilke linker, der ville virke bedst for hvert molekyle. I alt blev fire prodrugs (to af hver) syntetiseret. Hver af de endelige produkter blev isoleret i ~10-20 mg. Kompleksdannelsen af de syntetiseret prodrugs blev analyseret via ITC. Fem forskellige β-cyclodextrin derivater blev udvalgt og de opnåede $K_A$ værdierne blev sammenlignet.

## Abbreviations

| | |
|---|---|
| μM | Micromolar |
| Aq. | Aqueous |
| AcOH | Acetic acid |
| Boc | Di-*tert*-butyl dicarbonate |
| BtCl | 1-chlorobenzotriazole |
| °C | Celsius (unit) |
| CD | Cyclodextrin |
| $CDCl_3$ | Deuturized chloroform |
| $CD_3OD$ | Deuturized methanol |
| $(CD_3)_2SO_2$ | Deuturized dimethyl sulfate |
| $CH_2$ | Methylene group |
| $CH_3CN$ | Acetonitrile |
| CO | Carbon monooxide |
| $CO_2$ | Carbon dioxide |
| d | Dublet (in relation to NMR) |
| DβCD | Dextran-β-cyclodextrin |
| dd | Dobble dublet (in relation to NMR) |
| DCC | N,N'-Dicyclohexylcarbodiimide |
| DCM | Dichloromethane |
| DIPEA | N,N-Diisopropylethylamine |
| DMF | Dimethylformamide |
| DMAP | 4-dimethylaminopyridine |
| DMSO | Dimethyl sulfoxide |
| DNA | Deoxyribonucleic acid |
| Dox | Doxorubicin |
| dr. | Drops |
| EDC | 1-ethyl-3-(3-dimethylaminopropyl)carbodiimide |
| EPR | Enhanced permeability and retention |
| EtOAc | Ethyl acetate |
| Eq | Equivalent |
| Gem | Gemcitabine |
| GSH | Glutathione |
| h | Hour (unit) |
| $H_2O$ | Water |
| HBTU | (2-(1*H*-benzotriazol-1-yl)-1,1,3,3-tetramethyluronium hexafluorophosphate |
| HOBt | Hydroxybenzotriazole |
| HPβCD | Hydroxypropyl-β-cyclodextrin |
| ITC | Isothermal titration calorimetry |
| *J* | Coupling constant (in relation to NMR) |
| $K_2CO_3$ | Potassium carbonate |
| $KMnO_4$ | Potassium permanganate |
| LC-MS | Liquid chromatography-mass spectrometry |
| M | Molar |
| m | Multispot (in relation to NMR) |
| MβCD | Methyl-β-cyclodextrin |
| mg | Milligram |
| Me | Methyl |

| | |
|---|---|
| MeOH | Methanol |
| mM | milimolar |
| $Na_2CO_3$ | Sodium carbonate |
| $Na_2SO_4$ | Sodium sulfate |
| NaOCl | Sodium hypochlorite |
| NaOH | Sodium hydroxide |
| nM | nanomolar |
| nm | nanometer |
| NMR | Nuclear magnetic resonance |
| NO | Nitric oxide |
| OBt | O-benzotriazole |
| $^-$OH | Hydroyl group |
| p | Pentet (in relation to NMR) |
| p53 | Tumor protein p53 |
| PEG | Polyethylene glycol |
| ppm | Parts per million |
| Rf | Retention factor |
| ROS | Reactive oxygen species |
| rt | Room temperatur |
| s | Singlet (in relation to NMR) |
| SBEβCD | Sulfobutylether-β-cyclodextrin |
| TFA | Trifluoroacetic acid |
| THF | Tetrahydrofuran |
| TLC | Thin-layer chromatography |
| VEGF | Vascular endothelial growth factor |
| w/v | Weight/ volume |

# Synthesized compounds and target molecules



**1**



**2**



**3**



**4**

**5**

**6**

**7**

**8**

**9**

**10**

**11**

**12**

**13**

14
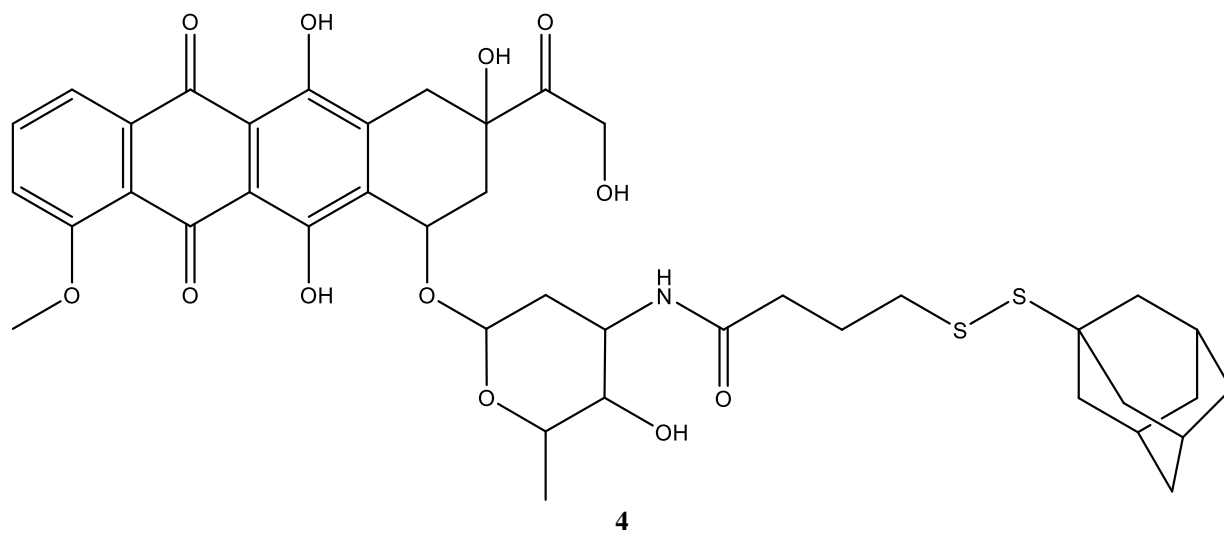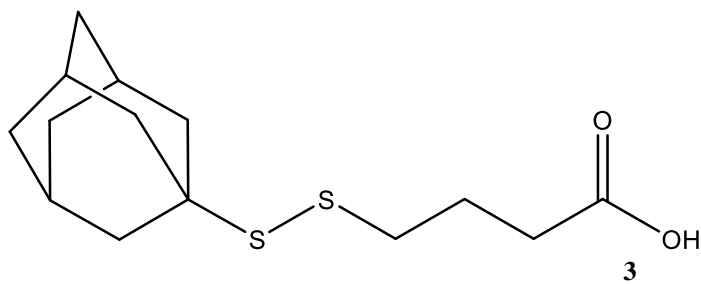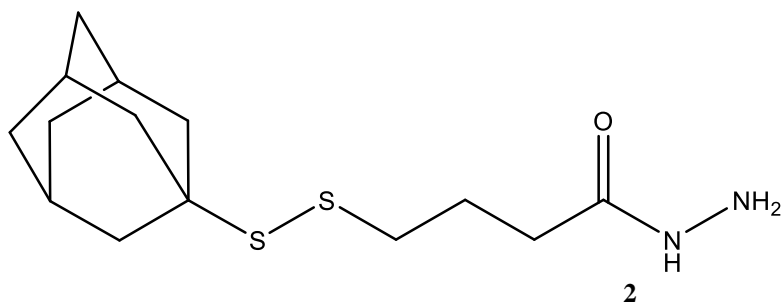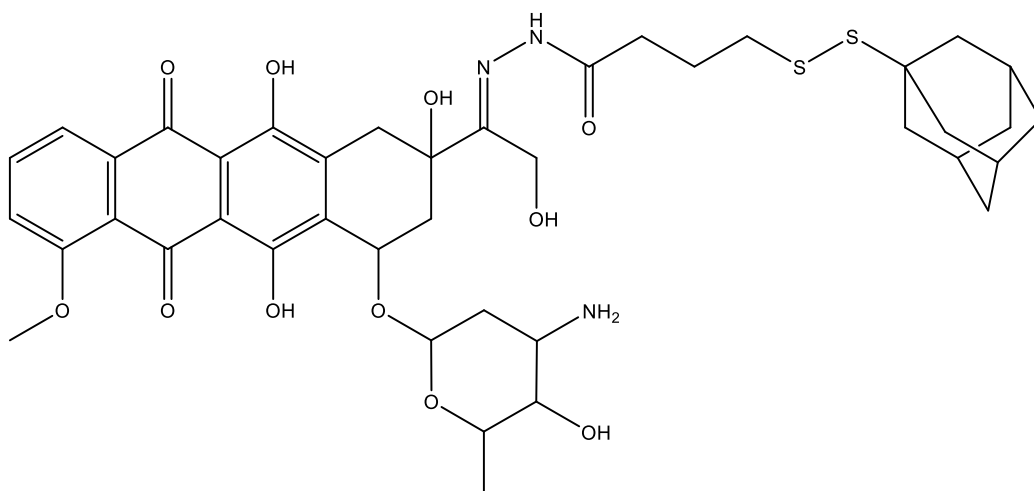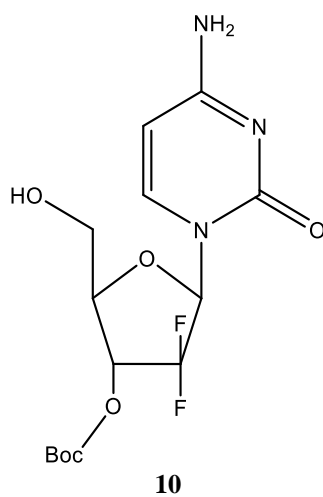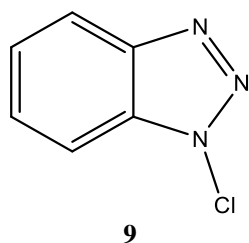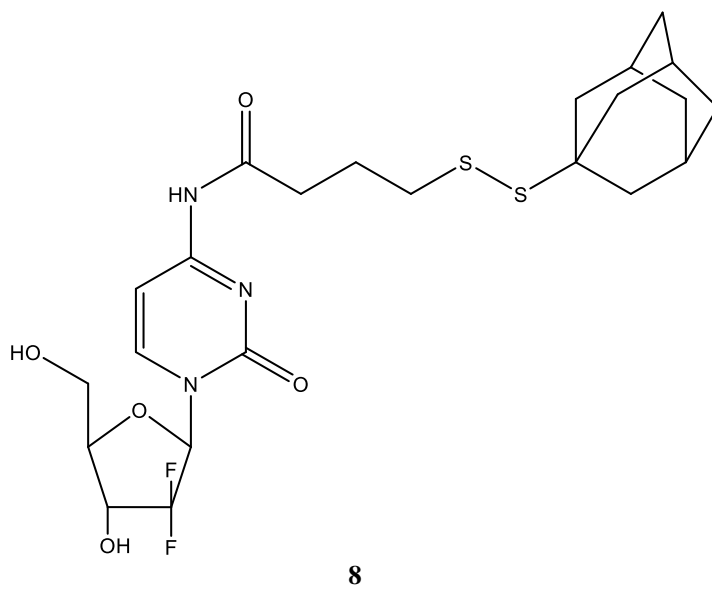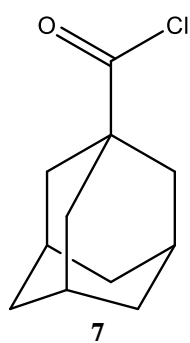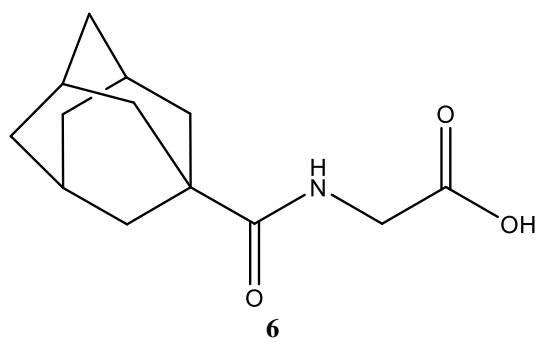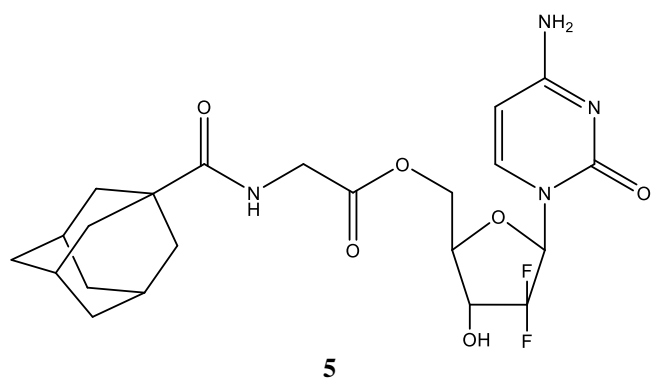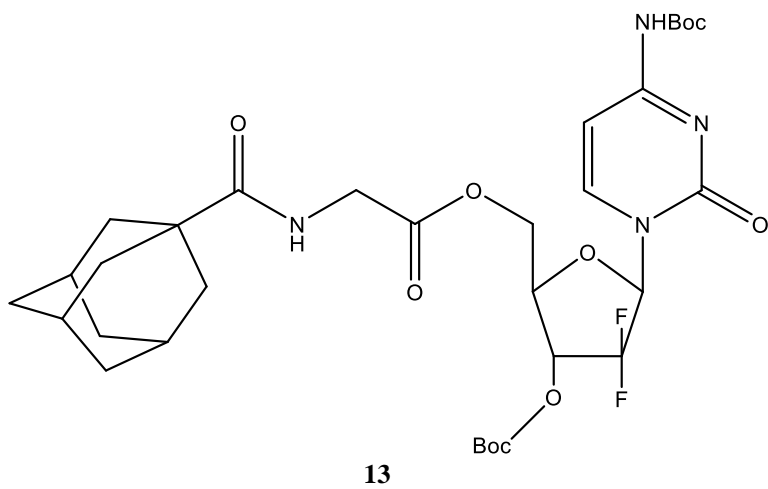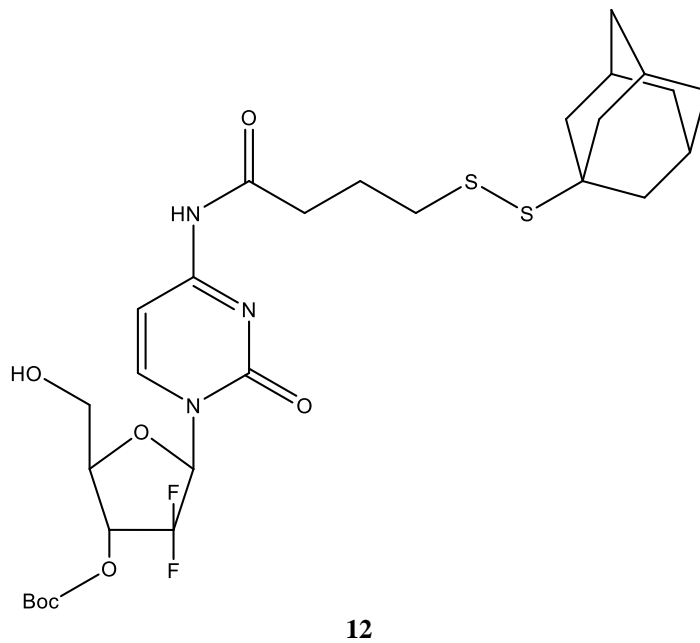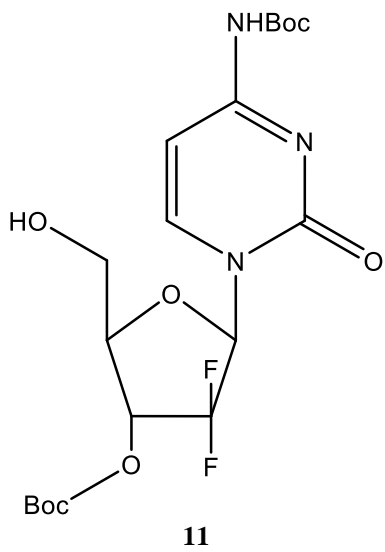
# 1. Introduction

In 2010, there were 14.1 million new cancer cases, 32.8 million individuals living with cancer within 5 years of diagnosis and 8.2 million cancer deaths, equivalent to an estimated 13 % of all deaths worldwide.[1] Cancer is a generic term for a large group of diseases, made up of different and distinctive diseases.[2] However, the diseases all have common traits. D. Hanahan and R. A. Weinberg proposed six so-called hallmarks of cancer in 2000.[3] These include sustaining proliferative signaling,[4] evading growth suppressors, and resisting cell death.[5] All six hallmarks can be seen in figure 1.
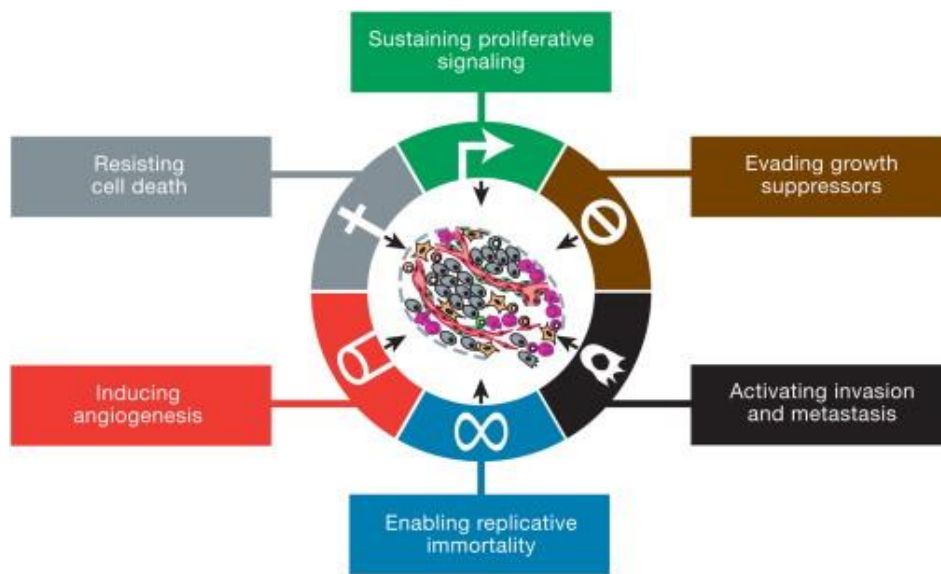


*Figure 1: Hallmarks of cancer as proposed by D. Hanahan and R. A. Wienberg.[5]*

Cancer can involve any tissue of the body and have many different forms in each body area. Most cancers are named for the type of cell or organ in which they start. Cancer often starts with abnormal cell growth, a neoplasm. These often grow faster than healthy cells and will continue to grow if not treated. A neoplasm can either be benign or malignant (cancerous). In the cancerous cases, a neoplasm is often referred to as tumor. Tumor cells accumulate mutations that result in unscheduled proliferation,[6] for example, knock down of p53 or Ras (an oncogene) becoming constitutively active.[5] Cancer cells also acquire genomic instability which leads to additional mutations and chromosomal instability. All this results in proliferative advantages and an increased susceptibility to accumulate additional genetic alterations.[7] An illustration of a cancer cell cycle can be seen in figure 2.
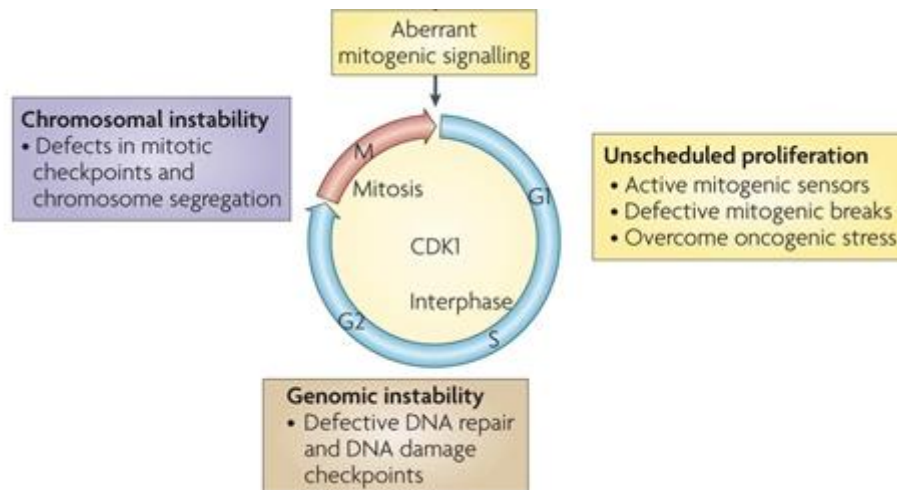
*Figure 2: Cancer Cell cycle.[7]*

The body is not without a defense system when it comes to preventing malignant neoplasms. P. Ehrlich proposed that both native and adaptive immune defenses play a role in preventing cancer. M. Burnet extended that theory and used the word *immunosurveillance* to describe the immunological resistance to cancer development.[8] The immunosurveillance theory was set forth over 50 years ago, and still has the immunological scientific community divided, mainly due to lack of convincing data of *in vivo* immunological eradication of precancerous lesions.[9] According to the immunosurveillance theory, the immune system should reject cancer cells based on their mutated profile. However, due to tolerance, the immune system sees some cancer cells as "self".[10] Treatment is therefore necessary and can come in the form of surgery, chemotherapy, radiotherapy and immunotherapy.

## 1.1 Chemotherapy

A chemotherapeutic is a chemical that binds to and specifically kills microbes or tumor cells, in short, a drug therapy for cancer. Chemotherapeutic drugs are classified according to their mechanism of action and are divided into five subcategories: alkylating agents, antimetabolites, anti-microtubule agents, topoisomerase inhibitors and cytotoxic agents.[11] A single chemotherapy drug can be used as treatment, but often multiple drugs with different mechanisms of action are used in combination. This improves the chances of killing cancer cells and reduces the chance of cancer cells becoming resistant to any one drug. Resistance, in this case, is defined as either a lack of tumor size reduction or the occurrence of relapse after an initial positive response.[12] Most chemotherapeutic agents target dividing cells, regardless of whether it is a dividing tumor cell or active intestinal epithelial cell.[13, 14] They do so with the same potency, which results in low specificity and systemic toxicity.[15, 16] Treatment is therefore a balance between killing the cancer cells and sparing the normal cells.

### 1.1.1 Doxorubicin

Doxorubicin (Dox), also known as Adriamycin, is an anticancer drug. Dox, shown in figure 3, is used to treat several cancers including breast, lung, gastric, ovarian, thyroid, non-Hodgkin's and Hodgkin's lymphoma, multiple myeloma, sarcoma, and pediatric cancers.[17] There are two proposed mechanisms of action for Dox. One is the intercalation into DNA, which leads to breaking of DNA[18] or poisoning of topoisomerase II,[19, 20] which leads to cell death.
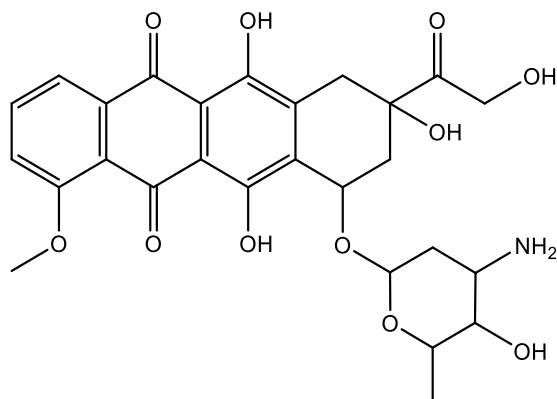


*Figure 3: Structure of Dox.*

The other is generation of free radicals.[21] Dox can generate free radicals by undergoing a one-electron reduction to form a DOX-semiquinone radical, doxorubicinol. This radical can be re-oxidized back to DOX, which leads to the formation of reactive oxygen species (ROS).[22] ROS ultimately leads to cell death. However, the use of Dox is limited due to systemic toxicities, primarily cardiotoxicity and immunosuppression.[17, 23]

### 1.1.2 Gemcitabine

Gemcitabine (Gem), shown in figure 4, is an anticancer nucleoside and an analog of deoxycytidine.[24] It is used intravenously and is active against solid tumors, including colon, lung, pancreatic, breast, bladder, and ovarian cancers.[25] Gem works as an antimetabolite towards pyrimidine.[26] Gem is formulated as a prodrug and needs to be phosphorylated by deoxycytidine kinase into its active form, the 5'-triphosphategemcitabine, which is incorporated into the DNA strand, halting its elongation and causing cell death. Gem has high toxicity and a very short plasma half-life due to rapid metabolizing in the blood, liver and kidneys as a consequence of deamination by cytidine deaminase into the inactive uracil derivative.[27] Gem has a hydrophilic nature and cannot cross cell membranes through passive diffusion.[28]
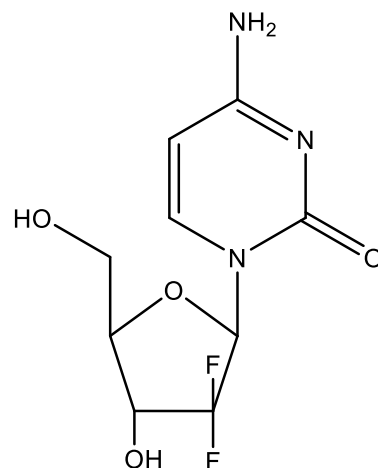


*Figure 4: Structure of Gem.*

## 1.2 Prodrug design

A prodrug is defined as a chemically modified bioreversible derivate of a drug molecule that undergoes an *in vivo* transformation, either enzymatic or chemical, to release the active drug.[29] The formulation of a prodrug is an established strategy to improve the physicochemical, biopharmaceutical or pharmacokinetic properties.[30] The drug–promoiety is pharmacologically inactive and made up of a pharmacologically active drug and a promoiety, as seen in figure 5. The drug is covalently bound to the promoiety via bioreversible groups that are chemically or enzymatically labile, such as an ester bond.[31]
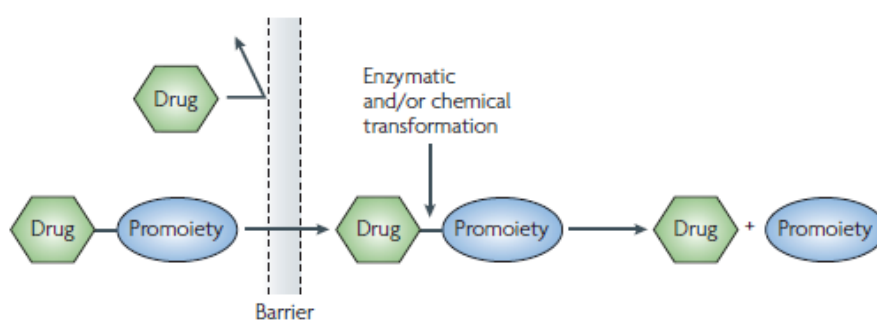


*Figure 5: Schematic of prodrug design.[30]*

Prodrugs make it possible to overcome a variety of barriers to drug formulation and delivery, such as, poor aqueous solubility, chemical instability, insufficient oral absorption and toxicity.[30] Another advantage of prodrugs is the possibility for improved drug targeting through site specific delivery.[30]

### 1.2.1 Enhanced permeability and retention

Tumor tissue has anatomical and pathophysiological abnormalities compared to healthy tissue.[32] When tumor cells reach a size of 2– 3 mm, angiogenesis is induced, to provide more nutrition and oxygen to the tumor cell.[33] The blood vessels in the tumor are irregular in shape, dilated, leaky or defective, and the endothelial cells are poorly aligned, as illustrated in figure 6.[34]
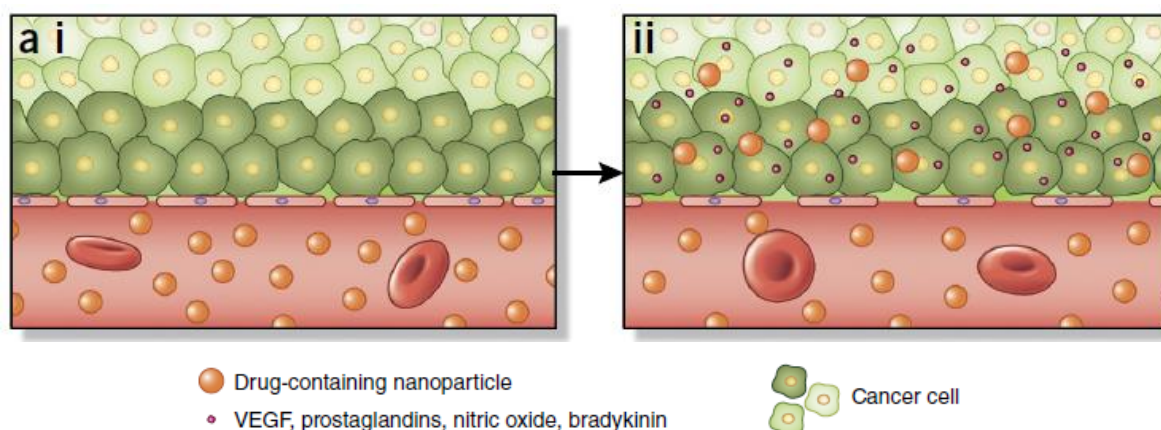


*Figure 6: Accumulation of nanoparticle in tumor cell through EPR.[35]*

Tumor cells also overproduce vascular mediators, such as bradykinin, nitric oxide (NO), vascular endothelial growth factor (VEGF), etc.[36] All these different factors lead to abnormal transport dynamics, especially for macromolecular drugs.[37] This phenomenon was later termed enhanced permeability and retention (EPR) effect and paved the way for the passive targeting of tumors using nanosized drugs. EPR-based tumor targeting, requires macromolecular drugs to have longer half-life. Drugs can therefore be modified with water-soluble polymers such as polyethylene glycol (PEG), cyclodextrin (CD), etc.[36] The polymers can further help in site specific delivery. Research has shown that tissue and cell distribution profiles of anticancer drugs can be controlled by their entrapment, and thereby increase the antitumor efficacy and reduce systemic side-effects.[12]

## 1.3 Host-guest supramolecular chemistry

J.-M. Lehn, D. J. Cram and C. J. Petersen won the Nobel prize in 1987,[38] on account of "*their development and application of molecules with highly selective structurespecific interaction, i.e. molecules that can "recognize" each other and choose with which other molecules they will form complexes*".[39] Host-Guest systems utilize non-covalent interactions, which include hydrogen-bonding interactions, π-π stacking, van der Waals forces, hydrophobic/hydrophilic attractions and electrostatic interactions.[40] These non-covalent interactions provide an easy approach for building supramolecular structures. A wide-range of non-covalent supramolecular systems such as vesicles and nanoparticles has been developed as drug carriers. If designed correctly these may act as vehicle and be able to target tumor cells, while protecting the drug from degradation.[12]

### 1.3.1 Cyclodextrins

CDs are nanometric biomaterials with supramolecular properties.[41] CDs are one among the many host molecules discovered and utilized for building up supramolecular systems. CDs can enhance apparent water solubility by forming dynamic, non-covalent, water-soluble inclusion complexes. CDs are a class of macrocyclic rings composed of α-1,4-glycosidic bond linked oligosaccharides. They are classified as either natural or derived CDs.[42] Most used are CDs containing six, seven or eight glucose units, commonly known as α-, β-, and γ-CDs.[40] The internal diameter varies, being 0.57 nm, 0.78nm and 0.95 nm respectively. CDs generally have a truncated structure, as seen in figure 7, due to the lack of free rotation around the bonds connecting the glucopyranose units.[43]
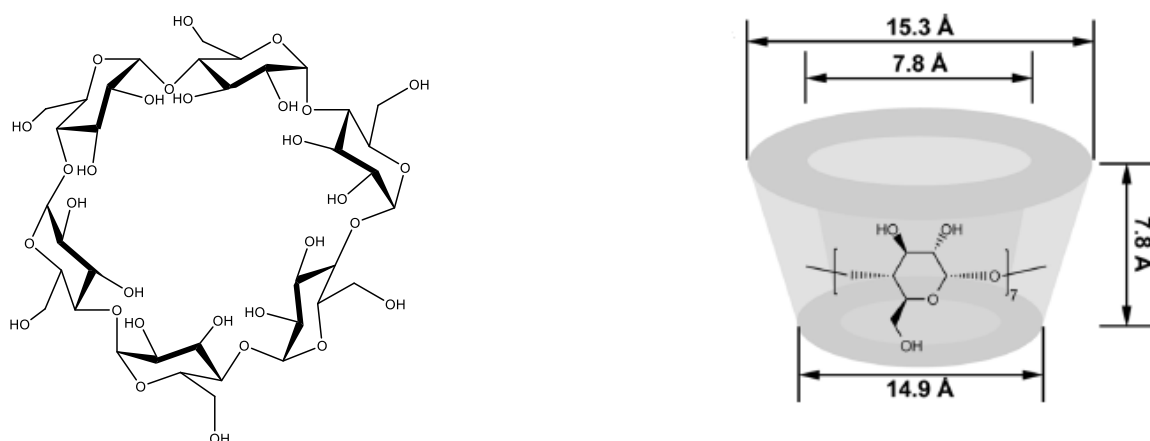
The internal cavity of CDs contains only hydrogen atoms and oxygen bridges, while the hydroxyl groups are forced on the outer edge.[45] The exterior is therefore hydrophilic while the interior cavity is hydrophobic. The hydrophobic region can serve as a reservoir for hydrophobic drugs while the hydrophilic exterior keeps it from being absorbed by macrophages.[14] They have insignificant toxicity and their improved bioavailability renders them suitable for functional delivery systems.[44] CDs form an inclusion complex, often 1:1, through an equilibrium process where the free guest molecules are in equilibrium with molecules in the complex, as described in equation 1.[46, 47] The cavity of CDs is occupied by water in aqueous solutions.[48] The occupancy by water is energetically unfavorable, while the displacement of water is a driving force for the complexation.

$$Drug_{free} + CD_{free} \rightleftarrows Drug/CD_{complex}$$
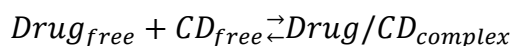
*Equation 1: equilibrium between free CD and CD complex*

CDs are mainly used in the pharmaceutical industry as complexing agents to increase the aqueous solubility of poorly water-soluble drugs, to increase their bioavailability and stability.[46, 49] $\beta$-CD is ideal for this purpose because of its cavity size, efficient drug loading, availability and cost.[42] CDs do not readily cross biological membranes and CD-drug complexes are therefore mostly administered by injection.[47] In 2010 there were 35 different pharmaceutical products containing CDs on the marked.[50] β-CDs are the most studied when it comes to pharmaceutical application,[51] however, the aqueous solubility is low.[41, 46] Derivatives of β-CDs with higher aqueous solubility have been synthesized, such as methyl-β-CD (MβCD), hydroxypropyl-β-CD (HPβCD), and sulfobutylether-β-CD (SBEβCD). Methyl-derivatives of β-CDs are highly soluble, but were found to have strong systemic toxicity, whereas the two others have the lowest hemolytic effect.[50] CDs generally have a great functionalization capacity[52] and the progress within this field has contributed to advancement in chemotherapy. The development of CD-chemotherapy delivery systems offers the possibility of more effective treatment with fewer side effects.[42]

### 1.3.2 CD-Adamantane complex

Among the many hydrophobic or amphiphilic molecules studied as guests in complexation with CDs, special attention has been given to β-CD complexation with adamantyl.[45] Adamantane is a symmetrical and stable structure. The adamantyl group has a diameter of 7 Å.[53] In 1989, M. R. Eftink *et al.*[54] determined the thermodynamic parameters for interaction of alicyclic carboxylic acids (including 3-homoadamantanecarboxylate; adamantanecarboxylate and cyclohexane acetic acid amongst others) with α- and β-cyclodextrin hosts. The study showed that adamantyl fits tightly in the β-CD cavity,[54] as illustrated in figure 8.
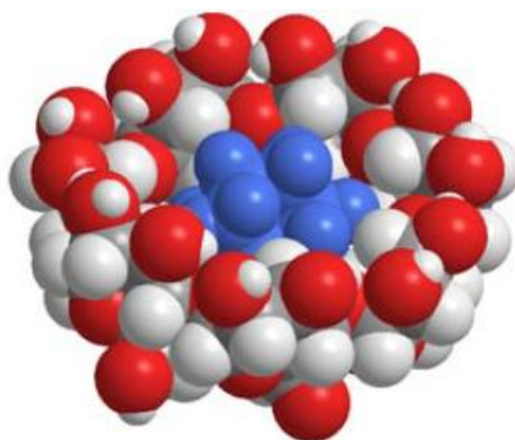
*Figure 8: Illustration of β-CD complex with adamantyl.[53]*

Because of the tight fit, adamantyl and adamantane derivatives form 1:1 inclusion complexes with β-CD, normally with an equilibrium constant between $10^4$–$10^5$ $M^{-1}$.[53, 45] The interior of the cavity of β-CD is not a smooth cone. H3 and H5 atoms of each glucose residue protrude into the cavity, and thereby forms a constricted entrance.[55] This gives way to two different isomeric complexes between adamantyl derivatives, and β-CD can be formed.[55]

# 2. Thesis statement

The overall concept of this project is to investigate the possibilities of modifying anticancer drugs to enhance their complexation with CDs. In order to keep the pharmaceutical properties of the drug, a prodrug will be designed. The formation of the prodrugs will be based on two anticancer drugs; Dox and Gem. Both these drugs are highly water soluble, which means that they do not complex well with CDs without modifications.

CD and adamantane is an easily assembled and well demonstrated system.[56] Therefore, in order to enhance complexation between the two drugs and CDs, an adamantyl moiety will be linked to the drugs. As mentioned earlier, there are different things that need to be considered when designing a prodrug. In the case of Dox and Gem, they both possess more than one functional group, therefore the coupling with the linker needs to be chemoselective. An ester bond would be an ideal choice as it is biodegradable. However, there is an amine present in both molecules and the formation of amide bonds is favored in conventional carboxylate coupling reactions when both amine and hydroxyl groups are present.
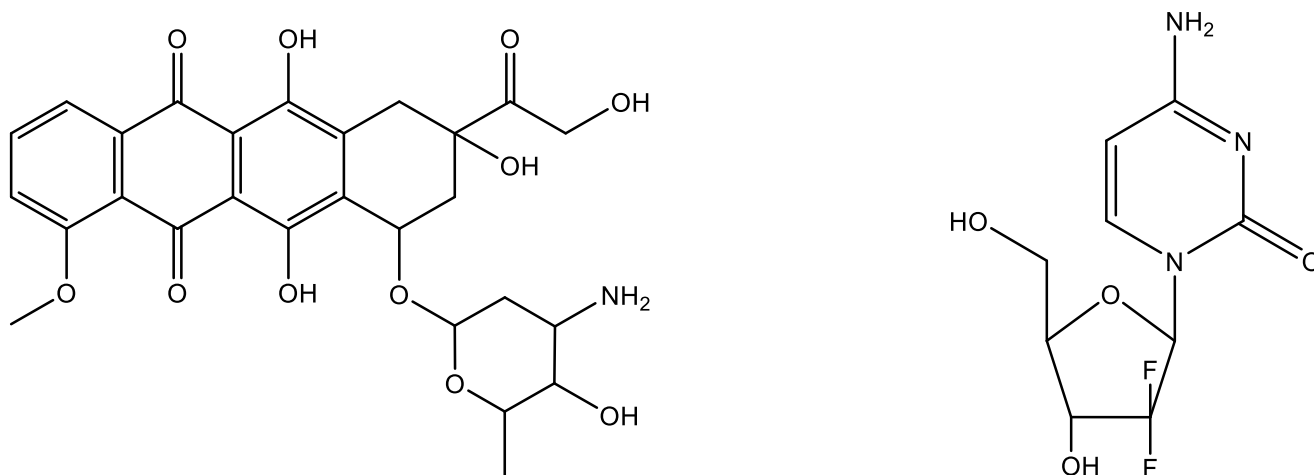


*Figure 9: Structure of Dox (left) and Gem (right).*

# 3. Theoretical considerations

## 3.1 Retrosynthesis of Doxorubicin

Dox bears a lot of functional groups such as amine-, ketone-, phenol- and hydroxyl-groups as seen in figure 9. An ester bond would be ideal, but to facilitate such a reaction, protection of the amine group before, and deprotection after, the conjugation is required. It is possible but given the multifunctional structure, it may result in degradation.[57] Alternative options will therefore be explored.

### 3.1.1 Retrosynthesis of (1) via a hydrazine bond

One alternative to the ester bond would be a conjugation between the ketone group in 13th position on Dox and hydrazine groups of polymeric carriers by forming an acid-labile hydrazine bond.
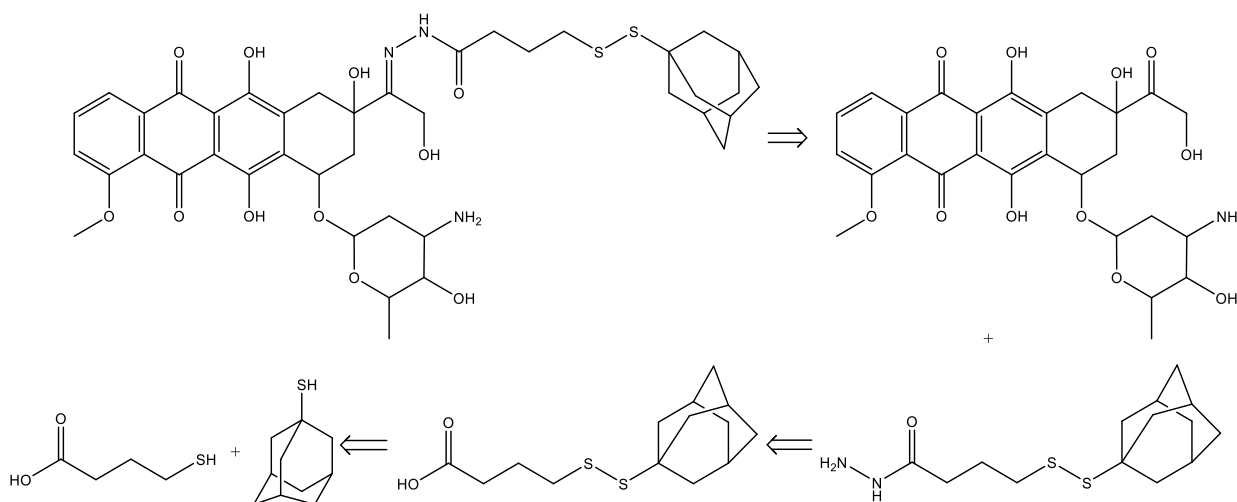


*Figure 10: Retrosynthesis of (1).*

### 3.1.2 Retrosynthesis of (4) via an amide bond

As mentioned, an amide bond is not biodegradable. However, H. Han *et al*.[58] demonstrated that a disulfide carbonate bond could be reduced by glutathione (GSH) and generate a thiol intermediate, which would release the drug through an intramolecular cyclization.[27]
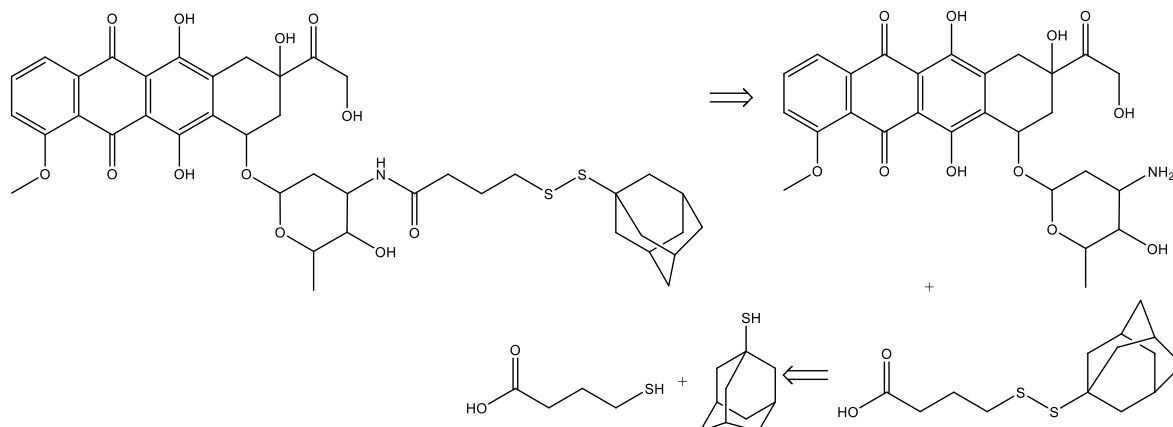


*Figure 11: Retrosynthesis of (4) through an amide bond.*

## 3.2 Retrosynthesis of Gemcitabine

Gem bears both an amine and two hydroxyl groups, as seen in figure 9.

### 3.2.1 Retrosynthesis of (5) via an ester bond

An ester bond would be ideal and achievable through conventional carboxylate coupling, with the amine group protected to avoid any unwanted side reactions.
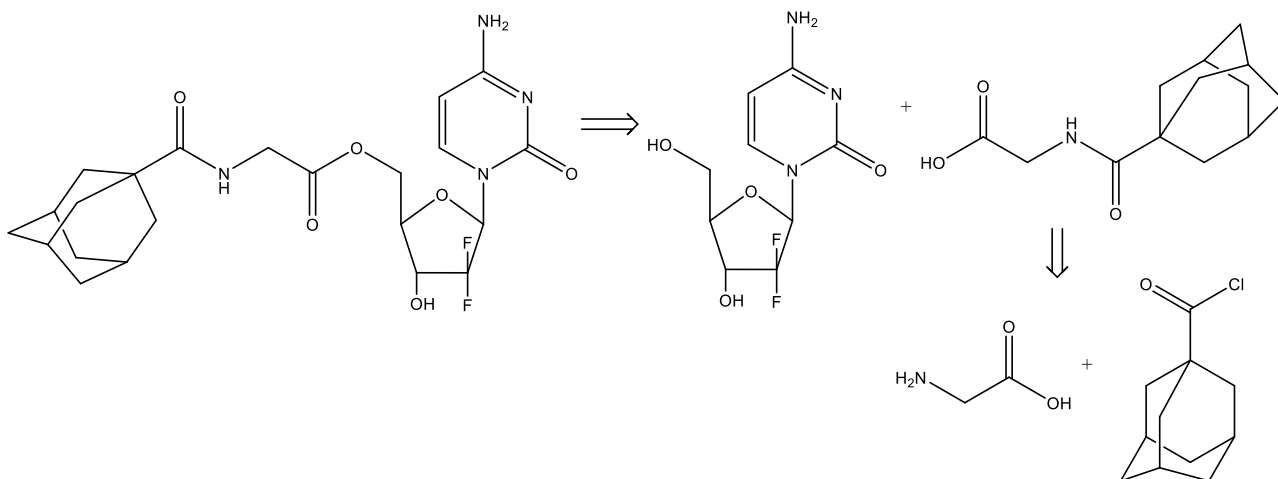


*Figure 12: Retrosynthesis of (5) through ester bond.*

### 3.2.2 Retrosynthesis of (8) via an amide bond

As mentioned, a disulfide carbonate bond could be reduced by GSH, generating a thiol intermediate, which would release the drug through an intramolecular cyclisation.[27, 58] This method would provide protection of the amine by forming an amide bond and it would eliminate the protection steps taken in the previous retrosynthesis.
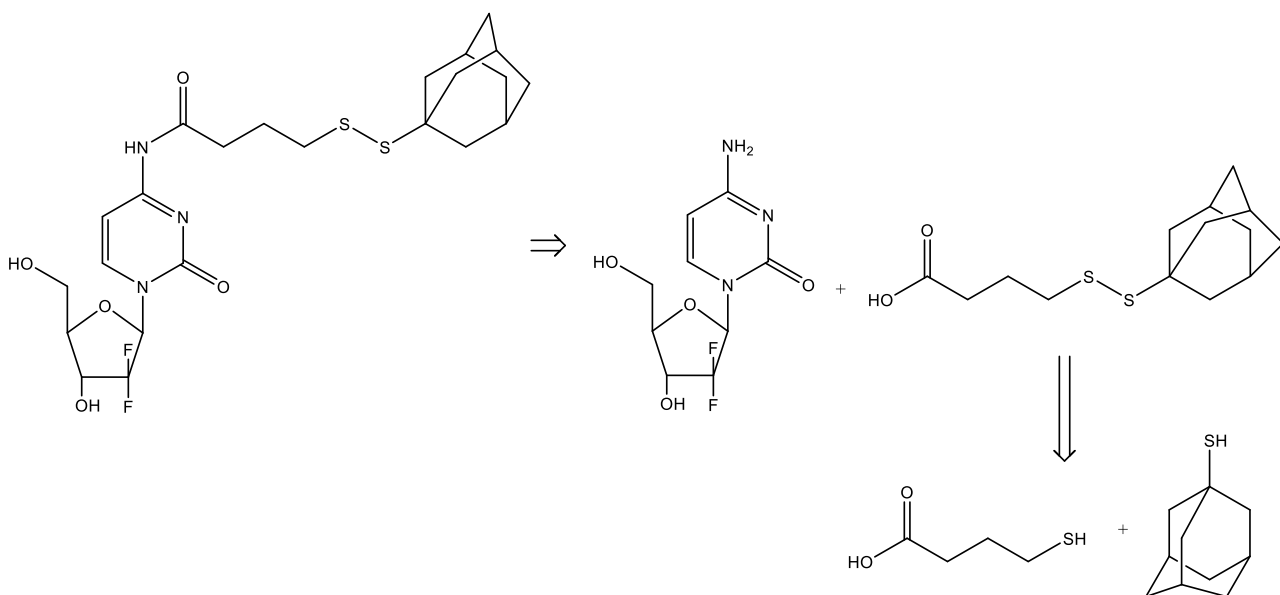


*Figure 13: Retrosynthesis of (8) through amide bond.*

## 3.3 Synthesis strategies and mechanisms

This section covers the considerations made about the individual reaction steps and the associated mechanisms.

### 3.3.1 Reactants

*3.3.1.1 1-adamantanecarbonyl chloride (7)*

1-adamantanecarbonyl chloride can be easily made from 1-adamantanecarboxylic acid by refluxing it in thionyl chloride or by reacting it with oxalyl chloride and a catalytic amount of DMF.
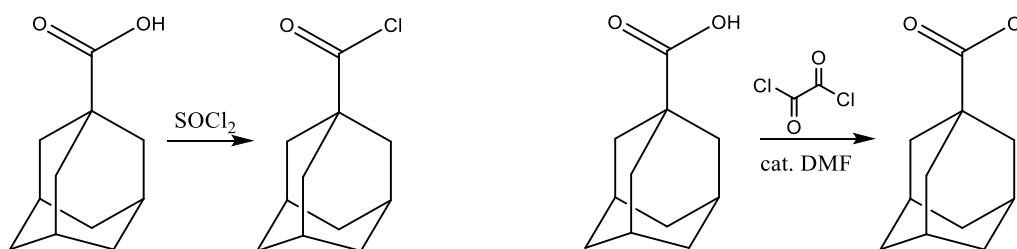


Figure 14: Synthesis of (7).

The electrophilic sulfur atom of thionyl chloride is attacked by the carboxylic acid and eliminates a chloride ion and forms an unstable electrophilic intermediate. The intermediate is then attacked by the chloride ion to give tetrahedral intermediate, which collapses to produce the acyl chloride with sulphur dioxide and hydrogen chloride as gasses. This is illustrated in figure 15.
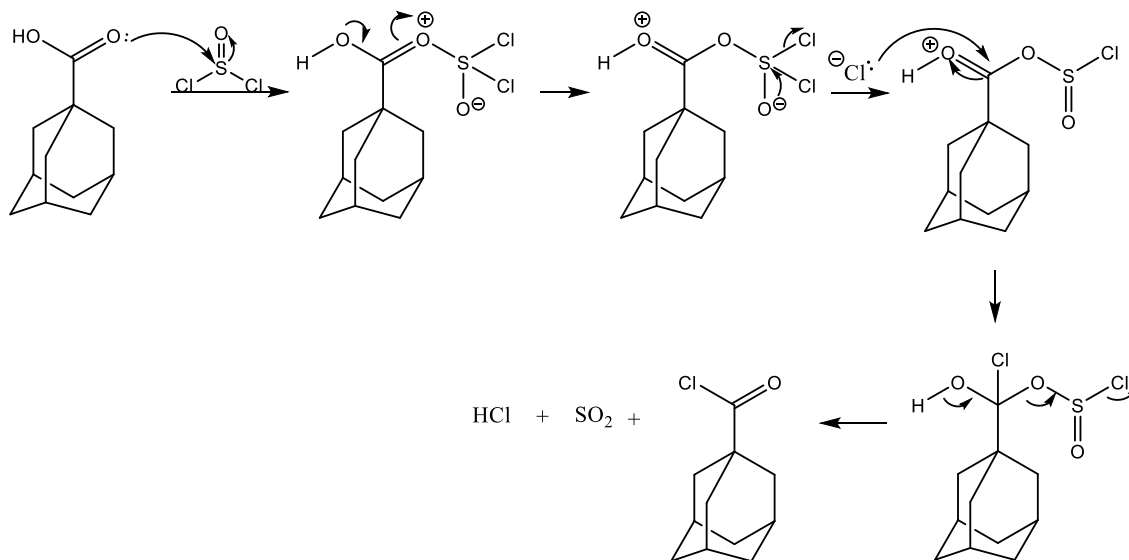


Figure 15: Reaction mechanism for the formation of (7) by thionyl chloride.

The reaction mechanism of oxalyl chloride involves the formation of the Vilsmeier Haack reagent, imidoyl chloride. Imidoyl chloride is the active chlorinating agent, which reacts with 1-adamantane carboxylic acid to produce 1-adamantanecarbonyl chloride and regenerates DMF. The mechanism described can be seen in figure 16.

25
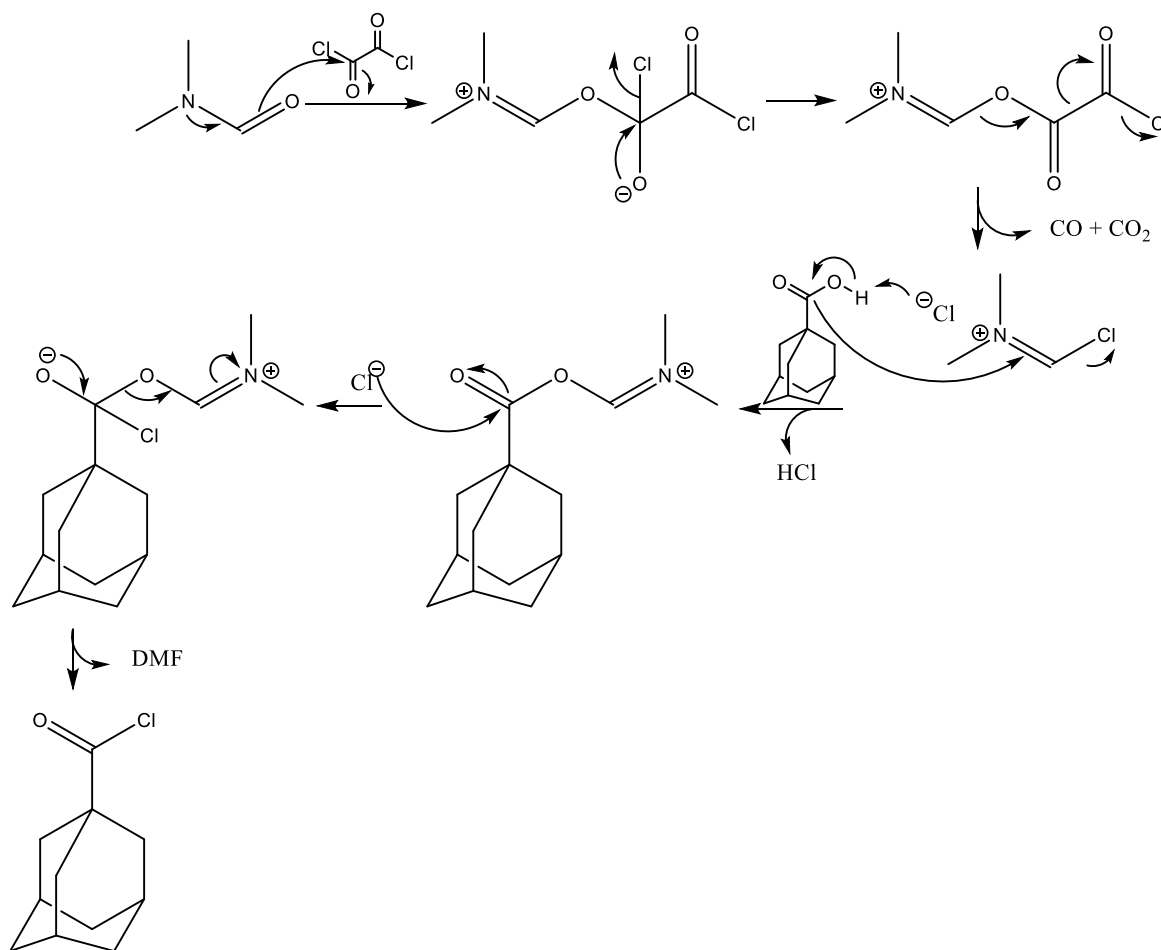
*Figure 16: Reaction mechanism for formation of (**7**) by oxalyl chloride with DMF catalyst.*

### 3.3.1.2 Chloronation of benzotriazole (**9**)

Benzotriazoles have a very useful set of properties. It is stable and a good leaving group and derivatives can easily be prepared.[59]
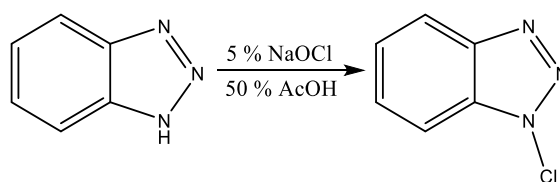


*Figure 17: Synthesis of (**9**).*

1-chlorobenzotriazole (BtCl) can be prepared by reacting benzotriazole with hypochlorite. Sodium hypochlorite is inexpensive and a strong oxidizing agent. The mechanism shown in figure 18 resembles the first step of a Weerman degradation.
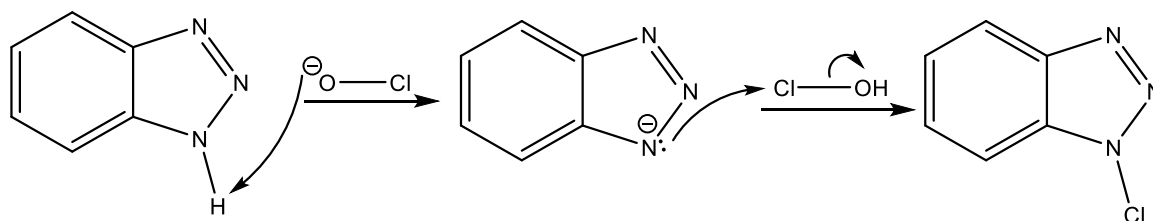


*Figure 18: Mechanism for synthesis (**9**).*

26

### 3.3.2 Doxorubicin

*3.3.2.1 Disulphide bond formation (**3**)*

This is an asymmetrical disulphide bond formation reaction. This can be done with the assistance of BtCl without the need for toxic and/or harsh oxidizing agents.
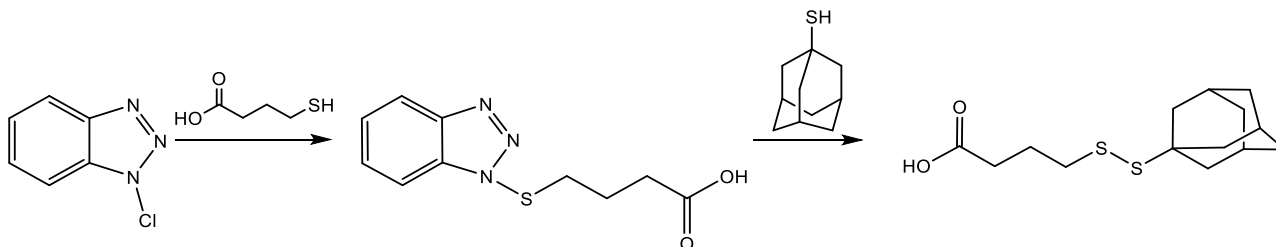


Figure 19: Asymmetric disulfide bond for the formation of (**3**).

Hunter *et. al.*[60] designed an effective protocol for the synthesis of unsymmetrical aliphatic–aliphatic disulfide. The authors proposed this mechanistic cycle, shown in figure 20.
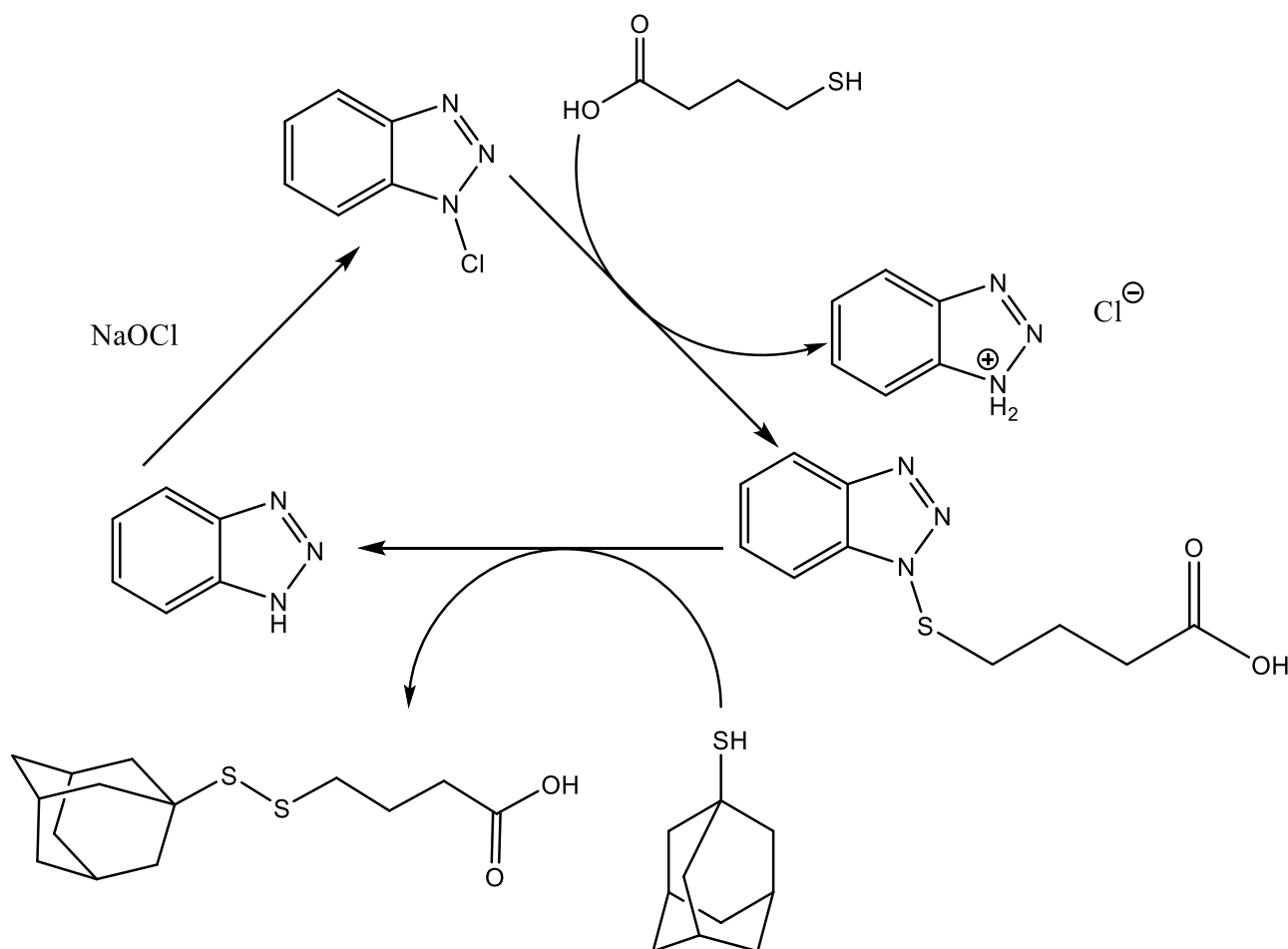


Figure 20: Asymmetric disulfide bond schematic.

The reaction mechanism involves two $S_N2$ like reactions,[61] as shown in figure 21. The nucleophilic attack from sulfur leads to displacement of chloride and benzotriazole respectively.
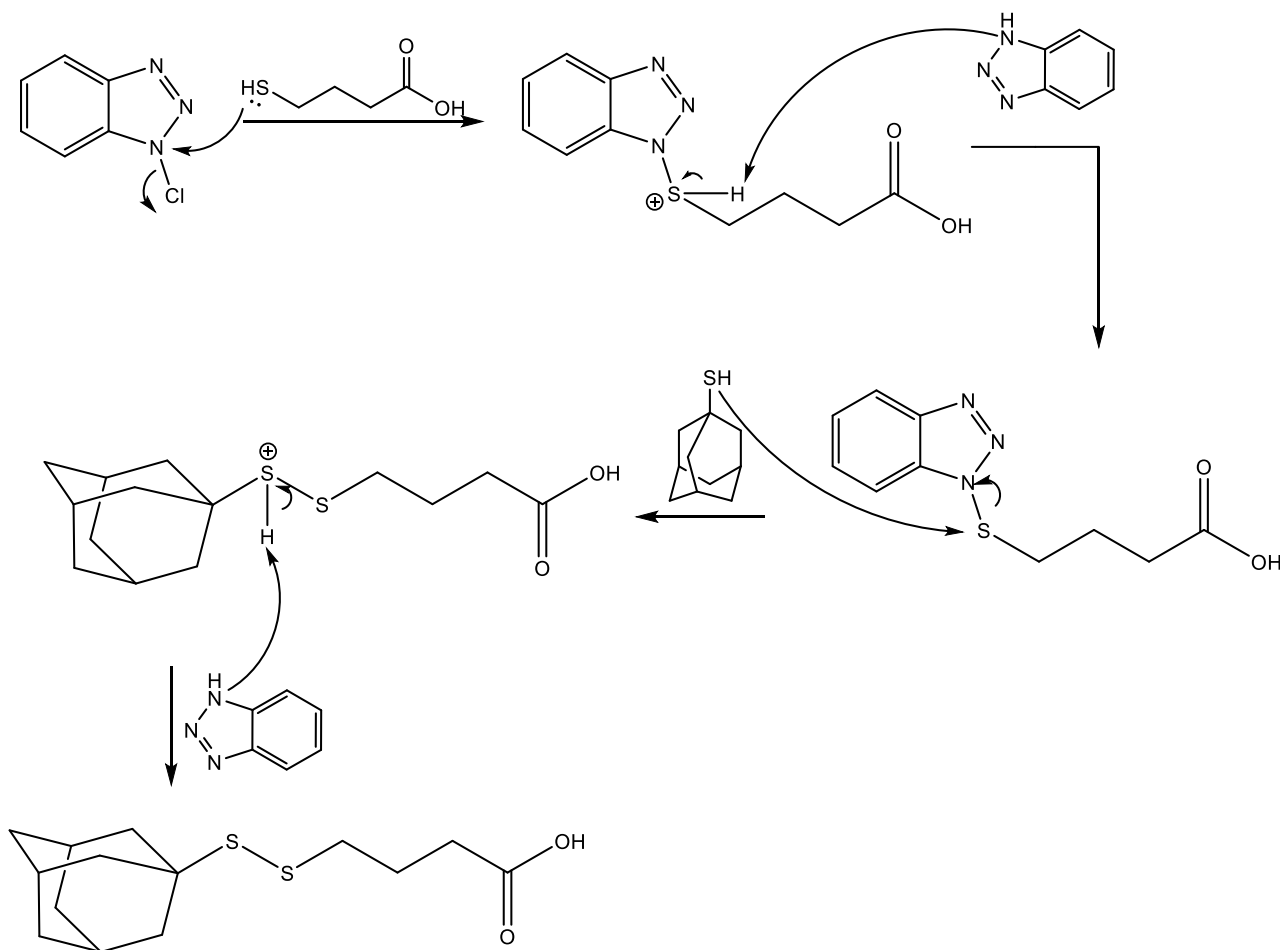


*Figure 21: Reaction mechanism for synthesis of (3).*

### 3.3.2.2 Amide bond (4)

This reaction relies on the formation of amide bonds being favored in conventional carboxylate coupling reactions.
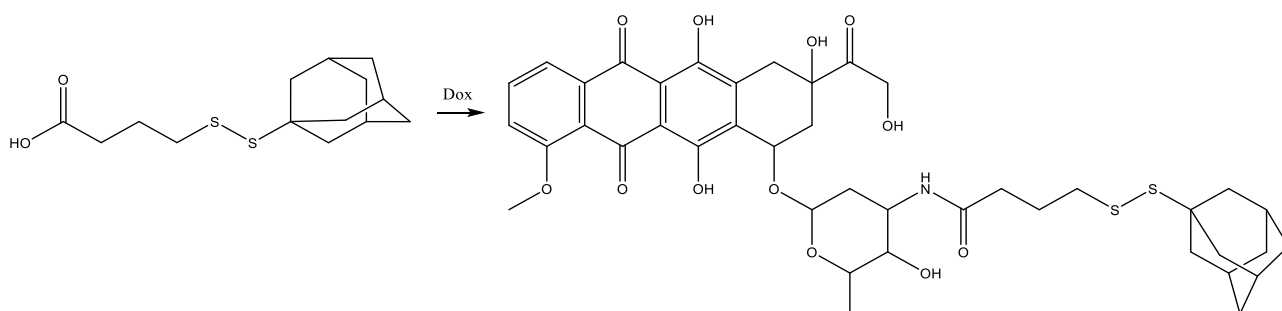


*Figure 22: Formation of (4).*

The carboxylic acid is deprotonated by DIPEA and HBTU to give an O-acylurea and then an O-benzotriazole (OBt) active ester, which in turn is more reactive. The OBt ester reacts with the amine to form the amide, as shown in figure 23.
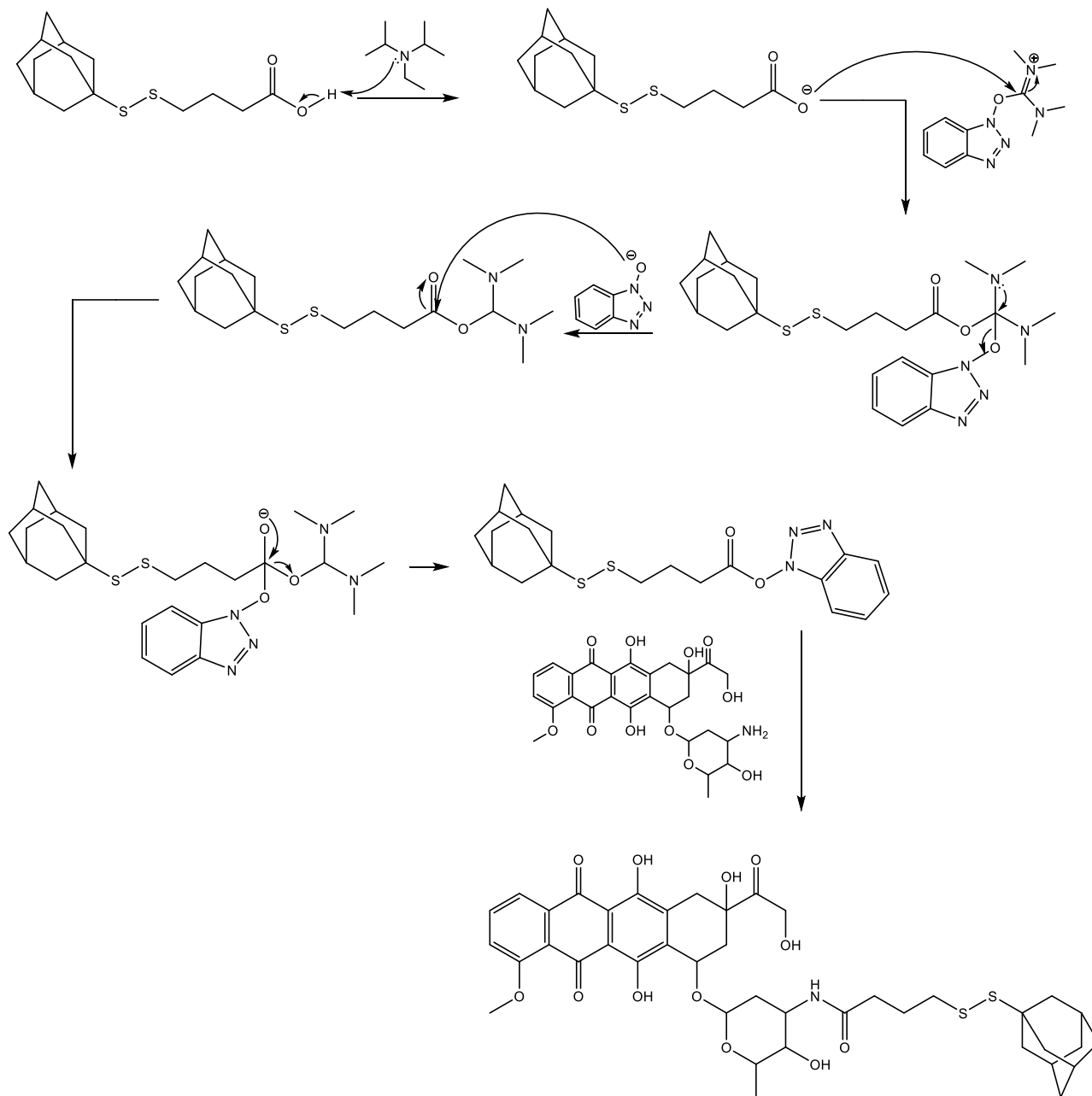
### 3.3.2.3 Hydrazone (2)

Hydrazine, which is more nucleophilic than a regular amine, reacts with the carbonyl to form a hydrazone.
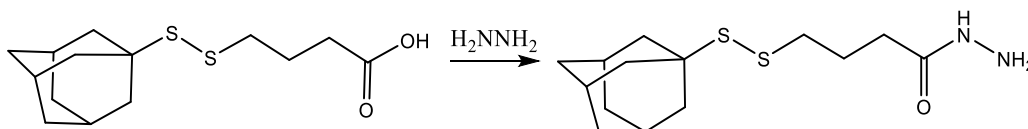


*Figure 24: Hydrazone formation (2).*

The nucleophilic nitrogen from the hydrazine attacks the carbonyl which leads to the elimination of water and the formation of a hydrazone.
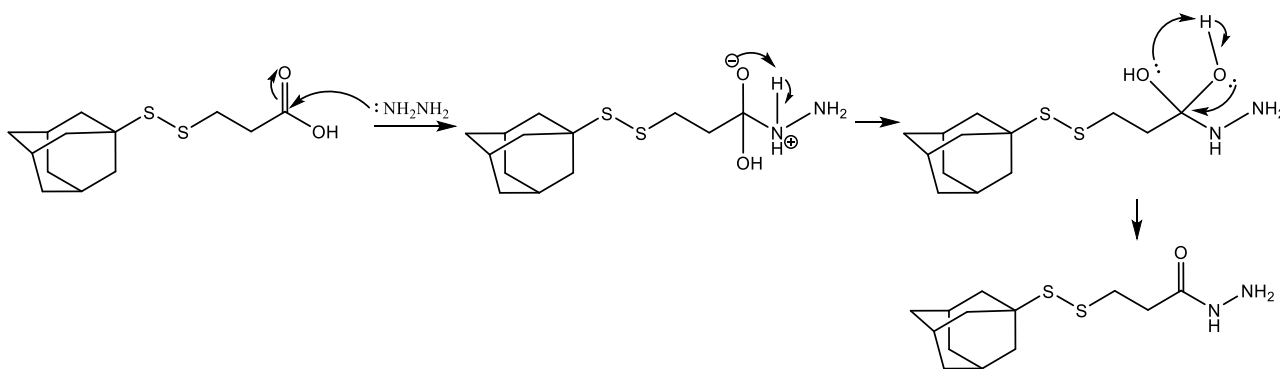


*Figure 25: Reaction mechanism to form (2).*

### 3.3.2.4 Imine formation (1)

The imine is formed when the primary amine reacts with the ketone group in 13$^{th}$ position on Dox.
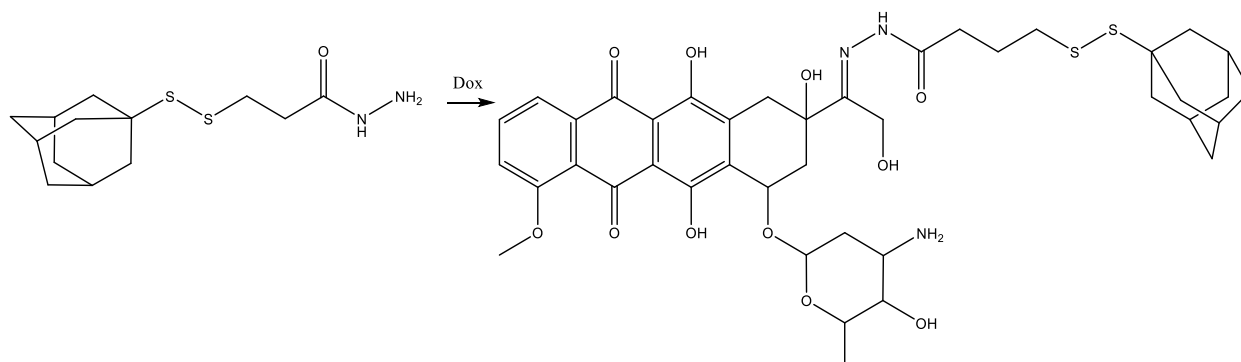


*Figure 26: Imine formation (1).*

Normally, imine formation uses an acid catalyst, to speed up the reaction. However, this reaction is not catalyzed, due to the unstable nature of Dox. The mechanism shown in figure 27 is therefore without a catalyst.
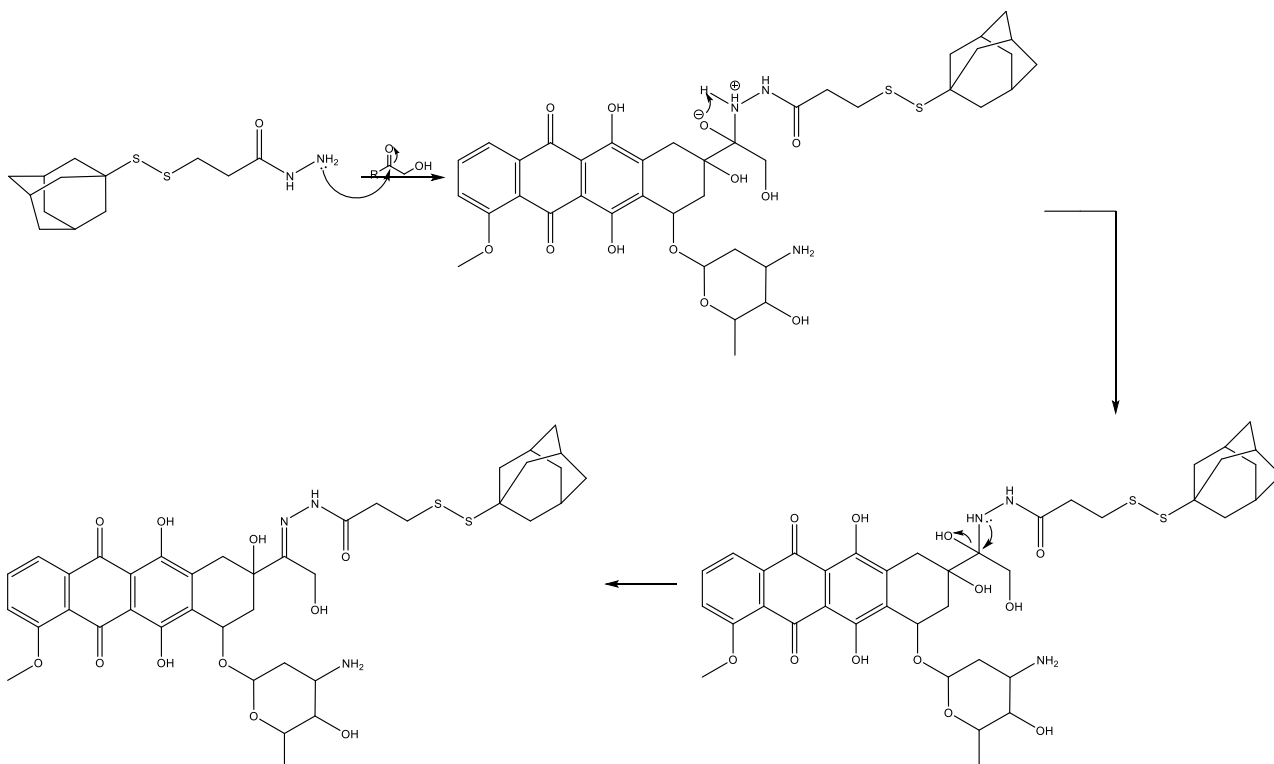
*Figure 27: Reaction mechanism for imine formation (**1**).*

### 3.3.3 Gemcitabine

*3.3.3.1 N-Adamantanoylglycine (**6**)*

This is a nucleophilic acyl substitution.
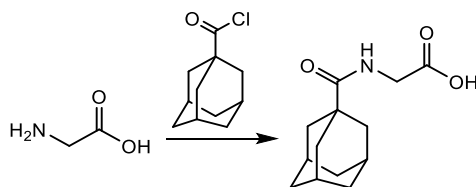


*Figure 28: Synthesis of (**6**).*

The lone pair on nitrogen will attack the fairly positive carbon atom of the acyl chloride and eliminate the chloride.
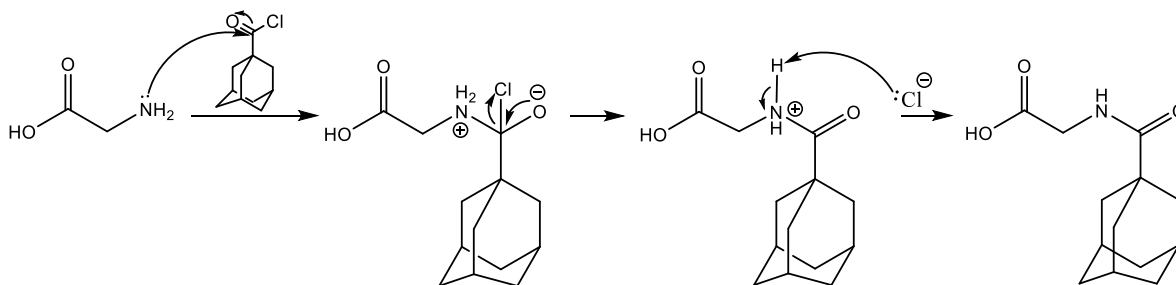


*Figure 29: Reaction mechanism for the formation of (6) by nucleophilic acyl substitution.*

The hydrogen ion from the nitrogen can either be removed by the chloride ion (as shown in figure 29) or by a glycine molecule.

The protection of amine group is necessary in order to avoid any unwanted side reactions in the following reaction steps. This can be done by using di-*tert*-butyl dicarbonate (boc) as a protecting group.
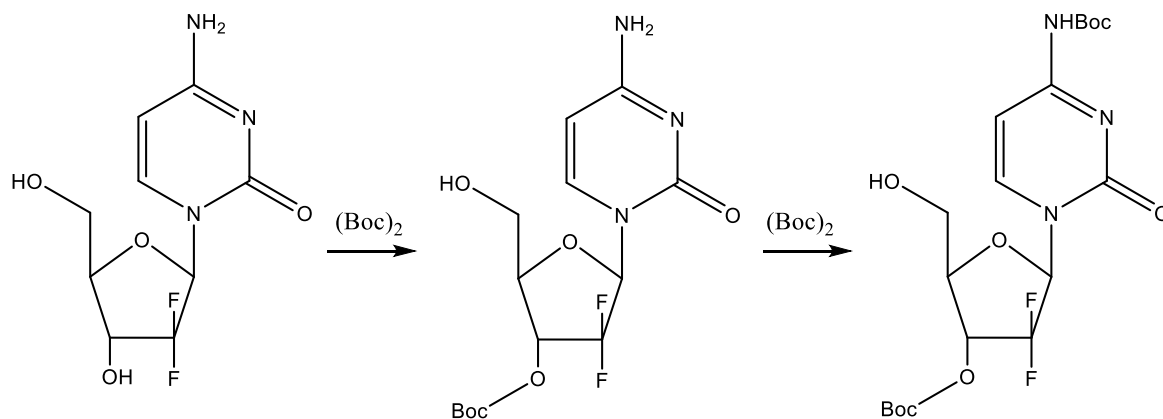


*Figure 30: Protection of Gem to produce (**10**) and (**11**).*

This is done in two steps: the first step protects the hydroxyl on position 3', as shown in figure 31, and the second protects the amine in 4th position, as seen in figure 32.
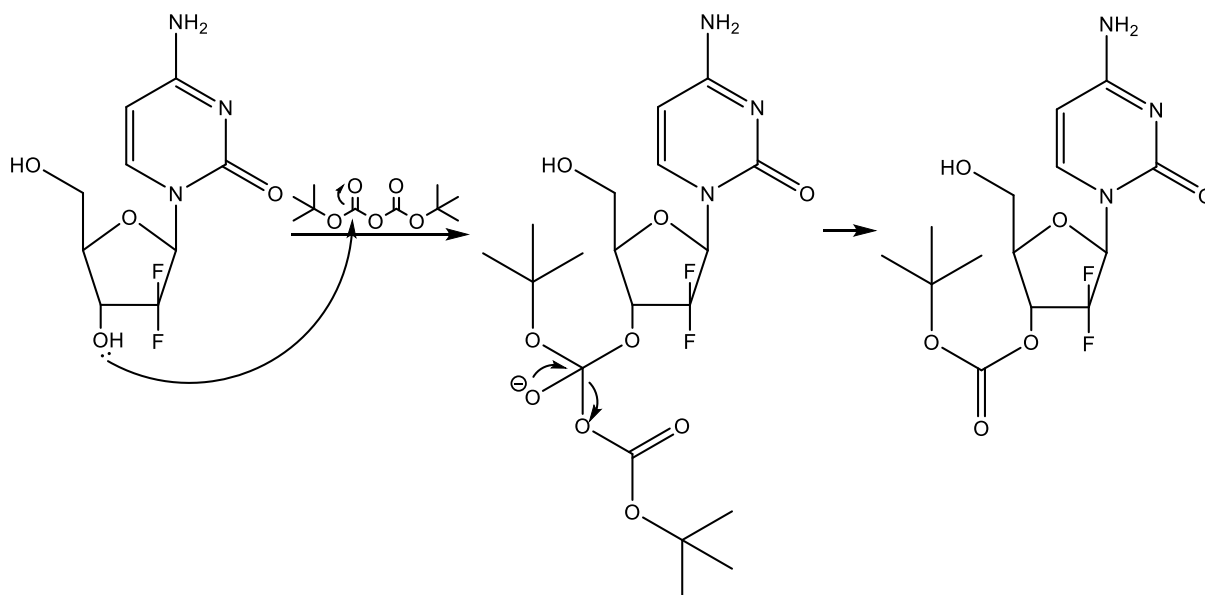


*Figure 31: Boc-protection mechanism to produce (**10**).*
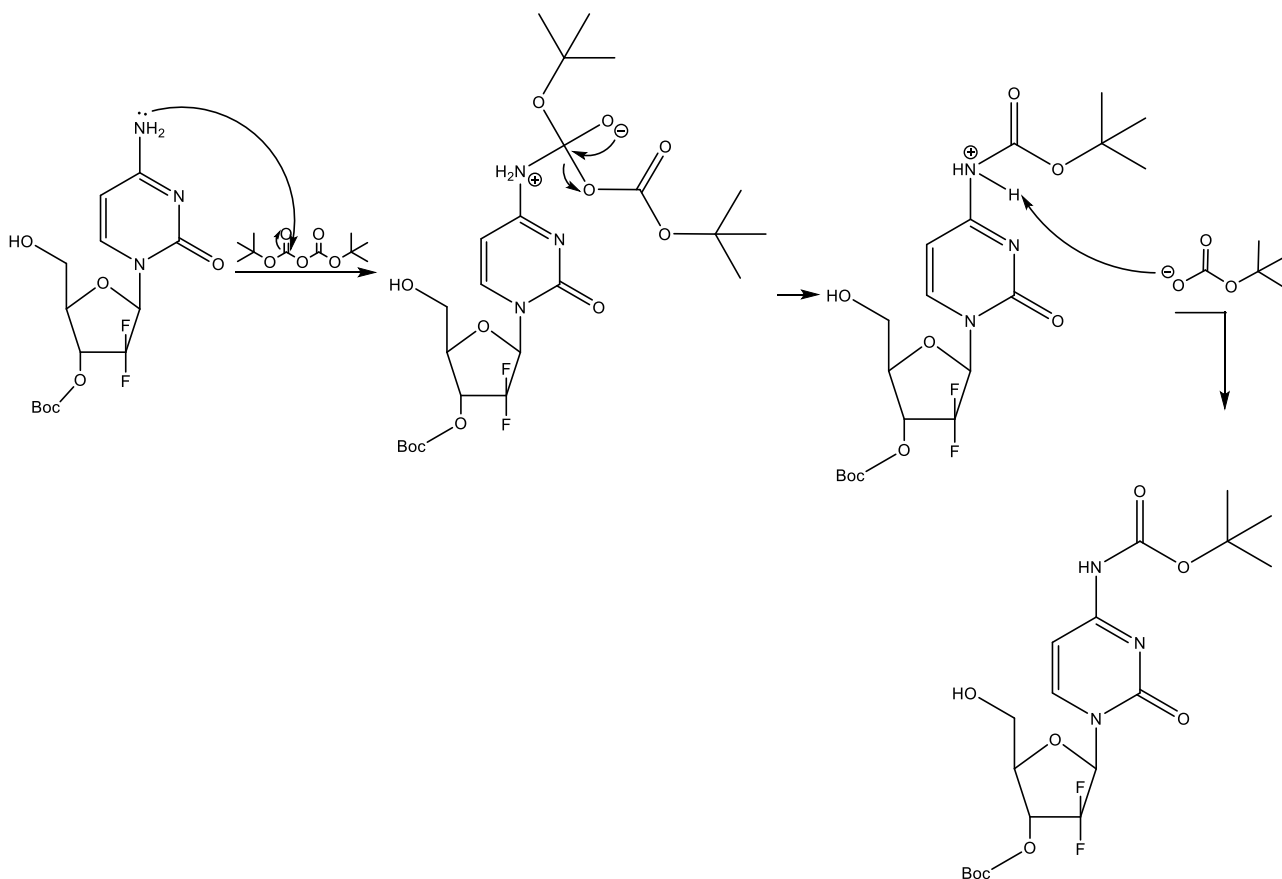
*Figure 32: Boc-protection mechanism to produce (**11**).*

### 3.3.3.3 Amide bond formation (*12*)

This reaction leads to an amide bond and is catalyzed by EDC and HOBt.
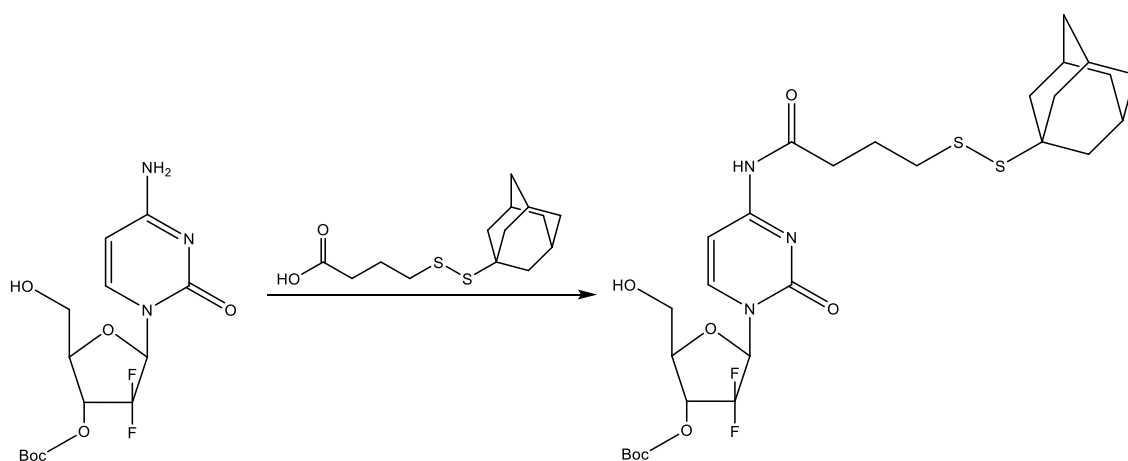


*Figure 33: Formation of (**12**) through an amide bond.*

The carboxylic acid is activated by EDC. This reaction gives an O-acylurea. HOBt then reacts with the O-acylurea to give the OBt active ester, which in turn is more reactive. The OBt ester reacts with the amine to form the amide and HOBt is restored. The mechanism can be seen in figure 34.
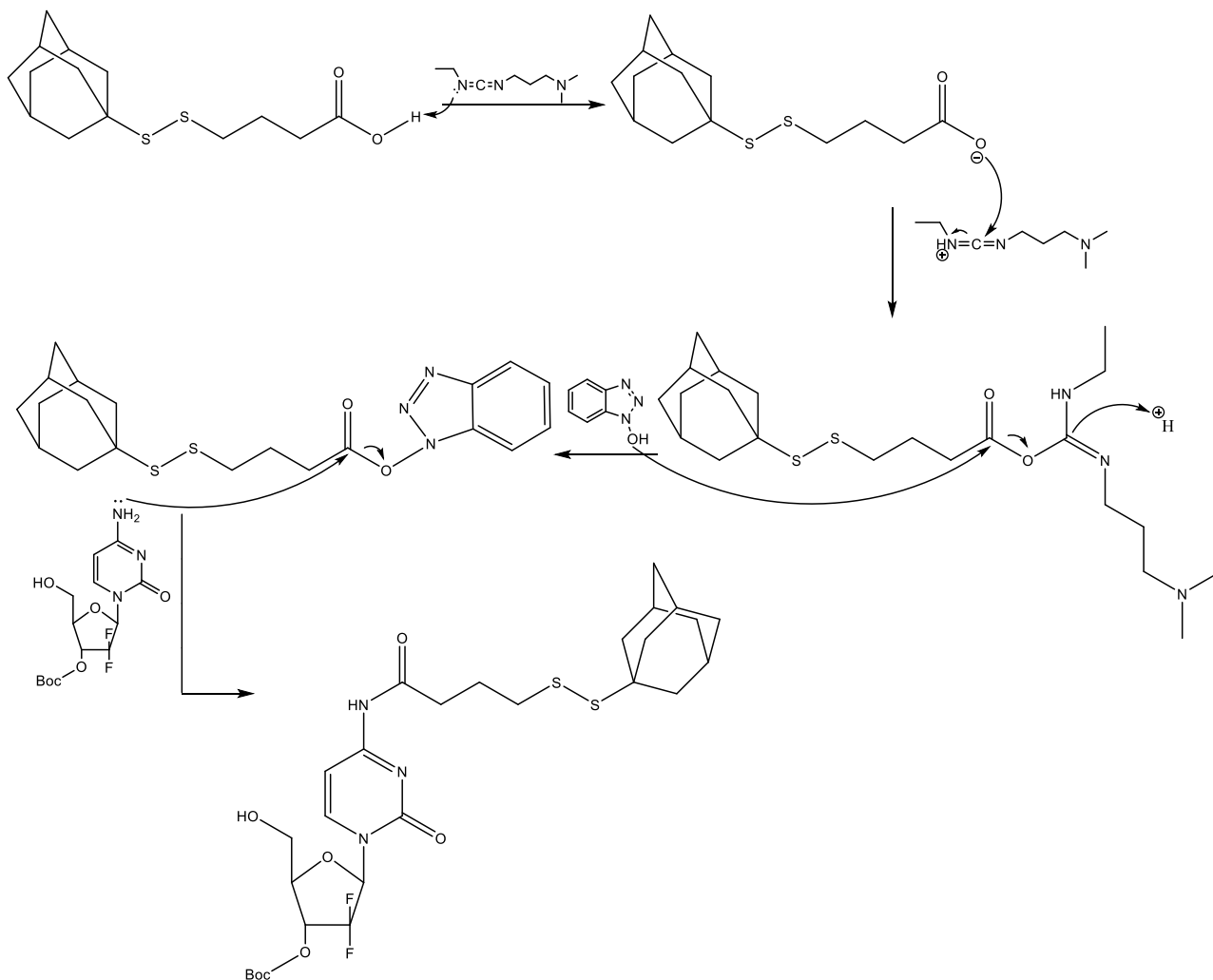


*Figure 34: Reaction mechanism for formation of (12), catalysed by EDC and HOBt.*

### 3.3.3.4 Esterification (13)

This is a standard esterification between a hydroxyl group and a carboxylic acid.
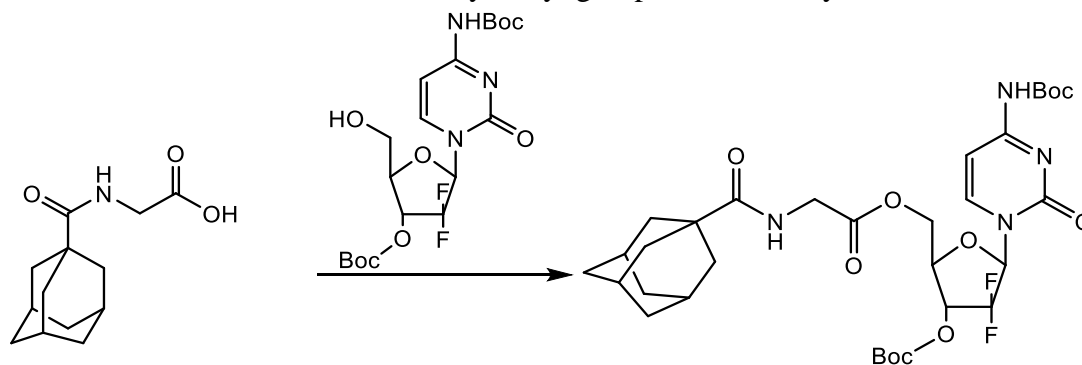


*Figure 35: Formation of (13) through esterification.*

The addition of a proton makes the carbonyl carbon more electrophile. The nucleophilic oxygen of the alcohol attacks and gives a tetrahedral intermediate with two hydroxyl groups. One of these hydroxyl groups is eliminated as water after a proton shift to the ester, as shown in figure 36.
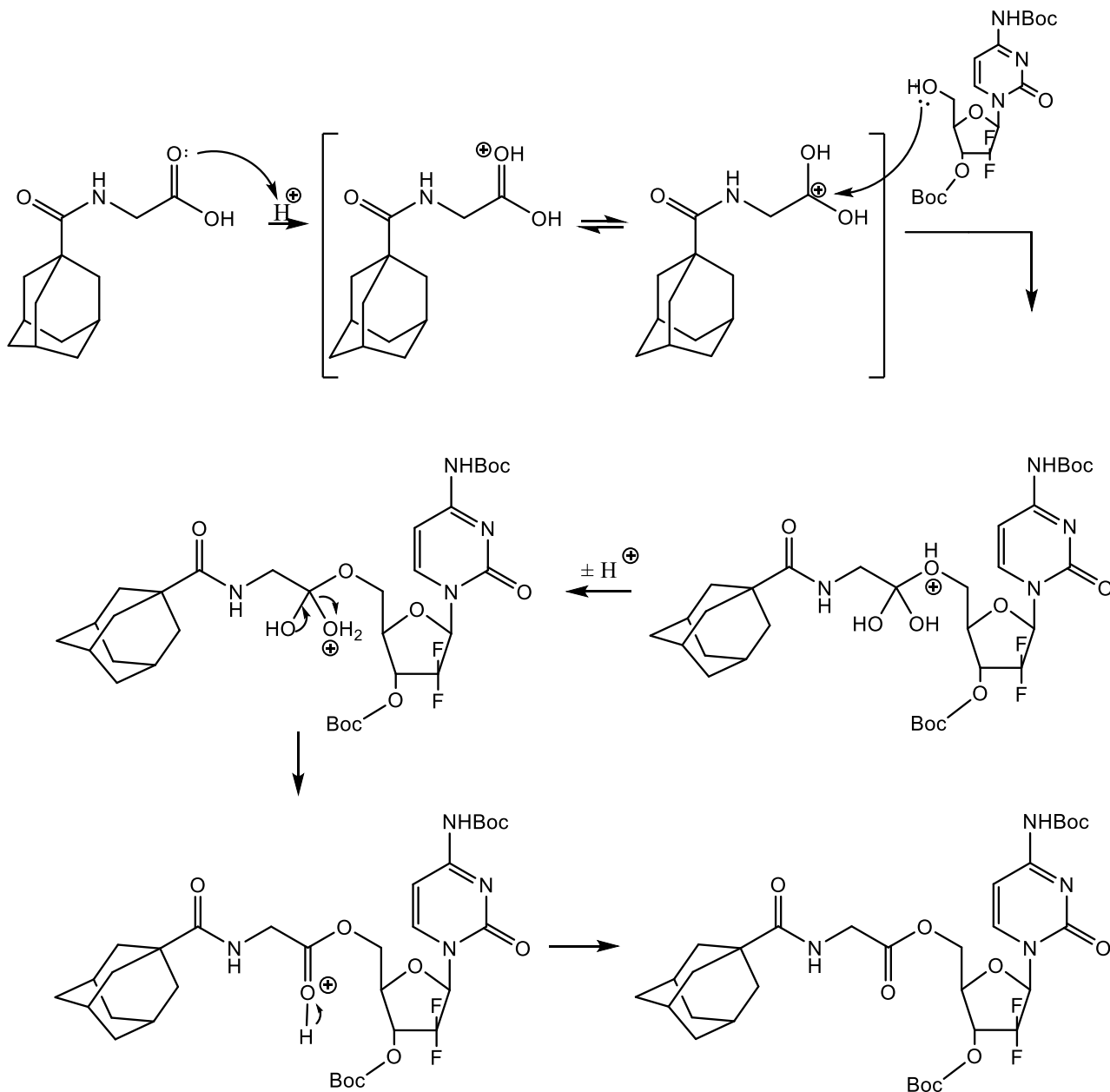


*Figure 36: Reaction mechanism for formation of (13) through esterification.*

35

### 3.3.3.5 Deprotection (5)

Boc is an acid labile protecting group and can therefore be removed by TFA, as shown in figure 37.
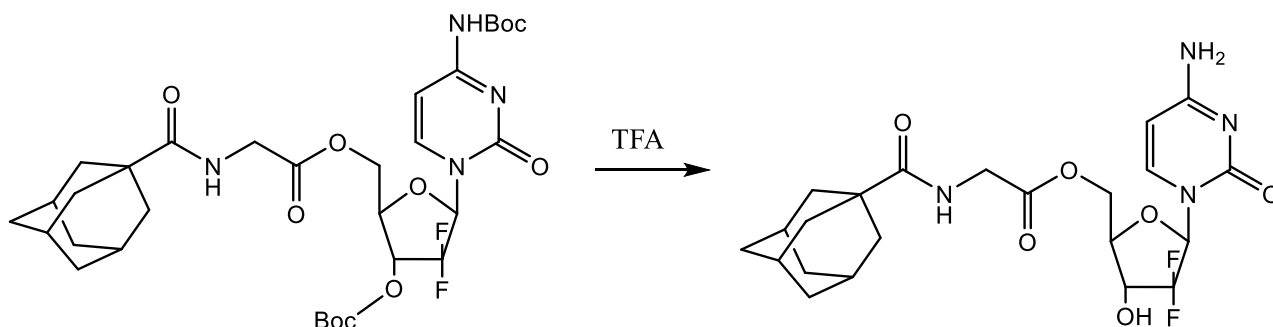


*Figure 37: Removal of Boc-protection to give (5).*

The tert-butyl carbamate becomes protonated and subsequently becomes carbamic acid through the loss of the tert-butyl cation. Decarboxylation leads to the free amine, as seen in figure 38.
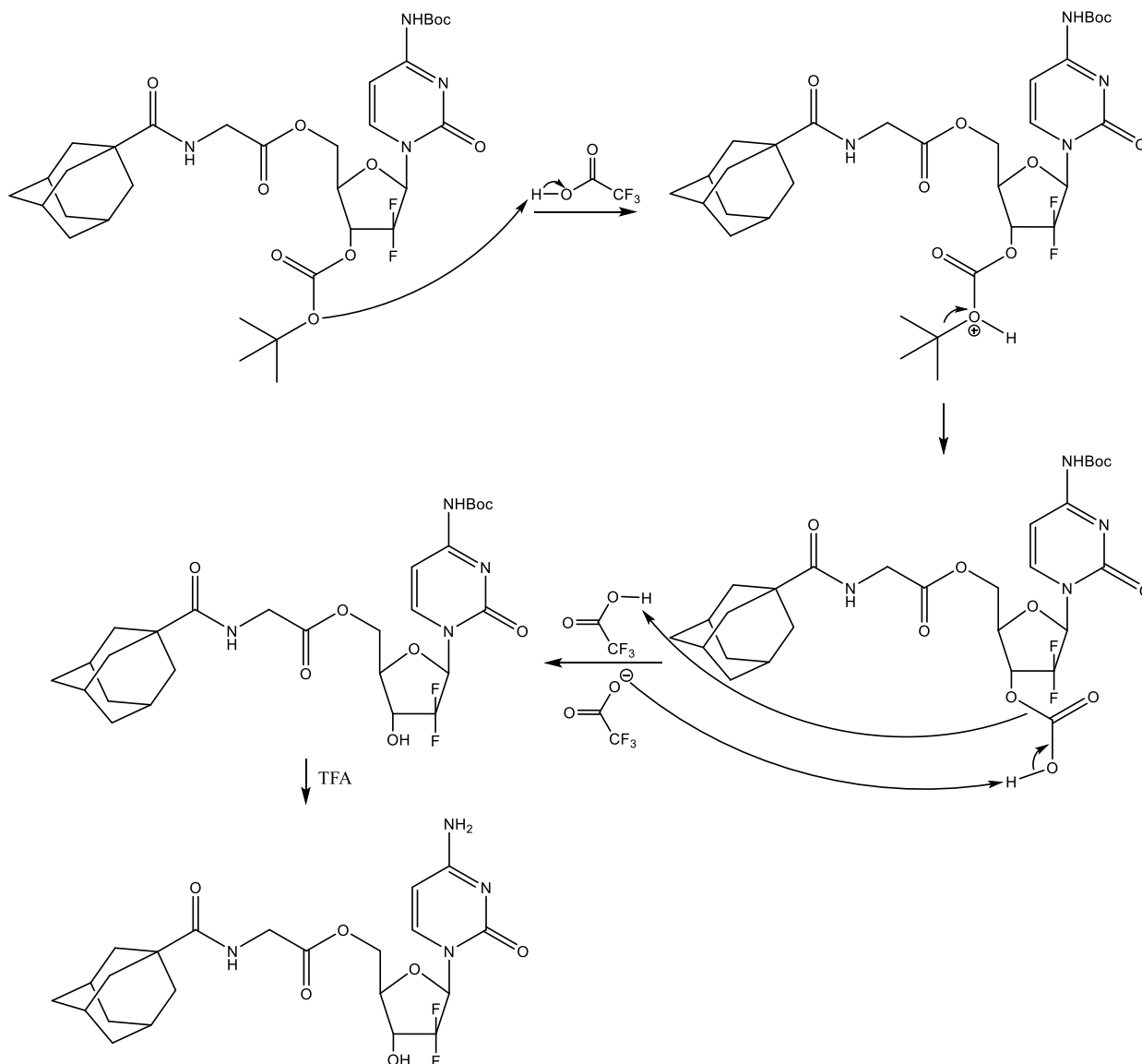


*Figure 38: Mechanism for boc-deprotection to give (5).*

## 3.4 Release of the active drugs

### 3.4.1 Release by GSH

GSH is made up of three amino acids: glutamate, cysteine and glycine, as seen in figure 39. The thiol in GSH is a reducing agent. GSH can reduce disulfide bonds by serving as an electron donor.
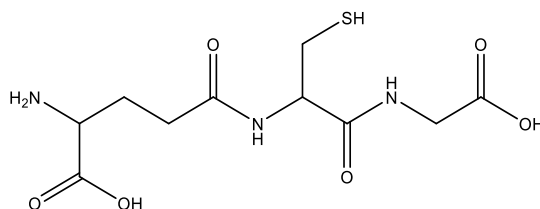


*Figure 39: Structure of GSH.*

GSH has a large gradient across membranes. The intracellular concentration range from 0.5~10.0 nM/g and extracellular concentration ~2-20 µM/g.[62] Furthermore, the concentration of GSH in tumor tissue is ~ 4 µM/g, which is about 4-fold higher concentrations of GSH than normal tissues where the concentration is ~1 µM/g.[58, 63] Two of the four synthesized prodrugs needs GSH to release the active drug. Figure 40 shows the release mechanism for (**4**) and figure 41 demonstrates the parallel mechanism for (**8**).
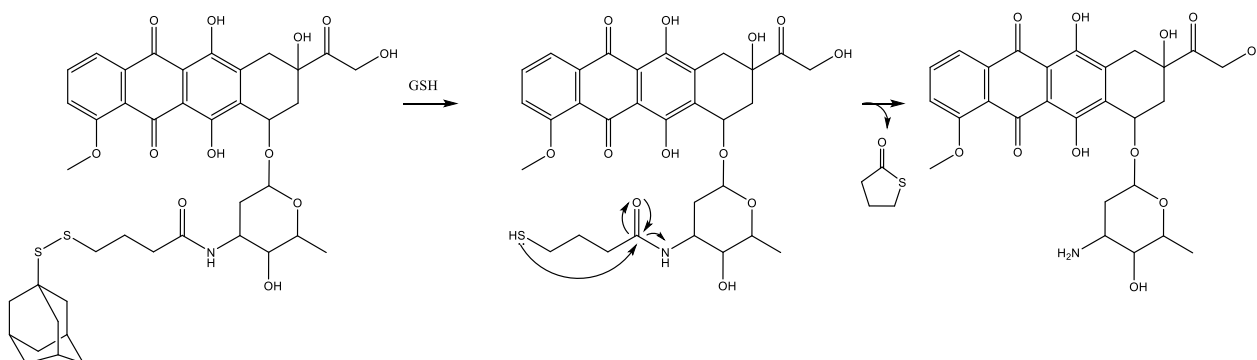


*Figure 40: Mechanism for release of Dox from prodrug (**4**).*

The low extracellular concentration of GSH makes it possible for the synthesized prodrugs to remain stable while in circulation and lead to an accumulation in the tumor tissue, through EPR. Once in the tumor tissue, the high concentration of GSH will ensure a rapid and efficient release of the active drug. [64]
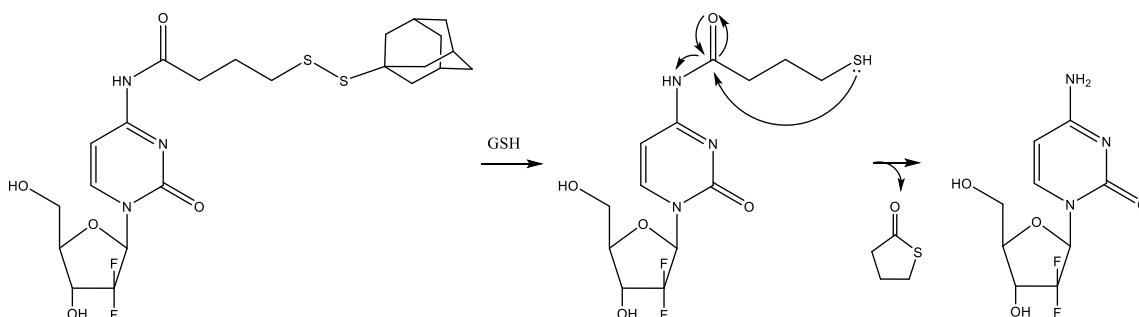


*Figure 41: Mechanism to release of Gem from prodrug (**8**)*

37

### 3.4.2 Release by hydrolysis

Imines are usually easily hydrolyzed. However, those imines that carry a nitrogen group, such as hydrazones and semicarbazones, are usually more stable.[65] The enhanced stability comes from the ability to delocalize the imine double bond, which decreases the partial positive charge on the carbon. This makes them less susceptible to nucleophilic attack. In chemistry, hydrolysis can either be acid or base catalyzed. Figure 42 shows the acid catalyzed mechanism
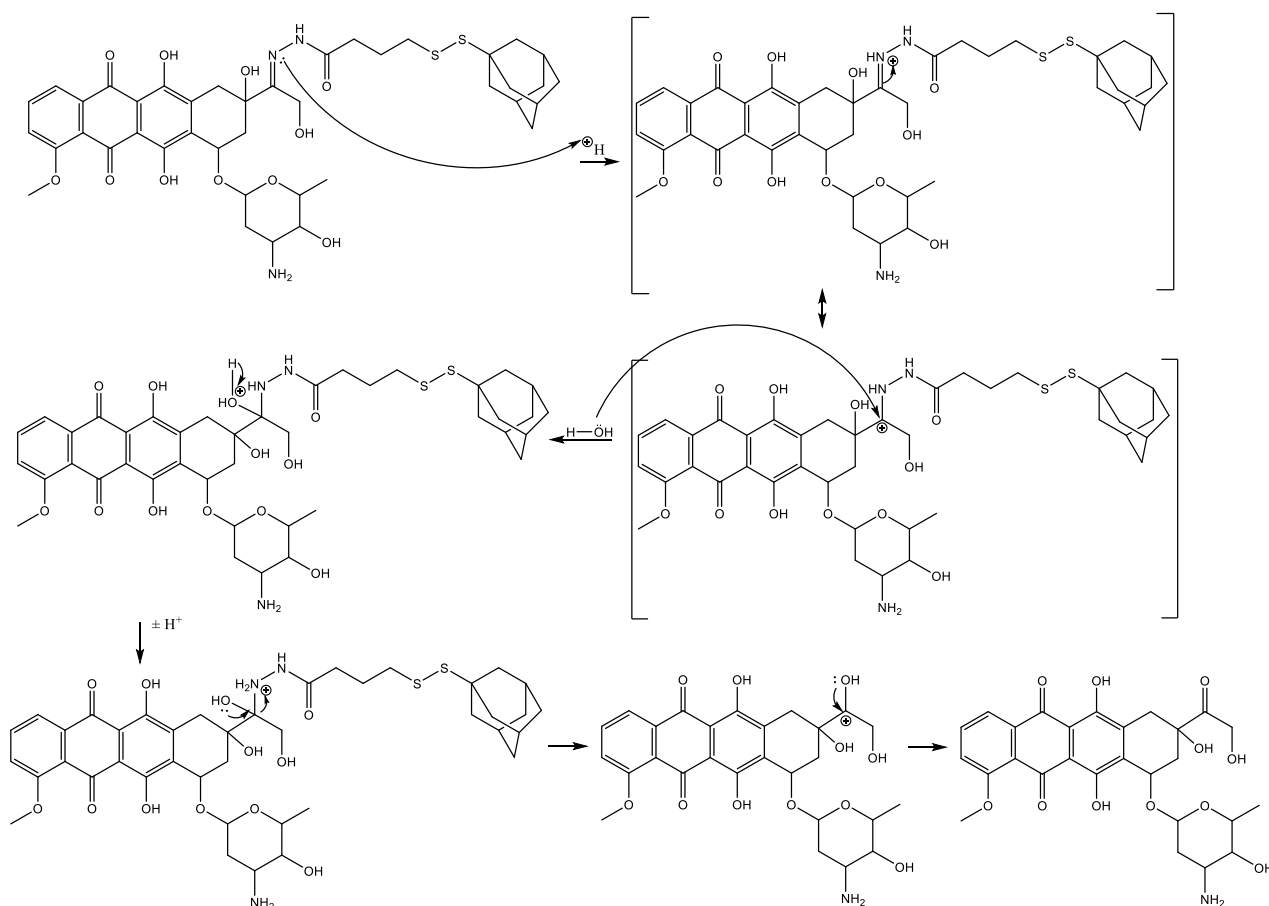
*Figure 42: Mechanism for hydrolysis of Imine bond to release Dox from prodrug (1).*

Ester bonds can be broken down in the body by esterase (hydrolase enzyme), which splits esters into acids and alcohols. The hydrolysis mechanism can either be acid or base catalyzed. The difference between the two mechanisms is the nucleophile. In the base catalyzed mechanism, shown in figure 43, $HO^-$ is the nucleophile whereas in the acid catalyzed the nucleophile is water.
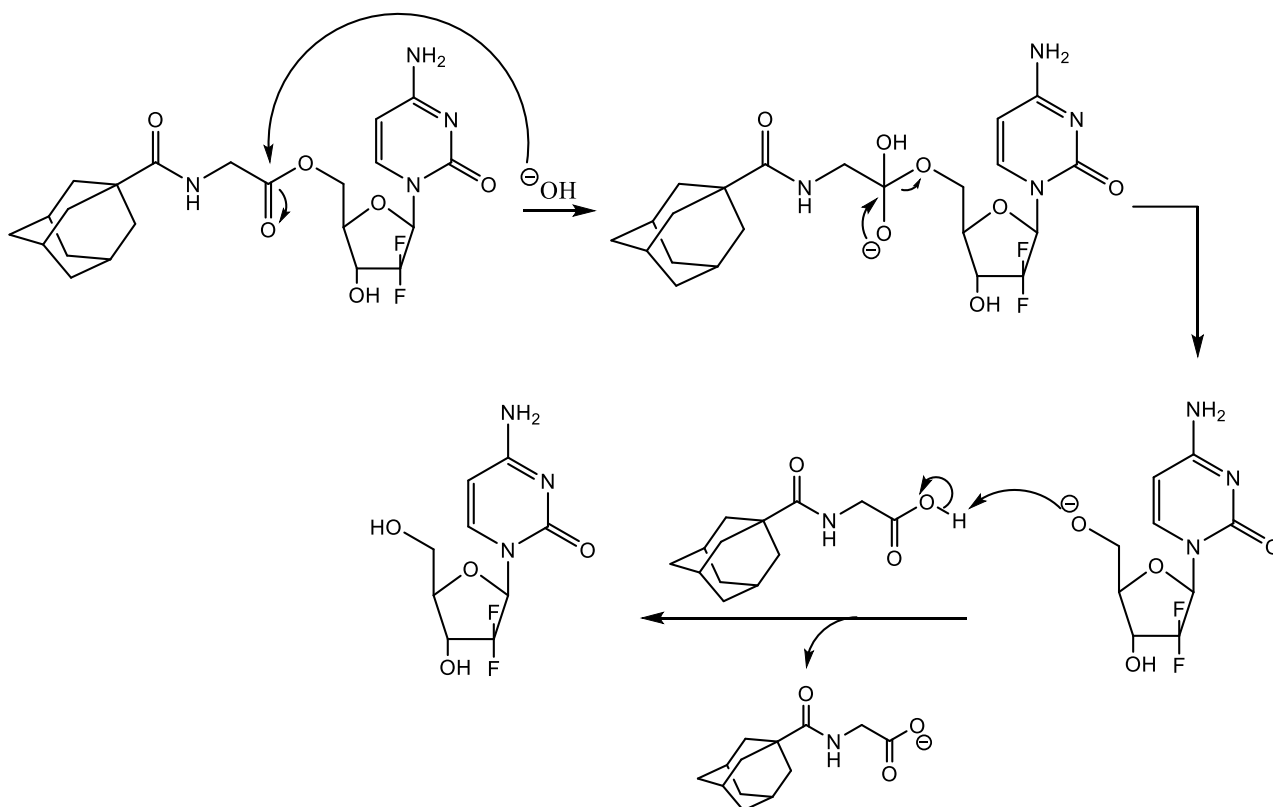
*Figure 43: Hydrolysis with basic catalyst to release Gem from prodrug (**5**).*

Figure 44 shows the acid catalyzed mechanism. The carbonyl oxygen is protonated, making the carbonyl carbon more electrophilic: this is necessary because of the low nucleophilicity of water.
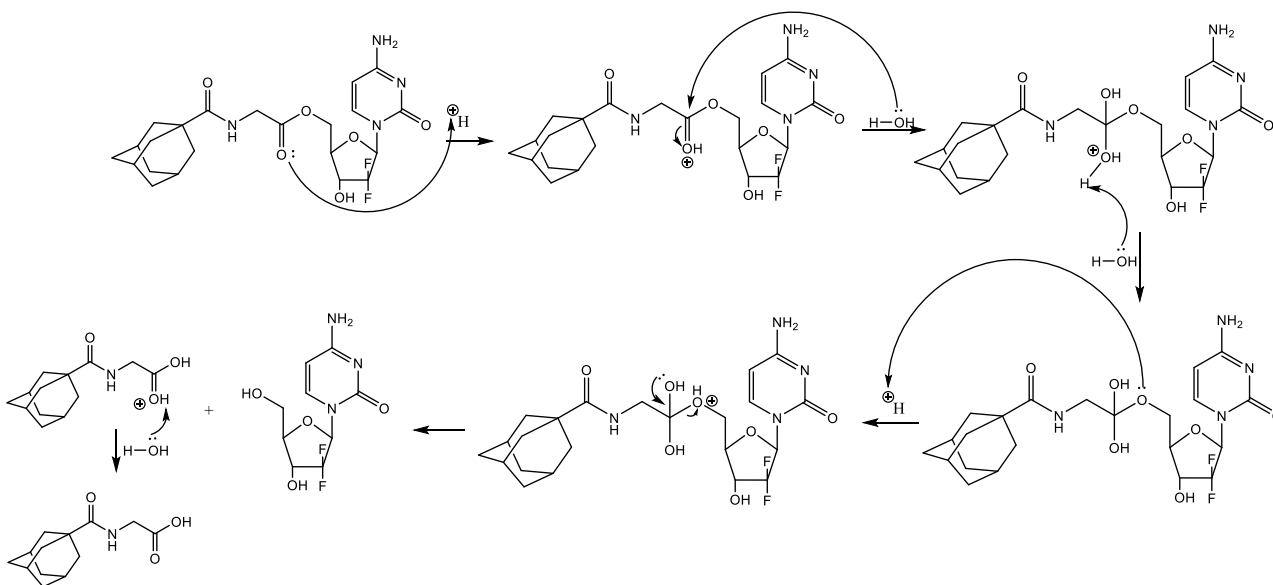


*Figure 44: Hydrolysis with acidic catalyst to release Gem from prodrug (**5**).*

# 4. Materials and methods

## 4.1 General

$^1$H-NMR spectrums were taken on a Bruker DRX600 spectrometer. Reference peaks were set for: CHCl$_3$ (7.26 ppm), DMSO (2.5 ppm), MeOH (3.31 ppm), H$_2$O (4.79 ppm) or DMF (8.03 ppm) during processing.[66] TLC were performed on ALUGRAM SIL G/UV$_{254}$ with 0.2 mm silica gel (Macherey-Nagel, Düren Germany), unless otherwise stated. Automated chromatographic column separation was performed on a Grace reveleris, Grace Davison Discovery science. Separation columns used were Grace Reveleris, Grace Davison Discovery science. Isothermal titration calorimetry measurements were carried out on a Malvern MicroCal PEAQ-ITC Automated.

### 4.1.1 Chemicals

Solvents (Sigma-Aldrich, Germany) used were of HPLC-quality, except for when performing TLC where technical solvents were considered adequate. Dry DCM and THF were bought and used as is. Reagents that were not synthesized during this thesis, were bought. 1-adamantane carboxylic acid 99%, 1-adamantanethiol, benzotriazole, DCC, di-tert-butyl dicarbonate (Boc), DMAP, EDC, hydrazine monohydrate, HOBt, Na$_2$SO$_4$ anhydrous, and thiourea were bought from Sigma-Aldrich (Steinheim, Germany). 4-mercaptobutyric acid technical grade and Gemcitabine were bought from Fluorochem (UK). Glycin was bought from Merck (Darmstadt, Germany), while Doxorubicin was bought from Molekular. For Isothermal titration calorimetry βCD, HPβCD and MβCD were from Wacker Chemie AG (Brughausen, Germany) and SBEβCD from ligand pharmaceuticals (USA). Dextran-βCD was previously synthesized[67] and kindly given by Thorbjørn T. Nielsen.

## 4.2 Synthesis of reactants

### 4.2.1 1-adamantanecarbonyl chloride (7)

*4.2.1.1 From thionyl chloride*

Adapted from literature.[68]
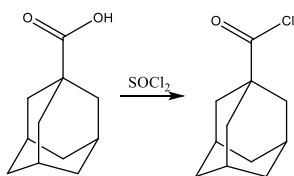
1-adamantanecarboxylic acid (6 g, 33 mmol) was dissolved in thionyl chloride (30 mL). The mixture was stirred under reflux for 4 h, and the excess thionyl chloride was evaporated under reduced pressure, to yield (**7A**) as an off-white powder (5.40 g, 81.76 %). The product was used without further purification. $^1$H NMR (CDCl$_3$): 2.14 (6H, m), 2.06 (3H, m), 1.75 (1H, m), 1.67 (4H), 1.60 (1H, m).

*4.2.1.1 From oxalyl chloride*

Adapted from literature.[69]
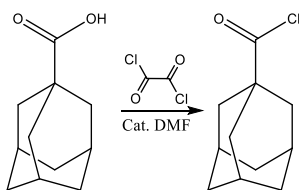
1-adamantanecarboxylic acid (3.0 g, 16 mmol) was dissolved in DCM (10 mL) and oxalyl chloride (3 mL, 19 mmol) was added slowly. A DMF solution was prepared by diluting DMF (5 dr.) in DCM (40 mL). DMF solution (3 dr.) was added and the solution was left to stir until the bubbles subsided. The solvents were evaporated under reduced pressure to yield (**7B**) as an off-white powder (2.08 g, 62.27 %). The product was used without further purification. $^1$H NMR (CDCl$_3$): 2.14 (6H, m), 2.07 (3H, m), 1.75 (1H, m), 1.68 (4H), 1.60 (1H, m).

### 4.2.2 1-chlorobenzotriazole (9)

Adapted from literature.[70]
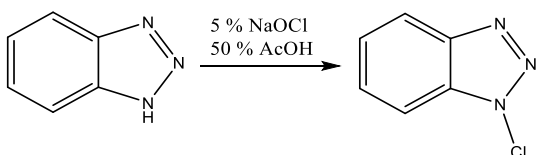
A 5% NaOCl solution (commercial bleach, 128 mL, 96 mmol) was added dropwise to a solution of benzotriazole (9.6 g, 80 mmol) in 50% AcOH (38.4 mL) with stirring. After the addition was complete, the solution was stirred for 2 h, filtered and the precipitate washed with water (0.5 L) until the washings were neutral. The solid was dried in vacuo to give (**9**) 1-chlorobenzotriazole (11.22 g, 91.15 %) $^1$H NMR (CDCl$_3$): δ 8.10 (1H, dt, *J*=8.32, 0.88 Hz) 7.62 (1H, m) 7.46 (1H, m).

## 4.3 Synthesis of Doxorubicin prodrug

### 4.3.1 3-(((3s,5s,7s)-adamantan-1-yl)disulfaneyl)butanoic acid (3)

Adapted from literature.[60]
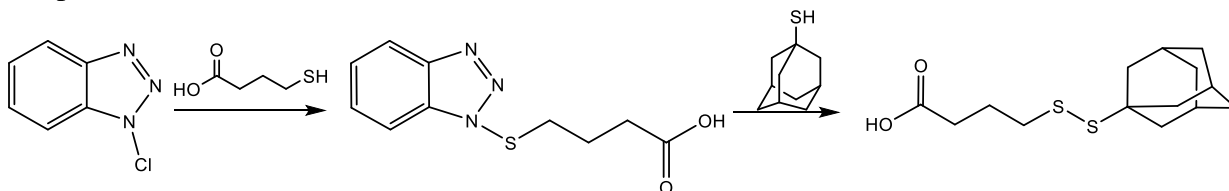


(**9**) (0.61 g, 4 mmol) and benzotriazole (0.24 g, 2 mmol) was dissolved DCM (20 mL) under argon. A solution of 4-mercaptobutyric acid (0.21 g, 2 mmol) in DCM (2 mL) was slowly added. After 10 min., a solution of thiourea (0.46 g, 6 mmol) in dry THF (5 mL) was added and the solution stirred for 10 min. 1-adamantanethiol (0.50 g, 3 mmol) in DCM (2 mL) was added slowly and the solution stirred for 18 h. The solvent was evaporated under reduced pressure and the crude material was loaded on to celite and purified column chromatography using DCM: MeOH mixture (0-25 %) to afford (**3**) (0.34 g, 59.64 %). ^{1}H NMR (CDCl$_3$) δ 2.00-2.05 (4H, p, $J$=6.16 Hz), 2.08-2.12 (7H, p, $J$=7.23 Hz), 2.44-2.49 (8H, m, $J$=6.16 Hz), 2.70-2.74 (2H, t, $J$=7.23 Hz), 2.90-2.93 (2H, t, $J$=7.23 Hz).

### 4.3.2 4-(((3s,5s,7s)-adamantan-1-yl)disulfaneyl)-N-(3-hydroxy-2-methyl-6-(3,5,12 trihydroxy-3-(2-hydroxyacetyl)-10-methoxy-6,11-dioxo-1,2,3,4,6,11-hexalhydrotetracen-1-yl)tetrahydro-2*H*-pyran-4-yl)butanamide (4)

Adapted from literature.[71]
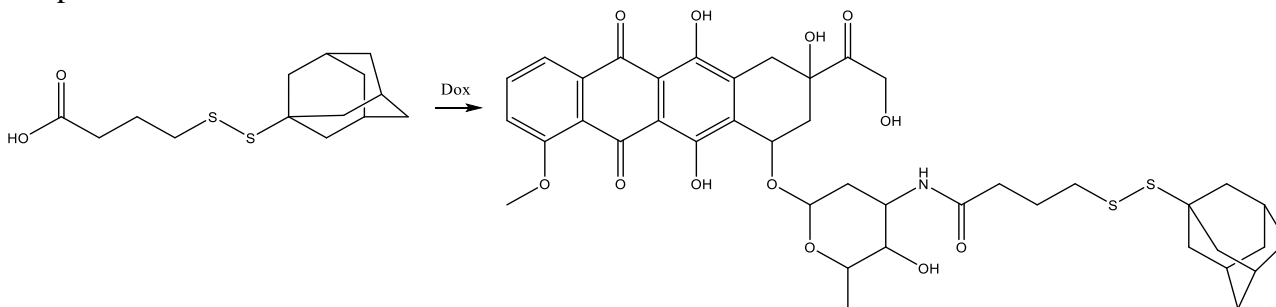


Dox (50 mg, 0.09 mmol) was suspended in dry DCM (10 mL). (**3**) (25 mg, 0.09 mmol) and HBTU (115 mg, 0.30 mmol) were dissolved in dry DCM (20 mL) and added slowly to the reaction mixture. DIPEA (100 mg, 0.77mmol) was added to the reaction mixture. The mixture was stirred for 3 h under argon. Water (50 mL) was added and the crude product was extracted with DCM (3 x 50 mL). The solvent was evaporated under reduced pressure and the crude product was purified by chromatography using DCM: MeOH (0-50 %) to afford (**4**) (10.5 mg, 14.87 %). ^{1}H NMR (CD$_3$OD): δ 8.01 (1H, d, $J$=7.46 Hz), 7.86 (1H, t, $J$=9.09 Hz), 7.60 (1H, d, $J$=8.37 Hz), 5.44 (1H, m), 5.22 (1H, m), 4.06 (3H, s), 3.64 (4H, m), 3.16 (1H, m), 3.02 (2H, d, $J$=4.45 Hz), 2.99 (3H, s), 2.48 (2H, m), 2.29 (1H, m), 1.73 (6H, m), 1.31 (8H, m), 1.18 (4H, m), 0.90 (2H, m).

### 4.3.3 3-(((3s,5s,7s)-adamantan-1-yl)disulfaneyl)propanehydrazine (2)

Adapted from literature.[72]
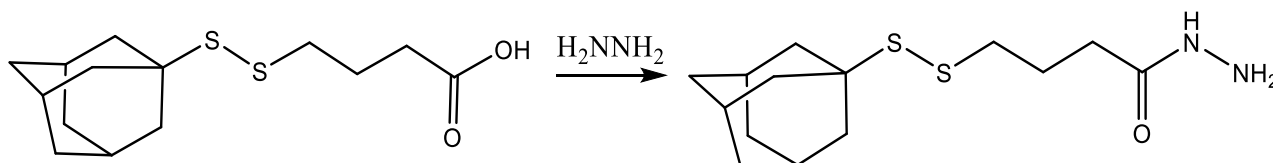


(**3**) (26 mg, 0.09 mmol) was dissolved in DMF (10 mL) at rt. HOBt (14 mg, 0.11 mmol) was added in one portion followed by EDC (20 mg 0.11 mmol). The mixture was stirred at rt, and the reaction progress was monitored by TLC until all of the acid was converted to the activated ester/amide mixture. The resulting mixture was then slowly added to a solution of hydrazine (9 mg, 0.18 mmol) in DMF (2 mL) while the temperature was maintained at rt. The reaction was complete upon the completion of addition. Water (40 mL) was added. The aqueous DMF mixture was extracted with EtOAc followed by a carbonate wash of the organic layer to remove HOBt. Removal of the solvents under reduced pressure yielded (**2**) (31.0 mg, < 100 %)[i]. $^1$H NMR (CDCl$_3$): δ 2.69 (2H, t, $J$=7.88 Hz), 2.28 (2H t, $J$=7.88 Hz), 2.06 (9H, m) 1.67 (6H, m).

### 4.3.4 4-(((1s,3R)-adamantan-1-yl)disulfaneyl)-N-((E(-1((2S,4S)-4-(((2R,4S,5R,6S)-1-amino-5-hydroxy-6-methyltetrahydro-2*H*-pyran-2-yl)oxy)-2,5,12-trihydroxy-7-methyoxy-6,11-dioxo-1,2,3,4,6,11-hexalhydrotetracen-2-yl)-2-hydroxyethylidene)butanehydrazide (1)

Adapted from literature.[72]
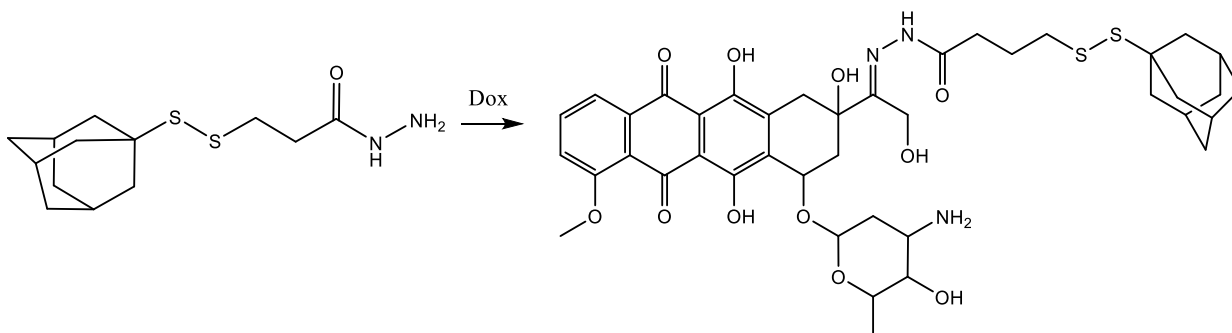


(**2**) (28 mg, 0.09 mmol) and Dox-HCl (48 mg, 0.083 mmol) were dissolved in MeOH (5 mL), covered in foil and stirred at rt. for 12 days. The reaction was followed by a reversed-phase TLC. After this period, the solvent was evaporated and the residue was chromatographed on a reverse phase column (MeOH: H$_2$O = 3:1, containing 3 % w/v ammonium acetate) to give (**1**) (10.6 mg, 15.52 %). $^1$H NMR (CD$_3$OD): δ 8.04 (2H, d, $J$=8.64 Hz), 7.87 (2H, t, $J$=8.13 Hz), 7.60 (2H, d, $J$=8.64 Hz), 5.49 (1H, m), 4.62 (2H, dd, $J$=23.39, 14.12Hz), 4.19 (1H, d, $J$=7.06 Hz), 4.04 (3H, s) 3.66 (1H, m) 3.62 (1H, m), 3.53 (1H, m) 3.37 (1H, m), 2.50 (2H, t, $J$=6.80 Hz), 2.45 (2h, t, $J$=7.38 Hz), 2.29 (2H, m) 2.02 (4H, m), 1.80 (6H, m) 1.76-1.64 (5H, m), 1.59 (2H, m), 1.31 (3H, d, $J$=6.5 Hz).

---

[i] High yield due to residue of DMF.

## 4.4 Synthesis of Gemcitabine prodrug

### 4.4.1 N-Adamantanoylglycine (6)

Adapted from literature.[73]
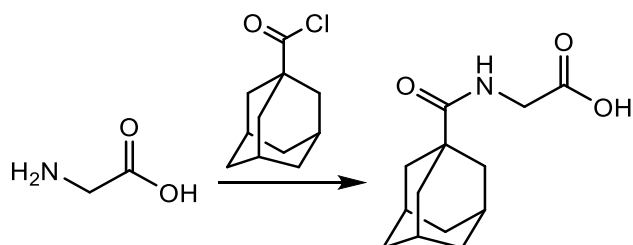


Glycine (0.15 g, 2 mmol) was partly dissolved in DMF (10 mL) and 4M aq. NaOH were successively added to obtain a pH~11. (**7**) (0.2 g, 1 mmol) was dissolved in DMF (5 mL) and added in five portions over 45 min while maintaining pH~11. Stirring was continued for 2h at rt. The solvent was concentrated under reduced pressure. The residue was extracted with EtOAc (5 x 20 mL) and evaporated under reduced pressure to yield (**6**) as a white powder (0.19 g, 79.37 %). ^{1}H NMR (DMF-d7): δ 8.79 (m), 3.49 (m), 2.08 (m), 1,28 (m), 1.09 (m), 0.89 (m).

### 4.4.2 3′-O-(tert-Butoxycarbonyl) gemcitabine (10)

Adapted from literature.[74]
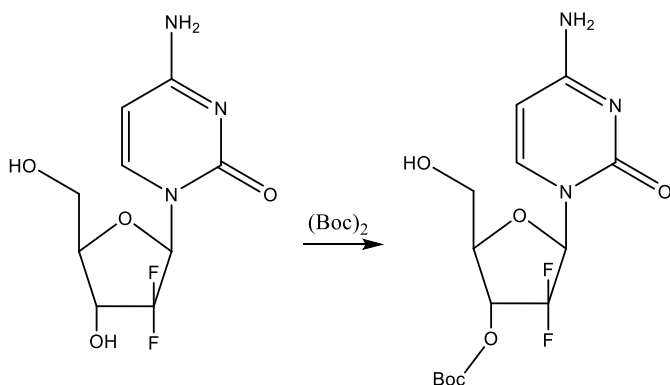


To a stirred mixture of Gemcitabine (0.50 g, 1.66 mmol) and $K_2CO_3$ (1.15 g, 8.33 mmol) in dioxane (20 mL) and water (5 mL) was added (Boc)$_2$O (0.36 g, 1.65 mmol), and the resulting mixture stirred at rt. for 48 h. After water (5 mL) was added, the mixture was extracted with of EtOAc (2 x 30 mL). The organic extracts were washed with water (5 mL) and brine (5 mL), dried over $Na_2SO_4$, and concentrated to dryness under reduced pressure to give (**10**) (0.46 g, 73.10 %). ^{1}H NMR ($(CD_3)_2SO_2$): δ 7.64 (1H, d, J=7.43 Hz), 7.43 (1H, d, J=13.86 Hz), 6.22 (1H, t, J=9.41 Hz), 5.81 (1H, d, J=7.43 Hz), 4.15 (1H, m) 3.74 (1H, m) 3.65 (1H, m), 1.45 (9H, s).

### 4.4.3 (5-(4-(4-(((1S,3s)-adamantan-1-yl)disulfaneyl)butanamido)-2-oxopyrimidin-1(2*H*)-yl)-4,4-difluoro-2-(hydroxymethyl)tetrahydrofuran-3-yl tert butylcarbonate (12)

Adapted from literature.[75]
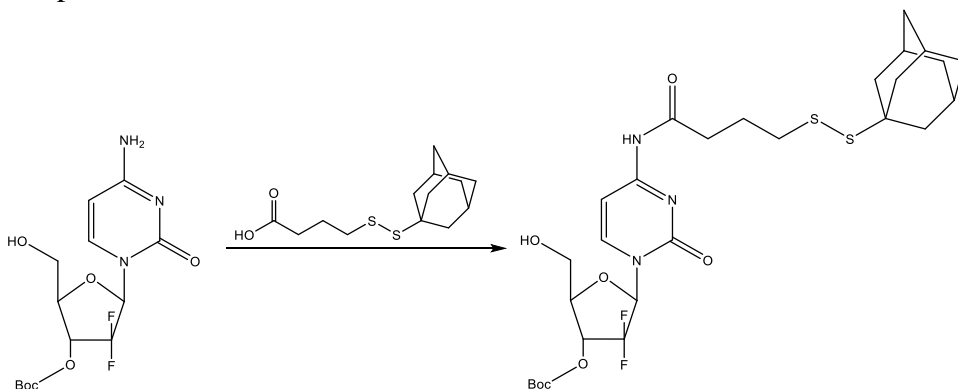


A mixture of (**3**) (40 mg, 0.144 mmol), EDC (50 mg, 0.267 mmol), and HOBt (36 mg, 0.267 mmol) in dry DCM (10 mL) was stirred for 0.5 h. A solution of (**10**) (50 mg, 0.132 mmol) in DCM (5 mL) was added, and then the resulting mixture was stirred at rt. overnight. The organic layer was washed with brine (3 x 10 mL), dried over anhydrous $Na_2SO_4$, and concentrated under reduced pressure. The residue was purified by the column chromatography with DCM: MeOH (0-10 %) to give the product (**12**) (27.2 mg, 18.52 % yield). $^1$H NMR ($CDCl_3$): δ 7.58 (1H, d, *J*=9.20 Hz), 6.27 (1H, m), 5.89 (1H, d, *J*=8.26 Hz), 4.14 (1H, m), 4.08 (1H d, *J*=12.56) 3.84 (2H, dd, *J*=9.11, 2.83 Hz), 2.11 (2H, m), 1.92 (2H, m), 1.70 (3H, m), 1.53 (4H, m), 1.52 (14H, m), 1.28 (3H, m), 0.87 (2H, m).

### 4.4.4 4-(((1S,3s)-adamantan-1-yl)disulfaneyl)-N-(1-(2R,4R,5R)-3,3-difluoro-4-hydroxy-5-(hydroxymethyl)tetrahydrofuran-2-yl)-2oxo-1,2-dihydropyrimidin-4-yl)butanamide (8)

Adapted from literature.[71]
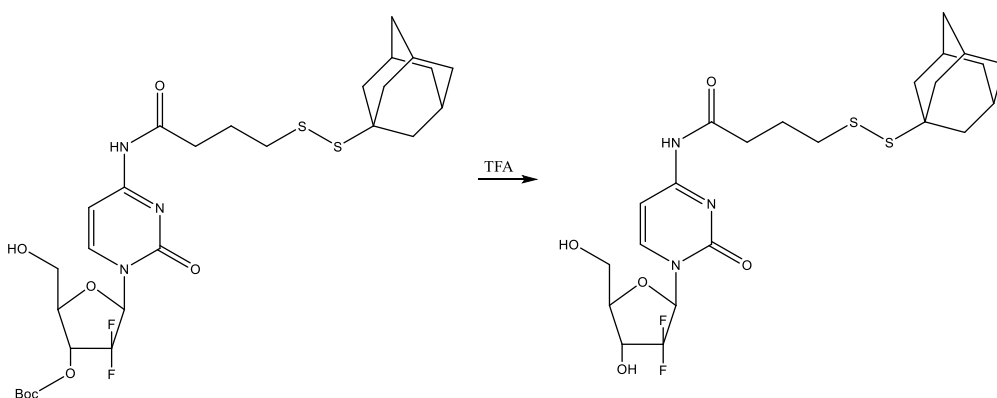


(**12**) (27 mg, 0.04 mmol) was treated with TFA solution (4 mL – 3:1 TFA: DCM). After 24 h the solvent was evaporated under reduced pressure to yield (**13**) as a white solid (22.8 mg, 99.60 %). $^1$H NMR ($CD_3OD$): δ 8.21 (1H, d, *J*=7.82 Hz), 6.20 (1H, dd, *J*=4.94, 4.61 Hz), 6.11 (1H, d, *J*=7.82 Hz), 4.31 (1H, m), 3.98 (1H, m), 3.82 (2H, dd, *J*=9.62, 3.81 Hz), 2.37 (2H, t, *J*=7.31 Hz), 2.29 (2H, t, *J*=7.27 Hz), 1.31 (3H, m), 1.21 (2H, m), 1.14 (2H, t, *J*=7.34 Hz), 0.91 (2H, t, *J*=7.25 Hz).

### 4.4.5 4-N-3′-O-Bis(tert-Butoxycarbonyl) Gemcitabine (11)

#### 4.4.5.1 From Gemcitabine

Adapted from literature.[74]
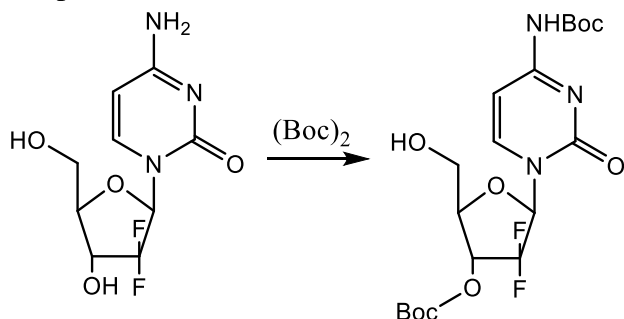


To a stirred mixture of Gemcitabine (0.24 g, 0.8 mmol) and $Na_2CO_3$ (0.55 g, 4.0 mmol) in dioxane (10 mL) and water (2 mL) was added (Boc)$_2$O (0.35 g, 1.6 mmol), and the resulting mixture was stirred at rt for 48 h. Water (2 mL) was added and the mixture was extracted with EtOAc (2 x 30 mL). The organic extracts were washed with water (5 mL) and brine (5 mL), dried over $Na_2SO_4$, and concentrated to dryness under reduced pressure to give (11) (0.14 g, 37.95 %).^{1}H NMR (($CD_3$)$_2$$SO_2$): δ 8.10 (1H, d, J=7.58 Hz), 7.09 (1H, d, J=7.51 Hz), 6.27 (1H, t, J=9.33 Hz), 5.32 (1H, d, J=4.96 Hz), 4.23 (1H, m) 3.77 (1H, m) 3.68 (1H, m), 1.47 (9H, s) 1.46 (9H, s).

#### 4.4.5.2 From (10)

Adapted from literature.[74]



To a stirred solution of (10) (73 mg, 0.2 mmol) in anhydrous dioxane (8 mL) was added (Boc)$_2$O (0.436 g, 2 mmol). The reaction mixture was stirred at rt. for 24 h. $Na_2CO_3$ (5 eq.) was added and the mixture stirred for an additional 24 h. Water (2 mL) was added and the mixture was extracted with EtOAc (2 x 30 mL). The organic extracts were washed with water (5 mL) and brine (5 mL) and dried over $Na_2SO_4$, and concentrated to dryness under reduced pressure to give (11) (70.2 mg, 73.12 %). ^{1}H NMR (($CD_3$)$_2$$SO_2$): δ 8.09 (1H, d, J=6.97 Hz), 7.08 (1H, d, J=8.22 Hz), 6.27 (1H, t, J=8.82 Hz), 5.31 (1H, t, J=6.30 Hz), 4.23 (1H, m) 3.77 (1H, m) 3.67 (1H, m), 1.46 (9H, s) 1.45 (9H, s).
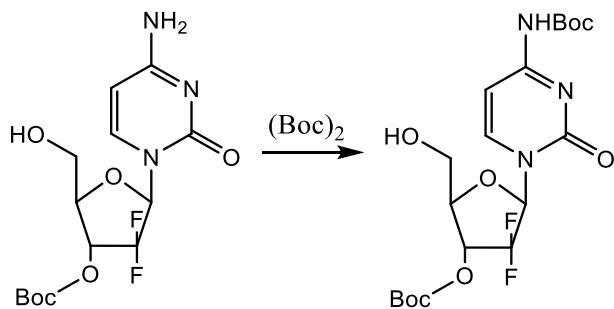
### 4.4.6 ((2R,3R,5R)-5-(4-((*tert*-butoxycarbonyl)amino)-2-oxopyrimidin-1(2H)-yl)-3- ((*tert*-butoxycarbonyl)oxy)-4,4-difluoro-5-methyltetrahydrofuran-2-yl)methyl ((3R,5R,7R)-adamentane-1-carbonyl)glycinate (13)

Adapted from literature.[71]
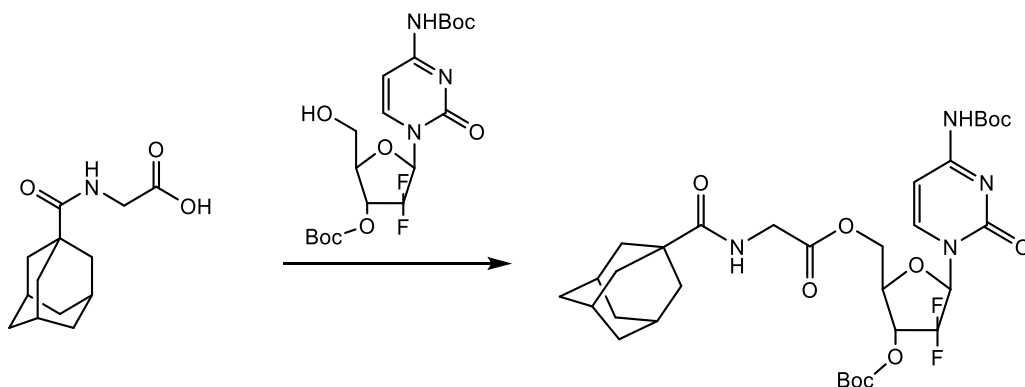


(**6**) (0.23 g, 1.0 mmol), DCC (0.20 g, 1.0 mmol), and DMAP (12.2 mg, 0.10 mmol) were allowed to react with (**11**) (0.447 g, 1.0 mmol) in DMF (10 mL). The reaction mixture was stirred at rt. for 24 h and monitored by TLC. After 24 h, the solvent was evaporated under reduced pressure at 50-55 °C. The residue was dissolved in ethyl acetate (30 mL) and washed with water (2 x 20 mL), saturated $NaHCO_3$ (2 x 20 mL), and brine (1 x 20 mL). The organic layer was dried over $NaSO_4$ and concentrated in vacuo to yield (**13**) as an oil (21.3 mg, 24.21 %). ^{1}H NMR ($CDCl_3$): δ 7.92 (1H, d, *J*=7.51 Hz), 7.58 (1H, m), 6.36 (1H, t, *J*=7.76 Hz) 4.18 (2H, m), 4.05 (2H, d, *J*=12.22 Hz), 3.87 (2H, d, *J*=12.22 Hz), 1.93 (5H, m), 1.71 (4H, tt, *J*=13.86, 3.75 Hz), 1.51 (18H, m) 1.32 (4H, m), 1.11 (2H, m).

### 4.4.7 ((2R,3R,5R)-5-(4-amino-2-oxopyrimidin-1(2H)-yl)-4,4,-difluoro-3-3hydroxy-5-methyltetrahydrofuran-2-carbonyl)glycinate (5)

Adapted from literature.[71]
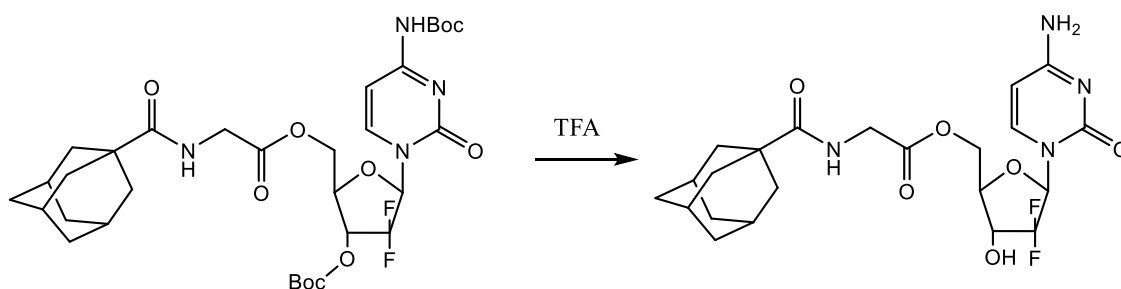


(**13**) was treated with TFA solution (4 mL – 3:1 TFA: DCM). After 24 h the solvent was evaporated under reduced pressure to yield (**5**) as a white solid (15.02 mg, 99.01 %). ^{1}H NMR ($CD_3OD$): δ 8.12 (1H, d, *J*=8.13 Hz), 6.21 (1H, m), 6.06 (1H, d, *J*=8.12 Hz), 4.30 (1H, m), 3.96 (2H, m), 3.81 (2H, dd, *J*=9.56, 3.20 Hz), 3.47 (1H, m), 1.87 (4H, dd, *J*=9.91, 3.30 Hz), 1.73 (1H, dt, *J*=13.89, 4.02 Hz) 1.37 (3H, m), 1.21 (2H, m), 1.14 (2H, m), 0.92 (2H, t, *J*=7.52 Hz).

# 5. Results and discussion

This section covers the experimental results and observations. It will be demonstrated which challenges arose and how they were resolved.

## 5.1 Synthesis of reagents

### 5.1.1 1-adamantanecarbonyl chloride (7)

1-adamantanecarbonyl chloride is commercially available, but it is just as easy to synthesize. This can be done in different ways. The first method tried was refluxing of 1-adamantanecarboxylic acid in thionyl chloride. This reaction afforded (**7A**), $^1$H NMR shown in figure 45, in ~ 80 % yield.
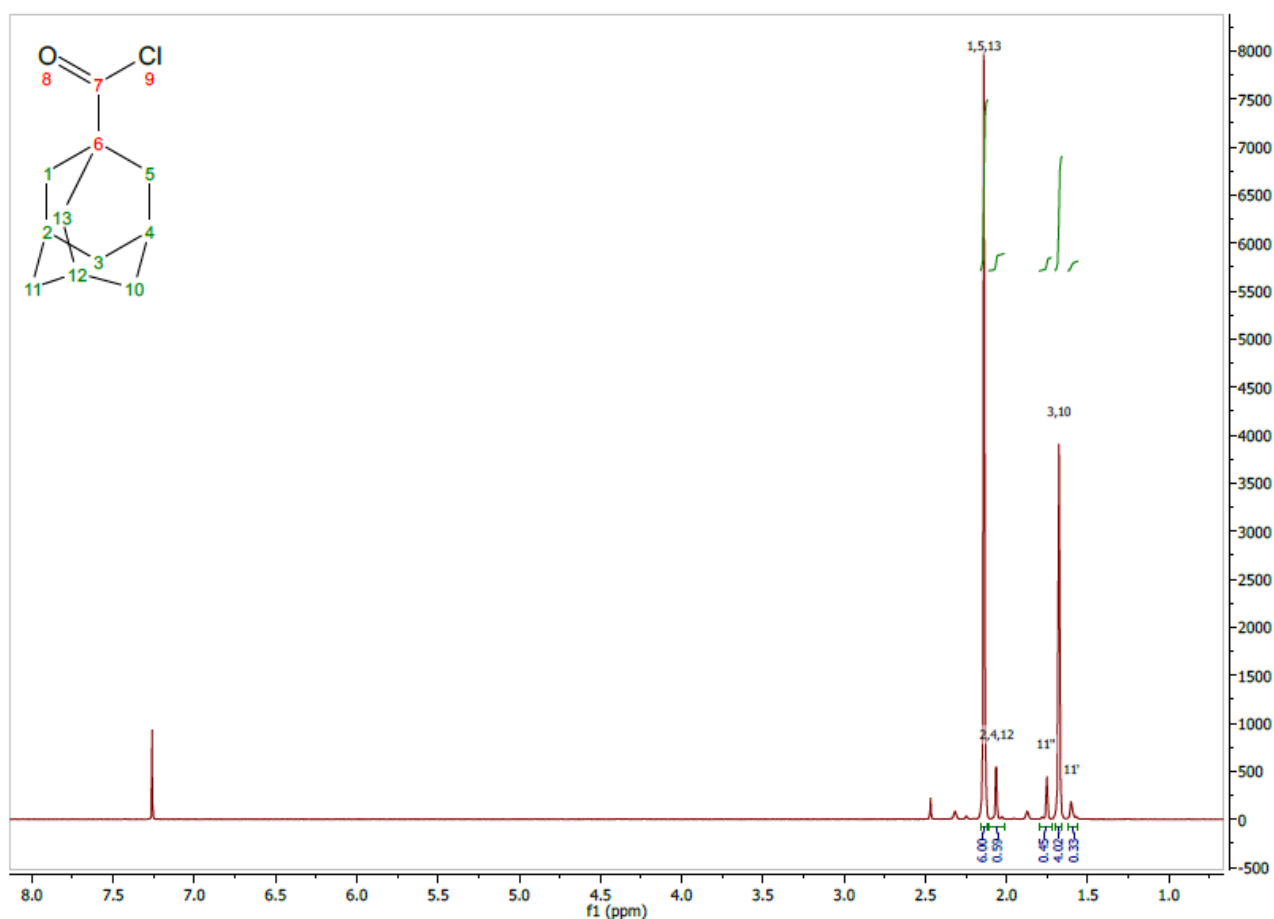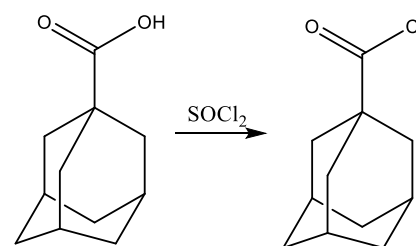




Figure 45: $^1$H NMR of (**7A**) synthesized from thionyl chloride.

Due to challenges in a later reaction, another method of synthesis (**7**) was tried. Thionyl chloride was switched for oxalyl chloride. 1-adamantane carboxylic acid was dissolved in DCM and 1.1 eq. oxalyl chloride was added to the mixture, followed by a catalytic amount of DMF. The addition of DMF caused the reaction to form bubbles (CO, $CO_2$ and HCl). This reaction yielded (**7B**), $^1$H NMR shown in figure 46, in ~ 60 %. Comparing the two reactions, it is clear that the yield is better when using thionyl chloride. However, the yield of **7B** could probably be improved by using more than 1.1 eq. oxalyl chloride. It should be noted that oxalyl chloride is more expensive than thionyl chloride which makes this synthesis less favorable in larger scale reactions.[76] However, it is worth noting that oxalyl chloride overall has a better success rate than thionyl chloride.
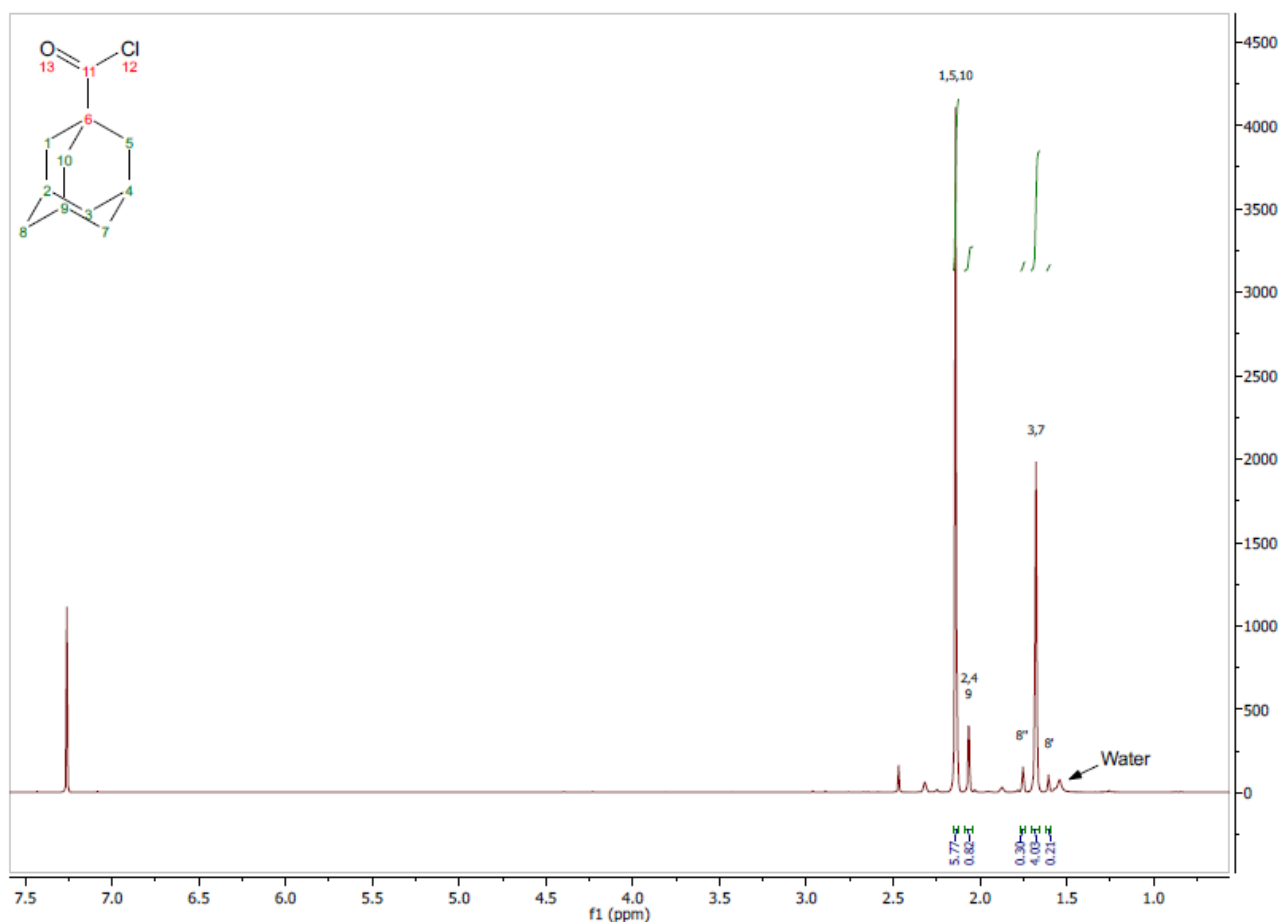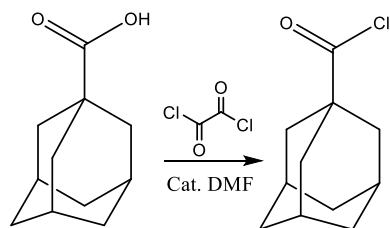


*Figure 46: $^1$H NMR of (**7B**) synthesized from oxalyl chloride.*

### 5.1.2 1-chlorobenzotriazole (9)

The chlorinated version of benzotriazole is fairly expensive compared to the unchlorinated. The synthesis was quite easy and straight forward.
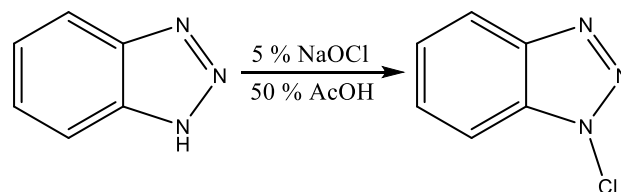


Benzotriazole was dissolved in AcOH and upon adding the hypochlorite solution, precipitation started. It yielded ~ 90 % and no further purification was done. $^1$H NMR can be seen in figure 47.

49
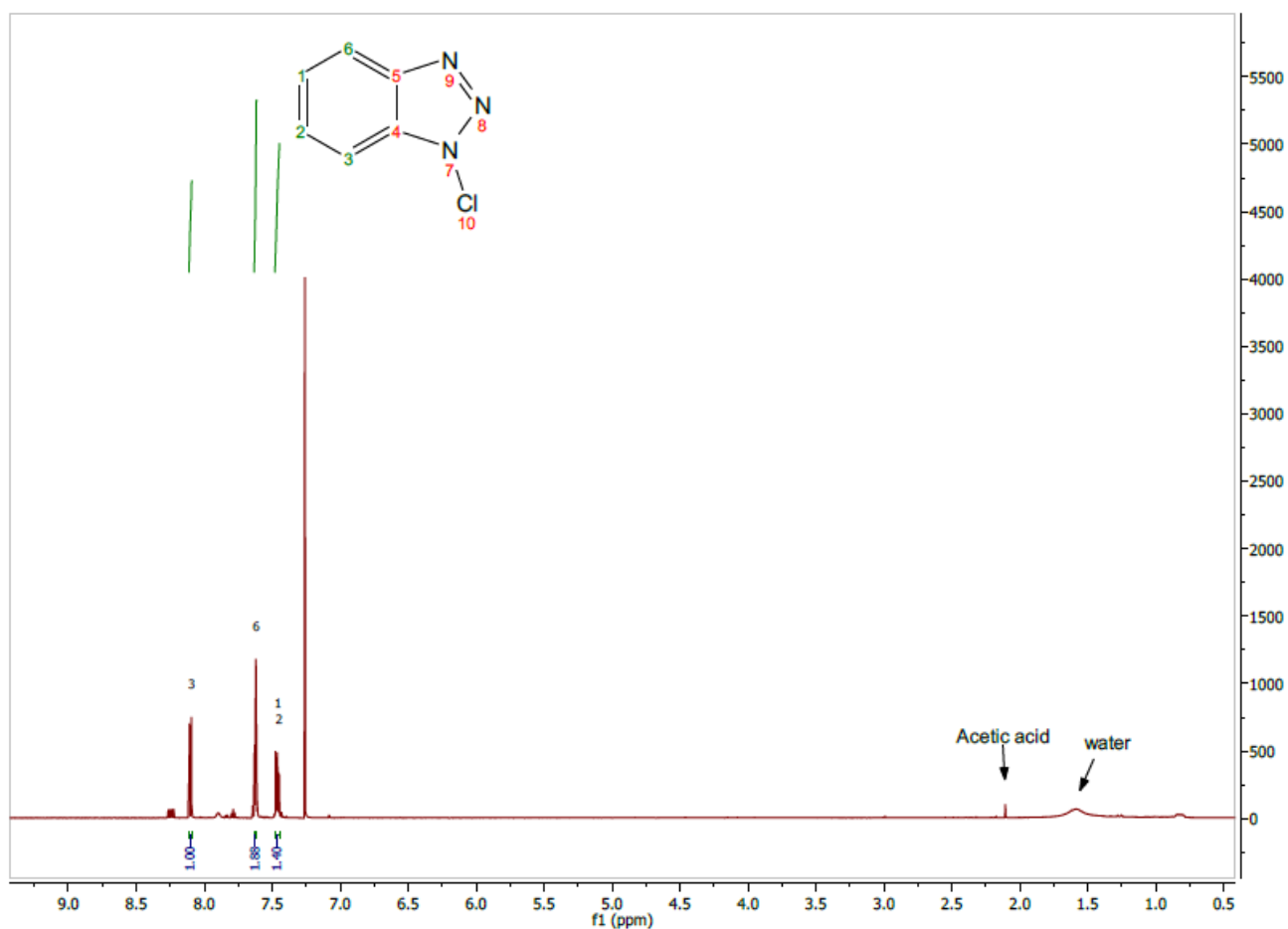
*Figure 47: ¹H NMR of (**9**).*

## 5.2 Synthesis of Dox prodrugs

### 5.2.1 Disulfide bond formation (3)

This reaction has been carried out twice, both attempts with 0.25 g 4-mercaptobutanoic acid. The first attempt was carried out under inert condition at -78 °C while adding in reactants. The temperature was allowed to rise to rt. overnight. The reaction was followed by TLC. It gave around 0.6 g crude product. For the second attempt, the reaction was carried under inert condition at rt. This attempt gave around 1.5 g crude product.
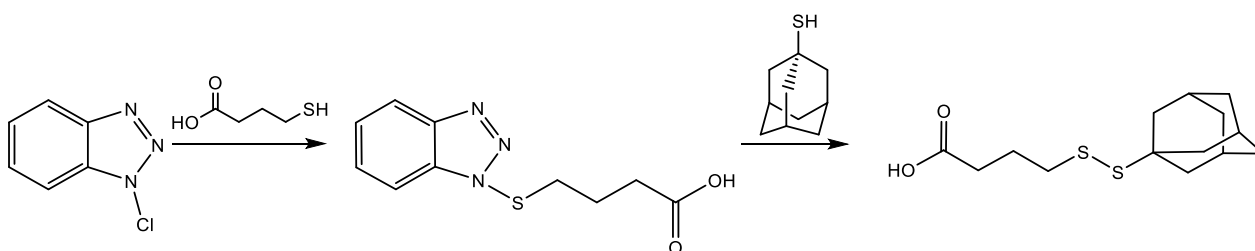


The crude product was only dissolvable in MeOH. Therefore, it was loaded on to celite and purified by column chromatography using a DCM: MeOH gradient. TLC was performed an all fractions (stained using KMnO₄). The following fractions were put together and evaporated.

| Fraction | Weight | Product |
|---|---|---|
| *First attempt* | | |
| 5-7 | 31.5 mg | 4-((1*H*-benzotriazol-1-yl)thio)butanoic acid & 1-((adamantane-1-yl)thiol)-1*H*-benzotriazole |
| 8-17 | 114.4 mg | Benzotriazole or 1-chlorobenzotriazole |
| 21-23 | 13.0 mg | Benzotriazole or 1-chlorobenzotriazole |
| 27-35 | 59.4 mg | 1-((adamantane-1-yl)thiol)-1*H*-benzotriazole |
| 45-49 | 10.7 mg | 4-((adamantan-1-yl)disulfaneyl)butanoic acid |
| *Second attempt* | | |
| 2-10 | 143.3 mg | 4-((adamantan-1-yl)disulfaneyl)butanoic acid |
| 15-23 | 170.4 mg | 4-((adamantan-1-yl)disulfaneyl)butanoic acid |
| 29-36 | 22.1 mg | 4-((adamantan-1-yl)disulfaneyl)butanoic acid |
| 40-56 | 580.8 mg | 1-((adamantane-1-yl)thiol)-1*H*-benzotriazole |
| 60-91 | 327.5 mg | Adamantanethiole |

*Table 1: Fractions collected.*

$^1$H NMRs were taken and analysed. The first attempt yielded ~1.5 % and the second attempt ~ 56 % (**3**). $^1$H NMR can be seen in figure 48.
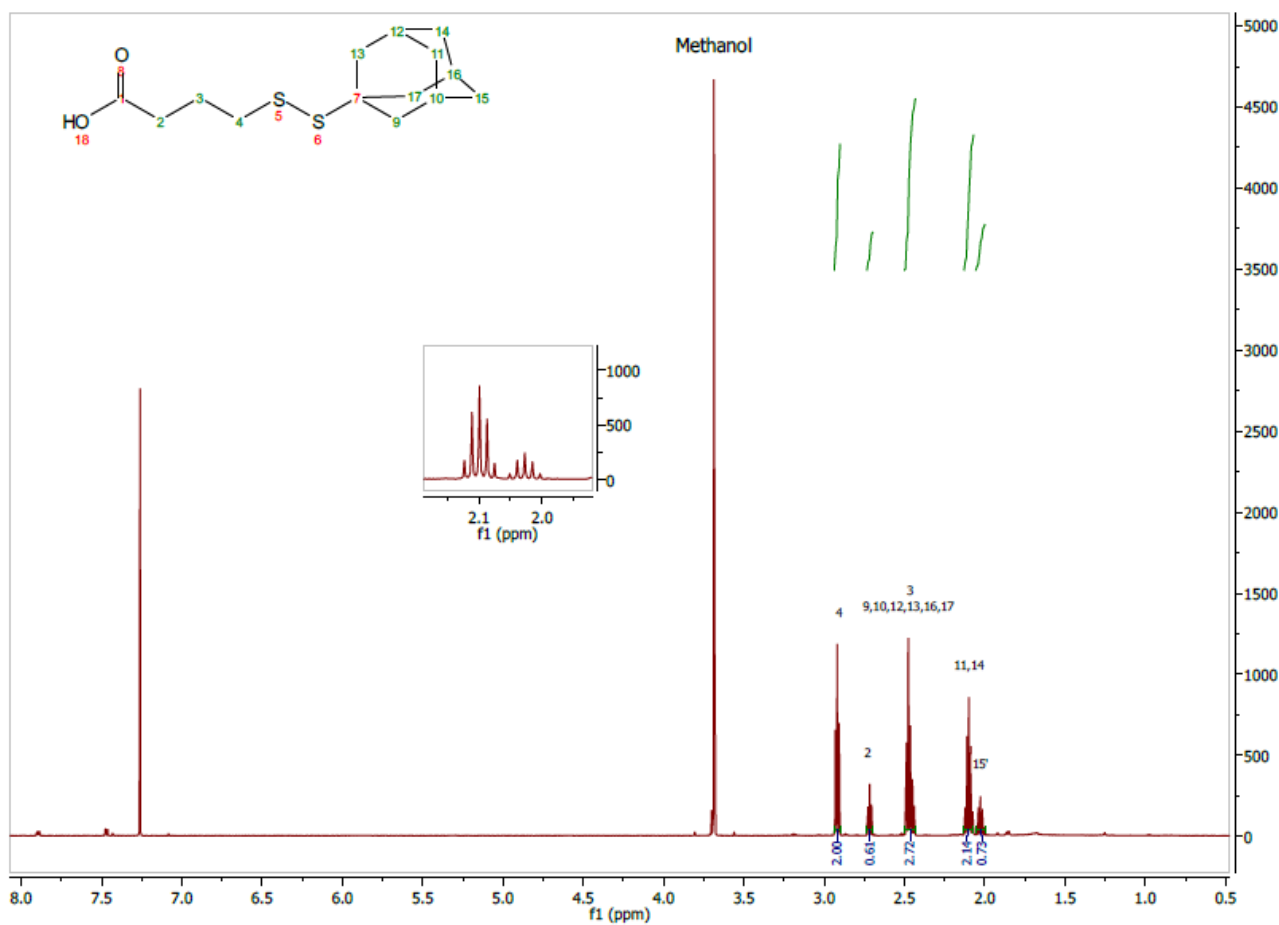


*Figure 48: $^1$H NMR of fraction 45-49, (**3**).*

## 5.2.2 Amide bond formation (4)

The reaction was first tried in small scale (50 mg), which went smoothly and yielded 0.13 g crude product. As seen in figure 49, the product needed purification. Looking at the structure of (**4**), it is quite easy to see that it is a polar molecule, which can complicate the purification.
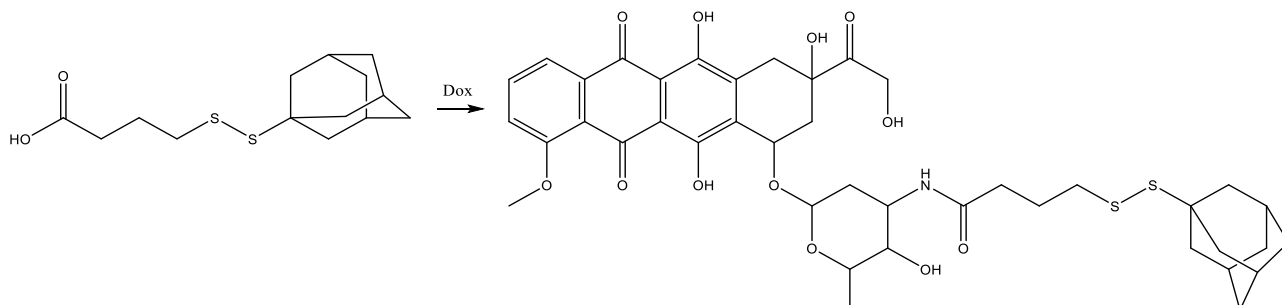


The preferred method for purification was column chromatography and a significant amount of time was therefore put in to finding a good solvent system for the purification. Given the structure of the product, reverse phase was considered. However, it was decided to see if the product could be purified using normal phase.
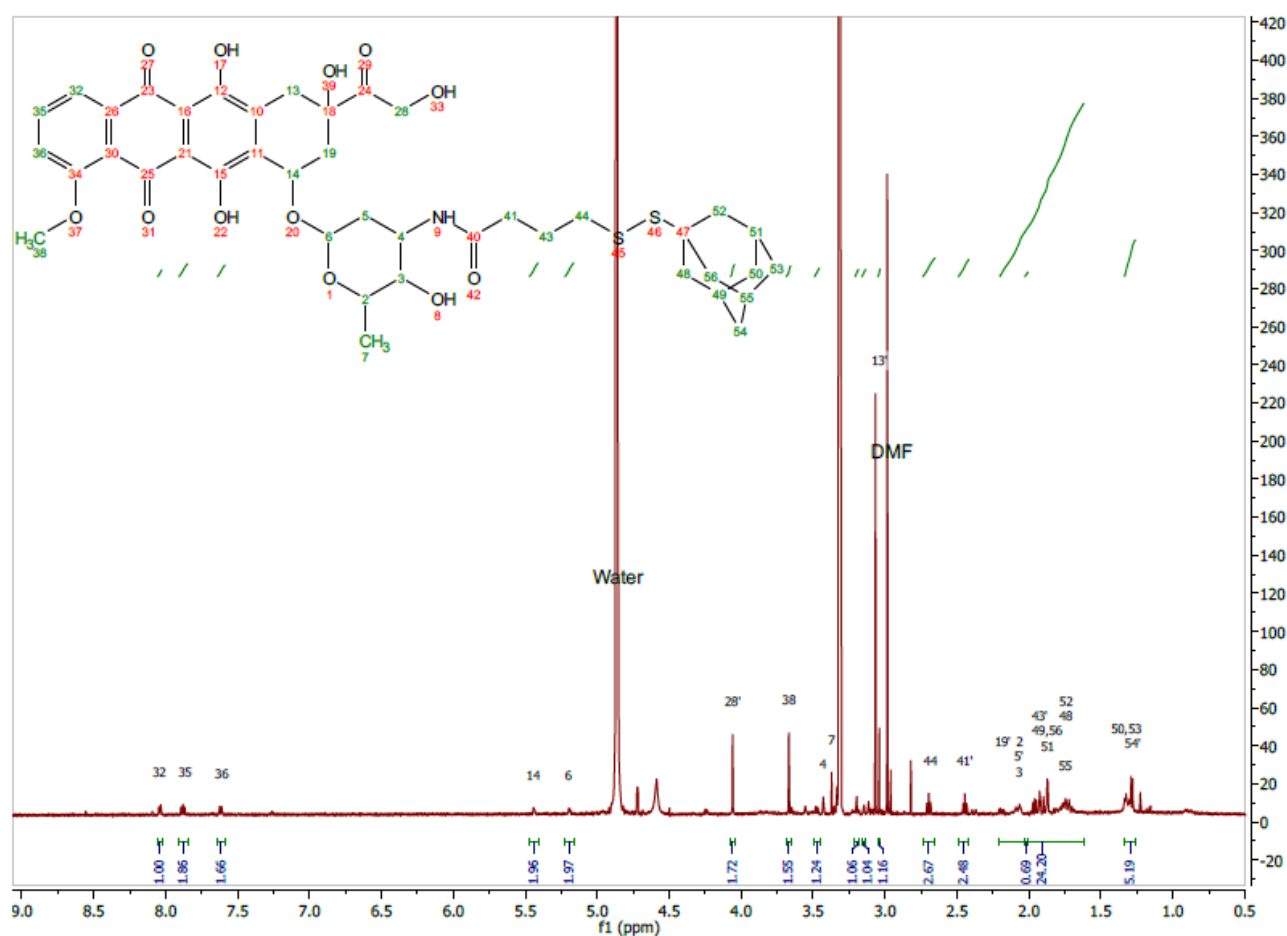


*Figure 49: ¹H NMR of (**4**) before purification.*

TLCs were made with different solvents systems (DCM: MeOH, CH₃CN: MeOH and heptane: MeOH) in different ratios. In the end, it was decided to use DCM: MeOH (0-35 %) as solvents. The product was dissolved in MeOH and loaded onto celite. TLCs were made of the collected fractions and combined accordingly. However, none contained the product, as seen on ¹H NMR (see appendix). It was therefore decided to flush the column with MeOH to see if it would be possible to get the product out. This was successful, as shown on the ¹H NMR in figure 50.
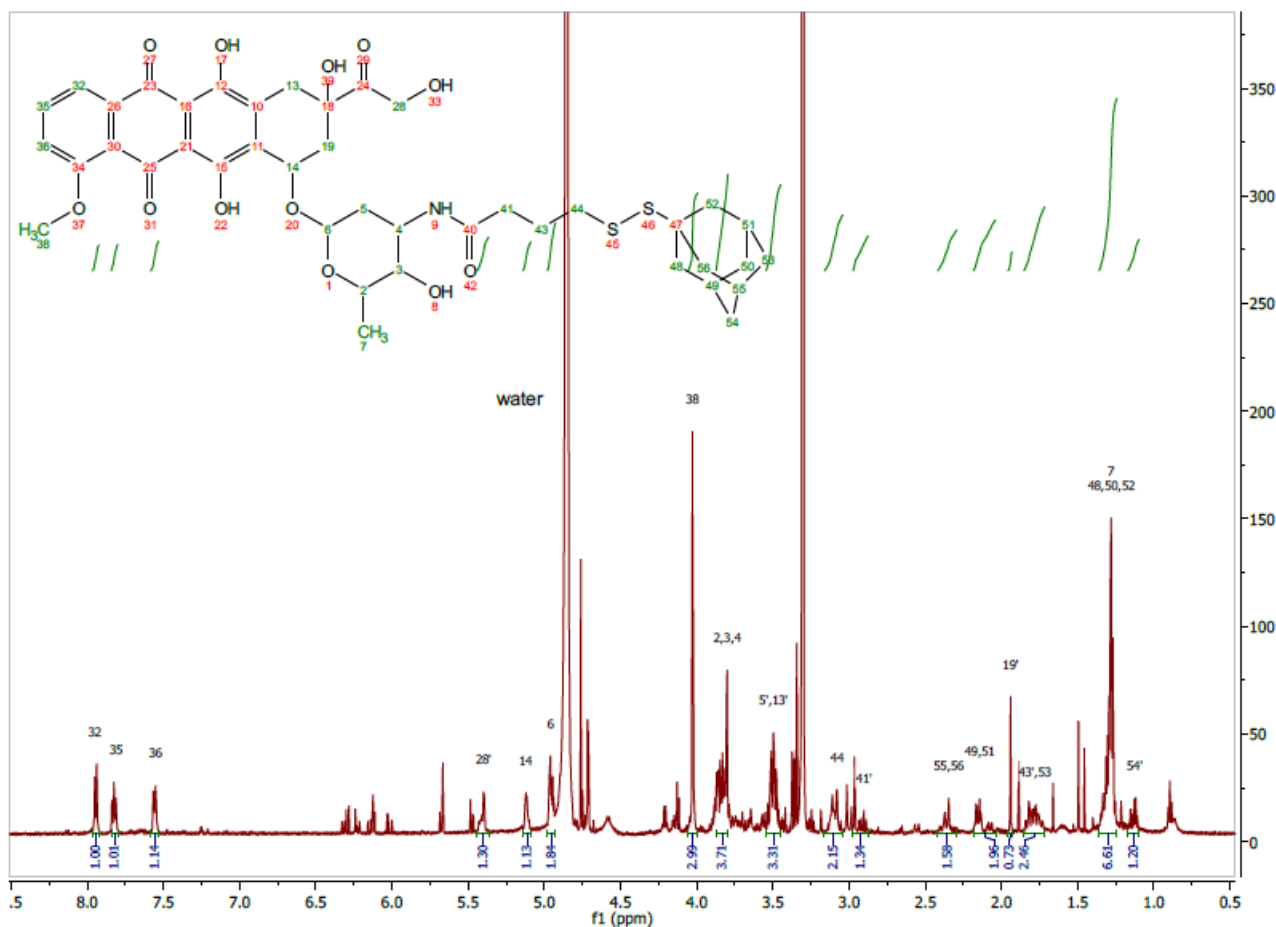


*Figure 50: ¹H NMR of (4) flushed out of column by MeOH*

However, as seen above, the product was less pure after purification than before. The purification was therefore repeated. The crude product was dissolved in MeOH and loaded on celite and purified by column chromatography with DCM: MeOH (0-50 %) as solvents. Fractions were collected and combined accordingly to give (4) in 14.87 % yield. A ¹H NMR of the purified product can be seen in figure 51.
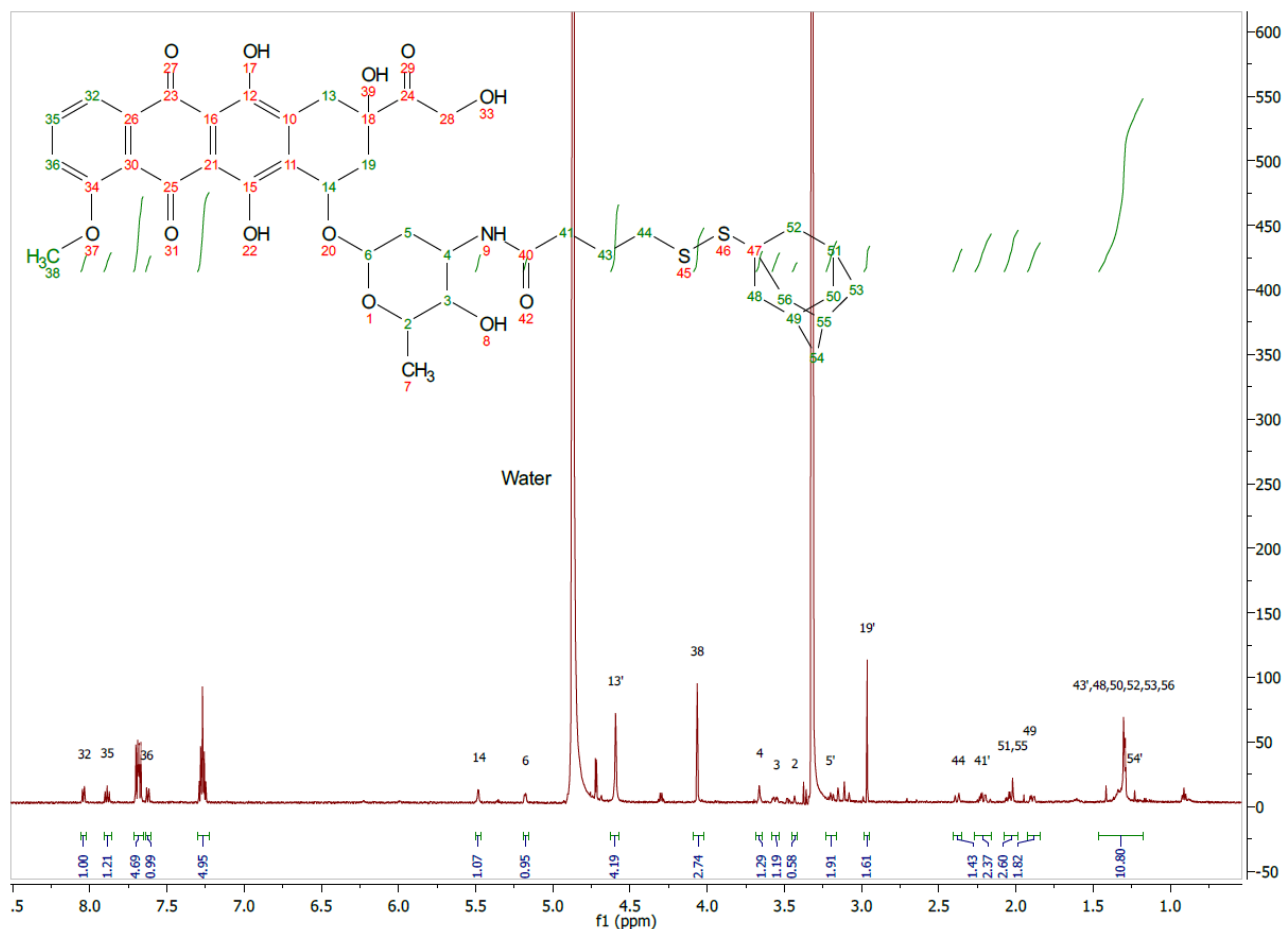
*Figure 51: $^1$H NMR of (**4**) after purification.*

The overall yield of the reaction was poor. Judging by the reaction, this is due to the method of purification (alternative purification will be discussed in section 5). However, the product seemed pure, judging by $^1$H NMR and therefore ready to be used for ITC. Before the ITC experiments were set up, LC-MS measurement was made of the product. 1 mg was partly dissolved in MeOH (10 mL). 100 µL was placed in a vial and measured. By LC-MS standards, the product did not seem pure. The LC-MS data can be seen in the appendix.

### 5.2.3 Hydrazone (2)

First the solvability of the (**3**) were tested. It was not dissolvable in acetonitrile, so the reaction was carried out in DMF. (**3**) was dissolved in DMF and reacted with HOBt and EDC in order to produce the activated ester/amide mixture. The reaction was followed by TLC and took around one hour before the reaction was judged complete.



54
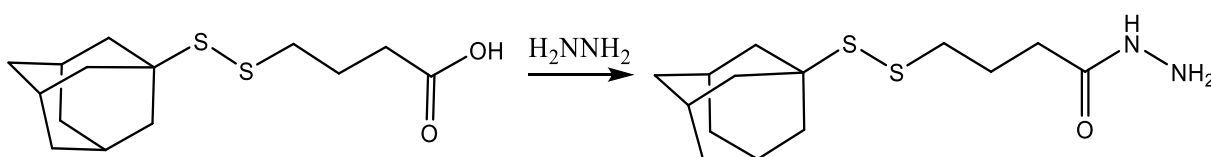
Hydrazine monohydrate was dissolved in DMF and the activated ester/amide mixture was slowly added. A TLC was taken immediately after the completion of addition, and it indicated a complete reaction. For good measure, the reaction was stirred for an additional two hours. Water was added and the aqueous DMF mixture was extracted with ethyl acetate. The organic phase was washed with a carbonate solution to remove 1-hydroxybenzotriazole. The solvent was evaporated under reduced pressure and yielded (2) in <100 %. The high yield is due to DMF residue as seen in figure 52. The yield is therefore not representative, but the reaction goes in quantitative yields in general.
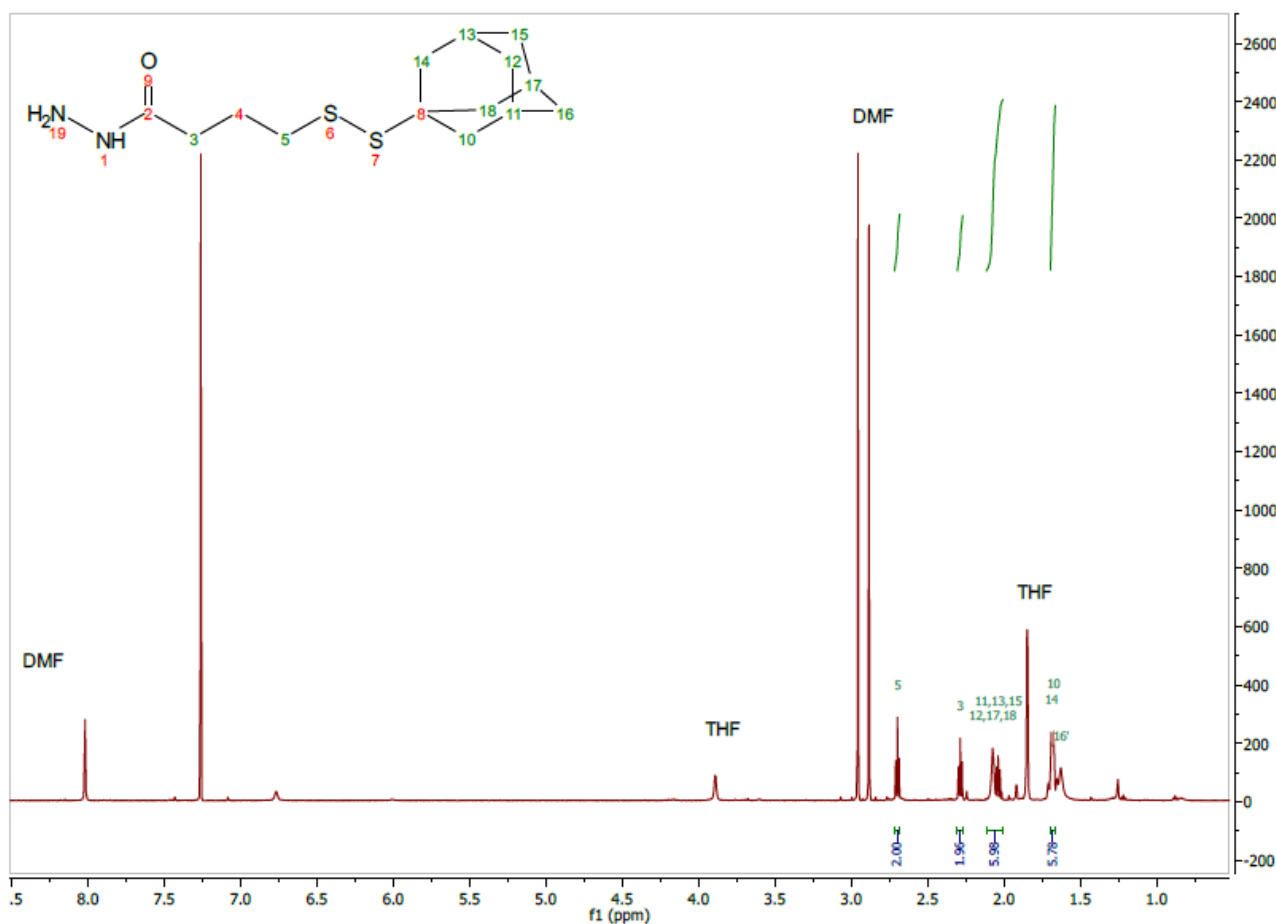


Figure 52: $^1H$ NMR of (2).

### 5.2.4 Imine formation (1)

(2) and Dox were dissolved in MeOH (5 mL) and stirred for 12 days, while covered in foil to keep the light out. The reaction was followed by reversed-phase TLC. A $^1H$ NMR was taken, and as seen



55
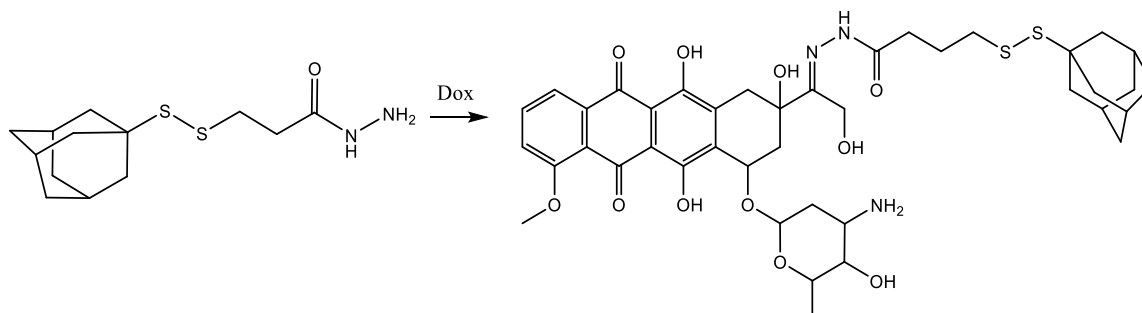
in figure 53, it was not pure. Different TLC solvents were tried in order to get a good rf value. The best system found was 3:1 MeOH: $H_2O$ with 3 % w/v ammonium acetate. This gave an rf ~0.1. The product was therefore purified by reverse phase column with this solvent system.
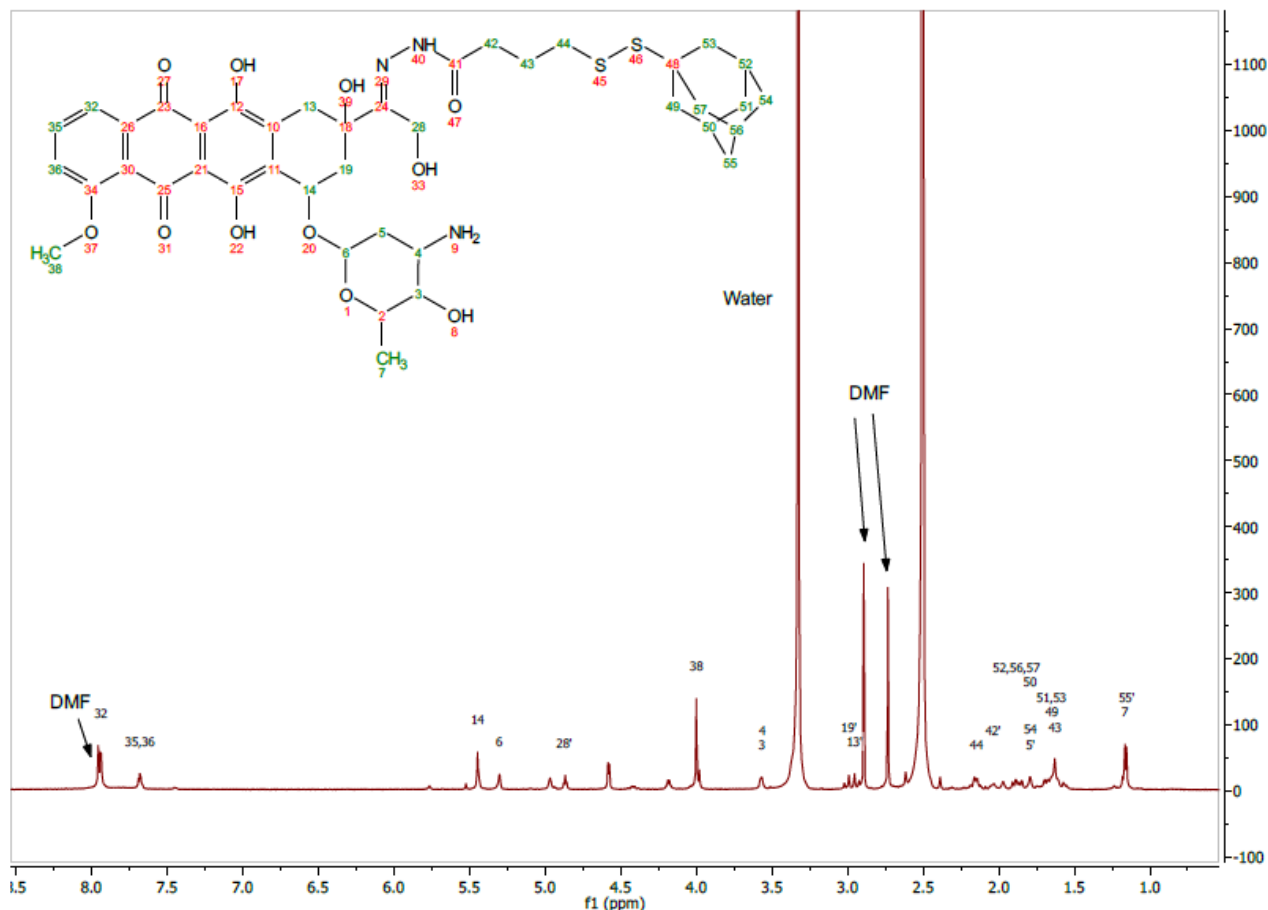


*Figure 53: $^1H$ NMR of (1) before purification.*

Both Dox and product has a clear red color and can therefore easily be seen. Fractions were collected and combined. The solvents were evaporated under reduced pressure. Getting an NMR of each fraction proved challenging as they all precipitated once placed on the spectrometer. A sample was prepared by dissolving a very small amount of fraction 63-70 in $CD_3OD$. This proved to be working and gave a $^1H$ NMR of the product which can be seen in figure 54. The reaction yielded (1) (10.6 mg, 15 %).
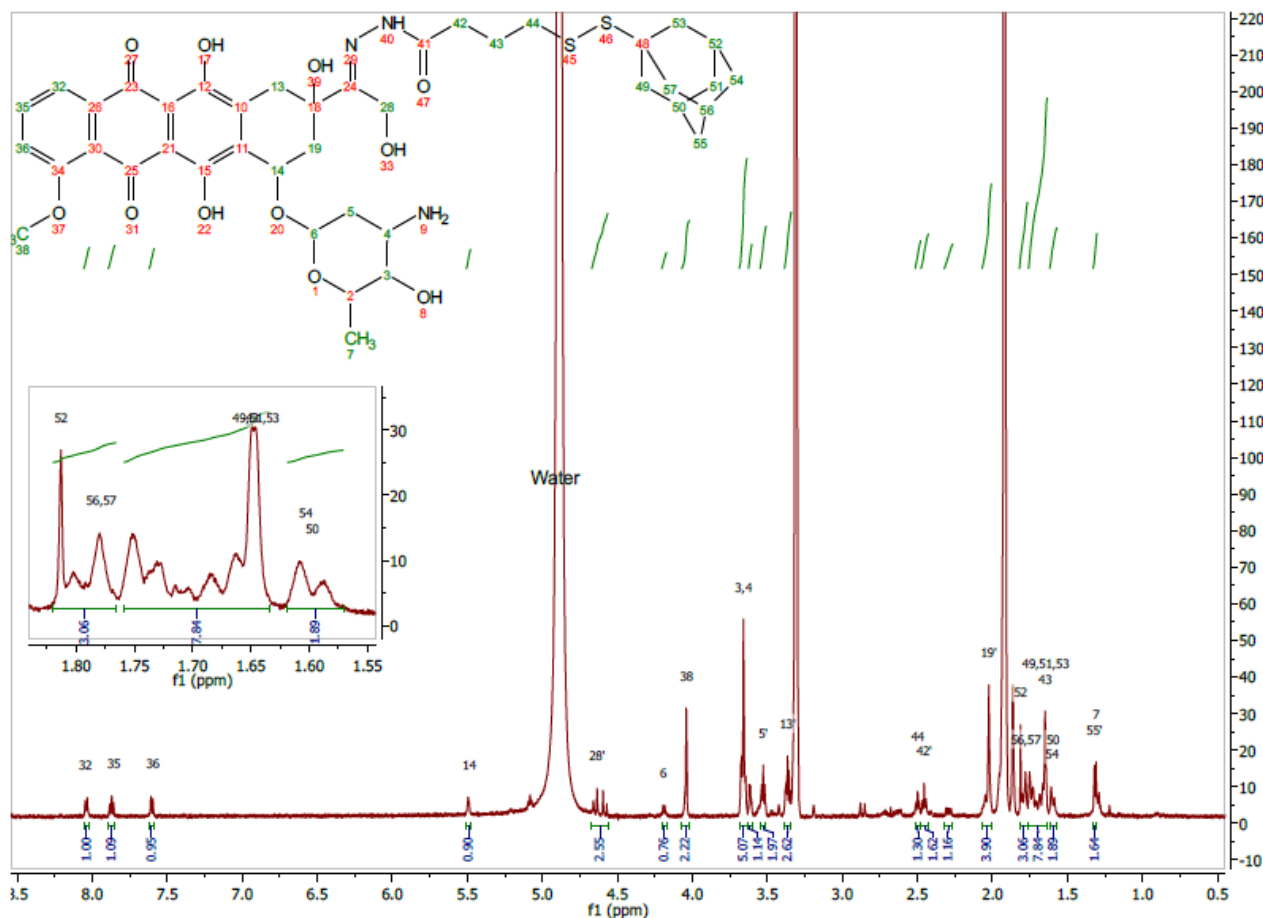
*Figure 54: ¹H NMR of (1) after purification*

Because of the low yield, the reaction was tried again. Two other experiments were set up, with varying temperatures. The reactions were followed by TLC.

| Name | Reactant | Temperature | Time | Crude | Yield |
|---|---|---|---|---|---|
| Reaction A | Dox | rt | 288 h | 86 % | 15 % |
| Reaction B | Dox | 35 °C | 48 h | 102 % | - |
| Reaction C | Dox | 45 °C | 72 h | 170 % | - |

*Table 2: Overview of reaction time and yield for Imine formation, (1).*

In order to compare all three reactions, the last two reactions were purified as well, using the same solvents system as for reaction A. The product from reaction C was purified first. However, this did not go as smoothly as anticipated for reaction C. Once the crude from reaction C was placed on the column it did not move. Hoping that this was due to air in the solvent wires, the same method was tried again without luck. The ammonium acetate concentration was increased to 10 % v/w. This however, made no difference. The solvent system was switched for acetonitrile and water with 10 % v/w ammonium acetate. This solvents system made some of the compound move, but not the product. In a last attempt, acetonitrile and MeOH was used as a solvent system. The product, did not move.

The only way left to retrieve the product would be to saw the column in half and try to extract the product with preferably MeOH: other possibilities could be DMF or DMSO. However, given that it was not crucial for the further work, the product was therefore considered "lost". Due to the trouble purifying and retrieving reaction C, it was decided to attempt purification of reaction B by normal phase. A lot of effort was therefore made to find a solvents system that could work. TLCs were made using DCM: MeOH, $CH_3CN$: MeOH and heptane: MeOH. The separation was not as good as on reverse phase, but DCM: MeOH gave the best result. Reaction B was only dissolvable in MeOH and was therefore placed on celite and purified by column chromatography. However, of the fractions collected from the purification, none contained the product. All this points to the same thing: the method of purification was not ideal, and in most, cases not effective. Both normal phase and reverse phase were tried and both fell short (alternative purification will be discussed in section 5). However, the product seemed pure, judging by $^1$H NMR and therefore ready to be used for ITC. Before the ITC experiments were set up, LC-MS measurement was made of the product isolated from reaction A. 1 mg was partly dissolved in MeOH (10 mL). 100 µL was placed in a vial and measured. By LC-MS standards, the product did not seem pure. The LC-MS data can be seen in the appendix.

## 5.3 Synthesis of Gemcitabine prodrugs

### 5.3.1 N-Adamantanoylglycine (6)

The reaction in itself is quite simple, however it proved to be a challenge. The first attempt was carried out in a mixture of water, dioxane and 4M NaOH aq. The first problem was keeping the pH level within range (9-11). Upon adding the first portion of (**7A** – synthesized from thionyl chloride) dissolved in dioxane the pH reached 13 and remained there for the duration of the reaction. The reaction was followed on TLC (stained with ninhydrin) which did not indicate a product forming. After stirring for 0.5 h, the reaction was quenched. Water was added to



the solution and precipitation began immediately. The precipitate was filtered of and washed with water till neutral. The reaction yielded 34 %. However, the $^1$H NMR did not show sign of glycine being present in the product. The signal from the $CH_2$ in glycine would be expected around 3.9 ppm. The spectrum of 1-adamantanecarbonyl chloride, shown in figure 55, is almost identical to that of 1-adamantanecarbonyl chloride shown in figure 45.
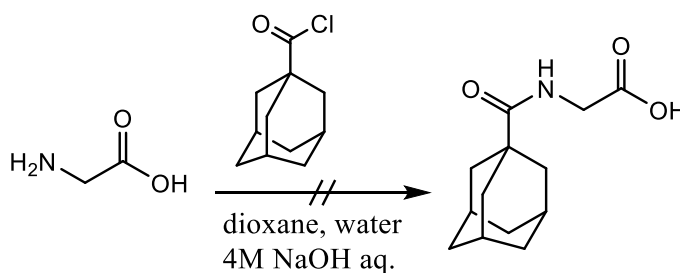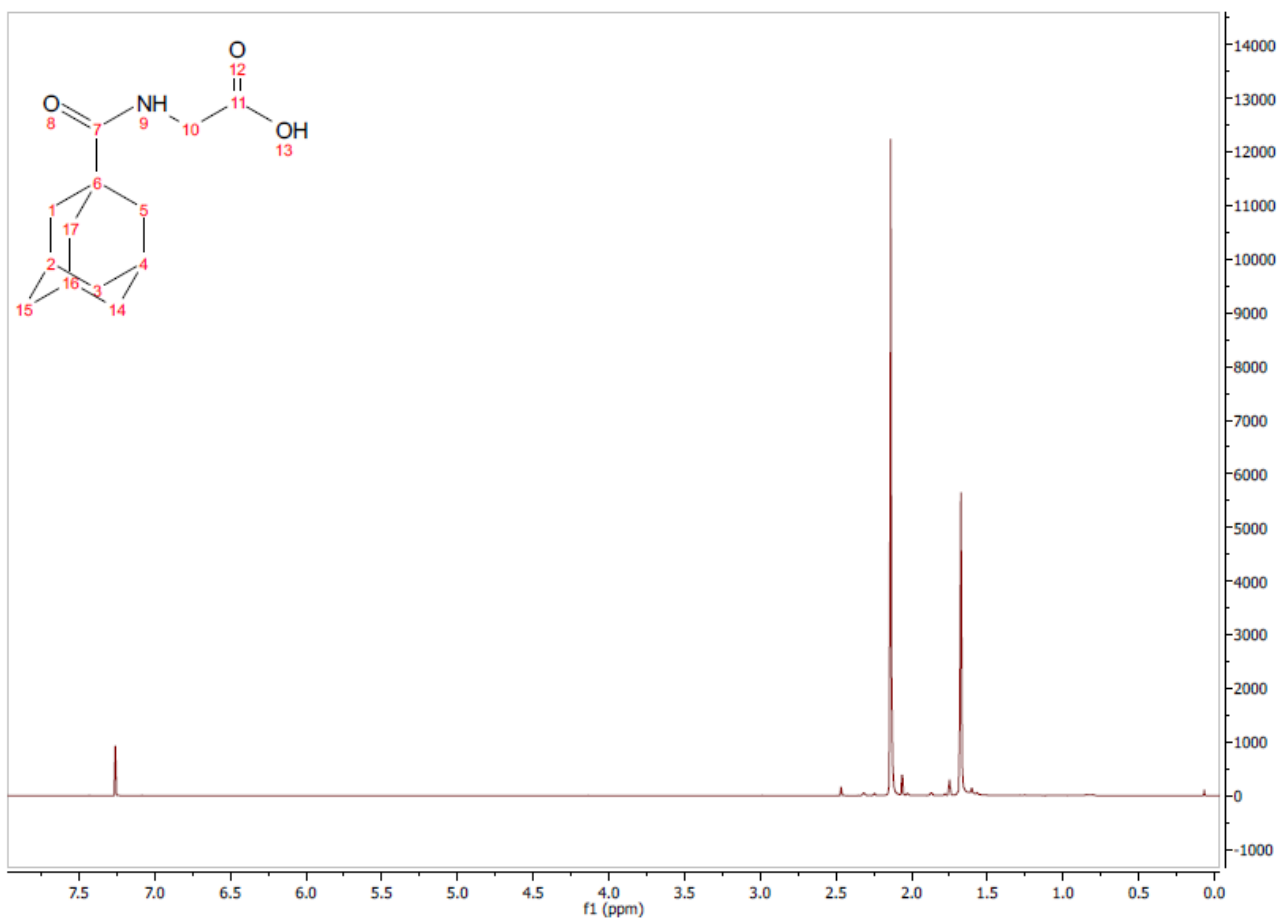
*Figure 55: ¹H NMR of, what should have been, 1-adamantanoylglycine.*

Two additional reactions, identical to the first, were carried out. One stirring for 1h and the other for
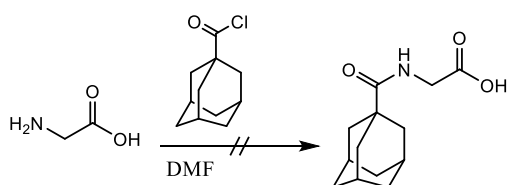


24h. Both produced results similar to the first attempt. In an attempt to keep the pH within range, a more diluted mixture of (**7A**) was made and less 4M NaOH was added. However, this did nothing to prevent the pH from reaching 13. This

reaction showed similar results to the first attempt. Another method was therefore tried. 3 eq. of glycine was dissolved in DMF and a bit of water and 1 eq. of (**7A**) was added, and the reaction was left to stir for 6 days. This did not produce the product either. The NMR was practically identical to the spectrum shown in figure 44. The conclusion was, therefore, that there could be a problem with (**7A**). Hence, (**7B**) made from oxalyl chloride was used in the following attempts. The first method tried with (**7B**) was identical to the first attempt with (**7A**). Similar problems arose and no product was indicated on TLC. The second attempt with (**7B**) was carried out in DMF with $Na_2CO_3$ as a base. The reaction indicated no product. The last attempt was carried out with (**7B**) in DMF with 4M NaOH and $Na_2CO_3$ as bases. Within 10 min of addition of (**7B**) the pH level dropped from 11 to 9. This was the first indication of product. The reaction was monitored closely by TLC (stained with ninhydrin). The mixture was filtered, and TLC was made of the isolated powder and the filtrated. Both powder

59

and filtrate indicated a present of glycine. However, the spot for the filtrate had a yellow color, indicating a secondary amine and the filtrate was therefore evaporated under reduced pressure to produce a white residue. The residue was dissolved in a small amount of water and a bit of DMF and extracted with ethyl acetate. The organic phase was evaporated to produce the product, which I believed to be the (**6**), as fine white powder in small yield (15.32 %).

| Reactant | Solvent | Time | Yield |
|----------|---------|------|-------|
| 1-adamantane carbonyl chloride[ii] | Water, dioxane, 4M NaOH aq. | 0.5 h | - |
| 1-adamantane carbonyl chloride[ii] | Water, dioxane, 4M NaOH aq. | 1 h | - |
| 1-adamantane carbonyl chloride[ii] | Water, dioxane, 4M NaOH aq. | 24 h | - |
| 1-adamantane carbonyl chloride[ii] | DMF | 24 h | - |
| 1-adamantane carbonyl chloride[iii] | Water, dioxane, 4M NaOH aq. | 24 h | - |
| 1-adamantane carbonyl chloride[iii] | DMF, $Na_2CO_3$ 4M NaOH aq. | 2 h | 15.32 % |
| 1-adamantane carbonyl chloride[iii] | DMF, 4M NaOH aq. | 2 h | 59.89 % |
| 1-adamantane carbonyl chloride[iii] | DMF, 4M NaOH aq. | 2 h | 82.60 % |

*Table 3: Overview of reaction conditions and yields.*

Getting a decent ^{1}H NMR was not easy at all. The product did not dissolve easily and even when it seemed it did (($CD_3$)$_2$SO, $D_2O$, $CD_3OD$) the ^{1}H NMR came back as either solvents or with only signals from glycine without trace of adamantyl or the other way around. To get an idea of whether it was the product or not the reaction to produce (**12**) was carried out and this paid off, as seen later in figure 62. It was therefore decided to see if a representative ^{1}H NMR could be obtained by dissolving the product in DMF. However, not much of the product (10 mg sample) dissolved and the ^{1}H NMR obtained was not that good, as shown in figure 56. It was not possible to obtain a better one.

---

[ii] Carried out with 7A
[iii] Carried out with 7B
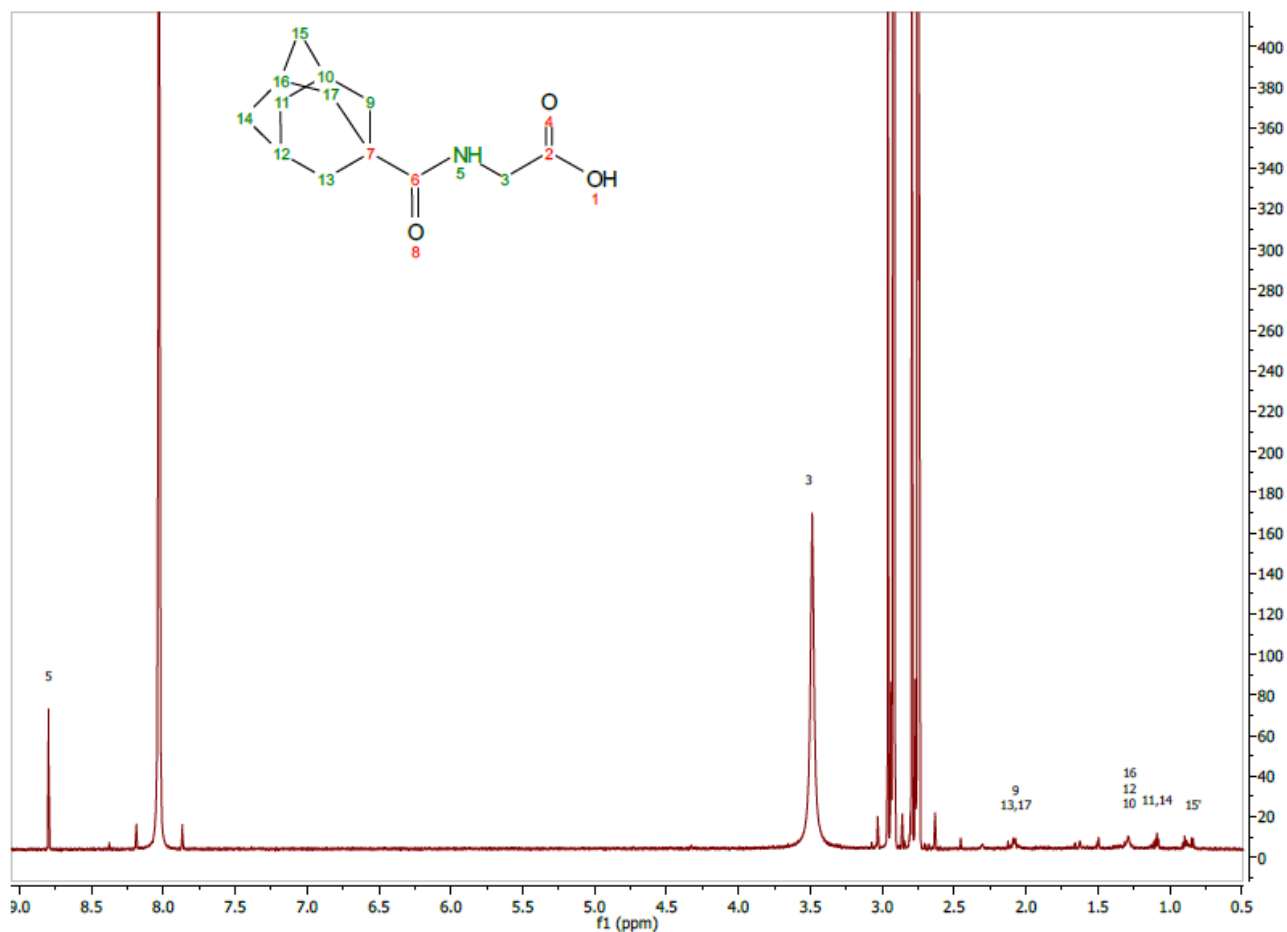
*Figure 56: 1H NMR of (**6**)*

In order to get an easier workup and to see if the yield could be improved, a new synthesis was carried out. Glycine (2 eq.) was dissolved in DMF and the solution was made basic (pH ~ 11) with 4M NaOH aq. (**7B**) was added in small portions and the pH level was monitored. The reaction was followed on TLC (stained with ninhydrin). After 2h the reaction was judged complete and the DMF/water mixture was extracted with ethyl acetate. The organic phases were combined and the solvent evaporated under reduced pressure to produce (**6**) in 59.89 % yield.  An identical reaction was carried out with (**7A**) to yield 82.6 %.

### 5.3.2 Protection of Gemcitabine (10)

The protection of Gem was not as straightforward as assumed. When using $Na_2CO_3$ as a base and letting the reaction stir at rt. for 48 h, the yield of the reaction was 40 %.
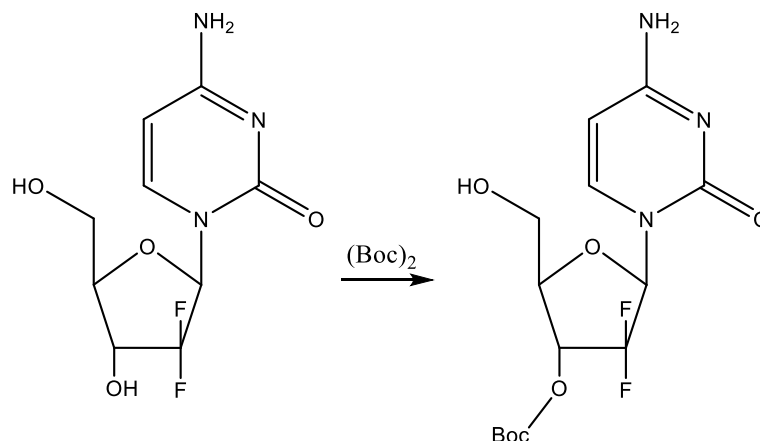


However, by looking at the $^1$H NMR below (figure 57), it seems there are two boc-groups present, given the two almost identical peaks around 1.47 ppm. This indicates that the reaction leads to a double protection and gives (11), instead of (10).
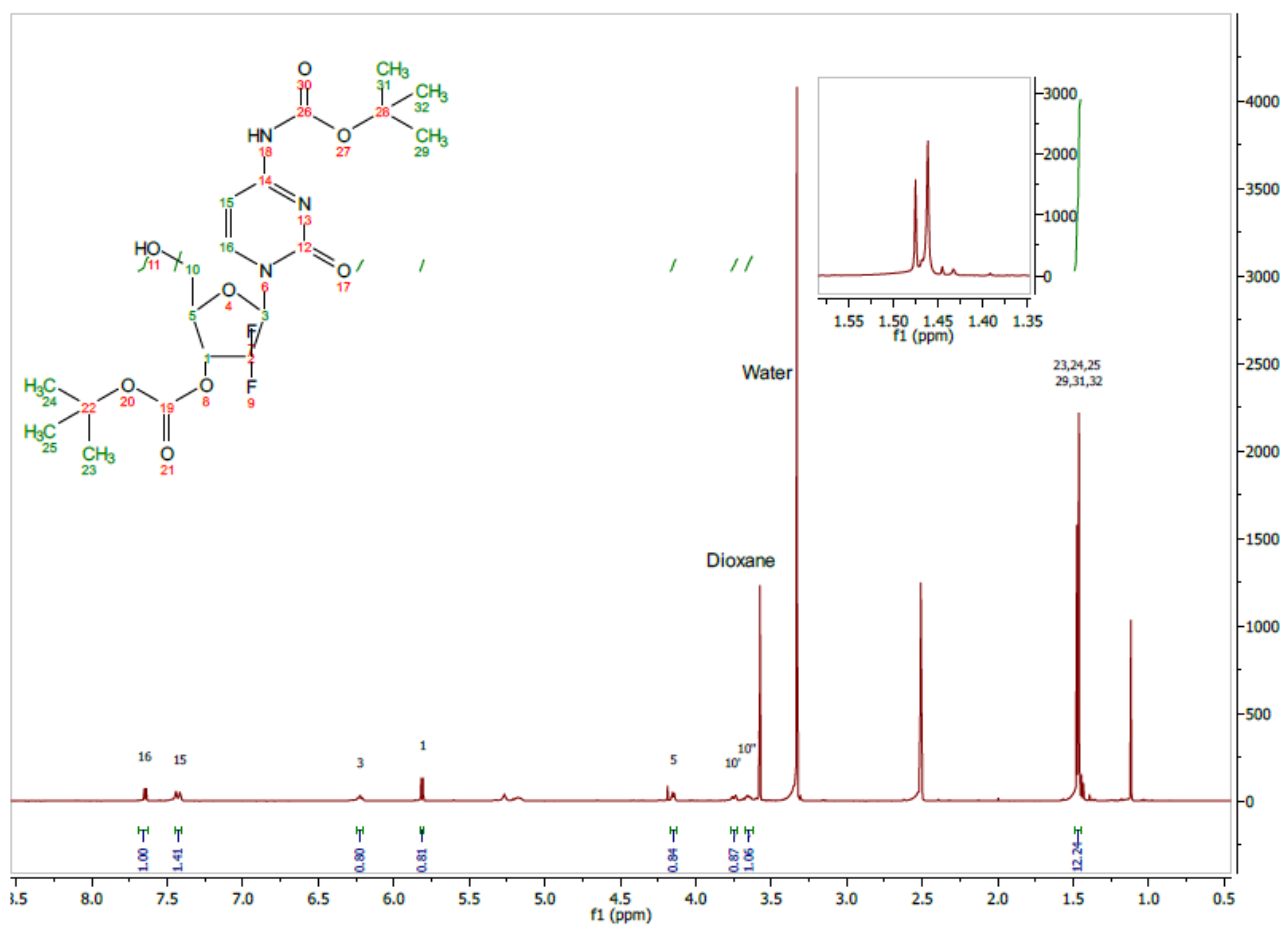


*Figure 57: $^1$H NMR of (11) catalyzed by $Na_2CO_3$.*

To see if the yield of the reaction could be improved, $Na_2CO_3$ was switched for $K_2CO_3$. All other conditions were kept the same and (**10**) was obtained in 73 % yield.
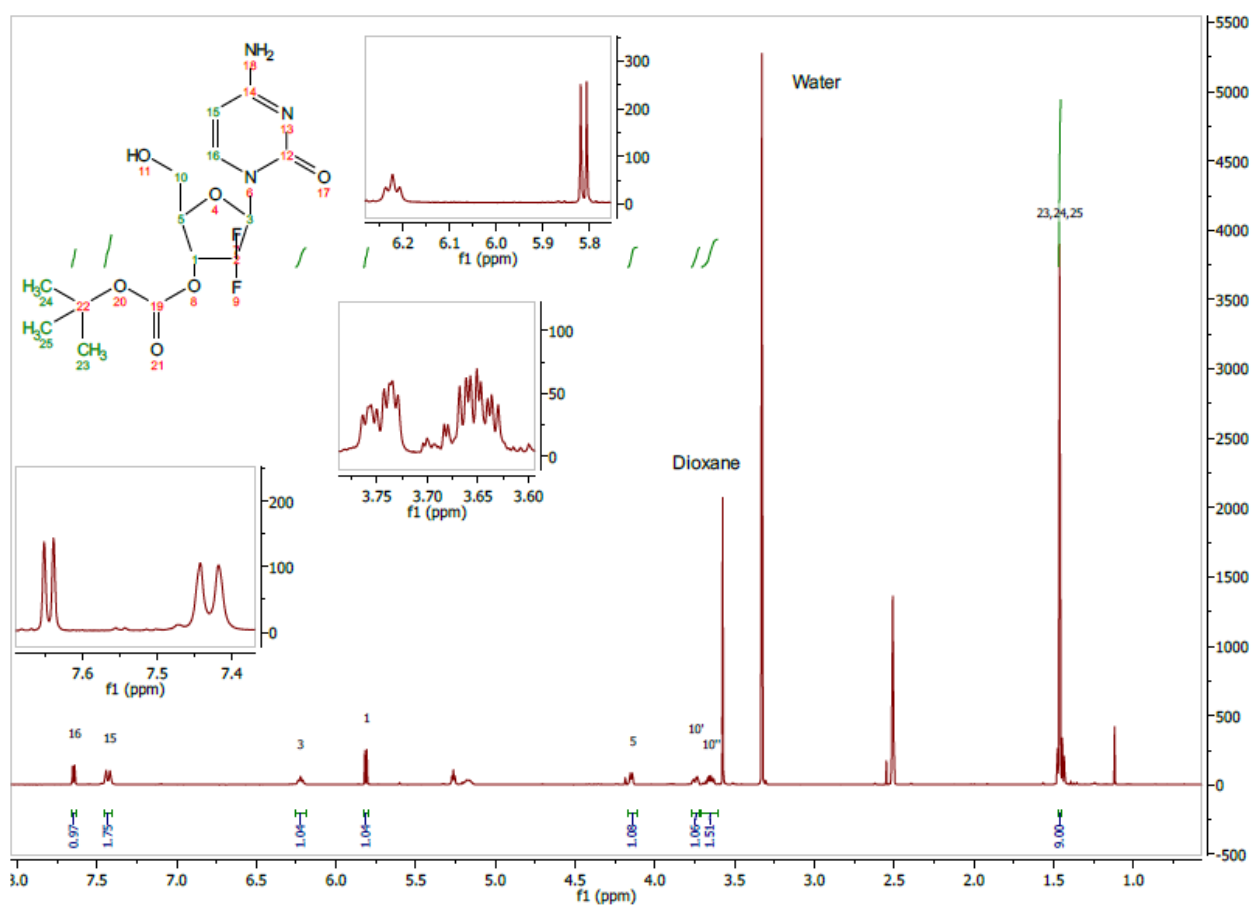


*Figure 58: $^1H$ NMR of (**10**) catalyzed by $K_2CO_3$.*

### 5.3.3 Second protection of Gemcitabine (11)

The protection of Gem with $Na_2CO_3$ yielded (**11**) as described in section 4.2.2. A reaction using 2 eq. of boc was carried out. The reaction was followed on TLC (stained with $KMnO_4$). The reaction yielded 37.95 %, which was lower than the first attempt. No further attempts were made to improve the yield of this reaction. The $^1H$ NMR of the product is shown in figure 59.



63
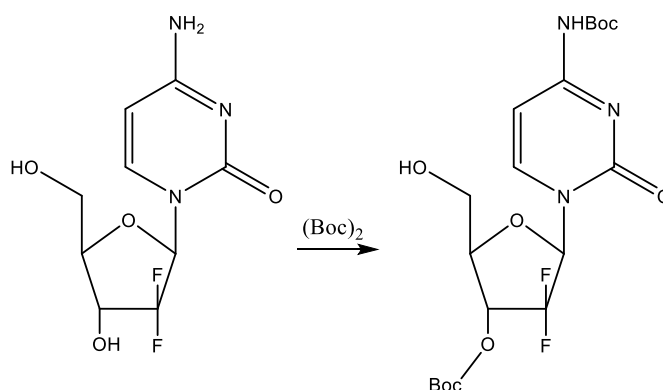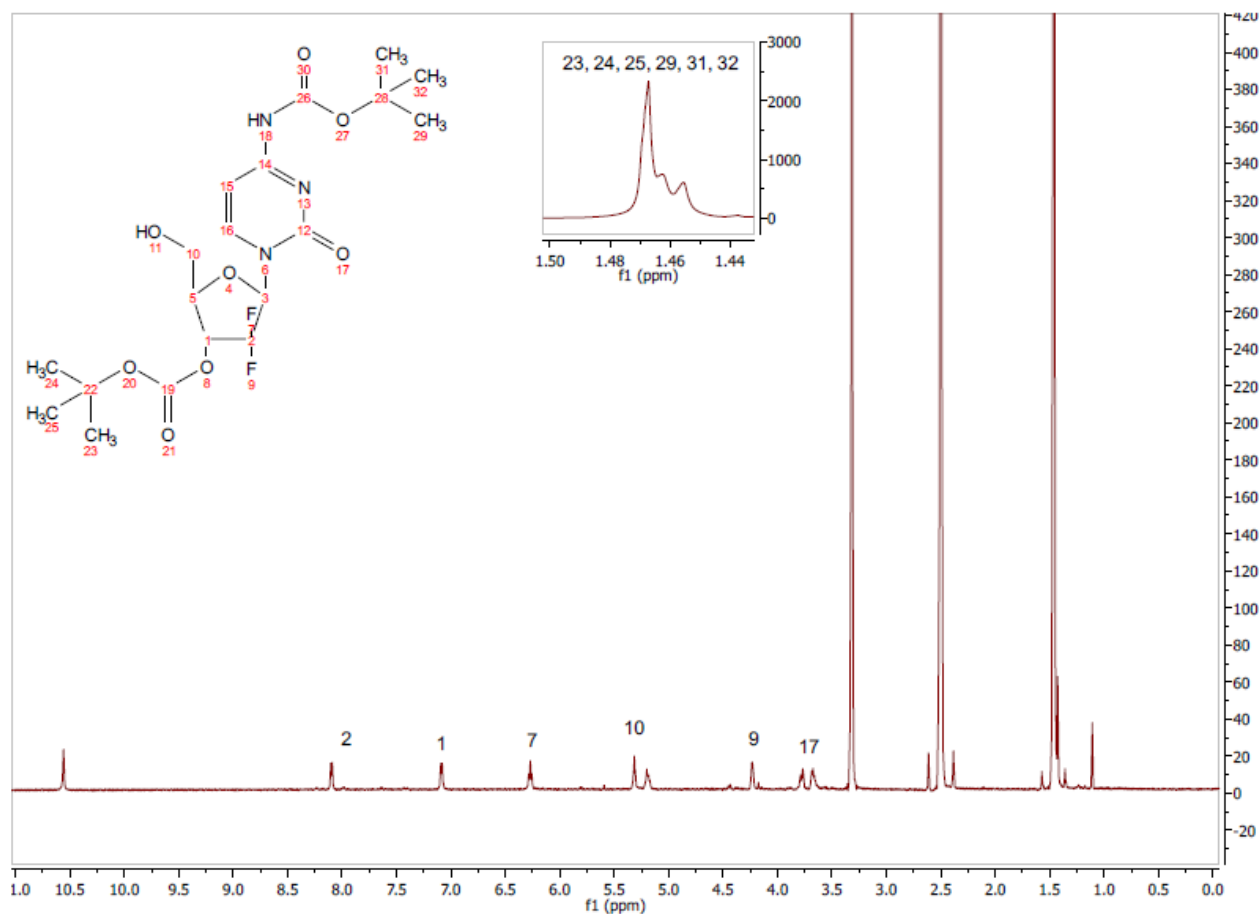
Figure 59: $^1H$ NMR of (**11**).

An attempt to produce (**11**) from (**10**) was made. (**10**) and (Boc)$_2$O was dissolved in dioxane and left to stir at rt. and the reaction was followed by TLC (stained with KMnO$_4$). After 70 h there was no change and the solvent was evaporated under reduced pressure. The reaction conditions were therefore change before attempting the synthesis once again. (**10**) and (Boc)$_2$O were dissolved in



dioxane and left to stir at rt. for 24h before adding Na$_2$CO$_3$ (5 eq.) as a base; the reaction was stirred
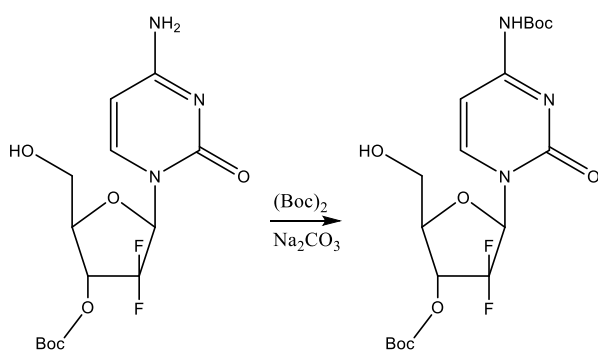


for another 24 h. The reaction was followed on TLC (stained with KMnO$_4$). After 72 h there was no reactant left, according to the TLC taken. The solvent was evaporated under reduced pressure to yield a white residue. The reaction yielded (**11**) in 73.12 %. A $^1H$ NMR was taken, which can be seen in figure 60.

64
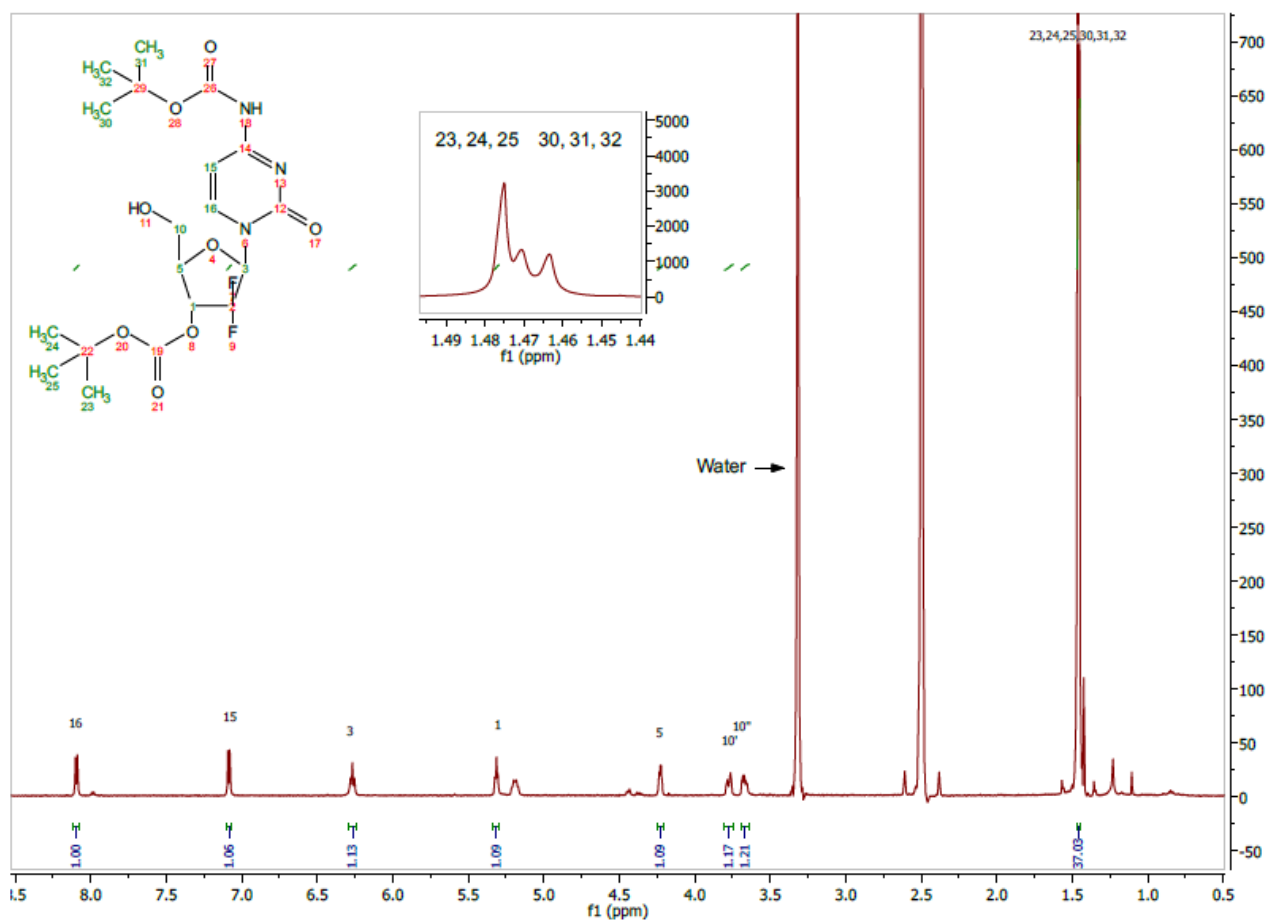
*Figure 60: $^1H$ NMR of (11).*

Comparing to two ways of synthesizing (**11**), it is clear that a higher yield (overall ~ 60 %) is obtained when the protection is carried out in two steps. However, that procedure combined takes 5 days, whereas the reaction using $Na_2CO_3$ and one reaction takes 2 days. The preferable method depends on which molecule one wish to attain. If the goal is (**11**), then the method using $Na_2CO_3$ is preferable despite the overall difference in yield (~ 20 %).

### 5.3.4 Amide bond to obtain (12)

This reaction was simple and straightforward. (**3**), EDC and HOBt was dissolved in dry DCM. (**10**) was added and the solution stirred overnight. The organic layer was washed with brine and dried over
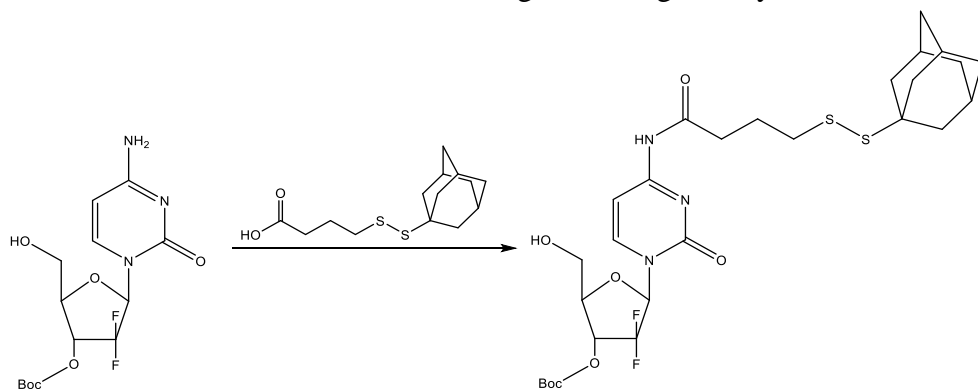


sodium sulphate. The solvent was evaporated under reduced pressure. Time was spend finding an optimal solvent system for

65

the purification. Different solvents were tried, but DCM: MeOH gave the best separation. The residue was purified by the column chromatography with DCM-MeOH (0-35 %). The product (**12**) was isolated across two fractions and yielded 18.52 %. Looking at the purification (which can be seen in the appendix), it is not the best separation made. The yield of the reaction is poor and some may be due to the purification (alternative purification will be discussed in section 5).
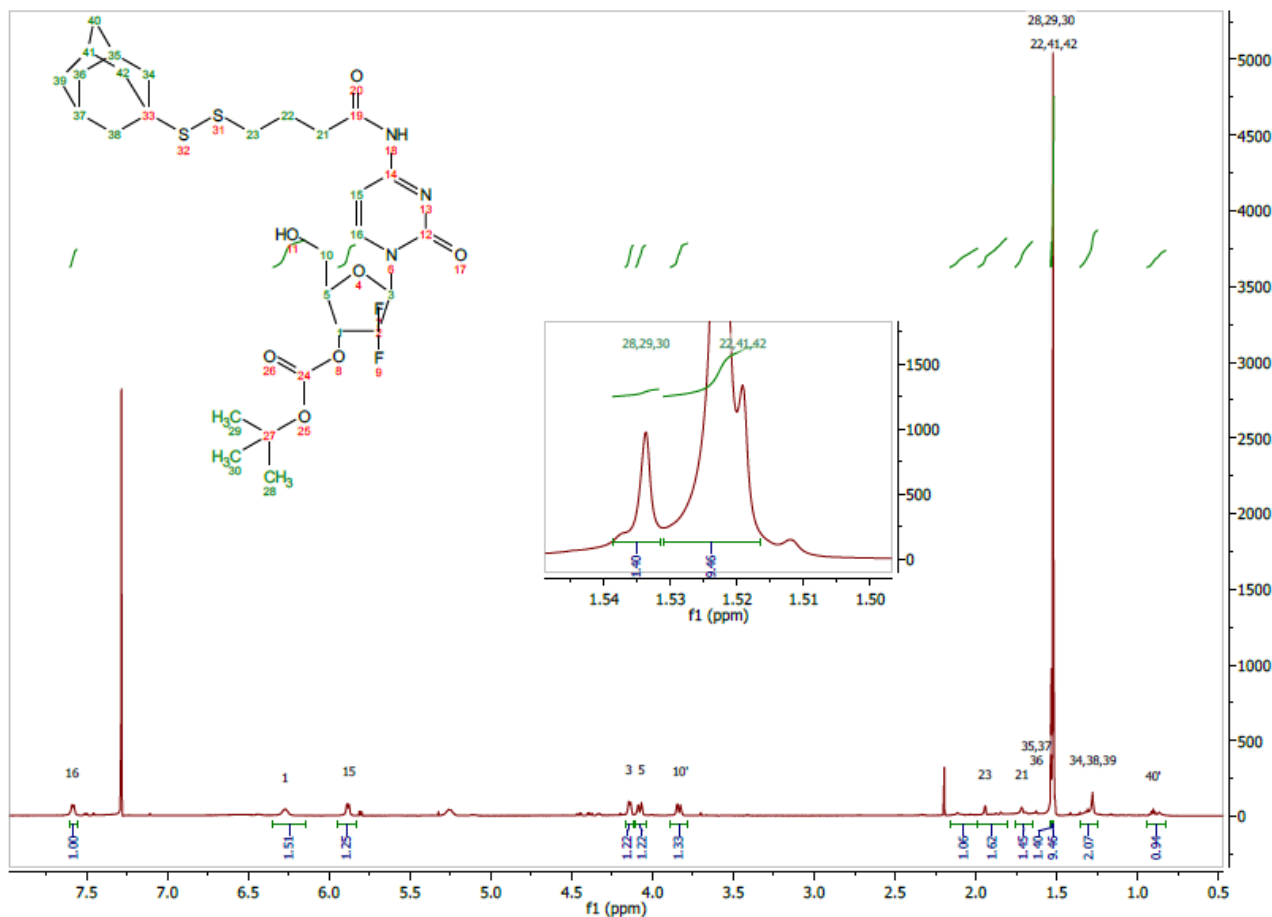


Figure 61: ¹H NMR of (**12**) after purification.

### 5.3.5 Deprotection to (8)

A small-scale experiment was carried out before any purification of (**12**) was done. This was in order to find the optimal amount of time and TFA concentration needed for complete deprotection, while not risking decomposing the molecule.
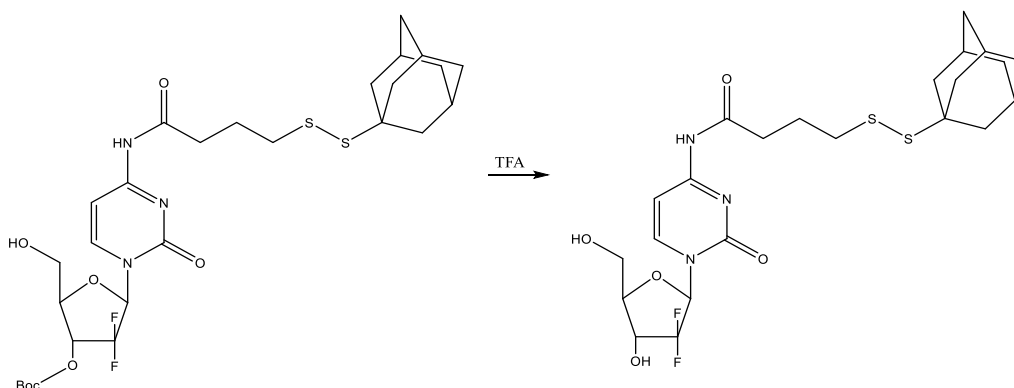
A TFA solution was made with a 3:2 TFA to DCM. 0.05 g (**12**) was dissolved in TFA (6 mL) solution and the deprotection was followed on TLC (stained with ninhydrin) for a total of 24 h. The TLC showed no sign of (**12**) after 4 h and after 24 h there were no sign of the molecule decomposing. It was therefore safe to go ahead and deprotect the purified (**12**). This was done by placing (**12**) in the TFA solution under stirring for ~ 4 h. The reaction was followed on TLC to make sure all was deprotected. The TFA solution was evaporated under reduced pressure to yield (**8**) a yellow/brown oil. The product needed no further purification, as seen on figure 62.
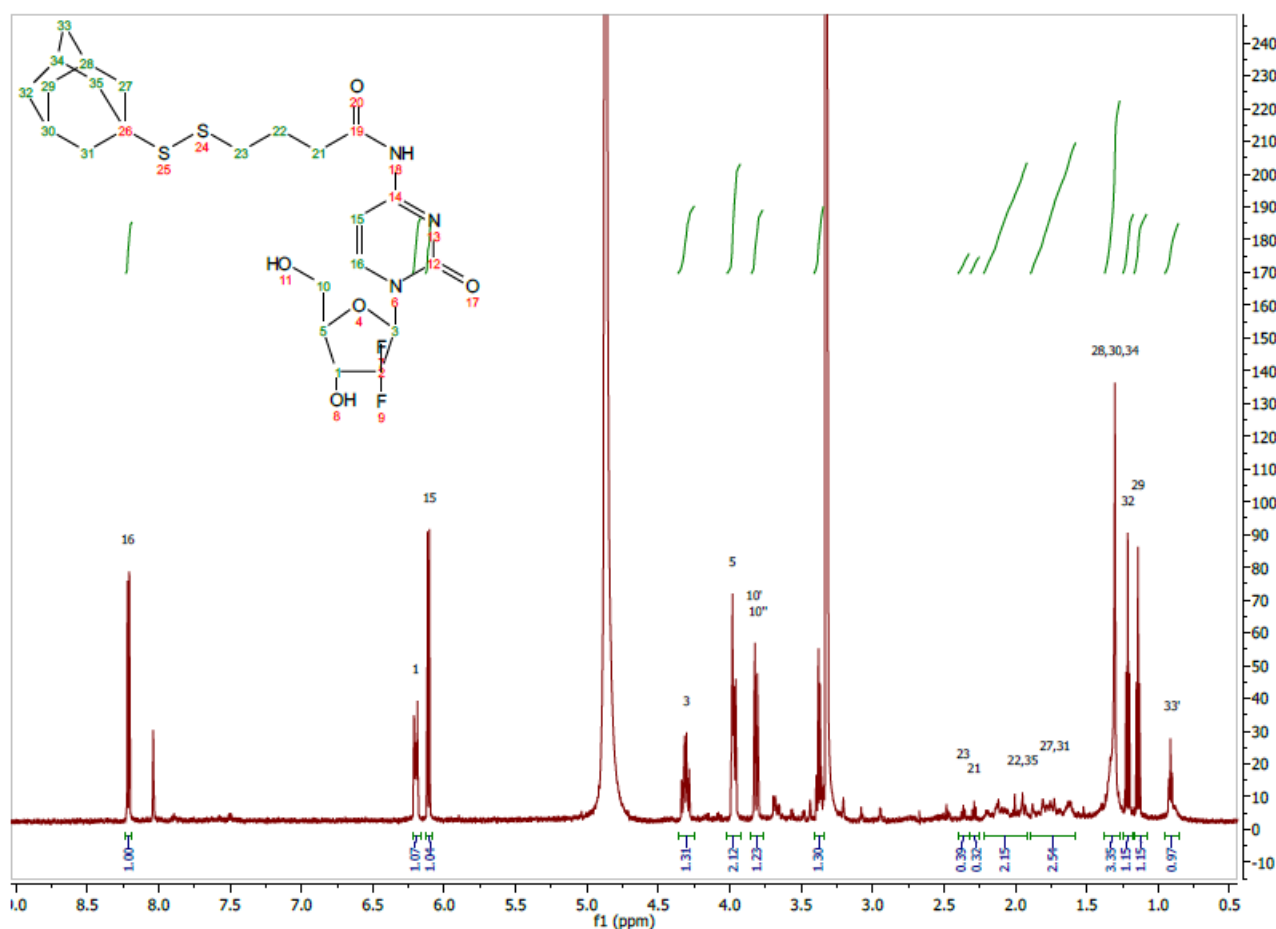


*Figure 62: ¹H NMR of (**8**).*

LC-MS measurement was made of the product. 1 mg was dissolved in MeOH (10 mL). 100 µL was placed in a vial and measured. By LC-MS standards, the product did not seem pure. The LC-MS data can be seen in the appendix.

### 5.3.6 Esterification to obtain (13)

This reaction was straightforward. (**6**), DCC and DMAP were dissolved in DMF. (**11**) was added and the solution turned light pink, and right thereafter, yellow which stayed.
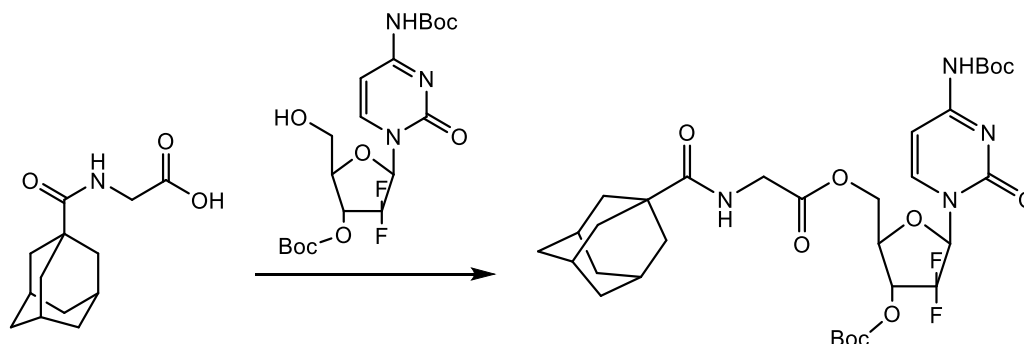


The solution was stirred for 24 h. The solvent was evaporated under reduced pressure to give a yellow substance, which was then dissolved in ethyl acetate. The organic phase was washed with water, saturated sodium bicarbonate and brine, and dried over Na₂SO₄. The solvent was evaporated under reduced pressure to yield a brownish oil.
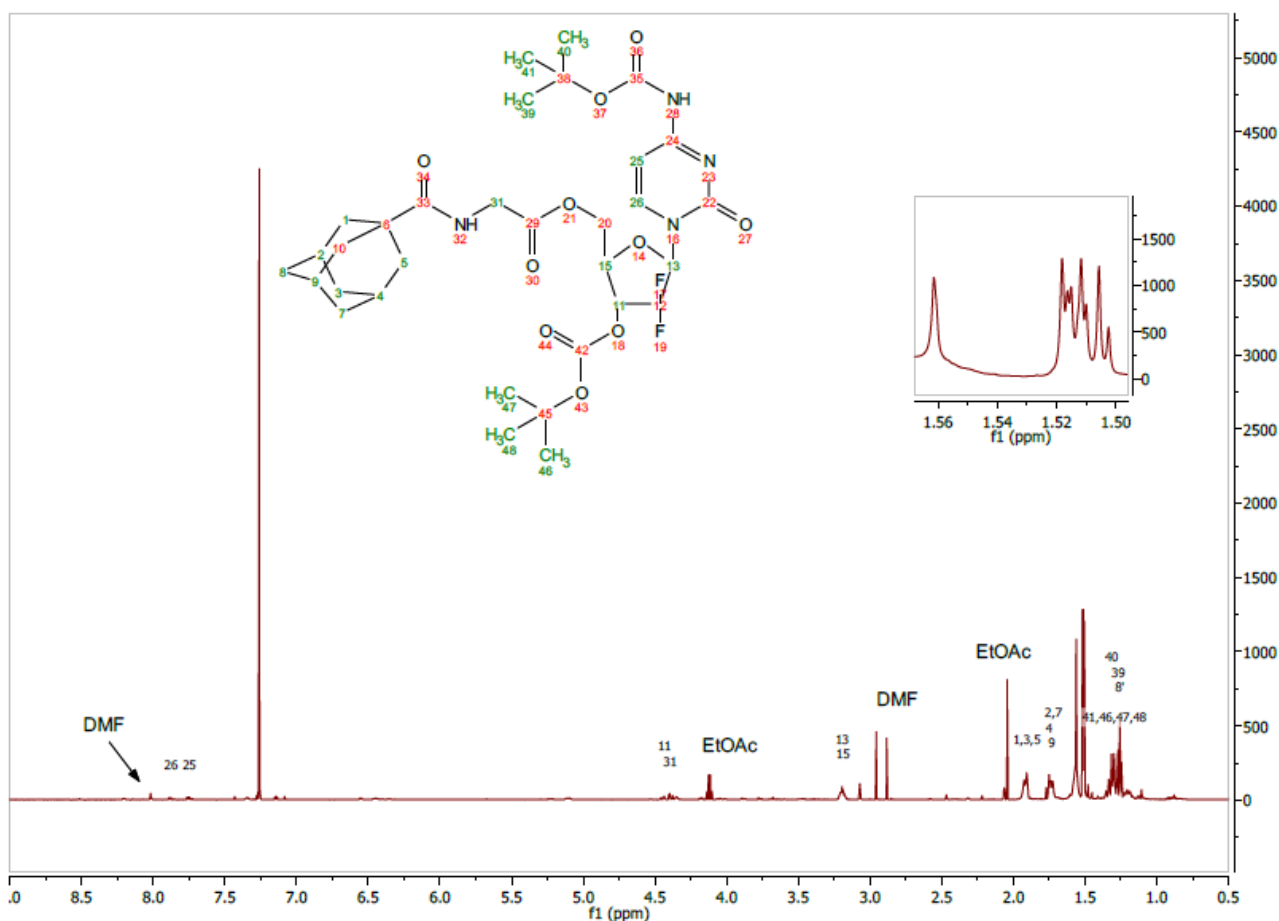


*Figure 63: ¹H NMR of (13) before purification.*

To make sure it would be possible to purify the molecule by column chromatography, different solvents were tried and tested and in the end DCM: MeOH seemed to give the best separation.

Different ratios were tried (20:1, 4:1, 3:1, 2:1 and 1:1) and the best rf was obtained with 20:1 ratio. The product was purified by column chromatography using DCM: MeOH (0-20 %). The product was isolated in across two fractions. One of the ^{1}H NMR is shown in figure 64. The product was obtained as a clear oil (21.3 mg, 24.21 %). The purification did not give the best separation (as can be seen in the appendix). The yield of the reaction is poor and some may be due to the purification (alternative purification will be discussed in section 5).
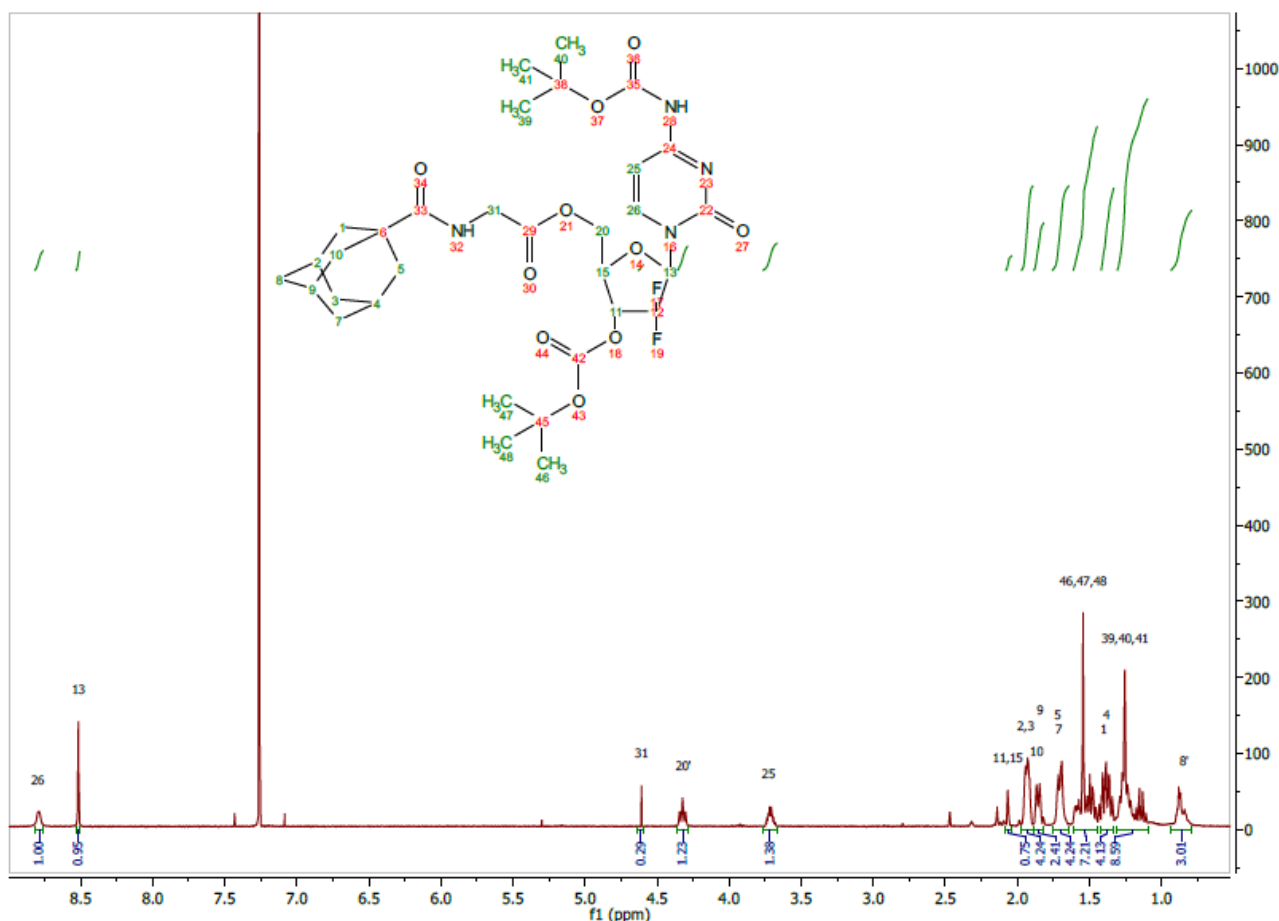


Figure 64: ^{1}H NMR of (13) after purification.

### 5.3.7 Deprotection to (5)

A small-scale trail was set up before any purification of (13) was done. This was to test the concentration of TFA and the time needed for complete deprotection without the molecule decomposing.



69
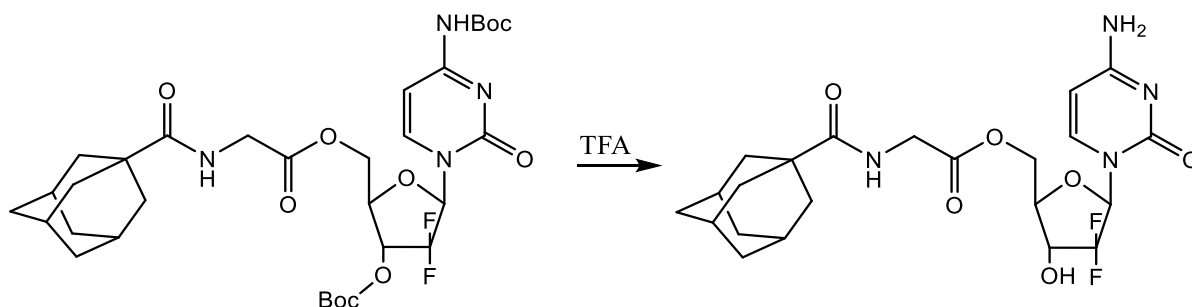
A TFA solution was made with a 3:2 TFA to DCM. 0.05 g was dissolved in TFA (6 mL) solution and the deprotection was follow on TLC (stained with ninhydrin) for a total of 24 h. The TLC showed no sign of (**13**) after 4 h and after 24 h there were no sign of the molecule decomposing. It was therefore safe to go ahead and deprotect the purified (**13**). This was done by placing (**13**) in the TFA solution under stirring for ~ 4 h. The reaction was followed on TLC to make sure all was deprotected. The TFA solution was evaporated under reduced pressure to yield (**5**) as white powder.
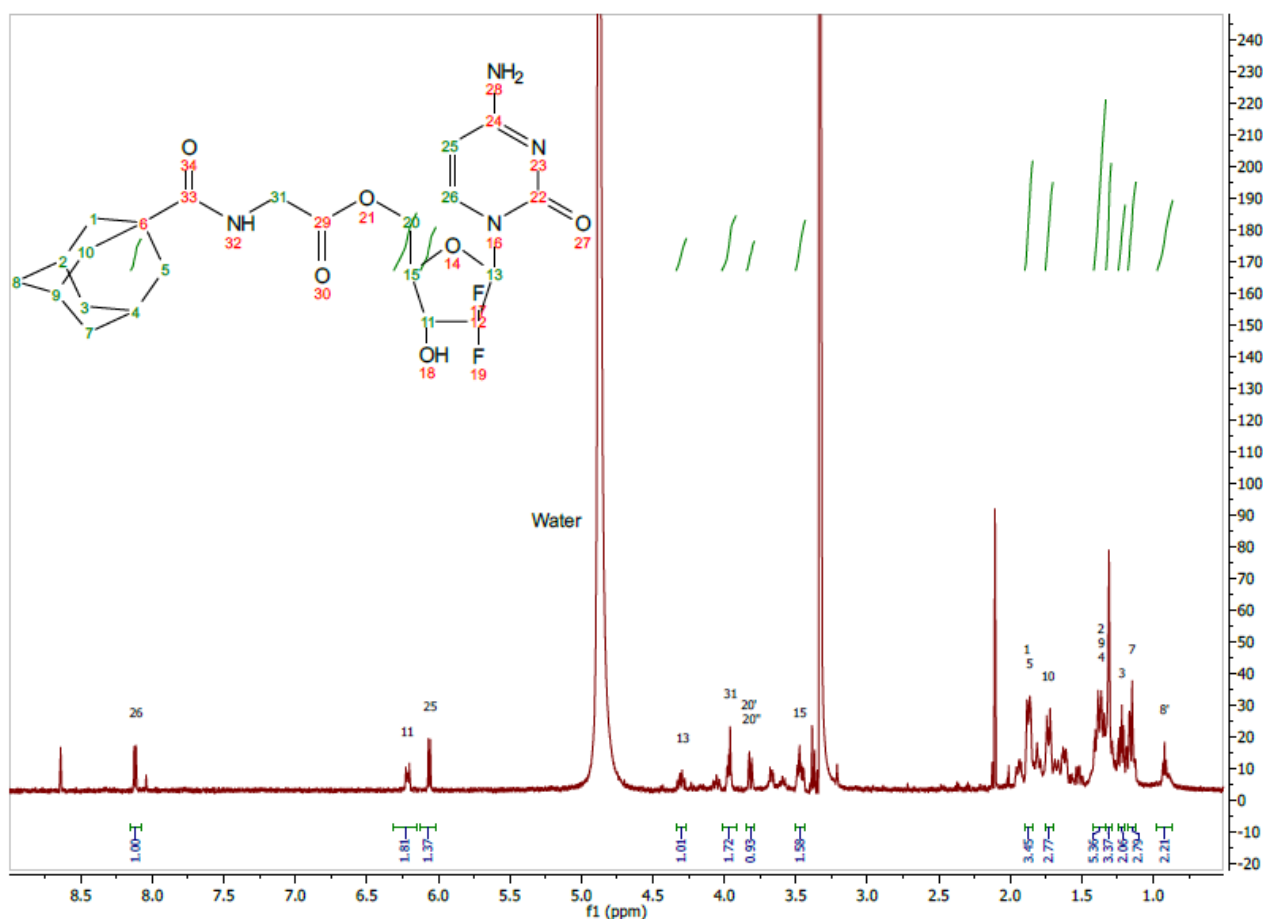


*Figure 65: ¹H NMR of (**5**).*

LC-MS measurement was made of the product. 1 mg was dissolved in MeOH (2 mL). 100 µL was placed in a vial and measured. By LC-MS standards, the product did not seem pure. The LC-MS data can be seen in the appendix.

# 6. Column purification

All purifications of Dox and Gem containing products were problematic and seemed to cause poor overall yields. Dox prodrugs were purified using both normal phase and reverse phase, whereas the Gem prodrugs were purified using only normal phase.

## 6.1 Normal phase purification

Normal phase chromatography is based on hydrophilic molecules adsorption on to a polar stationary phase. Normal phase silica consists of tetrahedral crosslinked polymers of $SiO_4$. The silanol groups, as seen in figure 66, gives the polar adsorption properties. This means that the least polar (hydrophobic) compounds elute first and the most polar (hydrophilic) compounds elute last.[77] Therefore, (**13**) eluted first and the unreacted and more polar structure (**11**) was kept back by the column. Same is true for structure (**12**) which is far less polar than that of structure (**10**). However, the purification was not good. The products, (**12**) and (**13**), eluted straight through indicating that the solvent system might have been too polar. This being said, a less polar solvent system was not an option as the product would not move on TLC when tested. Purification of both Dox prodrugs, (**1**) and (**4**), were also attempted using normal phase chromatography. When attempted on (**1**) it failed and neither product nor reactant was eluted. However, normal phase purification worked on (**4**). It gave poor yields, but the product was purified.
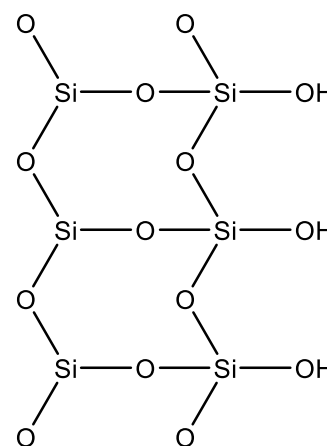
*Figure 66: Structure of normal phase silica.[78]*

## 6.2 Reverse phase purification

In reverse phase, hydrophobic molecules are adsorbed onto hydrophobic stationary phase. Reverse phase silica contains less polar or non-polar functional groups such as C18, as shown in figure 67. In this system, the most polar compounds elute first and the nonpolar last. This was thought to be ideal for the Dox prodrug (**1**). A C18 column was used with a high protic solvent system (water: MeOH). Water is the "weakest" as it is the most polar and repels hydrophobic molecules onto the stationary phase.[79] Decreasing the polarity by adding more methanol reduces the hydrophobic interaction and results in desorption. The molecules are, eluted in order of increasing hydrophobicity making the Dox product
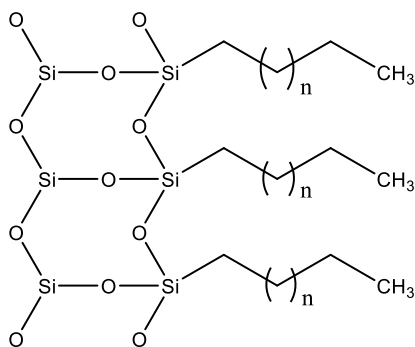
*Figure 67: Reverse phase silica.[78]*

(1) elute last. However, this succeeded only once and in poor yield. The second time, it failed all together.

## 6.3 Alternative purification

In hindsight, neither normal phase silanol nor reverse phase C18 was ideal. Luckily, there are a lot of different columns available and one of these may be the answer to the purification problem. The silica in these specialized columns have been "end-capped" with a functional group, as seen in figure 68. For silica, these include amino-, cyano- and diol functionalized. Both cyano-functionalized and amino-functionalized silica can be used in normal and reverse phase.[80] Both Cyano- and amino-functionalized silica can be used to separate moderately polar compounds in reverse phase and polar compounds normal phase. Amino-functionalized silica also has the ability to act as a proton donor. and generally[81] Cyano-functionalized silica



*Figure 68: Functionalized silica. FG=-NH$_2$. CN. etc.[78]*

has been shown to separate a wide range of drug compounds using DCM, THF, CH$_3$CN, hexane and water acetonitrile, n-hexane, and water.[82] These two systems could therefore be a good alternative for purification of both Dox and Gem containing products. However, none of these were tried as we did not have TLC plates that match the systems. This would mean that it would be trial and error trying to purify the product, which is not ideal.

# 7. Complexation with cyclodextrin

## 7.1 Isothermal titration calorimetry

Isothermal titration calorimetry (ITC) is used to measure interactions between ligands and host. All it requires is a measurable change in enthalpy (ΔH). ITC can calculate free energy (ΔG), entropy (ΔS), dissociation constant ($K_D$), and stoichiometry (n) of binding. It does so by measuring changes in temperature upon interaction, in this case, the interaction between the synthesized prodrugs and CDs, as shown in figure 69.
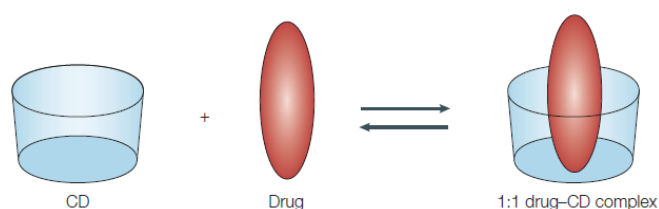


*Figure 69: Equilibrium between CD$_{free}$ and CD$_{complex}$.[44]*

If the interaction is exothermic (ΔH<0), the ITC uses less energy to heat the cell compared to the reference cell, whereas if it is an endothermic (ΔH>0) interaction, the ITC uses more energy to heat the cell compared to the reference cell. The raw data obtained shows the difference in power supplied to the two cells and look like figure 70.
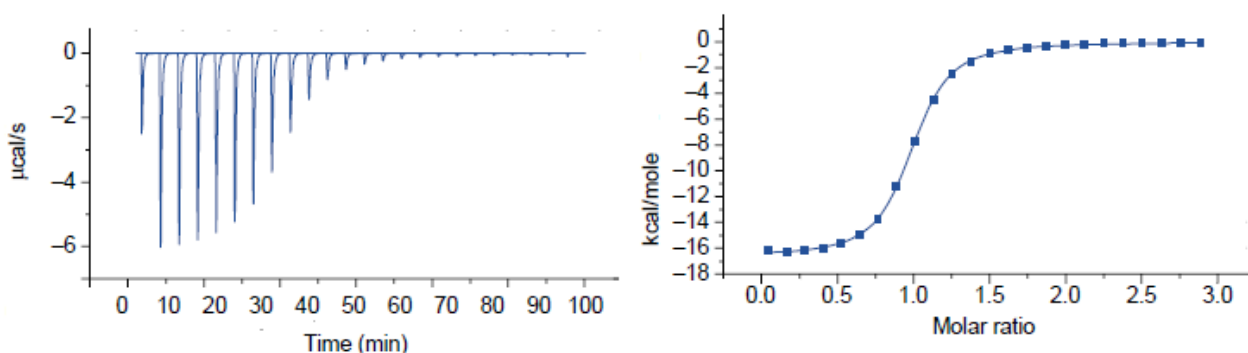


*Figure 70:Typical date obtained from ITC measurement. Heat vs. time (left) and heat change pr. injection with curve fitting (right).[83]*

From the data ΔG and ΔS can be calculated.

$$\Delta G = -RTlnK_A = \Delta H - T\Delta S$$

*Equation 2: Gibbs free energy.*

$K_A$ is known as the association constant, opposite the dissociation constant ($K_D$), which is used to evaluate the strengths of the interaction. The smaller the $K_D$ value, the greater the binding affinity meaning that a very small amount of drug will dissociate from the CD, as shown by equation 3.

$$K_D = \frac{[Drug]_{free}[CD]_{free}}{[Drug/CD]_{complex}} = \frac{1}{K_A}$$

*Equation 3: Association constant ($K_A$) and dissociation constant ($K_D$).*

The shape and position of the curve shown in figure 70 depends on multiple factors. The enthalpy affects the interception with the y-axis, the stoichiometry has an impact on the position of the inflection point and the shape of the curve depends on the unitless parameter C (also called the Wiseman C-parameter). C is influenced by the binding constant, concentration and stoichiometry and is given by:

$$C = K \times M \times n$$

*Equation 4: Parameter C, given by K (binding constant), M (total macromolecule concentration in the cell at the start of the experiment) and n (stoichiometry).*

When C is too high, the curvature in the binding isotherms for binding systems with varying K-values, will no longer appear unique. Likewise, when C is too low, the isotherms become too flat to be distinguishable. Ideally C should be somewhere above 10 (better if above 50) and below 3000.[84]

## 7.2 β-CD

As mentioned previously, adamantane and β-CD have a tight fit and it was therefore decided to test how the modified prodrugs would complex with native β-CD and β-CD derivatives. Four β-CD derivatives were chosen for the ITC measurements; 2-hydroxypropyl-β-CD (HP), methyl-β-CD (M), sulfobutylether-β-CD (SBE) and dextran-β-CD (DβCD). Looking at the chosen β-CD from a pharmaceutical point of view neither native β-CD or MβCD are ideal candidates as native βCD has low water solubility and MβCDs has strong systemic toxicity as mentioned earlier. Both SBEβCD and HPβCD have the lowest hemolytic effect and would therefore be good candidates. The hope is therefore that the binding affinity is higher for SBEβCD and HPβCD than native β-CD.

## 7.3 Complexation of Dox products

Solutions were made of each of the two synthesized Dox prodrugs (**1**) and (**4**). 2 mg were partly dissolved in water (150 ml). In order to get all the compound dissolved, both were placed in an ultrasonic bath for 5 min. and hereafter left to stir at 44°C overnight. This was enough for the remainder of the product to dissolve. The concentration of the solution came to 0.0161 mM for (**1**)

and 0.0164 mM for (**4**), which is low and not optimal for the ITC measurements. Therefore, solutions of the β-CDs were made in 1mM and 0.5mM. Measurements were carried out at 25 °C to ensure that the prodrugs. (**1**) formed complexes with all tested β-CDs (at 1 mM) except HPβCD, whereas (**4**) only formed complex with one β-CD derivative. Examples of the resulting data from the ITC measurement can be seen in figure 71 and 72.
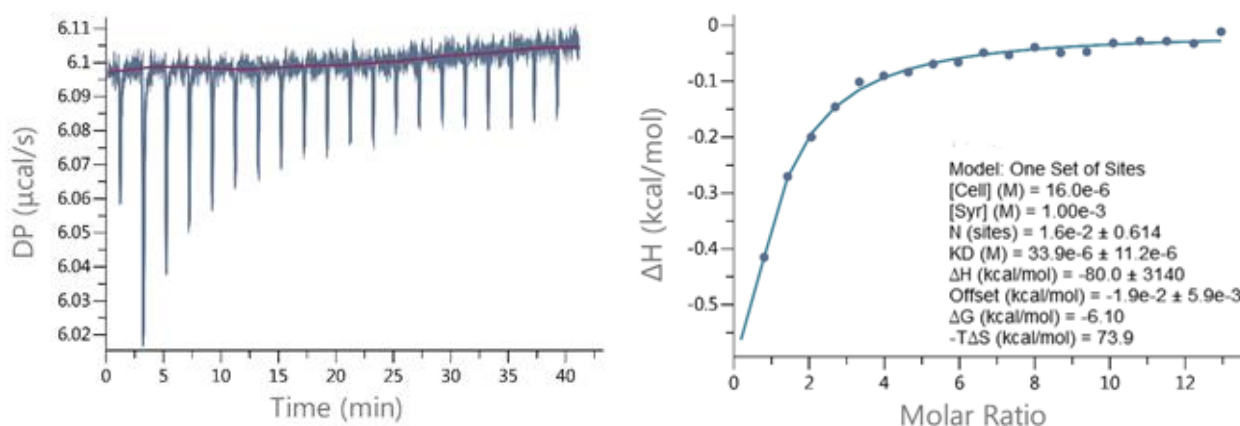


*Figure 71: ITC raw data (left) and Wiseman plot (right) of native β-CD and (1).*
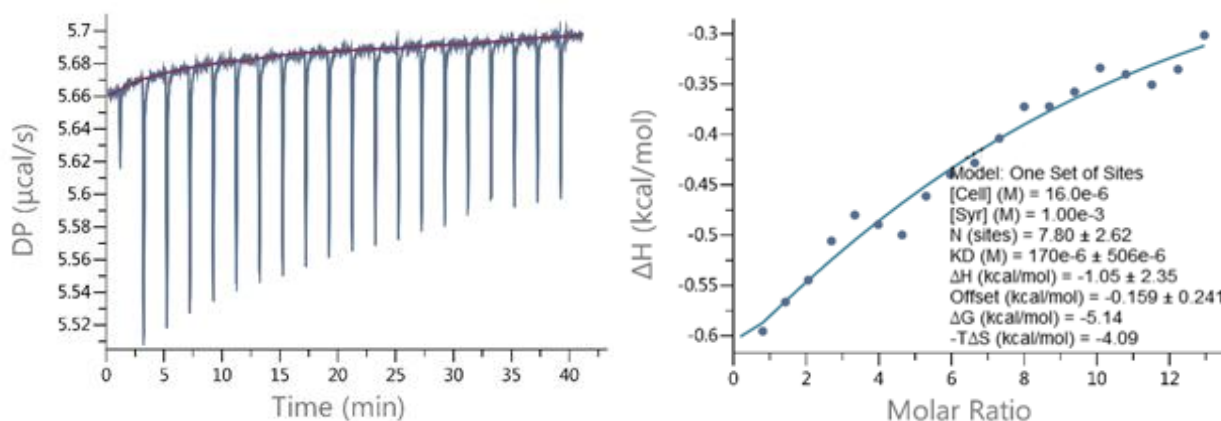


*Figure 72: ITC raw data (left) and Wiseman plot (right) of native SBEβCD and (4).*

The plots in general, are not the best, as the experiments were carried out with a low C parameter due to low concentration of prodrugs. Because of the poor fit it is justifiable to set the number of sites n=1 on condition that the data do not systematically deviate, examples can be seen in figure 73.
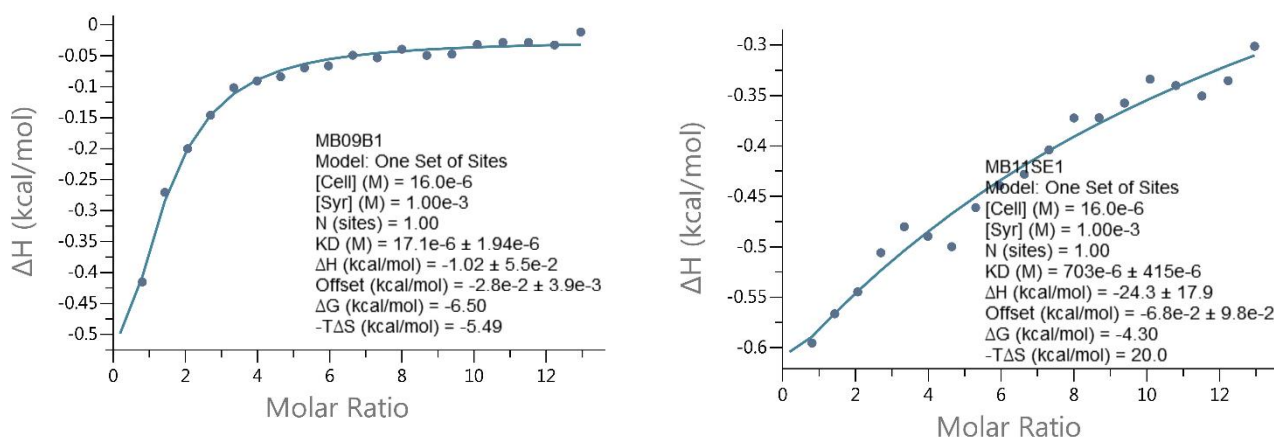
*Figure 73: Wiseman plot with N=1 for native βCD and (**1**)(right) and SBEβCD and (**4**) (left)*

All values seemed to improve upon fixating n=1. The reduced $\chi^2$ did not change significantly. $K_D$ got lower and the uncertainty attached to each value got smaller. $\Delta G$ remained approximately the same while $\Delta H$ and -T$\Delta S$ got less negative. These values were therefore judged to be valid and an overview of these can be seen in table 4.

| Compound | n | $K_A$ (M$^{-1}$) | $\Delta H$ (Kcal/mol) | -T$\Delta S$ (Kcal/mol) |
|---|---|---|---|---|
| (**1**)-βCD1 | 1 | 58480 | -1.02 | -5.49 |
| (**1**)-MβCD1 | 1 | 84746 | -0.424 | 6.30 |
| (**1**)-SBEβCD1 | 1 | 3802 | -9.79 | 4.90 |
| (**1**)-DβCD1 | 1 | 86957 | -1.20 | -5.54 |
| (**1**)-DβCD0.5 | 1 | 160772 | -0.852 | -6.25 |
| (**4**)-SBEβCD1 | 1 | 1422 | -24.3 | 20 |

*Table 4: Overview of measurements from ITC for (**1**) and (**4**).*

Figure 74 illustrates the binding affinities for complexes between prodrug (**1**) and the different β-CDs. The higher the $K_a$ value, the greater the binding affinity and from figure 74 it is clear to see that (**1**)-DβCD has the greatest binding affinity. Both native (**1**)-βCD and (**1**)-MβCD have high $K_a$ values ≥ 55000 Kcal/mol. (**1**)-SBEβCD and (**4**)-SBEβCD can be found in the lower end.
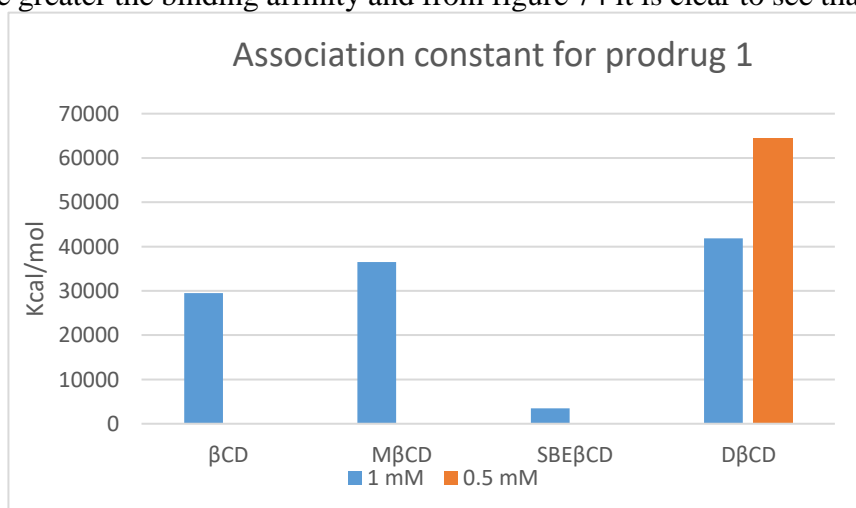


*Figure 74: Column diagram of $K_a$.*

## 7.4 Complexation of Gem products

2 mg of (**5**) was partly dissolved in water (100 ml). In order to get all the compound dissolved, it was placed in an ultrasonic bath for 5 min. and hereafter left to stir at 40°C. for 24 h. Unfortunately, the product did not dissolve completely. Because of this, it would not be possible to calculate an accurate concentration and the ITC measurement would not give useful results. It was therefore decided not to test the product any further. Prodrug (**8**) dissolved quite easily as 2 mg was dissolved in water (15 ml) giving a concentration of 0.251 mM. Solutions of the β-CDs were made in 5 and 2 mM. The measurements were carried out at 25 °C, as these were carried out along with measurements of (**1**) and (**4**). Both concentrations seemed to high as the curves indicated an almost complete saturation upon the first addition for all except HPβCD. The data from these measurements are therefore not reliable. New measurements were carried out with a concentration of βCD ~ 1mM. The plots in general, are not great as the C parameter is rather low. This makes the fitting difficult and because of the poor fit it is justifiable to set the number of sites n=1, however most of the data set systematically deviated and so these fits were discarded (can be seen in appendix).

| Compound | n | $K_A$ (M$^{-1}$) | ΔH (Kcal/mol) | -TΔS (Kcal/mol) |
|---|---|---|---|---|
| (**8**)-βCD5 | 0.00183 | 27173 | -80.0 | 74.0 |
| (**8**)-βCD2 | 0.00182 | 50000 | -80.0 | 73.6 |
| (**8**)-βCD1 | 0.00173 | 81301 | -80.0 | 73.3 |
| (**8**)-MβCD5 | 0.0012 | 12361 | -80.0 | 74.4 |
| (**8**)-MβCD2 | 0.001 | 43860 | -71.5 | 65.1 |
| (**8**)-MβCD1 | 0.001 | 123762 | -74.2 | 67.2 |
| (**8**)-HPβCD5 | 2.22 | 4386 | -0.256 | -4.71 |
| (**8**)-HPβCD2 | 0.0011 | 39841 | -80.0 | 73.7 |
| (**8**)-SBEβCD5 | 0.032 | 1767 | -80.0 | 75.6 |
| (**8**)-SBEβCD2 | 0.0084 | 5882 | -80.0 | 74.9 |
| (**8**)-SBEβCD1 | 0.0023 | 25773 | -80.0 | 74.0 |
| (**8**)-DβCD5 | 0.0026 | 23670 | -80.0 | 74.0 |
| (**8**)-DβCD2 | 0.0025 | 50000 | -80.0 | 73.6 |
| (**8**)-DβCD1 | 0.0026 | 60606 | -80.0 | 73.5 |

*Table 5: Overview of data obtained from ITC measurements of product (8) and β-CDs).*

In order to better show the difference in binding affinity, the $K_D$ values were converted to $K_A$ values as seen in figure 75. To illustrate the difference between the different concentrations $K_A$ values



Associaltion constant for prodrug 8
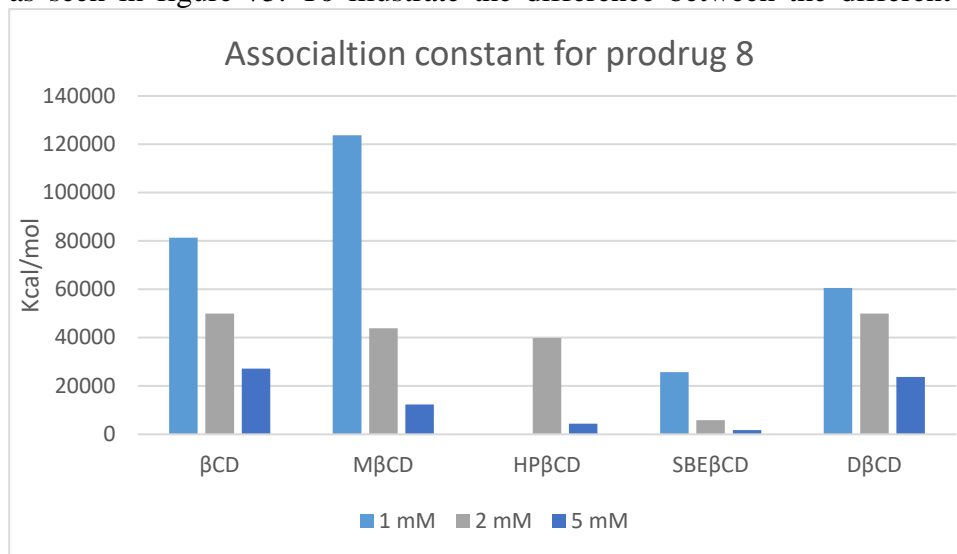
obtained from the experiment with 5 mM and 2 mM are shown as well. It is clear to see that MβCD has the greatest affinity followed by native βCD and DβCD. Neither HPβCD nor SBEβCD bind with great affinity.

*Figure 75: Column diagram of Ka.*

Apart from binding affinity, the ITC also gave ΔG, ΔH and ΔS, as shown in figure 76. All experiments showed a negative ΔG, as shown in table 5, which indicates that all complex formations are spontaneous. Another way to see this is to look at ΔS and ΔH. If $\Delta S > 0$ and $\Delta H < 0$ it is a spontaneous process, which is the case for almost all the investigated complexes; native βCD, MβCD, SBEβCD and DβCD. In the case of HPβCD where $\Delta S < 0$ and $\Delta H < 0$, the process will be spontaneous at low temperatures and non-spontaneous at high temperatures. Generally it is possible to assess which non-covalent interactions are involved by looking at ΔH and ΔS. Van der Waals interactions are entropy driven ($\left|\Delta H\right| > \left|T\Delta S\right|$) with minor entropies (favourable or unfavourable) while hydrophobic interactions are entropy driven ($\left|\Delta H\right| < \left|T\Delta S\right|$)



*Figure 76: ΔG, ΔH and ΔS.*

with small enthalpies.[85] The numeric difference between ΔH and -TΔS are too small to make an assessment.
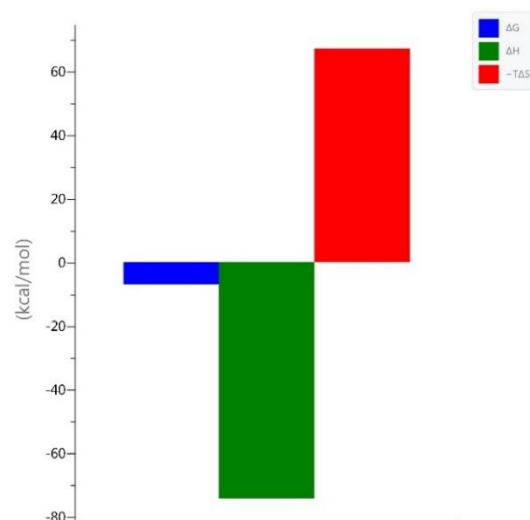
# 8. Conclusion

The overall aim was to investigate the possibilities of modifying Gem and Dox with adamantane to enhance complexation with cyclodextrins. There were some unforeseen issues along the way, however most were overcome. The synthesis of the two Gemcitabine prodrugs caused a lot of difficulty and made it necessary to find alternative methods of synthesis. The protection of Gem was the first issue and the overall yield ended up around 53 %. The synthesis of N-adamantanoylglycine was challenging and a variety of methods were employed and ended up yielding around 60-80 %. The two prodrugs were obtained in ~ 15-20 mg. The synthesis of the two Doxorubicin prodrugs were fairly straight forward. The reactions went in quite good yields with 4-((adamantan-1-yl)disulfaneyl)butanoic acid having the lowest yield of 56 %. The most difficulty was the purification of the final two products and the probable cause of the low yield. The two prodrugs were obtained in ~10 mg.

When it came time for the ITC measurements, the modified drugs had to be dissolved in water. This was not easy, but in the end three out of four were dissolved and ITC measurements were carried out on all three with five different β-CDs.

Prodrug (**4**) only showed an affinity for SBEβCD whereas prodrug (**1**) had affinity for four and (**8**) for all of the βCDs tested. The ITC measurements showed that the synthesized prodrugs generally have a high affinity for native βCD as well as MβCD and DβCD.

# 9. Further work

The purification (**1**) and (**4**) was not ideal and products were lost in the process. Should one want to synthesis these molecules again, it is worth looking into alternative columns that would suit the molecules better. The same goes for (**10**) and (**13**) which had some of the same difficulty as the Dox prodrugs.

Looking beyond the synthesis and with the products in hand, it should be tested if the release mechanism, as proposed in section 2.5, works as intended. Assuming that it works as planned, it would be interesting to study the release rate of the prodrug from the CD complex. This is an aspect this study did not touch on and it would give an indication as to whether or not these prodrug designs are adequate. If not, new modifications could be made.

# 10. References

1.          Cancer, I. A. f. R. o. All Cancers (excluding non-melanoma skin cancer) Estimated Incidence, Mortality and Prevalence Worldwide in 2012. (accessed 31-08-2016).

2.          Are, C.; Rajaram, S.; Are, M.; Raj, H.; Anderson, B. O.; Chaluvarya Swamy, R.; Vijayakumar, M.; Song, T.; Pandey, M.; Edney, J. A.; Cazap, E. L., A review of global cancer burden: trends, challenges, strategies, and a role for surgeons. *Journal of surgical oncology* **2013,** *107* (2), 221-6.

3.          Hanahan, D.; Weinberg, R. A., The hallmarks of cancer. *Cell* **2000,** *100* (1), 57-70.

4.          *World Cancer Report 2014*. The International Agency for Research on Cancer: https://shop.iarc.fr/products/wcr2014, 2014

5.          Hanahan, D.; Weinberg, R. A., Hallmarks of cancer: the next generation. *Cell* **2011,** *144* (5), 646-74.

6.          Malumbres, M.; Barbacid, M., To cycle or not to cycle: a critical decision in cancer. *Nature reviews. Cancer* **2001,** *1* (3), 222-31.

7.          Malumbres, M.; Barbacid, M., Cell cycle, CDKs and cancer: a changing paradigm. *Nature reviews. Cancer* **2009,** *9* (3), 153-66.

8.          Lu, B.; Finn, O. J., T-cell death and cancer immune tolerance. *Cell death and differentiation* **2008,** *15* (1), 70-9.

9.          Corthay, A., Does the immune system naturally protect against cancer? *Frontiers in immunology* **2014,** *5*, 197.

10.         Topalian, S. L.; Taube, J. M.; Anders, R. A.; Pardoll, D. M., Mechanism-driven biomarkers to guide immune checkpoint blockade in cancer therapy. *Nature reviews. Cancer* **2016,** *16* (5), 275-87.

11.         Espinosa, E.; Zamora, P.; Feliu, J.; Gonzalez Baron, M., Classification of anticancer drugs--a new system based on therapeutic targets. *Cancer treatment reviews* **2003,** *29* (6), 515-23.

12.         Brigger, I.; Dubernet, C.; Couvreur, P., Nanoparticles in cancer therapy and diagnosis. *Advanced drug delivery reviews* **2002,** *54* (5), 631-51.

13.         Greish, K., Enhanced permeability and retention (EPR) effect for anticancer nanomedicine drug targeting. *Methods in molecular biology* **2010,** *624*, 25-37.

14.         Cho, K.; Wang, X.; Nie, S.; Chen, Z. G.; Shin, D. M., Therapeutic nanoparticles for drug delivery in cancer. *Clinical cancer research : an official journal of the American Association for Cancer Research* **2008,** *14* (5), 1310-6.

15.         Hassett, M. J.; O'Malley, A. J.; Pakes, J. R.; Newhouse, J. P.; Earle, C. C., Frequency and cost of chemotherapy-related serious adverse effects in a population sample of women with breast cancer. *Journal of the National Cancer Institute* **2006,** *98* (16), 1108-17.

16.         Russo, A.; Autelitano, M.; Bisanti, L., Re: Frequency and cost of chemotherapy-related serious adverse effects in a population sample of women with breast cancer. *Journal of the National Cancer Institute* **2006,** *98* (24), 1826-7.

17.         Thorn, C. F.; Oshiro, C.; Marsh, S.; Hernandez-Boussard, T.; McLeod, H.; Klein, T. E.; Altman, R. B., Doxorubicin pathways: pharmacodynamics and adverse effects. *Pharmacogenetics and genomics* **2011,** *21* (7), 440-6.

18.         Ross, W. E.; Glaubiger, D. L.; Kohn, K. W., Protein-associated DNA breaks in cells treated with adriamycin or ellipticine. *Biochimica et biophysica acta* **1978,** *519* (1), 23-30.

19.         Tewey, K. M.; Rowe, T. C.; Yang, L.; Halligan, B. D.; Liu, L. F., Adriamycin-induced DNA damage mediated by mammalian DNA topoisomerase II. *Science* **1984,** *226* (4673), 466-8.

20.         Bodley, A.; Liu, L. F.; Israel, M.; Seshadri, R.; Koseki, Y.; Giuliani, F. C.; Kirschenbaum, S.; Silber, R.; Potmesil, M., DNA topoisomerase II-mediated interaction of doxorubicin and daunorubicin congeners with DNA. *Cancer research* **1989,** *49* (21), 5969-78.

21.         Gewirtz, D. A., A critical evaluation of the mechanisms of action proposed for the antitumor effects of the anthracycline antibiotics adriamycin and daunorubicin. *Biochemical pharmacology* **1999,** *57* (7), 727-41.

22.         Minotti, G.; Recalcati, S.; Mordente, A.; Liberi, G.; Calafiore, A. M.; Mancuso, C.; Preziosi, P.; Cairo, G., The secondary alcohol metabolite of doxorubicin irreversibly inactivates aconitase/iron

regulatory protein-1 in cytosolic fractions from human myocardium. *FASEB journal : official publication of the Federation of American Societies for Experimental Biology* **1998,** *12* (7), 541-52.

23.     Garsky, V. M.; Lumma, P. K.; Feng, D. M.; Wai, J.; Ramjit, H. G.; Sardana, M. K.; Oliff, A.; Jones, R. E.; DeFeo-Jones, D.; Freidinger, R. M., The synthesis of a prodrug of doxorubicin designed to provide reduced systemic toxicity and greater target efficacy. *Journal of medicinal chemistry* **2001,** *44* (24), 4216-24.

24.     Malfanti, A.; Miletto, I.; Bottinelli, E.; Zonari, D.; Blandino, G.; Berlier, G.; Arpicco, S., Delivery of Gemcitabine Prodrugs Employing Mesoporous Silica Nanoparticles. *Molecules* **2016,** *21* (4), 522.

25.     Nussbaumer, S.; Bonnabry, P.; Veuthey, J. L.; Fleury-Souverain, S., Analysis of anticancer drugs: a review. *Talanta* **2011,** *85* (5), 2265-89.

26.     de Sousa Cavalcante, L.; Monteiro, G., Gemcitabine: metabolism and molecular mechanisms of action, sensitivity and chemoresistance in pancreatic cancer. *European journal of pharmacology* **2014,** *741*, 8-16.

27.     Dasari, M.; Acharya, A. P.; Kim, D.; Lee, S.; Lee, S.; Rhea, J.; Molinaro, R.; Murthy, N., H-gemcitabine: a new gemcitabine prodrug for treating cancer. *Bioconjugate chemistry* **2013,** *24* (1), 4-8.

28.     Dubey, R. D.; Saneja, A.; Gupta, P. K.; Gupta, P. N., Recent advances in drug delivery strategies for improved therapeutic efficacy of gemcitabine. *European journal of pharmaceutical sciences : official journal of the European Federation for Pharmaceutical Sciences* **2016,** *93*, 147-62.

29.     Muller, C. E., Prodrug approaches for enhancing the bioavailability of drugs with low solubility. *Chemistry & biodiversity* **2009,** *6* (11), 2071-83.

30.     Rautio, J.; Kumpulainen, H.; Heimbach, T.; Oliyai, R.; Oh, D.; Jarvinen, T.; Savolainen, J., Prodrugs: design and clinical applications. *Nature reviews. Drug discovery* **2008,** *7* (3), 255-70.

31.     Mahato, R.; Tai, W.; Cheng, K., Prodrugs for improving tumor targetability and efficiency. *Advanced drug delivery reviews* **2011,** *63* (8), 659-70.

32.     Iyer, A. K.; Khaled, G.; Fang, J.; Maeda, H., Exploiting the enhanced permeability and retention effect for tumor targeting. *Drug discovery today* **2006,** *11* (17-18), 812-8.

33.     Matsumura, Y.; Maeda, H., A new concept for macromolecular therapeutics in cancer chemotherapy: mechanism of tumoritropic accumulation of proteins and the antitumor agent smancs. *Cancer research* **1986,** *46* (12 Pt 1), 6387-92.

34.     Nakamura, Y.; Mochida, A.; Choyke, P. L.; Kobayashi, H., Nanodrug Delivery: Is the Enhanced Permeability and Retention Effect Sufficient for Curing Cancer? *Bioconjugate chemistry* **2016**.

35.     Blanco, E.; Shen, H.; Ferrari, M., Principles of nanoparticle design for overcoming biological barriers to drug delivery. *Nature biotechnology* **2015,** *33* (9), 941-51.

36.     Tanaka, T.; Shiramoto, S.; Miyashita, M.; Fujishima, Y.; Kaneo, Y., Tumor targeting based on the effect of enhanced permeability and retention (EPR) and the mechanism of receptor-mediated endocytosis (RME). *International journal of pharmaceutics* **2004,** *277* (1-2), 39-61.

37.     Maeda, H., The enhanced permeability and retention (EPR) effect in tumor vasculature: the key role of tumor-selective macromolecular drug targeting. *Advances in enzyme regulation* **2001,** *41*, 189-207.

38.     Lehn, J.-M., Supramolecular chemistry - Scope and perspectives. Molecules, supermolecules, and molecular devices, (Nobel Lecture, 8.12.1987). *Angew. Chem., Int. Ed. Engl* **1988,** *27*, 89-112.

39.     2014, N. M. A. Press Release: The 1987 Nobel Prize in Chemistry. (accessed 19-04-2017).

40.     Ma, X.; Zhao, Y., Biomedical Applications of Supramolecular Systems Based on Host-Guest Interactions. *Chemical reviews* **2015,** *115* (15), 7794-839.

41.     Trotta, F.; Zanetti, M.; Cavalli, R., Cyclodextrin-based nanosponges as drug carriers. *Beilstein journal of organic chemistry* **2012,** *8*, 2091-9.

42.     Gidwani, B.; Vyas, A., A Comprehensive Review on Cyclodextrin-Based Carriers for Delivery of Chemotherapeutic Cytotoxic Anticancer Drugs. *BioMed research international* **2015,** *2015*, 198268.

43.     Tiwari, G.; Tiwari, R.; Rai, A. K., Cyclodextrins in delivery systems: Applications. *Journal of pharmacy & bioallied sciences* **2010,** *2* (2), 72-9.

44.     Davis, M. E.; Brewster, M. E., Cyclodextrin-based pharmaceutics: past, present and future. *Nature reviews. Drug discovery* **2004,** *3* (12), 1023-35.

45.     Paolino, M.; Ennen, F.; Lamponi, S.; Cernescu, M.; Voit, B.; Cappelli, A.; Appelhans, D.; Komber, H., Cyclodextrin-Adamantane Host−Guest Interactions on the Surface of Biocompatible Adamantyl-Modified Glycodendrimers. *Macromolecules* **2013,** *46*, 3215-3227.

46. Loftsson, T.; Duchene, D., Cyclodextrins and their pharmaceutical applications. *International journal of pharmaceutics* **2007,** *329* (1-2), 1-11.

47. Stella, V. J.; He, Q., Cyclodextrins. *Toxicologic pathology* **2008,** *36* (1), 30-42.

48. Gigliotti, C. L.; Minelli, R.; Cavalli, R.; Occhipinti, S.; Barrera, G.; Pizzimenti, S.; Cappellano, G.; Boggio, E.; Conti, L.; Fantozzi, R.; Giovarelli, M.; Trotta, F.; Dianzani, U.; Dianzani, C., In Vitro and In Vivo Therapeutic Evaluation of Camptothecin-Encapsulated beta-Cyclodextrin Nanosponges in Prostate Cancer. *Journal of biomedical nanotechnology* **2016,** *12* (1), 114-27.

49. Brewster, M. E.; Loftsson, T., Cyclodextrins as pharmaceutical solubilizers. *Advanced drug delivery reviews* **2007,** *59* (7), 645-66.

50. Loftsson, T.; Brewster, M. E., Pharmaceutical applications of cyclodextrins: basic science and product development. *The Journal of pharmacy and pharmacology* **2010,** *62* (11), 1607-21.

51. di Cagno, M.; Terndrup Nielsen, T.; Lambertsen Larsen, K.; Kuntsche, J.; Bauer-Brandl, A., beta-Cyclodextrin-dextran polymers for the solubilization of poorly soluble drugs. *International journal of pharmaceutics* **2014,** *468* (1-2), 258-63.

52. Erdogar, N.; Esendagli, G.; Nielsen, T. T.; Sen, M.; Oner, L.; Bilensoy, E., Design and optimization of novel paclitaxel-loaded folate-conjugated amphiphilic cyclodextrin nanoparticles. *International journal of pharmaceutics* **2016,** *509* (1-2), 375-90.

53. Granadero, D.; Bordello, J.; Perez-Alvite, M. J.; Novo, M.; Al-Soufi, W., Host-guest complexation studied by fluorescence correlation spectroscopy: adamantane-cyclodextrin inclusion. *International journal of molecular sciences* **2010,** *11* (1), 173-88.

54. Eftink, M. R.; Andy, M. L.; Bystrom, K.; Perlmutter, H. D.; Kristolt, D. S., Cyclodextrin Inclusion Complexes: Studies of the Variation in the Size of Alicyclic Guests. *J. Am. Chem. Soc.* **1989,** *111* (17), 6765-6112.

55. Carrazana, J.; Jover, A.; Meijide, F.; Soto, V. H.; Vazquez Tato, J., Complexation of adamantyl compounds by beta-cyclodextrin and monoaminoderivatives. *The journal of physical chemistry. B* **2005,** *109* (19), 9719-26.

56. Fan, H.; Hu, Q. D.; Xu, F. J.; Liang, W. Q.; Tang, G. P.; Yang, W. T., In vivo treatment of tumors using host-guest conjugated nanoparticles functionalized with doxorubicin and therapeutic gene pTRAIL. *Biomaterials* **2012,** *33* (5), 1428-36.

57. Altreuter, D. H.; Dordick, J. S.; Clark, D. S., Nonaqueous biocatalytic synthesis of new cytotoxic doxorubicin derivatives: exploiting unexpected differences in the regioselectivity of salt-activated and solubilized subtilisin. *Journal of the American Chemical Society* **2002,** *124* (9), 1871-6.

58. Han, H.; Wang, H.; Chen, Y.; Li, Z.; Wang, Y.; Jin, Q.; Ji, J., Theranostic reduction-sensitive gemcitabine prodrug micelles for near-infrared imaging and pancreatic cancer therapy. *Nanoscale* **2016,** *8* (1), 283-91.

59. Joule, J. A.; Mills, K., *Heterocyclic Chemistry, fifth edition* Wiley: 2010.

60. Hunter, R.; Caira, M.; Stellenboom, N., Inexpensive, one-pot synthesis of unsymmetrical disulfides using 1-chlorobenzotriazole. *The Journal of organic chemistry* **2006,** *71* (21), 8268-71.

61. Mandal, B.; Basu, B., Recent advances in S-S bond formation. *RSC Adv.* **2014,** *4*, 13854-13881.

62. Lushchak, V. I., Glutathione homeostasis and functions: potential targets for medical interventions. *Journal of amino acids* **2012,** *2012*, 736837.

63. Lee, M. H.; Yang, Z.; Lim, C. W.; Lee, Y. H.; Dongbang, S.; Kang, C.; Kim, J. S., Disulfide-cleavage-triggered chemosensors and their biological applications. *Chemical reviews* **2013,** *113* (7), 5071-109.

64. Deng, B.; Ma, P.; Xie, Y., Reduction-sensitive polymeric nanocarriers in cancer therapy: a comprehensive review. *Nanoscale* **2015,** *7* (30), 12773-95.

65. Clayden, J.; Greeves, N.; Warren, S.; Wothers, P., *Organic chemistry*. Oxford University press: 2009.

66. Gottlieb, H. E.; Kotlyar, V.; Nudelman, A., NMR Chemical Shifts of Common Laboratory Solvents as Trace Impurities. *The Journal of organic chemistry* **1997,** *62* (21), 7512-7515.

67. Nielsen, T. T.; Wintgens, V.; Amiel, C.; Wimmer, R.; Larsen, K. L., Facile synthesis of beta-cyclodextrin-dextran polymers by "click" chemistry. *Biomacromolecules* **2010,** *11* (7), 1710-5.

68. Chen, Y.; Wang, A.; Tao, Z.; Deng, Y.; Hu, X., A facile synthesis of saxagliptin intermediate N-Boc-3-hydroxyadamantylglycine. *Res Chem Intermed* **2015,** *41*, 4113–4121.

69. Kuethe, J. T.; Beutner, G. L., Synthesis of 2-arylindole-4-carboxylic Amides: [2-(4-fluorophenyl)-1H-indol-4-yl]-1-pyrrolidinylmethanone. *Org. Synth.* **2009,** *86*, 92-104.

70.        Hughes , T. V.; Hammond, S. D.; Cava, M. P., A Convenient New Synthesis of 1-Cyanobenzotriazole and Its Use as a C-Cyanating Reagent. *J. Org. Chem.* **1998,** *63* (2), 401–402.

71.        Song, X.; Lorenzi, P. L.; Landowski, C. P.; Vig, B. S.; Hilfinger, J. M.; Amidon, G. L., Amino acid ester prodrugs of the anticancer agent gemcitabine: synthesis, bioconversion, metabolic bioevasion, and hPEPT1-mediated transport. *Molecular pharmaceutics* **2005,** *2* (2), 157-67.

72.        Greenfield, R. S.; Kaneko, T.; Daues, A.; Edson, M. A.; Fitzgerald, K. A.; Olech, L. J.; Grattan, J. A.; Spitalny, G. L.; Braslawsky, G. R., Evaluation in vitro of adriamycin immunoconjugates synthesized using an acid-sensitive hydrazone linker. *Cancer research* **1990,** *50* (20), 6600-7.

73.        Purygin, P. P.; Danilin, A. A.; Klenova, N. A.; Makarova, N. V.; Moiseev, I. K., Synthesis and membranotropic activity of N-adamantanoylamino and N-adamantylacetylamino acids. *Pharm. Chem. J.* **1999,** *33* (3), 132-133.

74.        Guo Zw, Z.; Gallo, J. M., Selective Protection of 2',2'-Difluorodeoxycytidine (Gemcitabine). *The Journal of organic chemistry* **1999,** *64* (22), 8319-8322.

75.        Chhikara, B. S.; St Jean, N.; Mandal, D.; Kumar, A.; Parang, K., Fatty acyl amide derivatives of doxorubicin: synthesis and in vitro anticancer activities. *European journal of medicinal chemistry* **2011,** *46* (6), 2037-42.

76.        Williams, J. M. J., Acid Halides. In *Comprehensive Organic Functional Group Transformations*, Katritzky, A. R.; Meth-Cohn, O.; Rees, C. W., Eds. Elsevier Ltd.: 1995; Vol. 5, pp 1-21.

77.        Coskun, O., Separation techniques: Chromatography. *Northern clinics of Istanbul* **2016,** *3* (2), 156-160.

78.        Teledyne Isco, I., Effective Organic Compound Purification - Guidelines & Tactics for Flash Chromatography. Fourth Edition ed.; Teledyne Isco, Inc.: 2010.

79.        Chromacademy. Reverse Phase Chromatography.pdf, p. 1-93.

80.        Kim, I. W.; Lee, H. S.; Lee, Y. K.; Jang, M. D.; Par, J. H., Selectivity of amino-, cyano- and diol-bonded silica in reversed-phase liquid chromatography. *Journal of chromatography. A* **2001,** *915* (1-2), 35-42.

81.        Rabel, F. M., *Encyclopedia of Chromatography*. CRC Press: 2009; Vol. 1.

82.        Smith, R. M.; Miller, S. L., Comparison of the selectivity of cyano-bonded silica stationary phases in reversed-phase liquid chromatography. *Journal of Chromatography A* **1989,** *464*, 297-306

83.        Holdgate, G. A.; Ward, W. H., Measurements of binding thermodynamics in drug discovery. *Drug discovery today* **2005,** *10* (22), 1543-50.

84.        Malvern,        ITC        Expert        User's        Manual.        Malvern: https://biochem.wisc.edu/sites/default/files/facilities/bif/instrument_pdfs/ITC_Expert_Users_Manual.pdf, Vol. 2017, pp 1-18.

85.        Bouchemal, K.; Mazzaferro, S., How to conduct and interpret ITC experiments accurately for cyclodextrin–guest interactions. *Drug discovery today* **2012,** *17* (11-12), 623-629.

# 11. Appendix

## 11.1 1-adamantanecarbonyl chloride (7)

### 11.1.1. From thionyl chloride
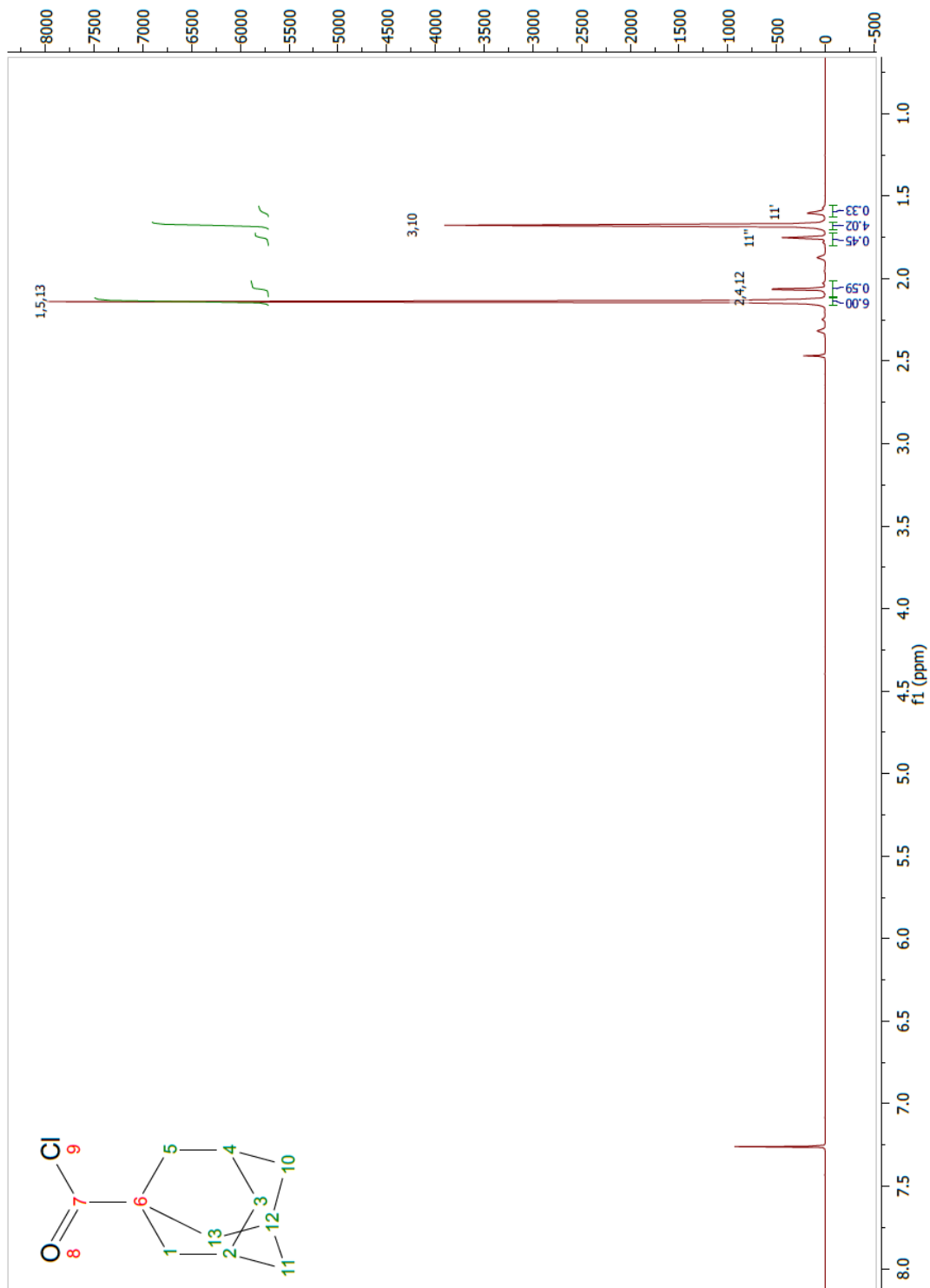


$^1$H NMR (CDCl$_3$): δ 2.14 (6H, m), 2.06 (3H, m), 1.75 (1H, m), 1.67 (4H), 1.60 (1H, m).

## 11.1.2 From oxalyl chloride
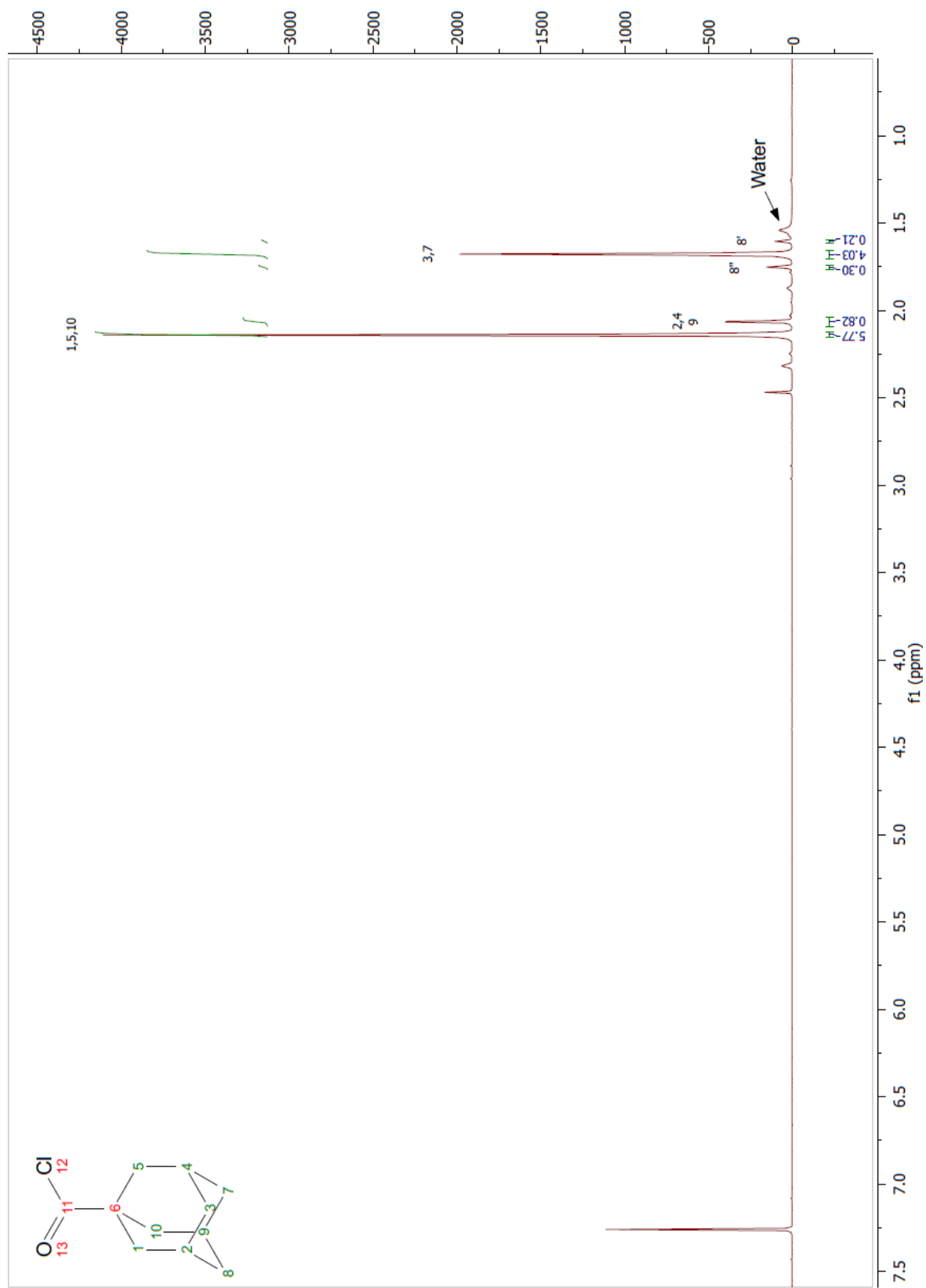


$^{1}$H NMR (CDCl$_3$): δ 2.14 (6H, m), 2.07 (3H, m), 1.75 (1H, m), 1.68 (4H), 1.60 (1H, m).

## 11.2 1-chlorobenzotriazole (9)
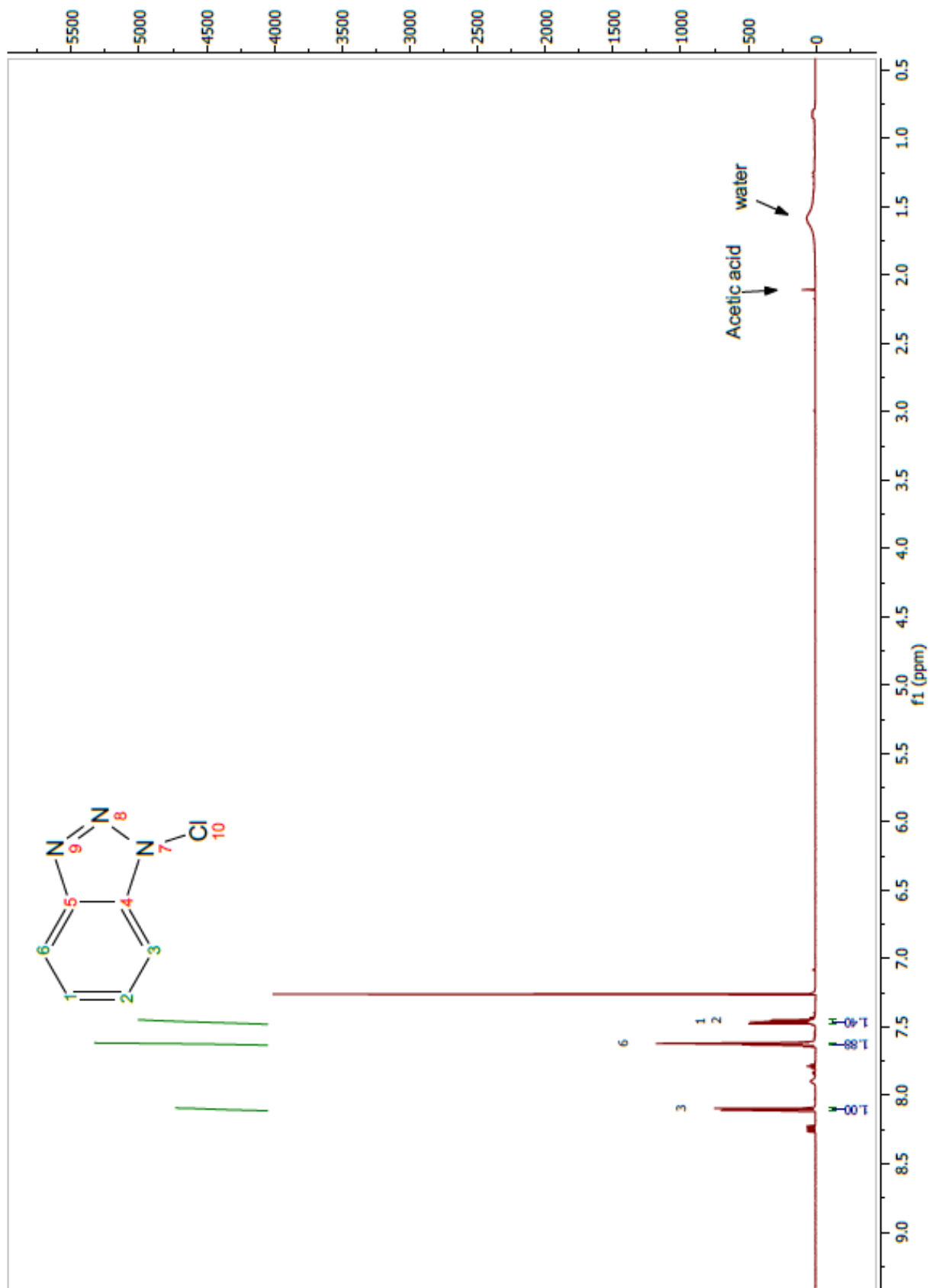


$^1$H NMR (CDCl$_3$): δ 8.10 (1H, dt, $J$=0.88, 8.32 Hz) 7.62 (1H, m) 7.46 (1H, m).

## 11.3 3-(((3s,5s,7s)-adamantan-1-yl)disulfaneyl)butanoic acid (3)

### 11.3.1 First attempt - purification

**REVELERIS™**
Flash Chromatography System

**Method Name:**
Run Name: 2017-01-11_10-33-19mb04
Run Date: 2017-01-11 10:45

Column: Reveleris® Silica 40g
Flow Rate: 40 mL/min
Equilibration: 7.1 min
Run Length: 30.5 min
Air Purge Time: 1 min

Slope Detection: Off
ELSD Threshold: 5 mV
UV Threshold: 0.02 AU
UV1 Wavelength: 254 nm
UV2 Wavelength: 280 nm

Collection Mode: Collect Peaks
Per-Vial Volume: 7 mL
Non-Peaks: 8.5 mL
Injection Type: Dry

ELSD Carrier: Iso-propanol
Solvent A: Methylene chlorid
Solvent B: Methanol
Solvent C: <No solvent chose
Solvent D: <No solvent chose
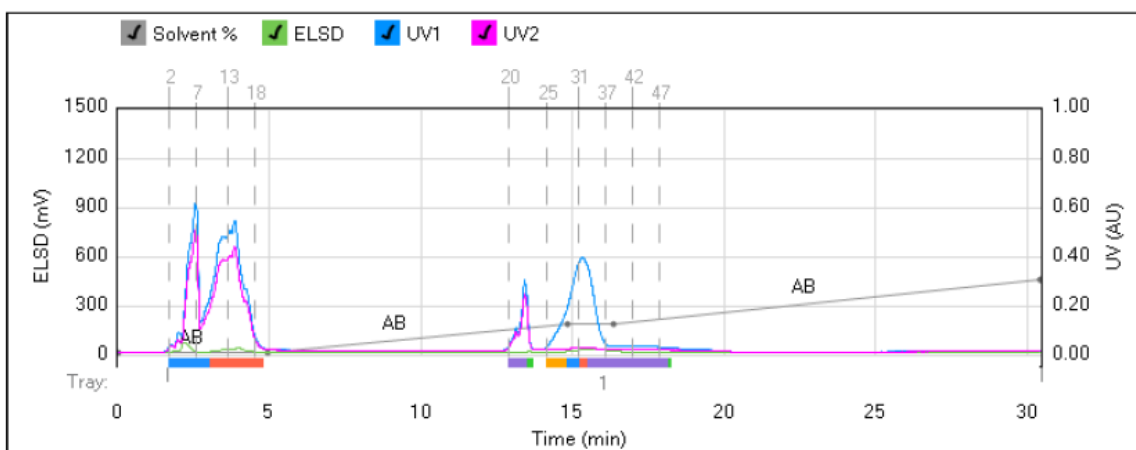


1 - 4019
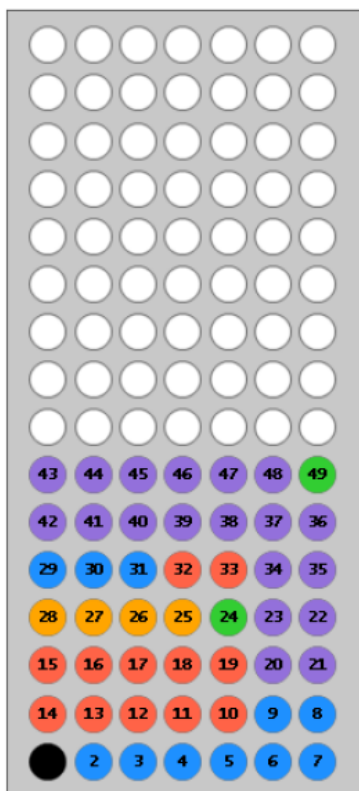


**Gradient Table**

|   | Min  | Solvents | % 2nd |
|---|------|----------|-------|
| 1 | 0.0  | AB       | 0     |
| 2 | 4.9  | AB       | 0     |
| 3 | 9.9  | AB       | 12    |
| 4 | 1.5  | AB       | 12    |
| 5 | 14.1 | AB       | 30    |

**Vial Mapping Table**

| Peak # | Start Tray:Vial | End Tray:Vial |
|--------|-----------------|---------------|
| 1      | 1:2             | 1:9           |
| 2      | 1:10            | 1:19          |
| 3      | 1:20            | 1:23          |
| 4      | 1:24            | 1:24          |
| 5      | 1:25            | 1:28          |
| 6      | 1:29            | 1:31          |
| 7      | 1:32            | 1:33          |
| 8      | 1:34            | 1:48          |
| 9      | 1:49            | 1:49          |

*¹H NMR fraction 5-7*
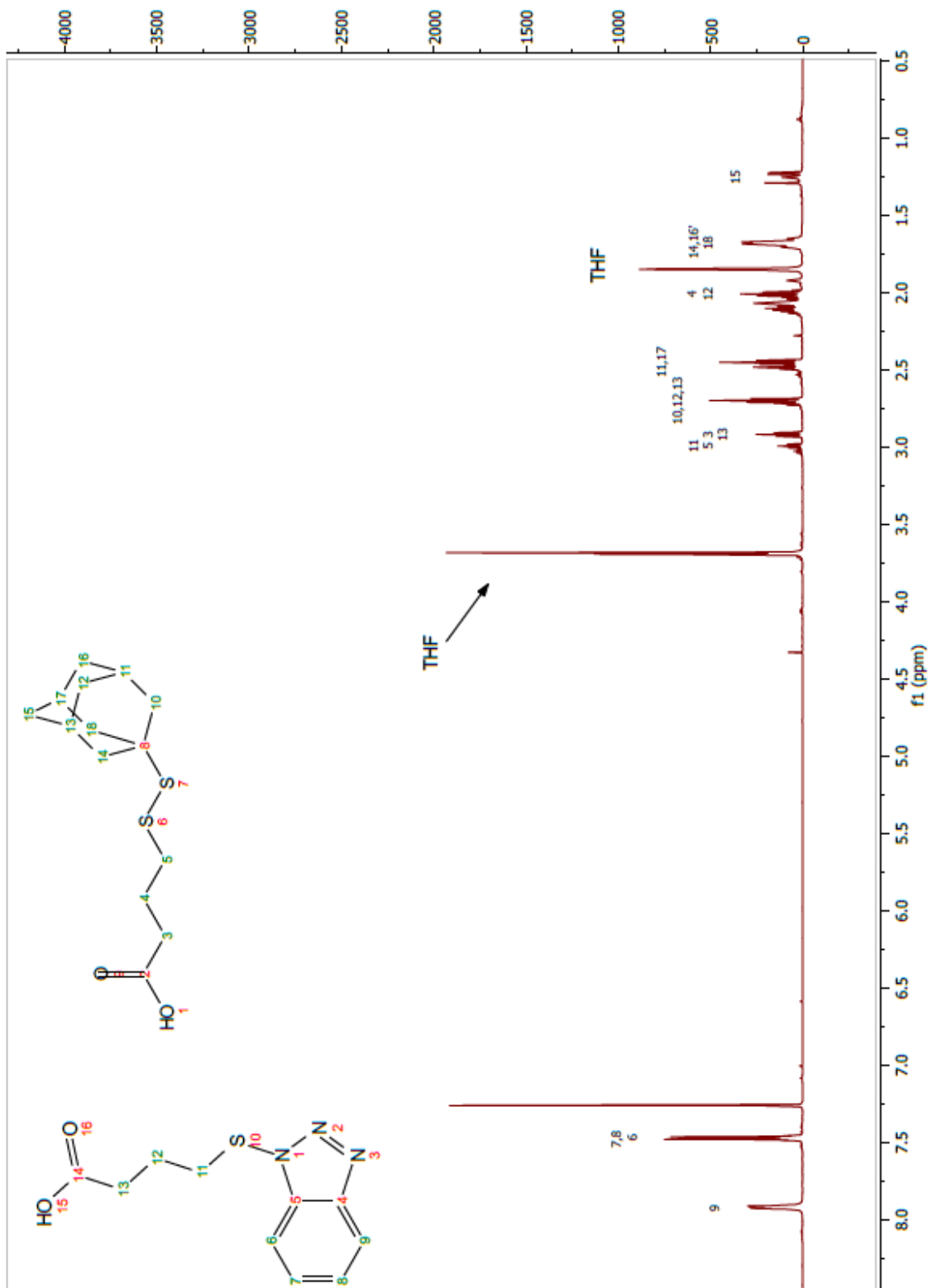


¹H NMR (CDCl₃): δ 7.92 (1H, m), 7.47 (3H, m), 2.99 (m), 2.92 (m), 2.69 (m), 2.49-2.43 (m), 2.14-1.97 (m), 1.85 (m), 1.68 (m), 1.29 (m), 1.23 (m).

*¹H NMR fraction 8-17*
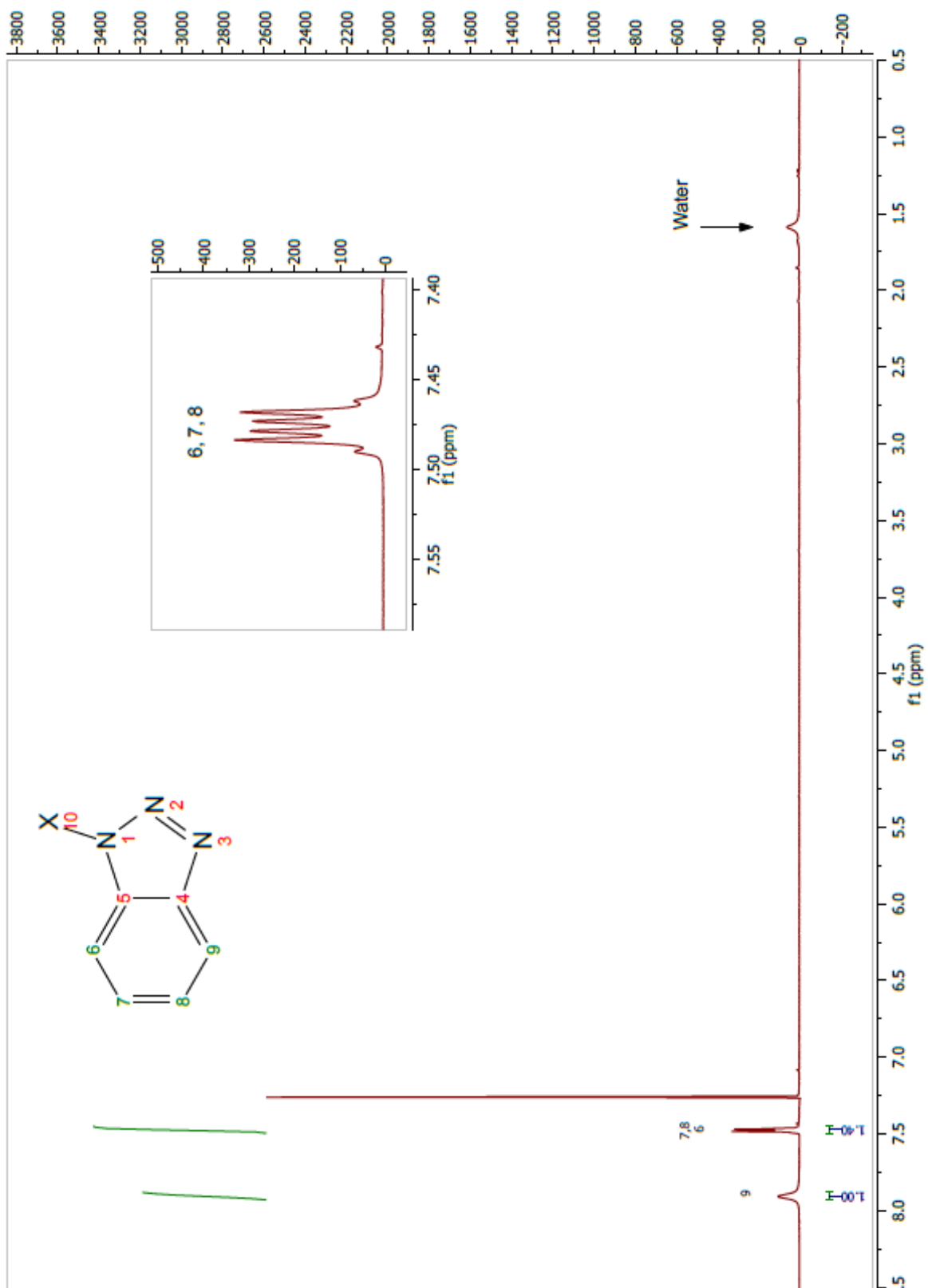


X= Cl or H
¹H NMR (CDCl₃): δ 7.91 (1H), 7.48 (3H, m).
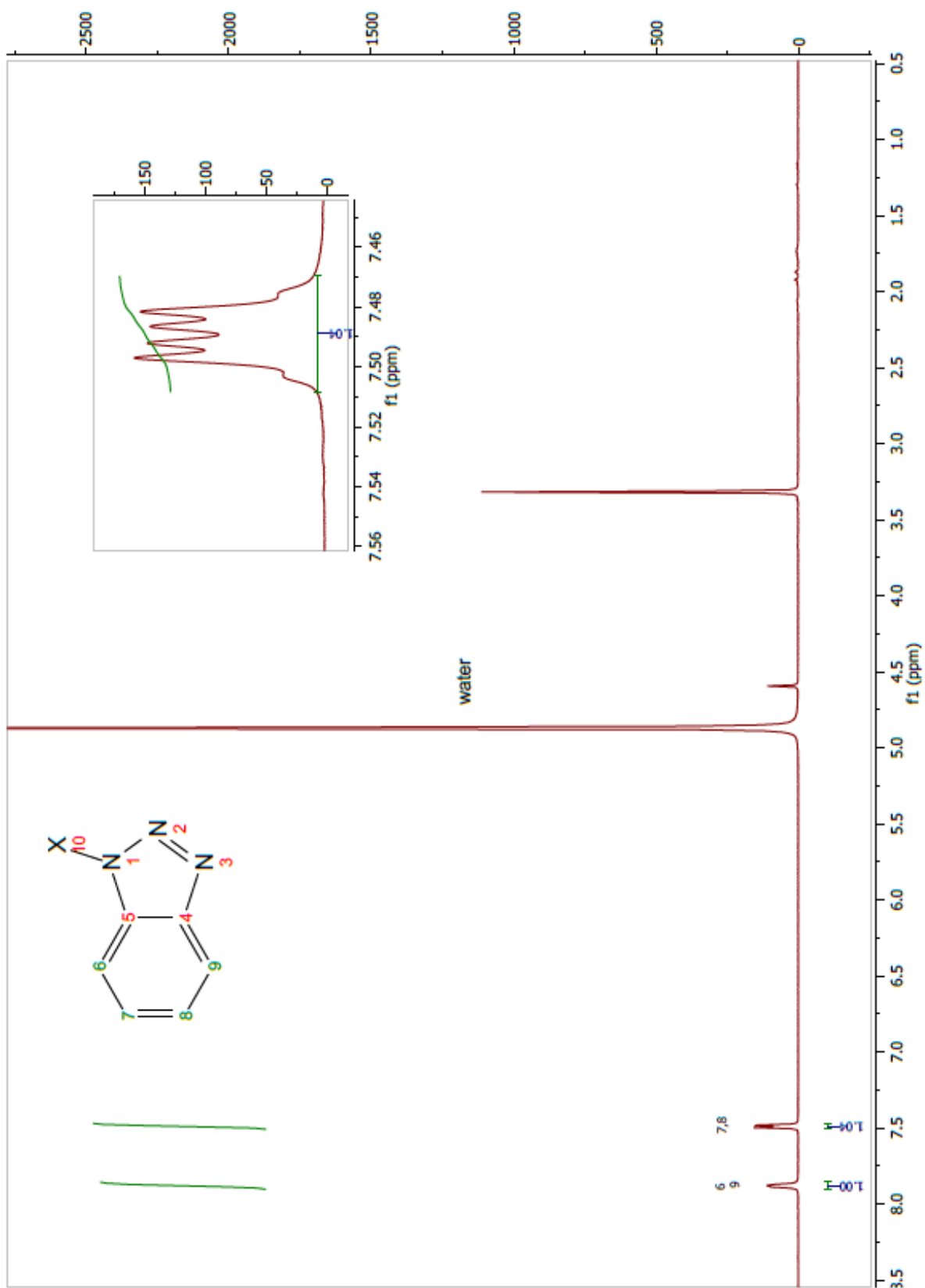
X= Cl or H
$^{1}$H NMR (CD$_3$OD): δ 7.88 (2H, m), 7.49 (2H, m, *J*=9.03, 2.89 Hz).
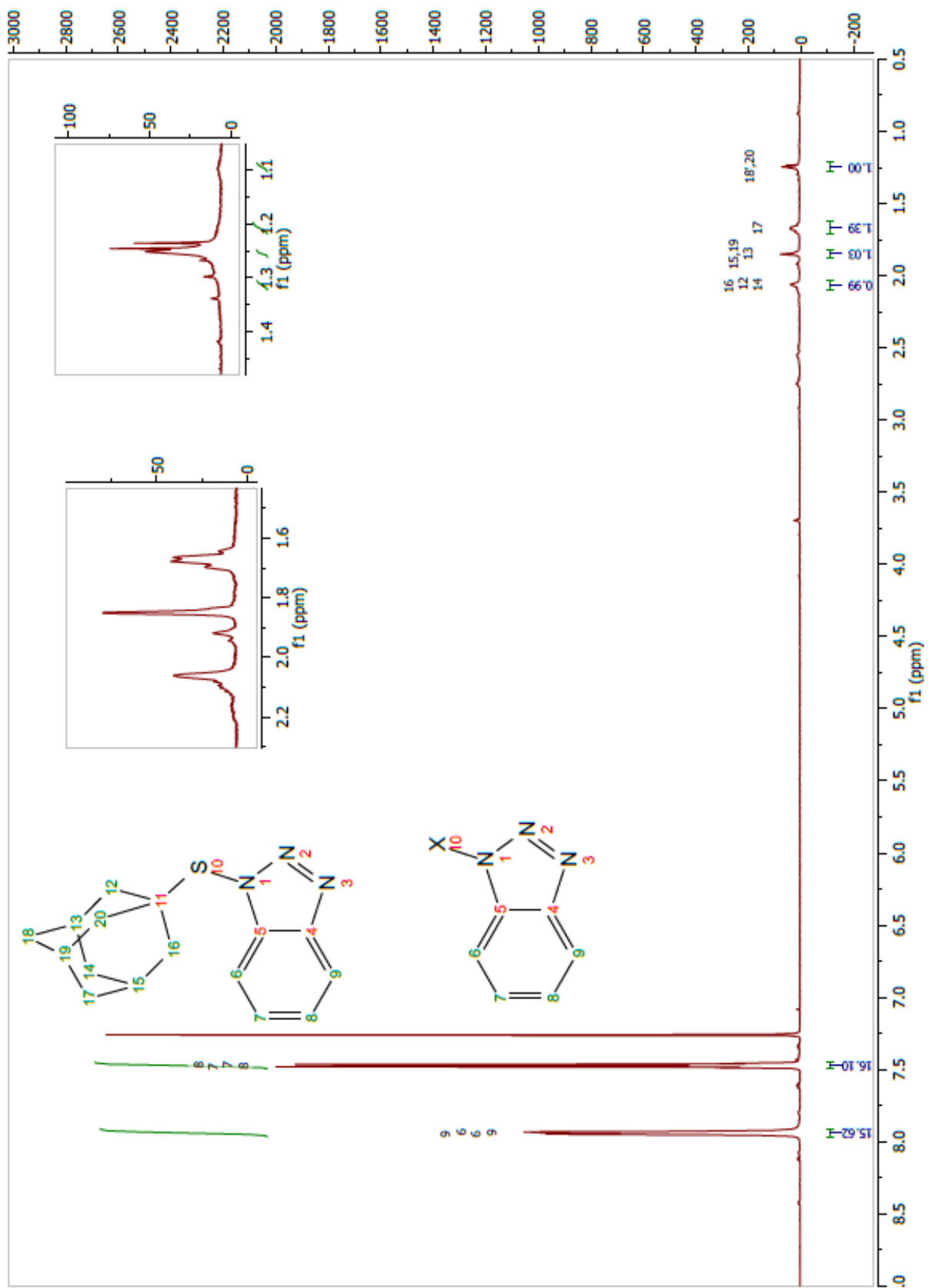
$^{1}$H NMR (CDCl$_3$): δ 7.94 (m), 7.47 (m), 2.06 (m), 1.85 (m), 1.66 (m), 1.25 (m).
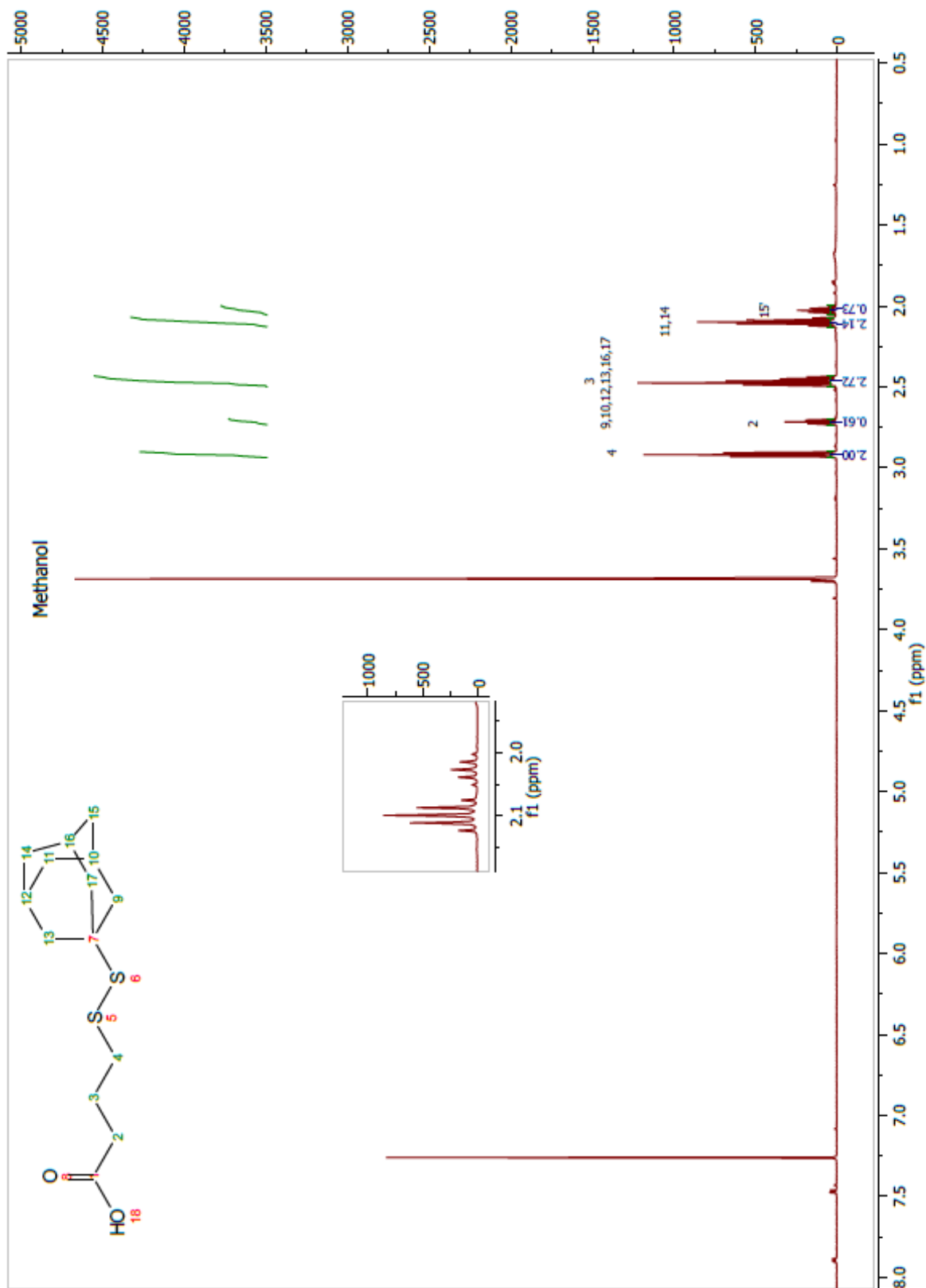
$^1$H NMR (CDCl$_3$): δ 2.92 (2H, t, *J*=7.17 Hz), 2.48 (2H, m), 2.10 (p, *J*=7.34 Hz), 2.03 (1H, p, *J*=7.47Hz).

### 11.3.3 Second attempt - purification

**REVELERIS™**
Flash Chromatography System

**Method Name:**
**Run Name:** 2017-01-18_13-00-01mb04a
**Run Date:** 2017-01-18 13:08

Column: Reveleris® Silica 40g
Flow Rate: 40 mL/min
Equilibration: 7.1 min
Run Length: 38.0 min
Air Purge Time: 1 min

Slope Detection: Off
ELSD Threshold: 5 mV
UV Threshold: 0.02 AU
UV1 Wavelength: 254 nm
UV2 Wavelength: 280 nm

Collection Mode: Collect Peaks
Per-Vial Volume: 5 mL
Non-Peaks: 8.5 mL
Injection Type: Dry

ELSD Carrier: Iso-propanol
Solvent A: Methylene chlorid
Solvent B: Methanol
Solvent C: <No solvent chose
Solvent D: <No solvent chose
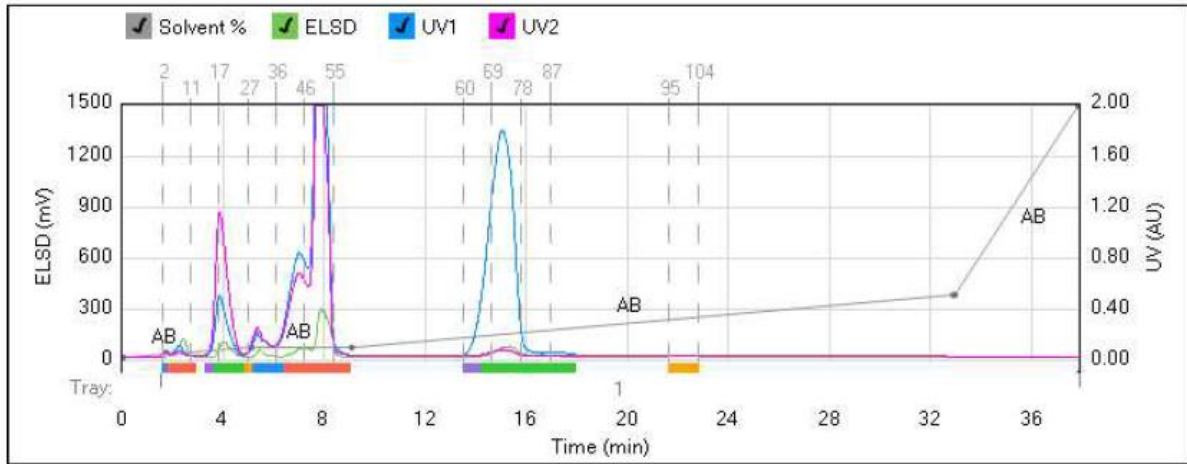


1 - 4019
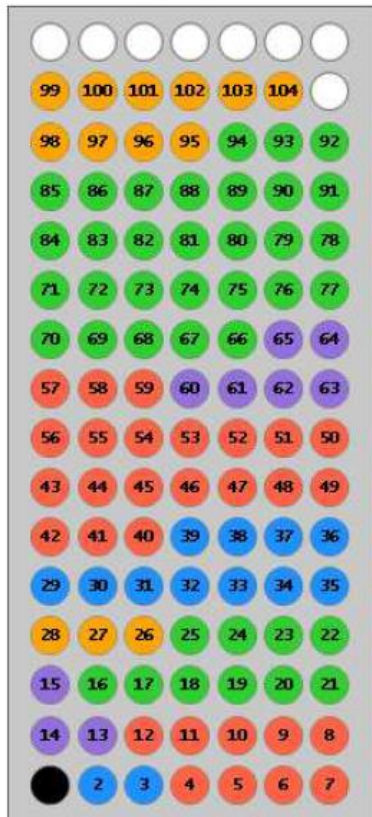


#### Gradient Table

|   | Min  | Solvents | % 2nd |
|---|------|----------|-------|
| 1 | 0.0  | AB       | 0     |
| 2 | 5.1  | AB       | 4     |
| 3 | 4.0  | AB       | 4     |
| 4 | 23.9 | AB       | 25    |
| 5 | 0.1  | AB       | 25    |
| 6 | 4.9  | AB       | 100   |

#### Vial Mapping Table

| Peak # | Start Tray:Vial | End Tray:Vial |
|--------|-----------------|---------------|
| 1      | 1:2             | 1:3           |
| 2      | 1:4             | 1:12          |
| 3      | 1:13            | 1:15          |
| 4      | 1:16            | 1:25          |
| 5      | 1:26            | 1:28          |
| 6      | 1:29            | 1:39          |
| 7      | 1:40            | 1:59          |
| 8      | 1:60            | 1:65          |
| 9      | 1:66            | 1:94          |
| 10     | 1:95            | 1:104         |

Page 1

*^{1}H NMR Fraction 2-10*



^{1}H NMR (CDCl₃): δ 2.69 (2H, t, *J*=6.86 Hz), 2.44 (2H, t, *J*=7.24 Hz), 2.07 (6H, m), 2.0 (3H, m), 1.94 (2H, d, *J*=3 Hz), 1.92 (1H, t, J=2.68 Hz) 1.68 (4H, m), 1.42 (1H, s).

*¹H NMR Fraction 15-23*
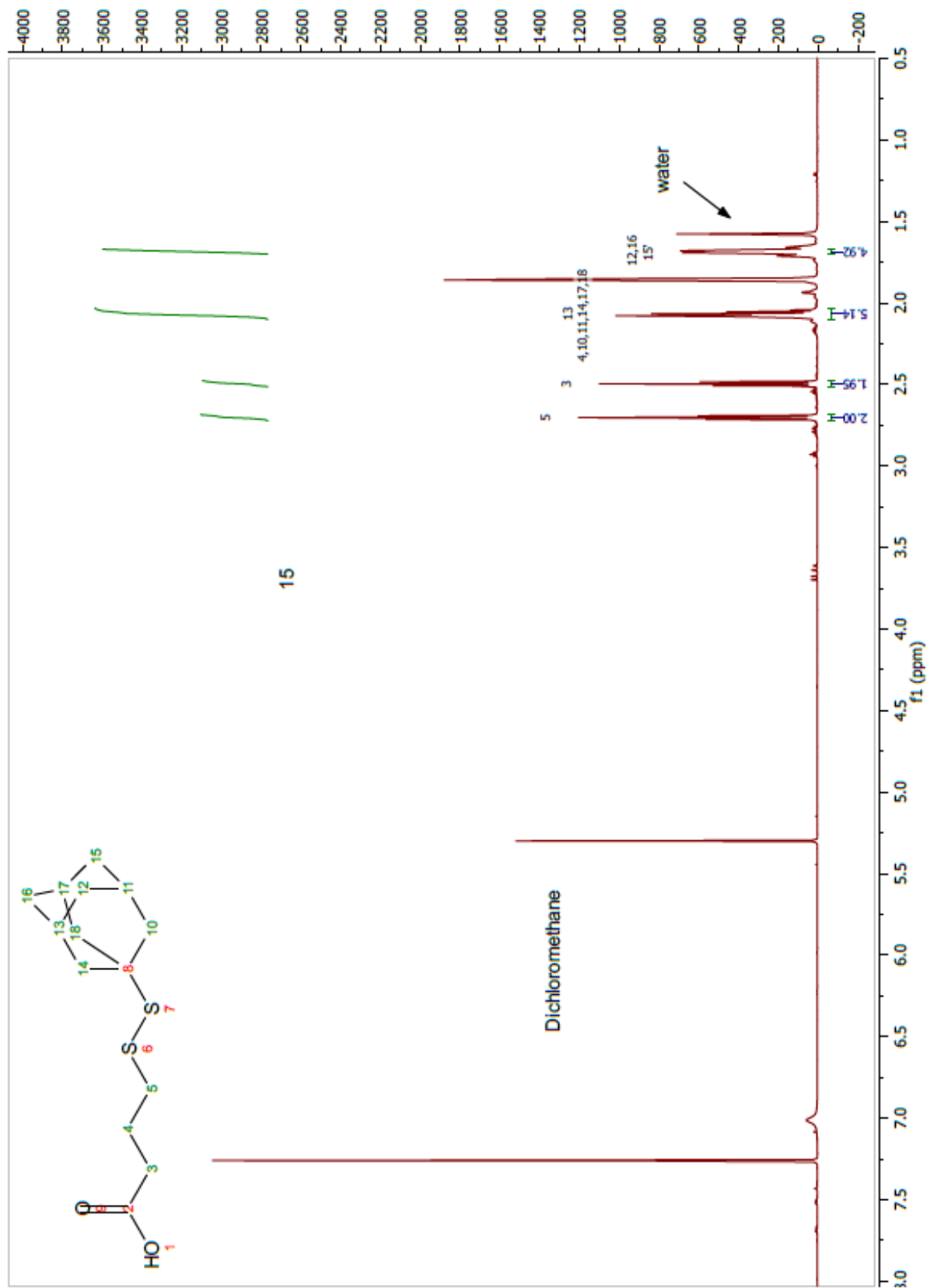


¹H NMR (CDCl₃): δ 2.70 (2H, t, *J*=7.10 Hz), 2.50 (2H, t, *J*=7.10 Hz), 2.08-2.06 (12H, m), 1.67 (4H, m).
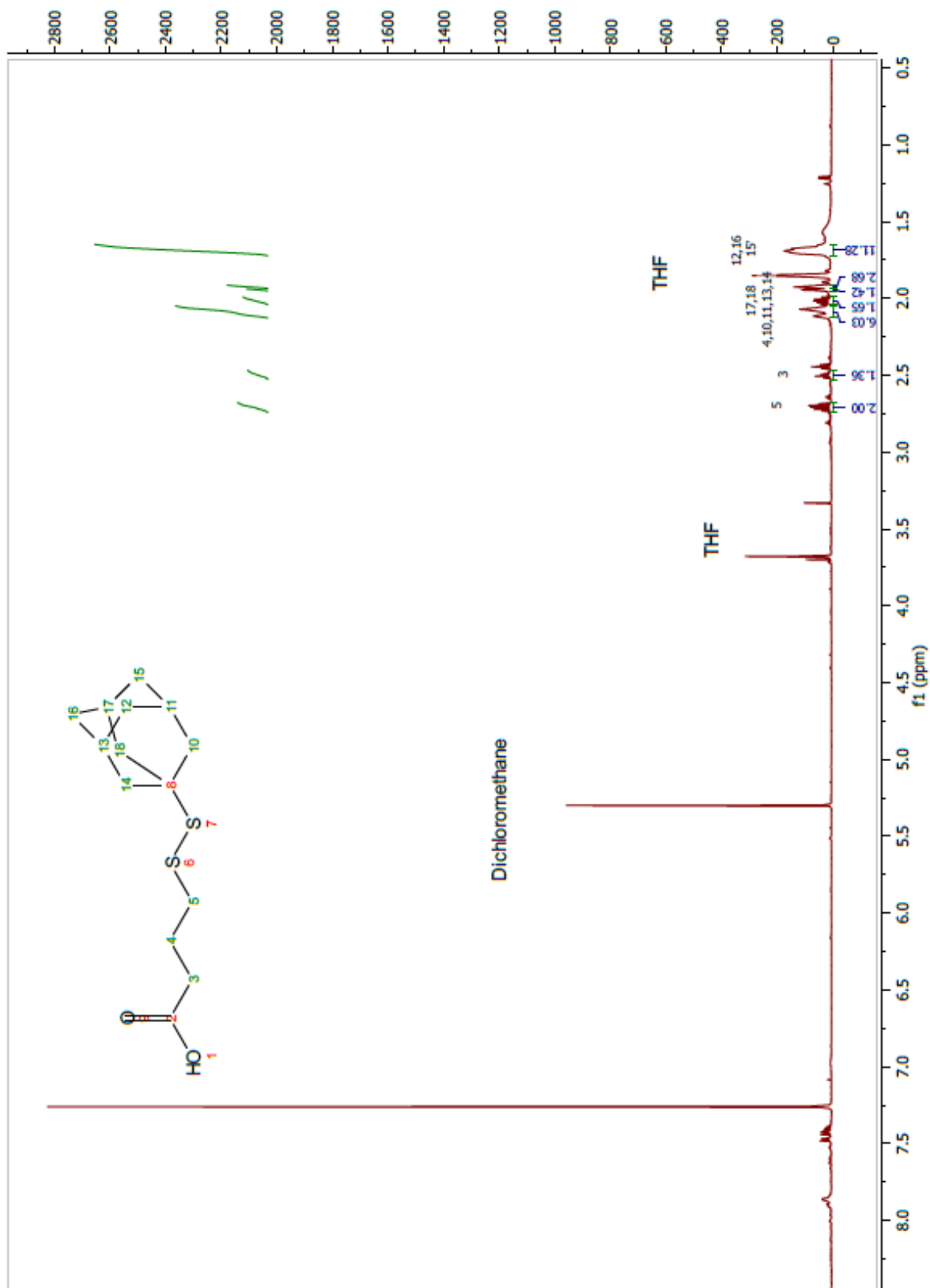
$^1$H NMR (CDCl$_3$): δ 2.71 (2H, m), 2.50 (2H, m), 2.10 (6H, m), 2.01(3H, m) 1.93, 1.94 (2H, m), 1.92 (1H, m), 1.69 (4H, m).

*¹H NMR Fraction 40-56*
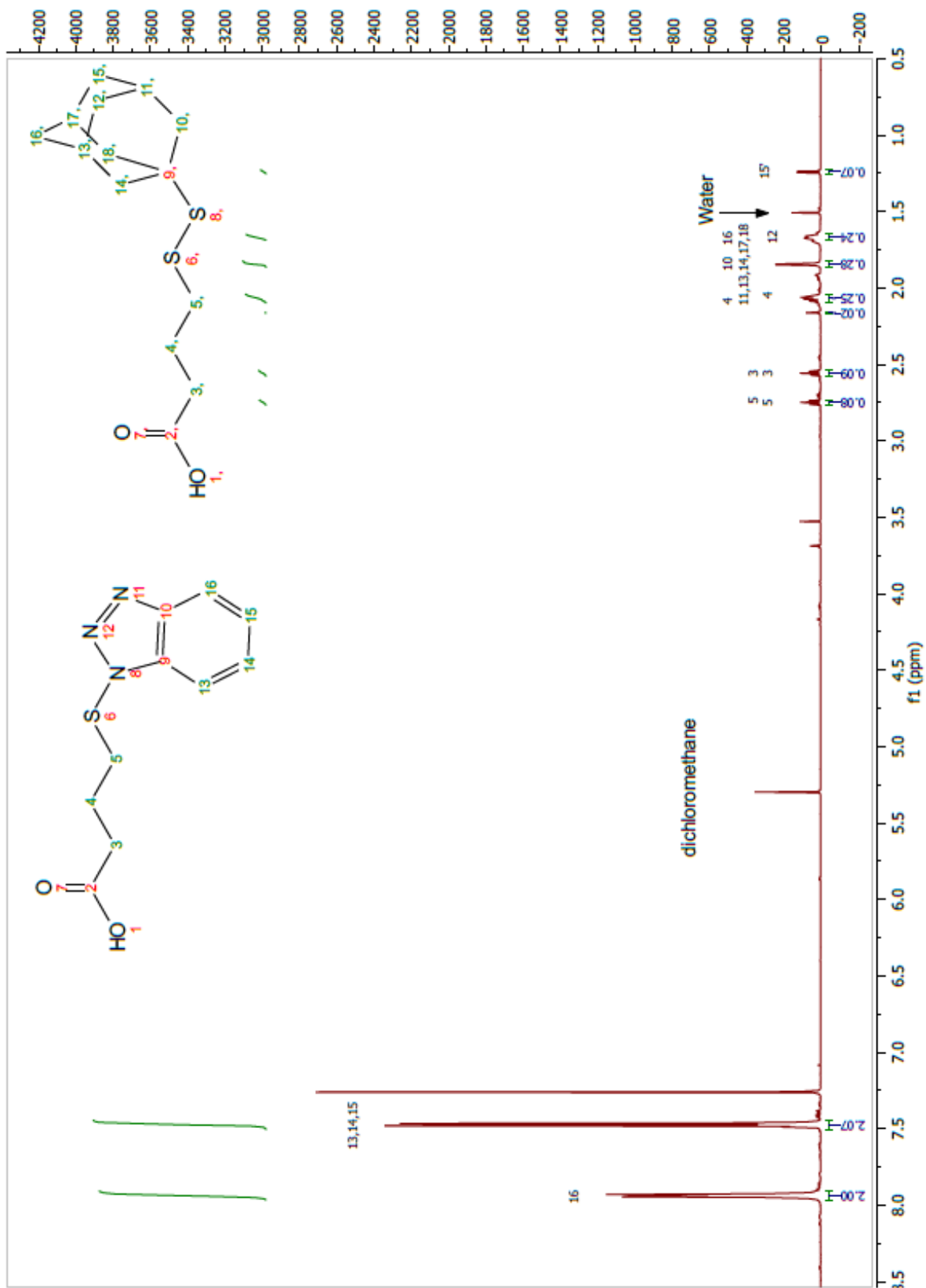


¹H NMR (CDCl₃): δ 7.94 (m), 7.47 (m), 2.75 (t, *J*=7.65 Hz), 2.55 (t, *J*=7.22 Hz), 2.16 (s), 2.06 (m) 1.85 1.67 (m), 1.24 (m).

¹H NMR (CD₃OD): δ 2.09, 1.89 (m), 1.74 (m).

## 11.4 4-(((3s,5s,7s)-adamantan-1-yl)disulfaneyl)-N-(3-hydroxy-2-methyl-6-(3,5,12 trihydroxy-3-(2-hydroxyacetyl)-10-methoxy-6,11-dioxo-1,2,3,4,6,11-hexalhydrotetracen-1-yl)tetrahydro-2*H*-pyran-4-yl)butanamide (4)

### 11.4.1 Before purification
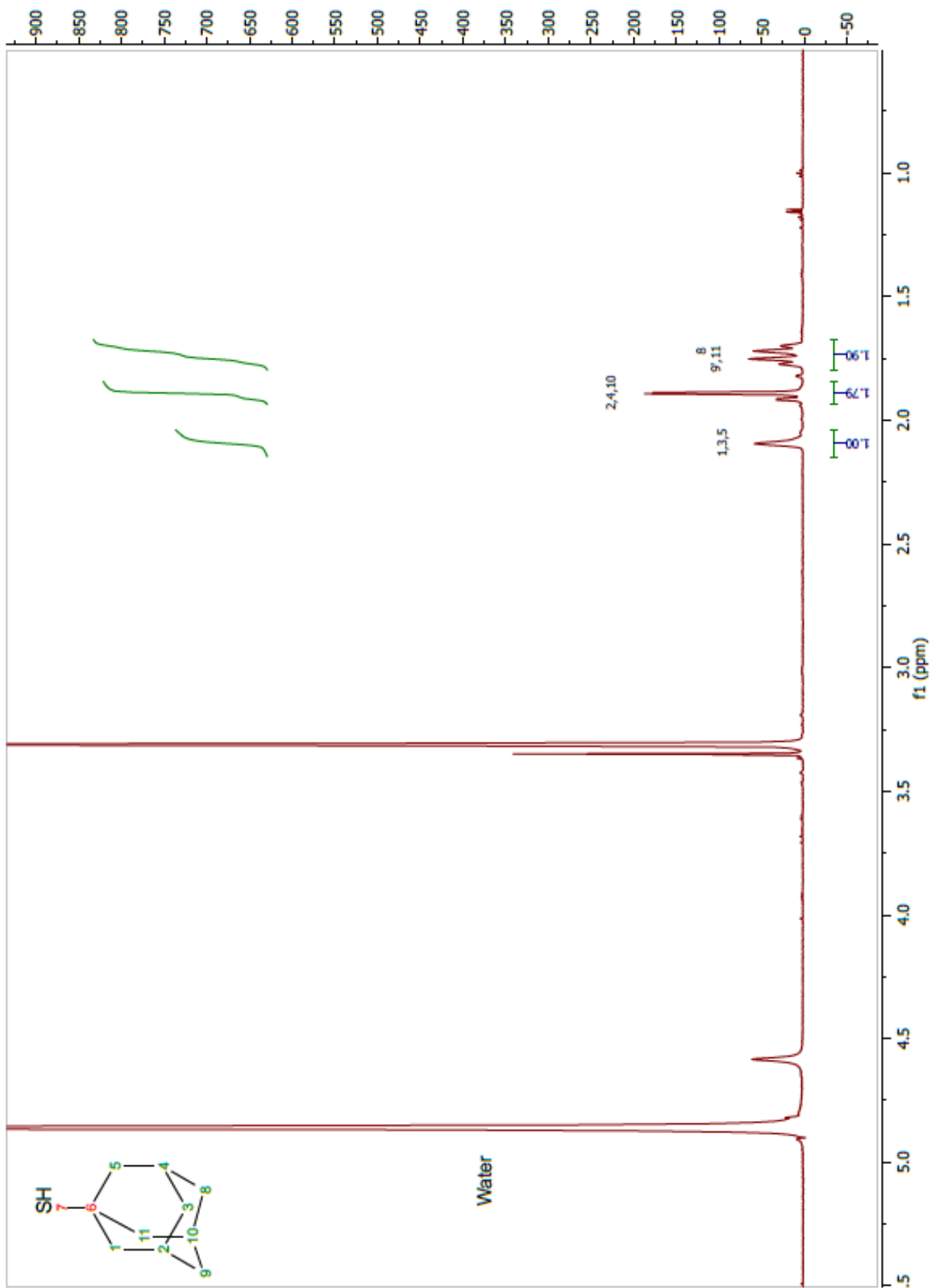


[^1]H NMR (CD₃OD): δ 8.04 (1H, d, *J*=8.42 Hz), 7.88 (1H, t, *J*=8.73 Hz), 7.62 (1H, d, *J*=7.61 Hz), 5.44 (1H, m), 5.18 (1H, m), 4.04 (2H, s), 3.64 (3H, s) 3.45 (1H, m), 3.17 (3H, m), 2.70 (2H, t, *J*=7.05 Hz), 2.44 (2H, t, *J*=7.47 Hz), 1.97-1.86 (6H, m), 1.83-1.69 (11H, m), 1.34-1.27 (5H, m).

## 11.4.2 First attempt - purification

**REVELERIS® PREP**

Method Name:
Run Name: MFB/2017-05-01_10-14-25 mb11
Run Date: 2017-05-01 10:27

| | | |
|---|---|---|
| Column: Reveleris® Silica 40g | Solvent A: Methylene chloride | UV Threshold: 0.05 AU |
| Flow Rate: 40 mL/min | Solvent B: Methanol | UV Sensitivity: Low |
| Equilibration: 7.1 min | Solvent C: Empty | UV1 Wavelength: 254 nm |
| Run Length: 39.3 min | Solvent D: Empty | UV2 Wavelength: 265 nm |
| Mode: Flash Dry | Slope Detection: Off | UV3 Wavelength: 280 nm |

ELSD Threshold: 20 mV
ELSD Sensitivity: Low
Collection: Collect Peaks
Per-Vial Volume: 25 mL
Non-Peak Volume: 25 mL



FLOW RATE ALTERED
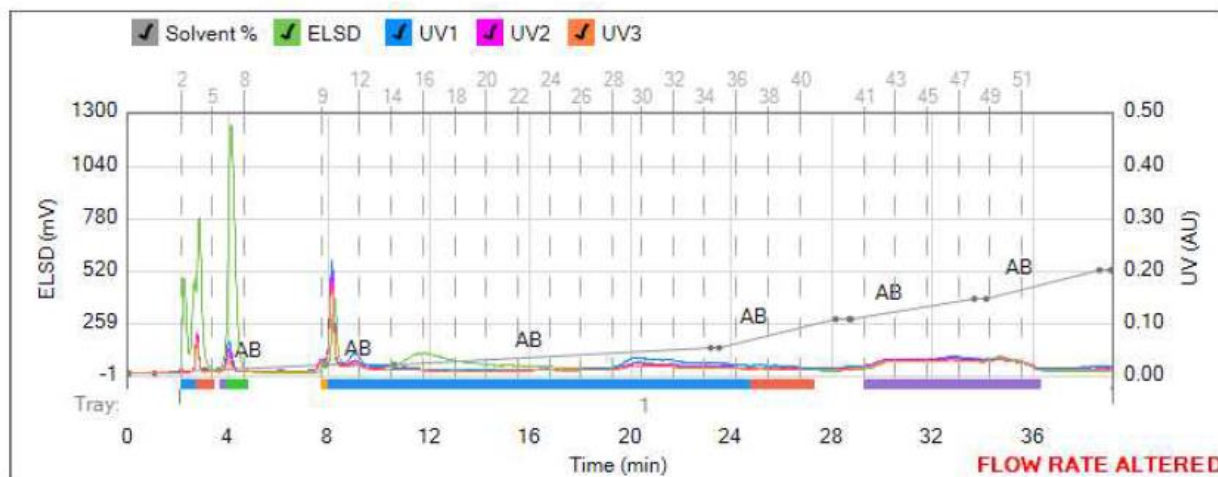
1 - F333
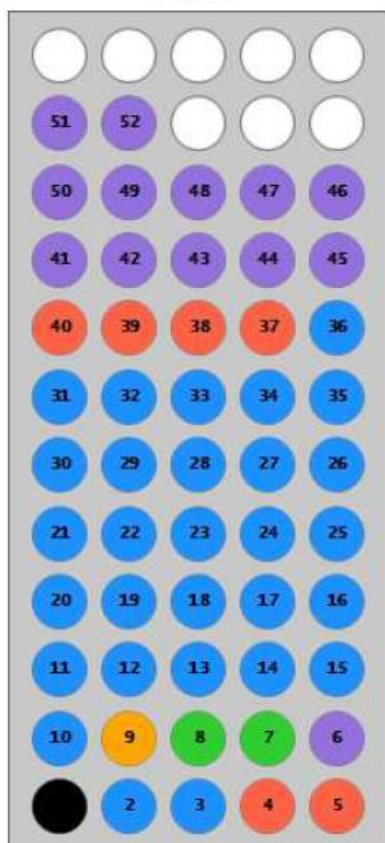


### Gradient Table

| | Min | Solvents | % 2nd |
|---|---|---|---|
| 1 | 0.0 | AB | 0 |
| 2 | 1.0 | AB | 0 |
| 3 | 2.1 | AB | 1 |
| 4 | 0.5 | AB | 1 |
| 5 | 4.2 | AB | 3 |
| 6 | 2.8 | AB | 3 |
| 7 | 12.7 | AB | 10 |
| 8 | 0.4 | AB | 10 |
| 9 | 4.7 | AB | 21 |
| 10 | 0.5 | AB | 21 |
| 11 | 0.1 | AB | 21 |
| 12 | 4.9 | AB | 29 |
| 13 | 0.5 | AB | 29 |
| 14 | 4.5 | AB | 40 |
| 15 | 0.5 | AB | 40 |

### Vial Mapping Table

| Peak # | Start Tray:Vial | End Tray:Vial |
|---|---|---|
| 1 | 1:2 | 1:3 |
| 2 | 1:4 | 1:5 |
| 3 | 1:6 | 1:6 |
| 4 | 1:7 | 1:8 |
| 5 | 1:9 | 1:9 |
| 6 | 1:10 | 1:36 |
| 7 | 1:37 | 1:40 |
| 8 | 1:41 | 1:52 |

Page 1

## 11.4.3 First attempt – after purification

*1H NMR fraction 9-29*
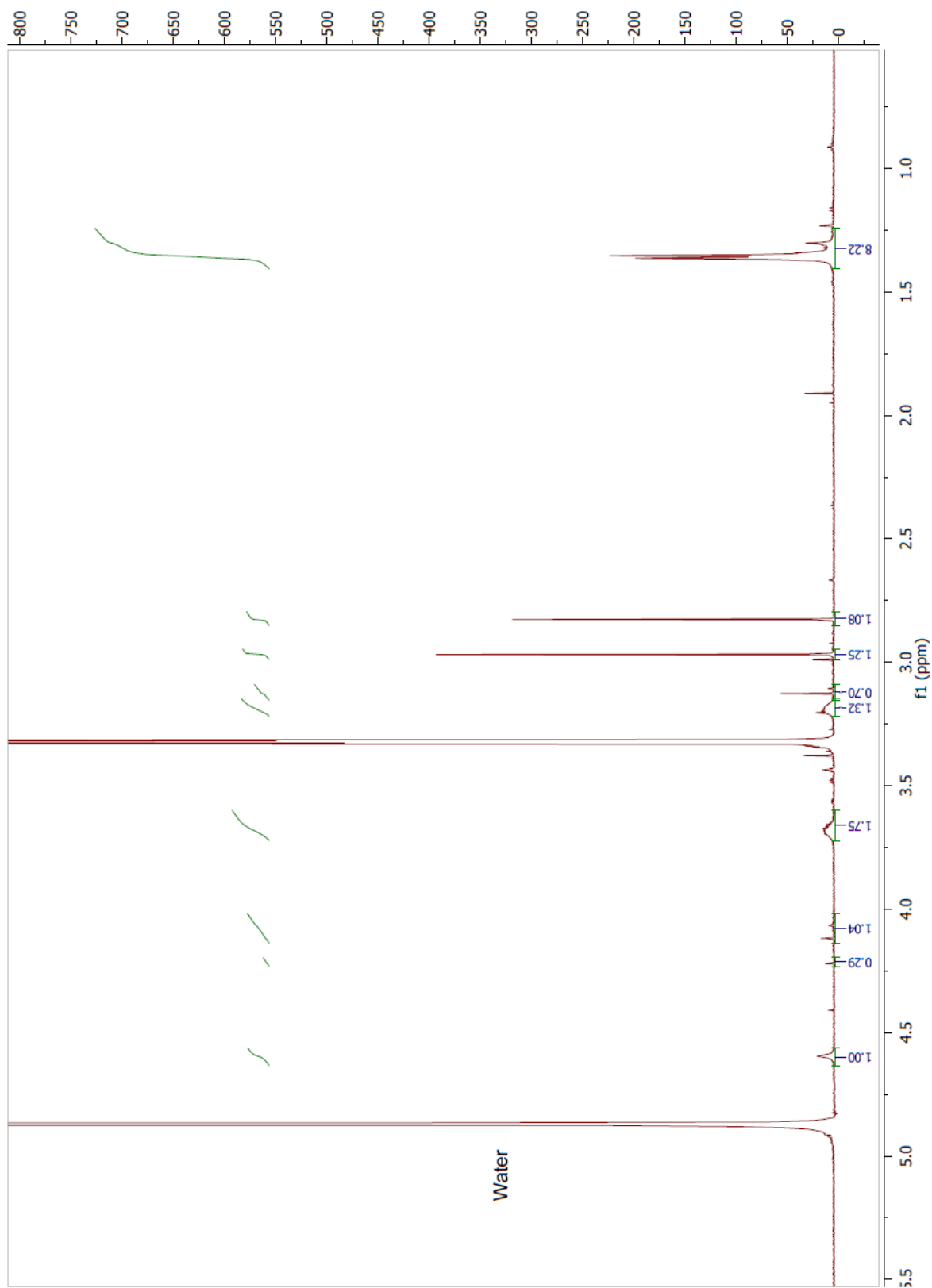


$^1$H NMR (CD$_3$OD): δ 4.59 (1H, s), 4.22 (1H, s), 4.07 (1H, m), 3.68 (2H, m), 3.20 (1H, m), 3.13 (1H, s), 2.97 (2H, s), 2.83 (1H, s), 1.35 (8H, m).

*¹H NMR fraction 30-38*
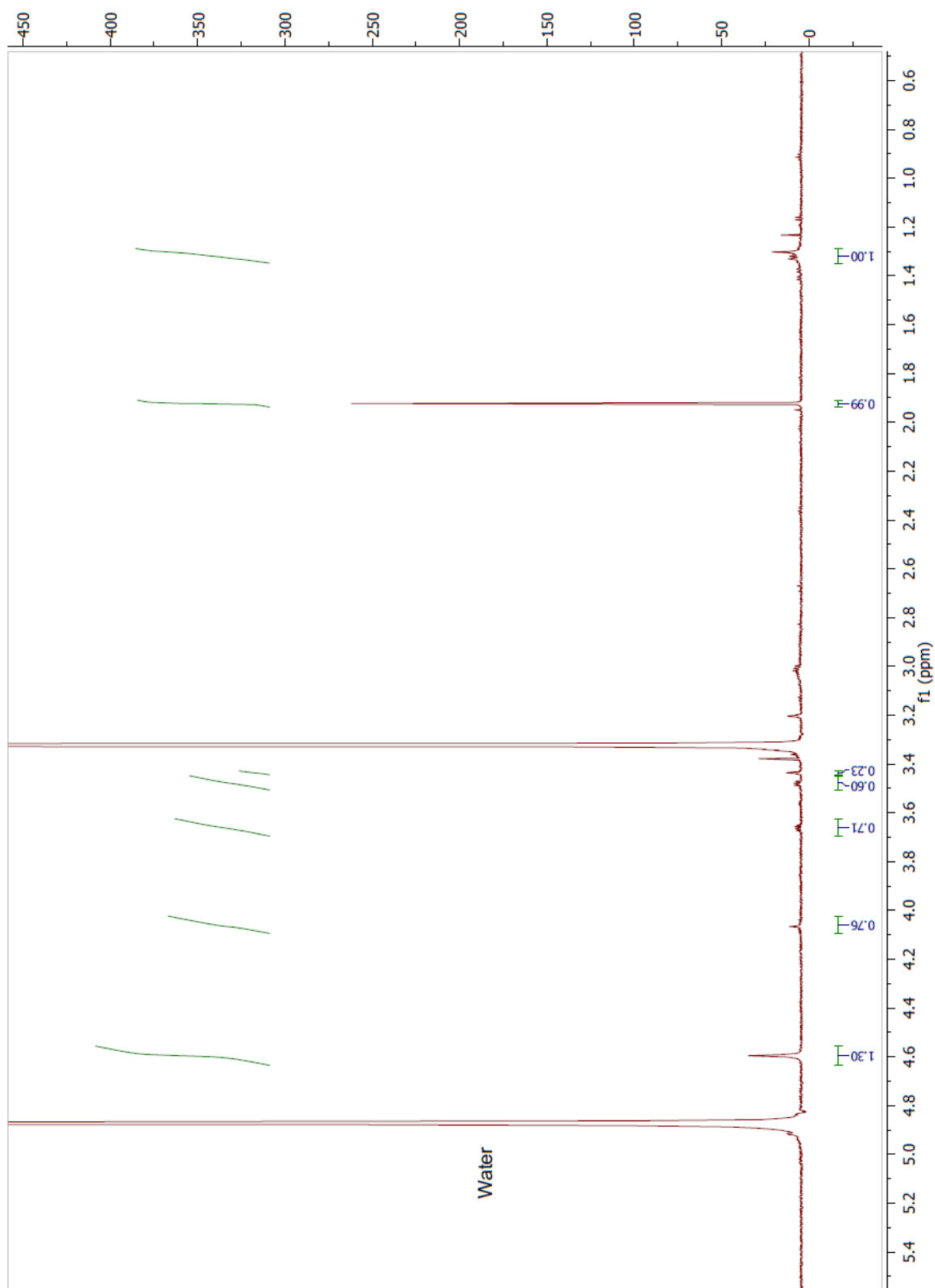


¹H NMR (CD₃OD): δ 4.60 (1H, s), 4.07 (1H, m), 3.66 (1H, q, *J*=4.98 Hz), 3.48 (1H, t, *J*=4.93 Hz), 3.44 (1H, p, *J*=4.98 Hz), 1.92 (1H, s), 1.33-1.29 (1H, m).
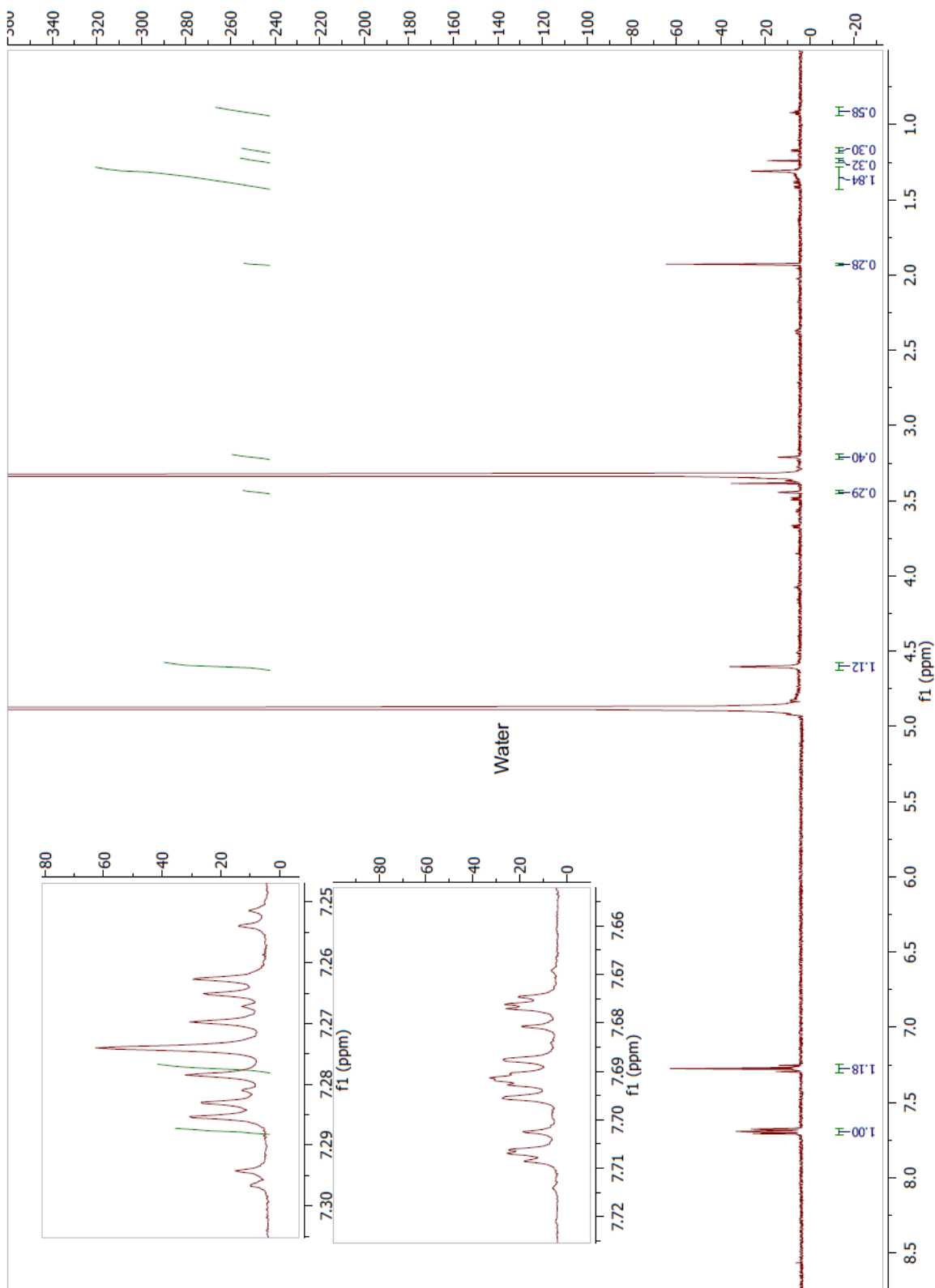
¹H NMR (CD₃OD): δ 7.71-7.67 (1H, m), 7.30-7.25 (1H, m), 4.60 (1H, s), 3.44 (0.3H, p, *J*=1.68 Hz), 3.21 (0.4H, p, *J*=1.68 Hz), 1.93 (1H, s), 1.43-1.28 (2H, m), 1.24 (0.3H, s), 1.17 (0.3H, d, *J*=6.32 Hz), 0.92 (1H, t, *J*=7.10 Hz)

## 11.4.4 First attempt – flushed through

**REVELERIS® PREP**

**Method Name:**
Run Name: MFB/2017-05-05_11-55-50 mb11 flush
Run Date: 2017-05-05 12:05

| | |
|---|---|
| Column: Reveleris® Silica 40g | Solvent A: Methylene chloride |
| Flow Rate: 40 mL/min | Solvent B: Methanol |
| Equilibration: 5.0 CV | Solvent C: Empty |
| Run Length: 20.4 CV | Solvent D: Empty |
| Mode: Flash Liquid | Slope Detection: Off |

| | |
|---|---|
| UV Threshold: 0.02 AU | ELSD Threshold: 5 mV |
| UV Sensitivity: Low | ELSD Sensitivity: Low |
| UV1 Wavelength: 254 nm | Collection: Collect Peaks |
| UV2 Wavelength: 265 nm | Per-Vial Volume: 7 mL |
| UV3 Wavelength: 280 nm | Non-Peak Volume: 8.5 mL |
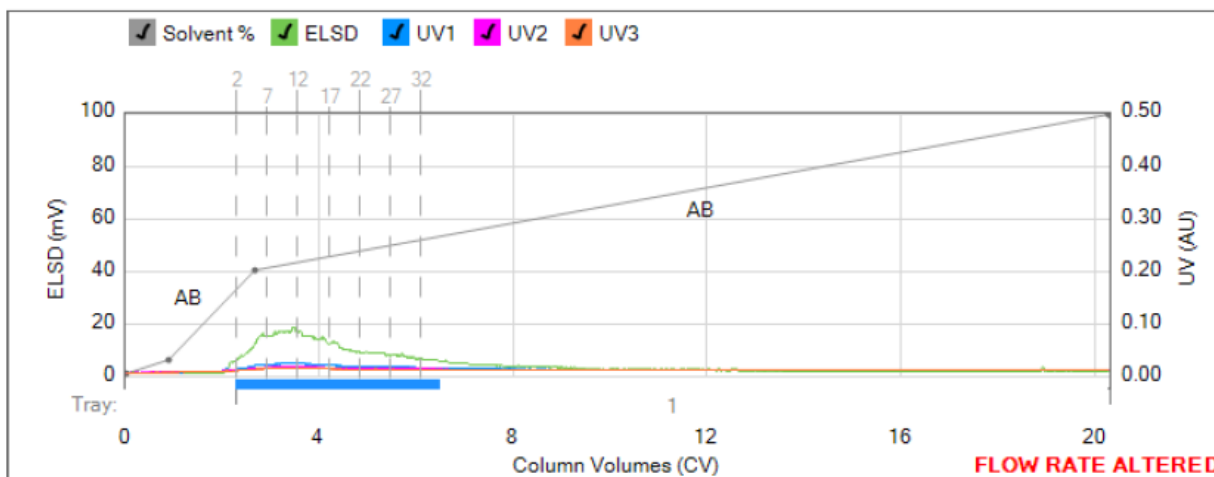


1 - 4019
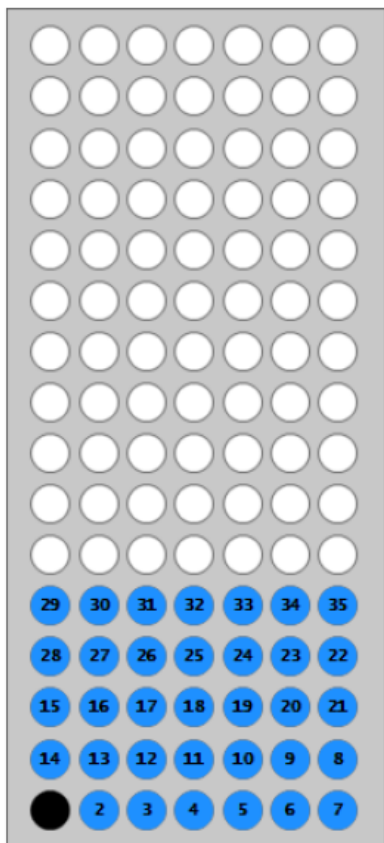


**Gradient Table**

| | CV | Solvents | % 2nd |
|---|---|---|---|
| 1 | 0.0 | AB | 0 |
| 2 | 0.9 | AB | 5 |
| 3 | 1.8 | AB | 40 |
| 4 | 17.7 | AB | 100 |

**Vial Mapping Table**

| Peak # | Start Tray:Vial | End Tray:Vial |
|---|---|---|
| 1 | 1:2 | 1:35 |
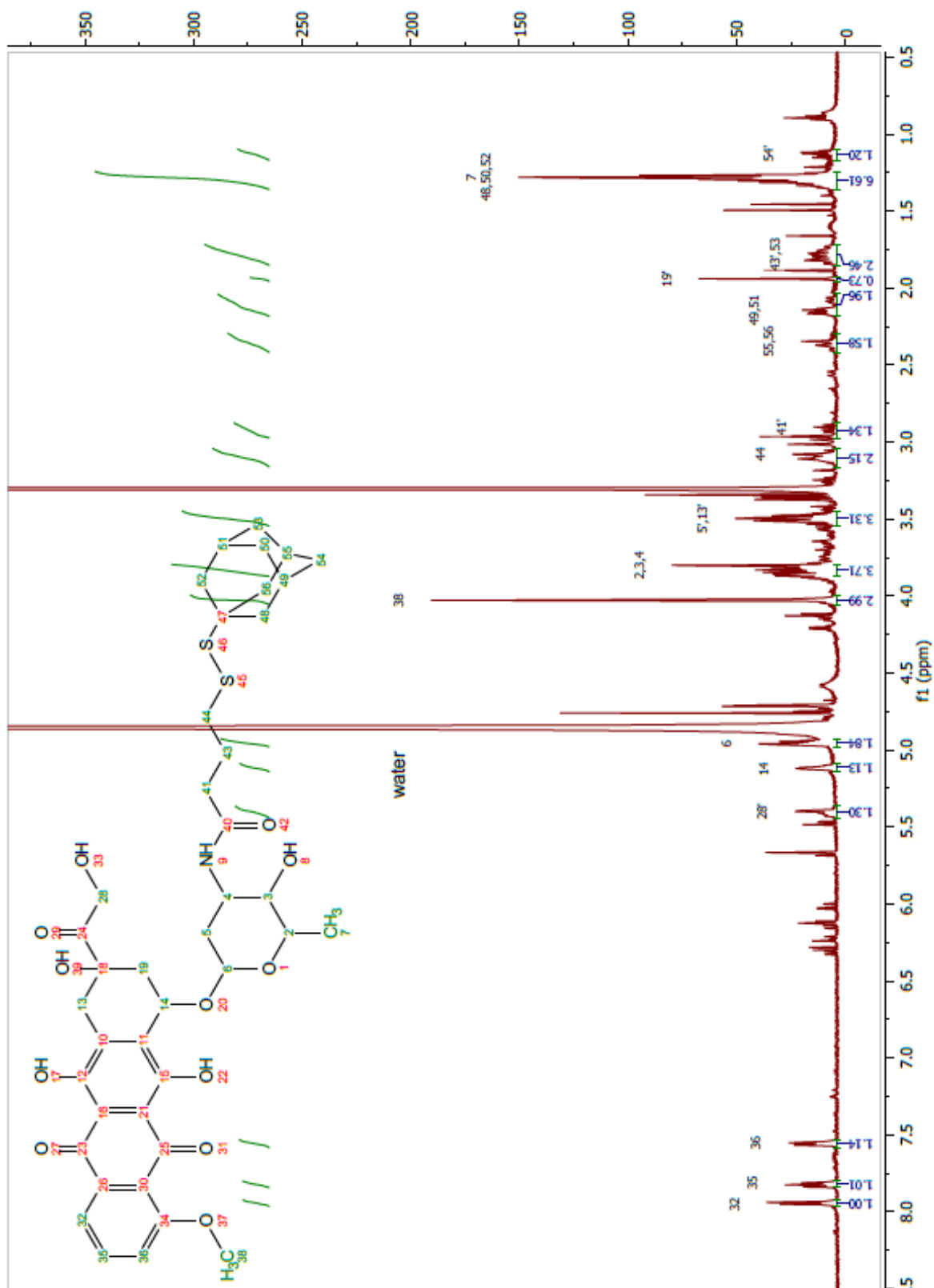
$^1$H NMR (CD$_3$OD): δ 7.94 (1H, d, *J*=7.66 Hz), 7.82 (1H, dt, *J*=2.59, 7.66 Hz), 7.55 (1H, dd, *J*=7.87, 3.15 Hz), 5.40 (2H, m), 5.12 (1H, m), 4.96 (1H, m), 4.03 (3H, s), 3.84 (3H, m) 3.50 (4H, m), 3.11 (2H, m), 2.90 (2H, m), 2.35 (3H, m), 2.14 (2H, m) 1.93 (2H, m), 1.78 (4H, m), 1.28 (9H, m) 1.12 (2H, m).

### 11.4.6 Second attempt – purification

**REVELERIS® PREP**

Method Name:
Run Name: MFB/2017-05-12_09-25-26 mbl1a
Run Date: 2017-05-12 09:34

Column: Reveleris® Silica 40g
Flow Rate: 40 mL/min
Equilibration: 7.1 min
Run Length: 30.0 min
Mode: Flash Dry

Solvent A: Chloroform
Solvent B: Methanol
Solvent C: Empty
Solvent D: Empty
Slope Detection: Off

UV Threshold: 0.05 AU
UV Sensitivity: Low
UV1 Wavelength: 254 nm
UV2 Wavelength: 265 nm
UV3 Wavelength: 280 nm

ELSD Threshold: 20 mV
ELSD Sensitivity: Low
Collection: Collect Peaks
Per-Vial Volume: 7 mL
Non-Peak Volume: 8.5 mL
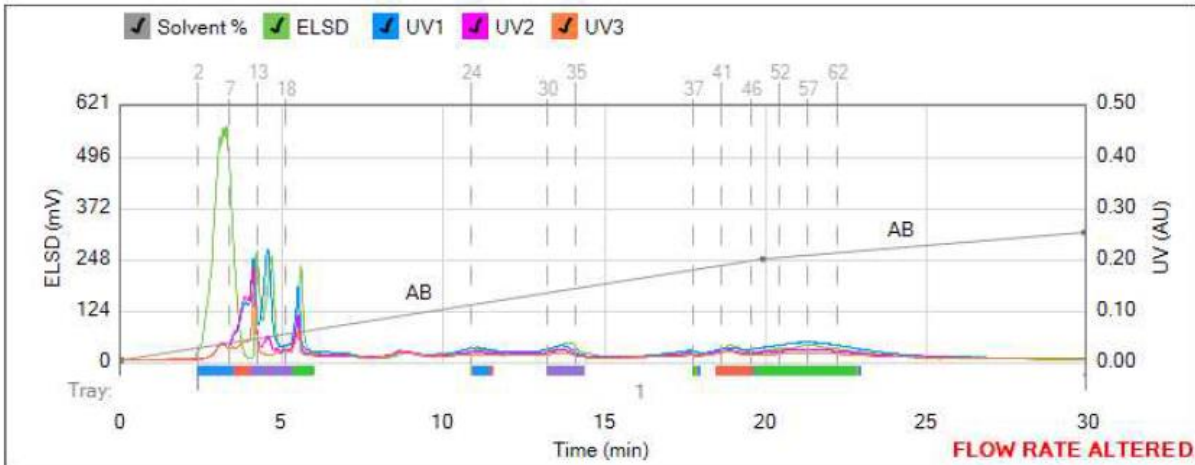


1 - 2F2A
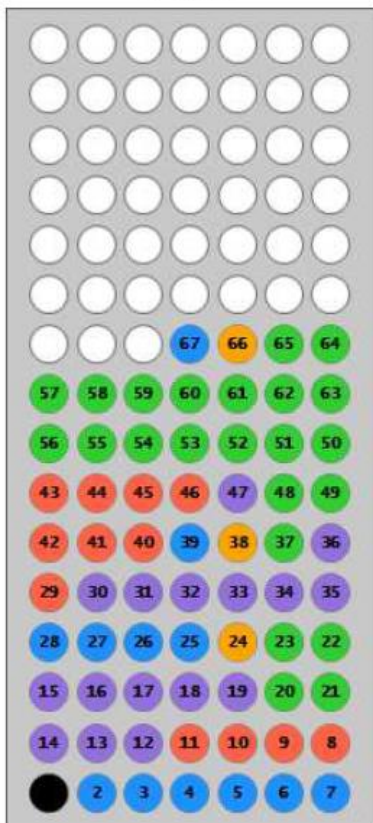


**Gradient Table**

|   | Min  | Solvents | % 2nd |
|---|------|----------|-------|
| 1 | 0.0  | AB       | 0     |
| 2 | 20.0 | AB       | 40    |
| 3 | 10.0 | AB       | 50    |

**Vial Mapping Table**

| Peak # | Start Tray:Vial | End Tray:Vial |
|--------|-----------------|---------------|
| 1      | 1:2             | 1:7           |
| 2      | 1:8             | 1:11          |
| 3      | 1:12            | 1:19          |
| 4      | 1:20            | 1:23          |
| 5      | 1:24            | 1:24          |
| 6      | 1:25            | 1:28          |
| 7      | 1:29            | 1:29          |
| 8      | 1:30            | 1:36          |
| 9      | 1:37            | 1:37          |
| 10     | 1:38            | 1:38          |
| 11     | 1:39            | 1:39          |
| 12     | 1:40            | 1:46          |
| 13     | 1:47            | 1:47          |
| 14     | 1:48            | 1:65          |
| 15     | 1:66            | 1:66          |
| 16     | 1:67            | 1:67          |
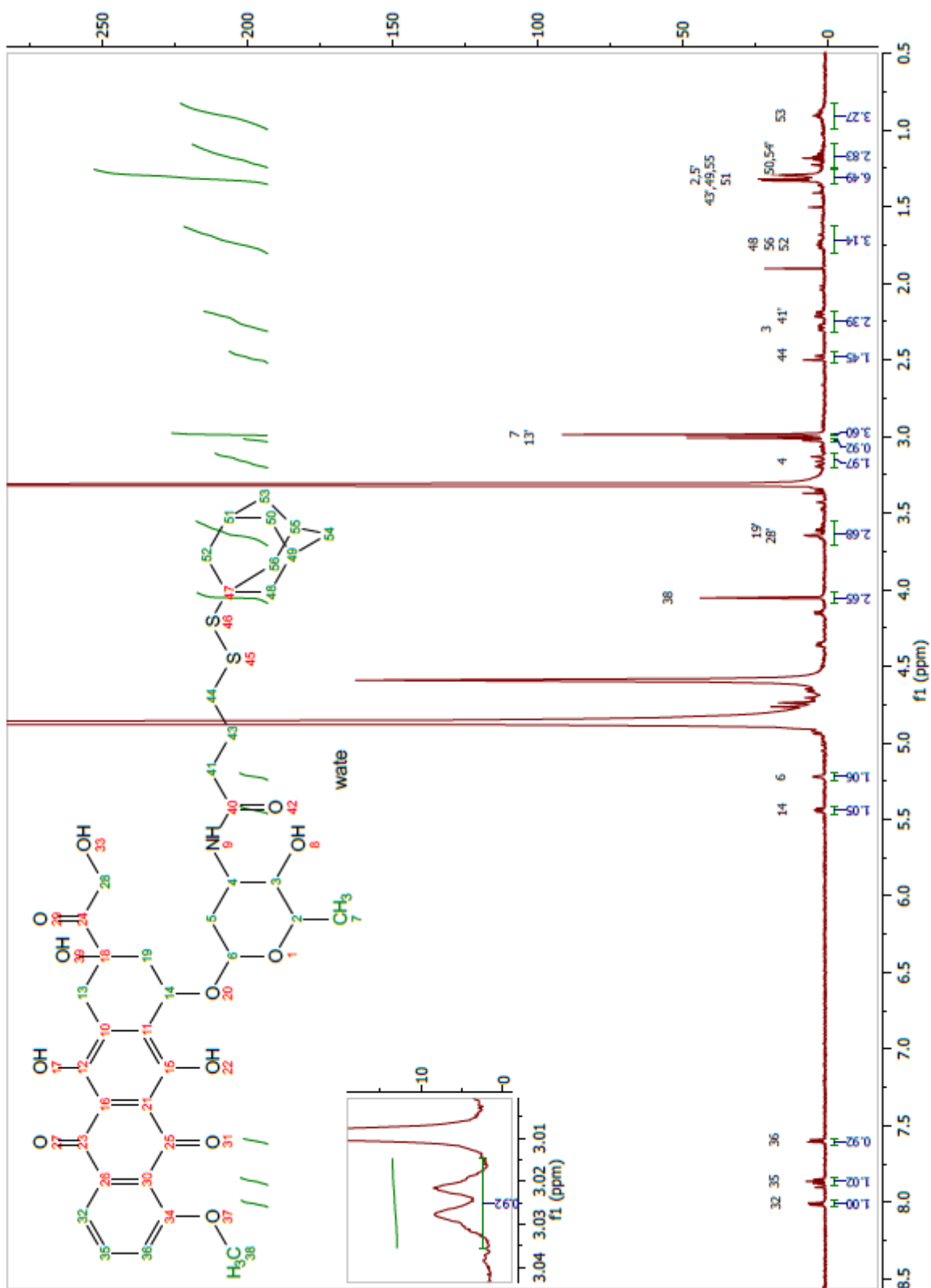
Page 1

107

*¹H NMR fraction 24-29*



¹H NMR (CD₃OD): δ 8.01 (1H, d, *J*=7.46 Hz), 7.86 (1H, t, *J*=9.09 Hz), 7.60 (1H, d, *J*=8.37 Hz), 5.44 (1H, m), 5.22 (1H, m), 4.06 (3H, s), 3.64 (4H, m), 3.16 (1H, m), 3.02 (2H, d, *J*=4.45 Hz), 2.99 (3H, s), 2.48 (2H, m), 2.29 (1H, m), 1.73 (6H, m), 1.31 (8H, m), 1.18 (4H, m), 0.90 (2H, m).
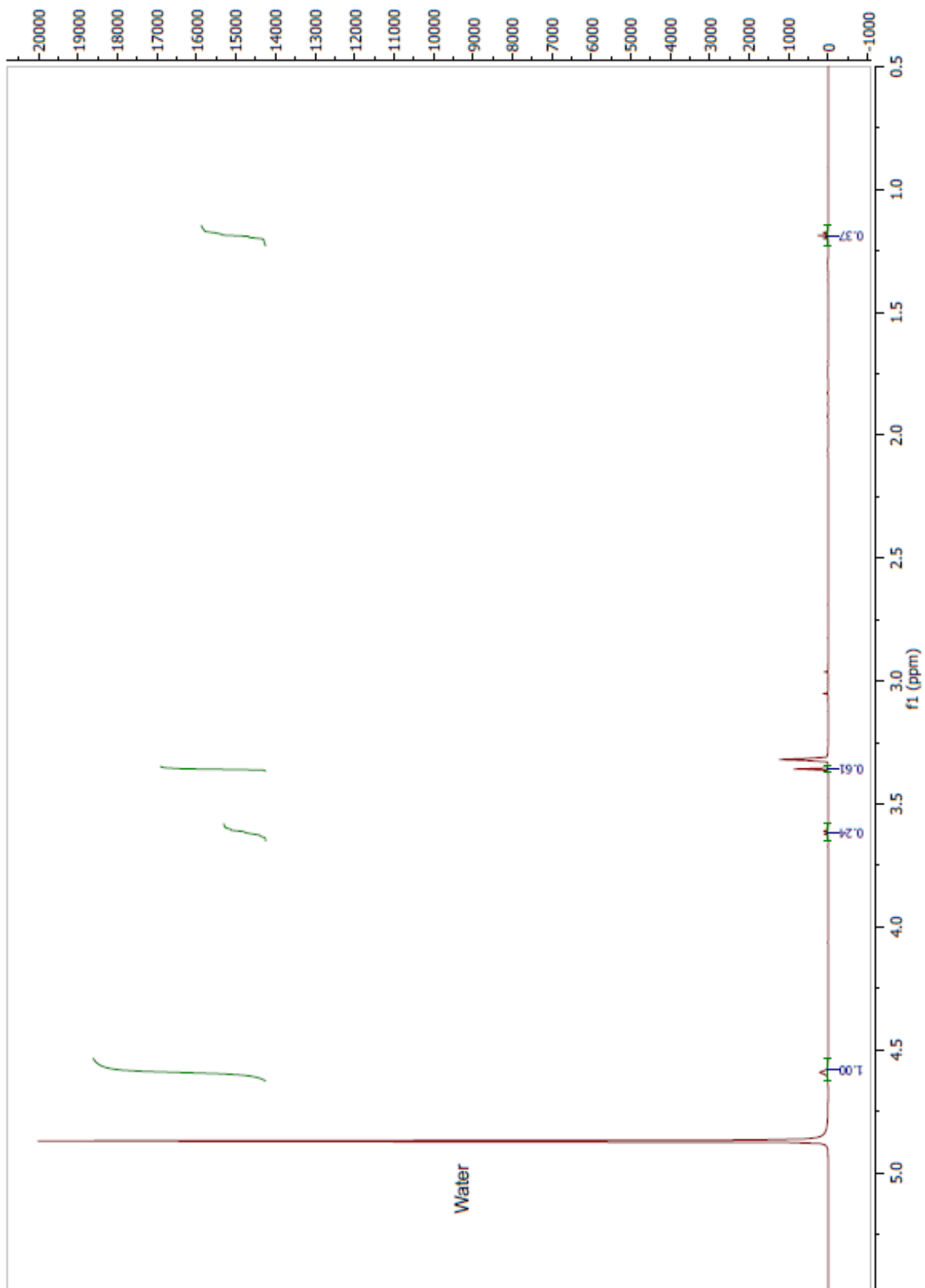
$^1$H NMR (CD$_3$OD): δ 4.58 (1H, s), 3.61 (0.25H, q, *J*=7.00 Hz), 3.36 (1H, s), 1.19 (0.5H, t, *J*=7.06 Hz).

$^1$H NMR (CD$_3$OD): δ 8.04 (1H, d, *J*=7.43 Hz), 7.89 (1H, t, *J*=7.83 Hz), 7.62 (1H, d, *J*=9.66 Hz), 5.48 (1H, m), 5.18 (1H, m), 4.59 (2H, s), 4.07 (3H, s), 3.66 (1H, m), 3.56 (1H, m), 3.44 (1H, m), 3.20 (1H, m), 2.97 (2H, s), 2.38 (1H, m), 2.21 (1H, m), 2.03 (2H, m), 1.89 (1H, m), 1.43-1.18 (14H, m).
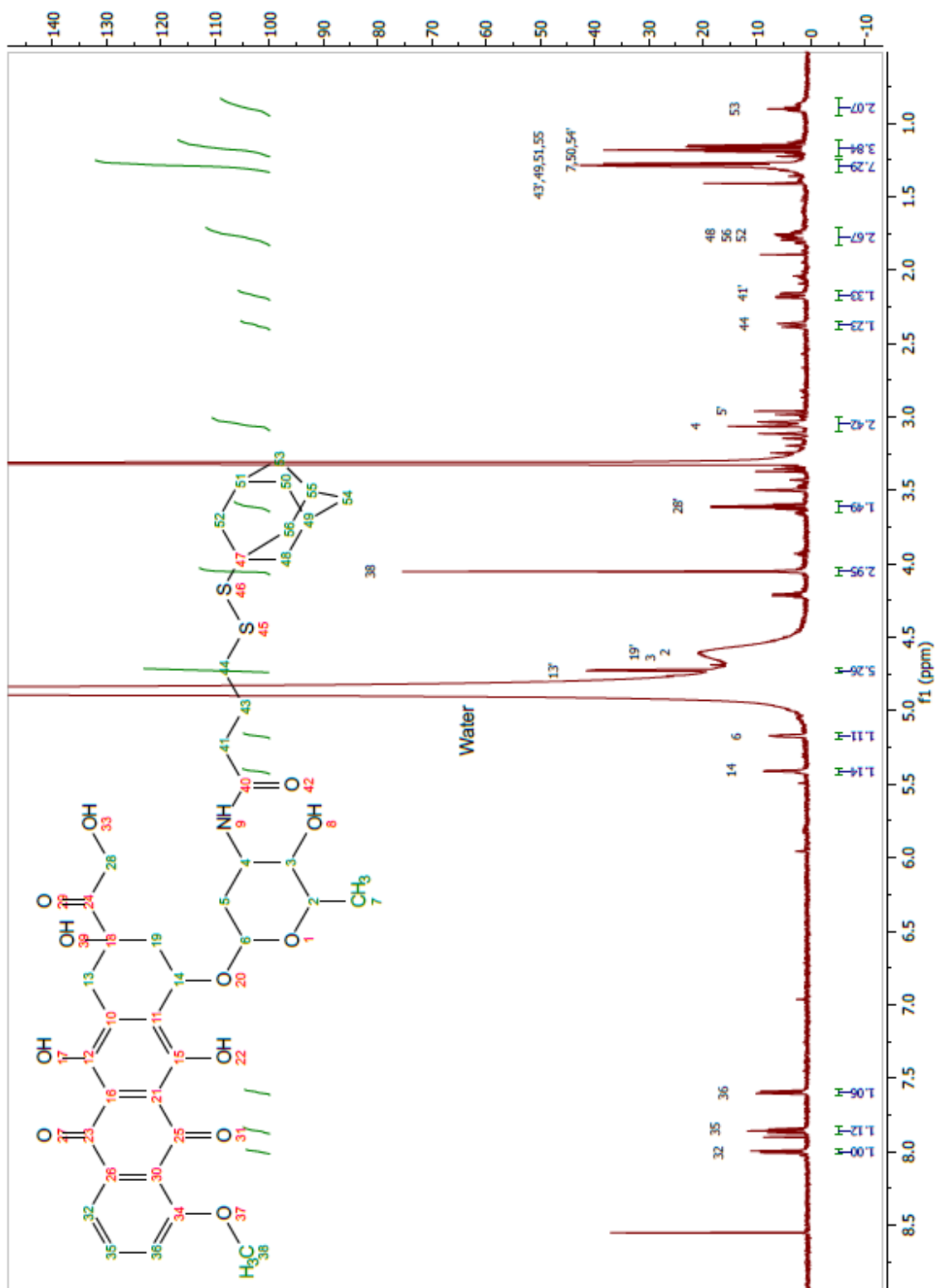
¹H NMR (CD₃OD): δ 8.00 (1H, d, *J*=7.49 Hz), 7.86 (1H, t, *J*=8.22 Hz), 7.60 (1H, d, *J*=7.40 Hz), 5.41 (1H, m), 5.17 (1H, m), 4.72 (2H, s), 4.60 (4H, m), 4.05 (3H, s), 3.61 (2H, q, *J*=7.17 Hz) 3.05 (3H, m), 2.37 (2H, m), 2.17 (2H, dd, *J*=10.44, 5.04 Hz), 1.78 (6H, m), 1.28 (5H, m), 1.18 (7H, m), 0.90 (2H, m).

**11.4.8 LC-MS**
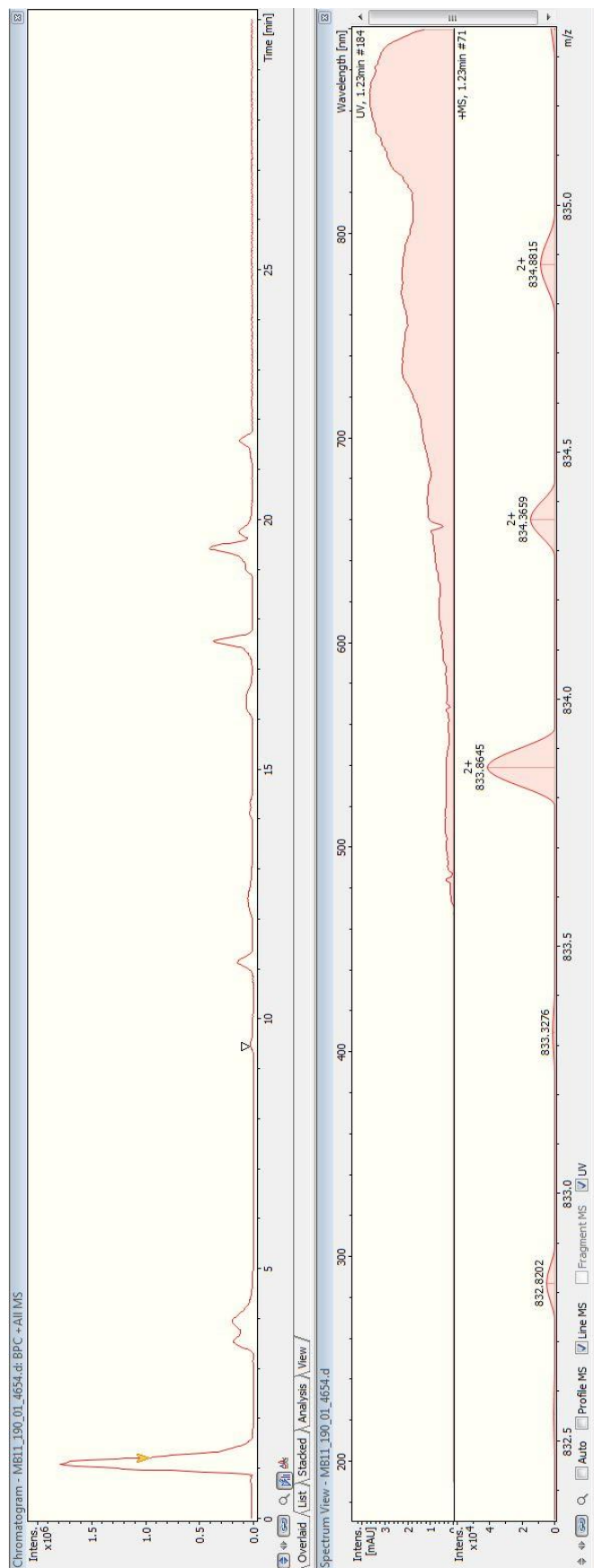


LC-MS: m/z = 834.3659 [M+Na$^+$], calc. for. (C$_{41}$H$_{49}$NO$_{12}$S$_2$ Na$^+$): m/z: 834.2588

Deviation of 0.1071 Da.

**11.4.9 ITC measurement - native β-CD**
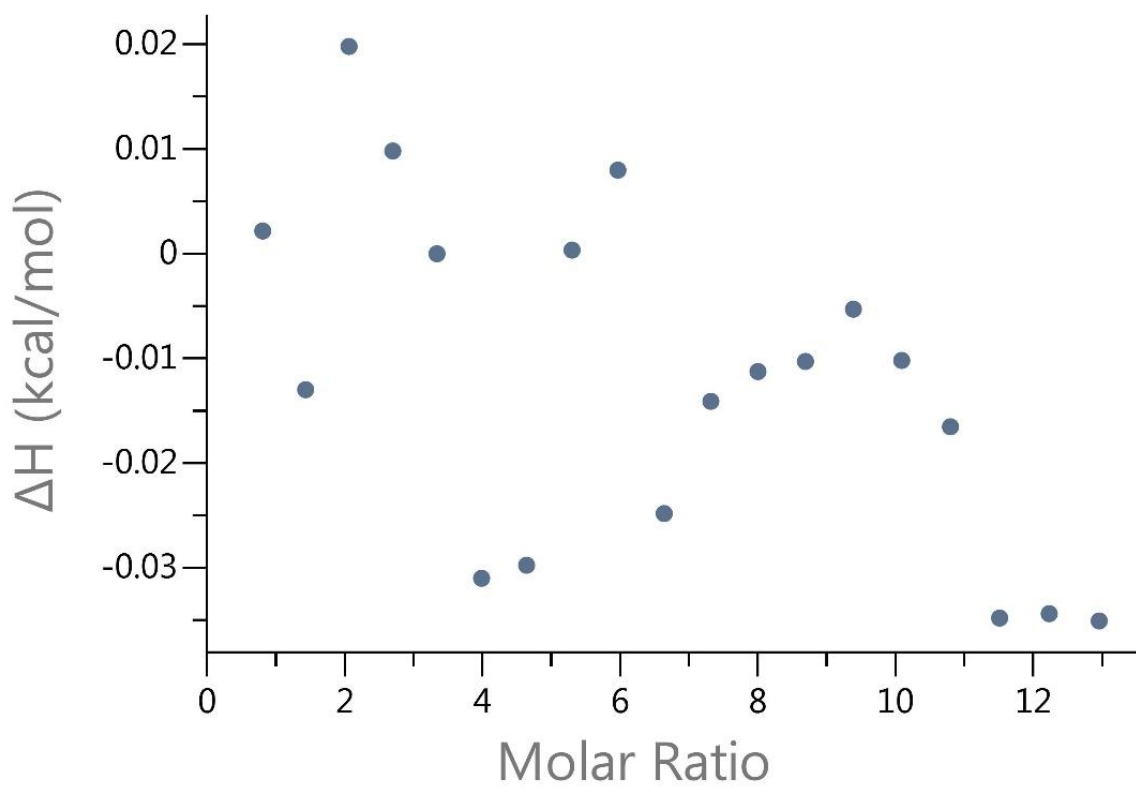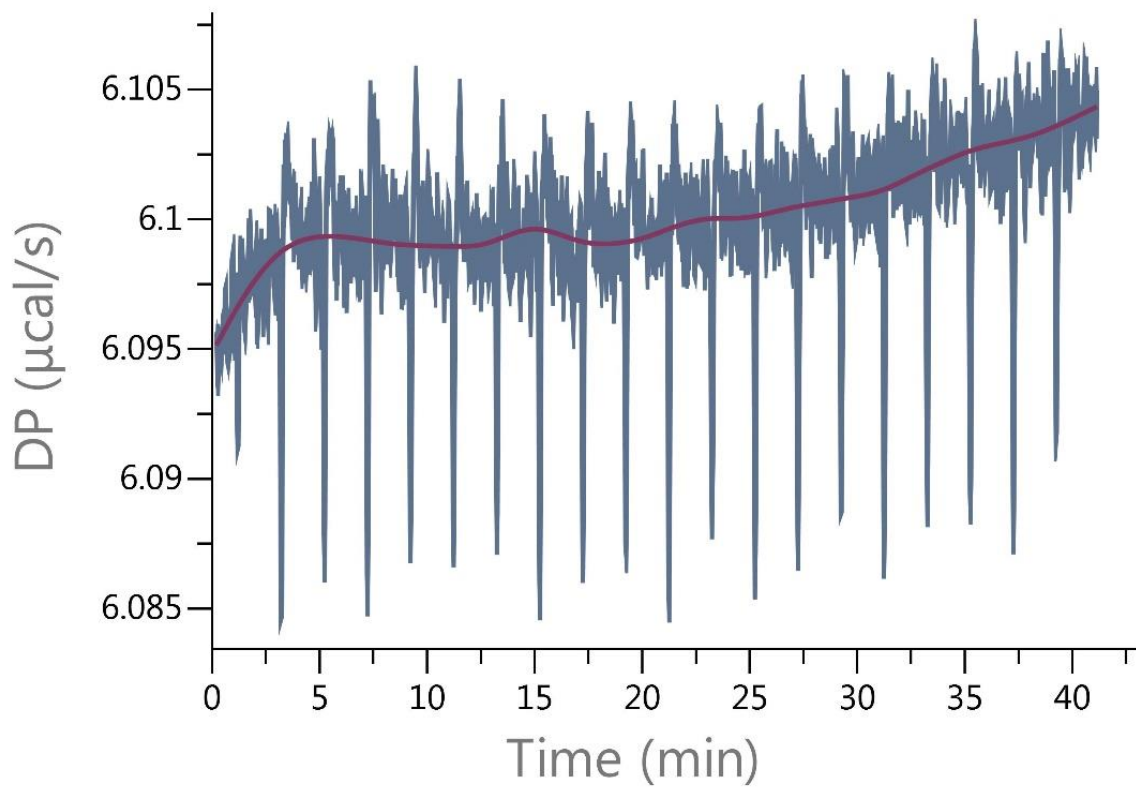
*At 1 mM*



No binding observed.
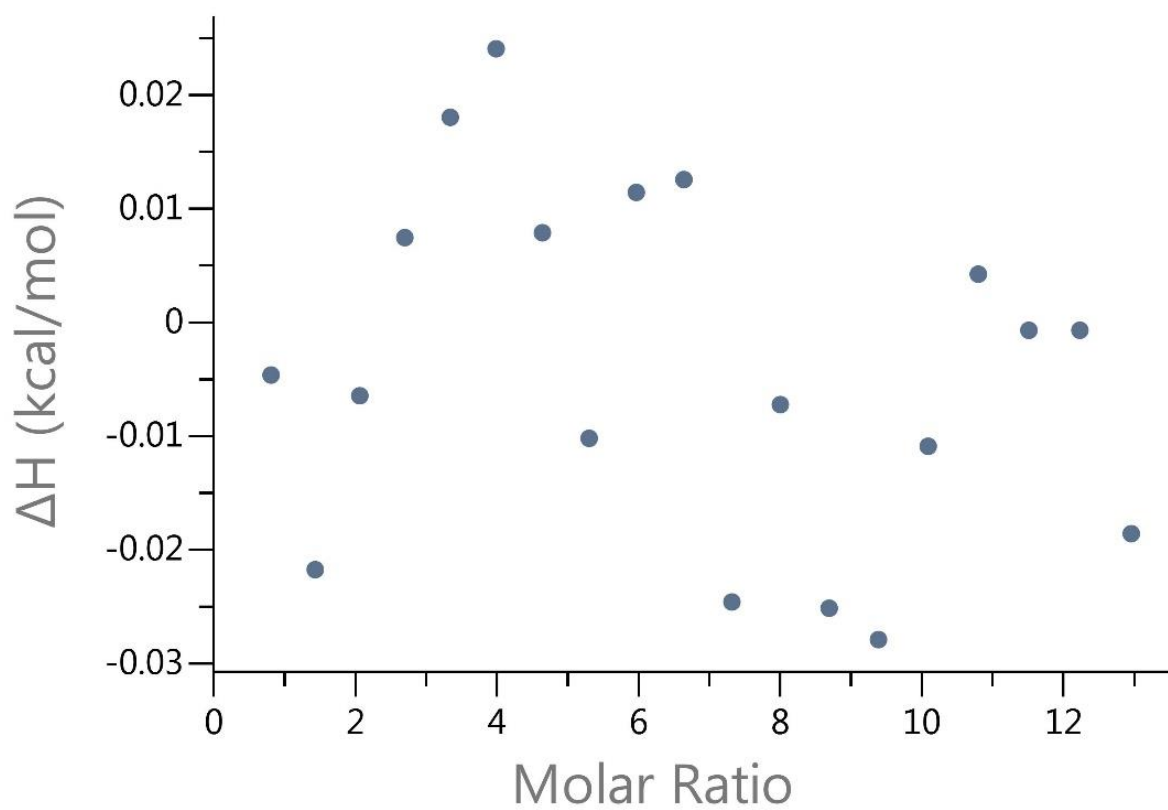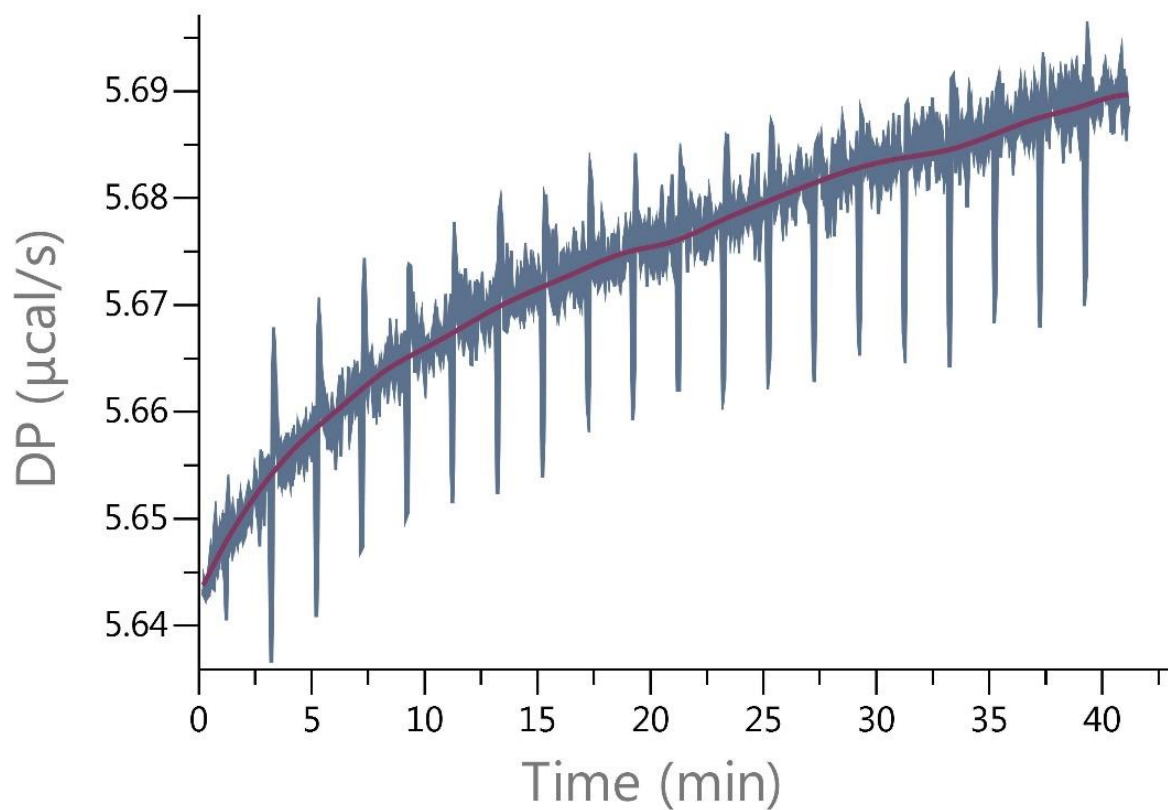
No binding observed.

**11.4.10 ITC measurement - MβCD**
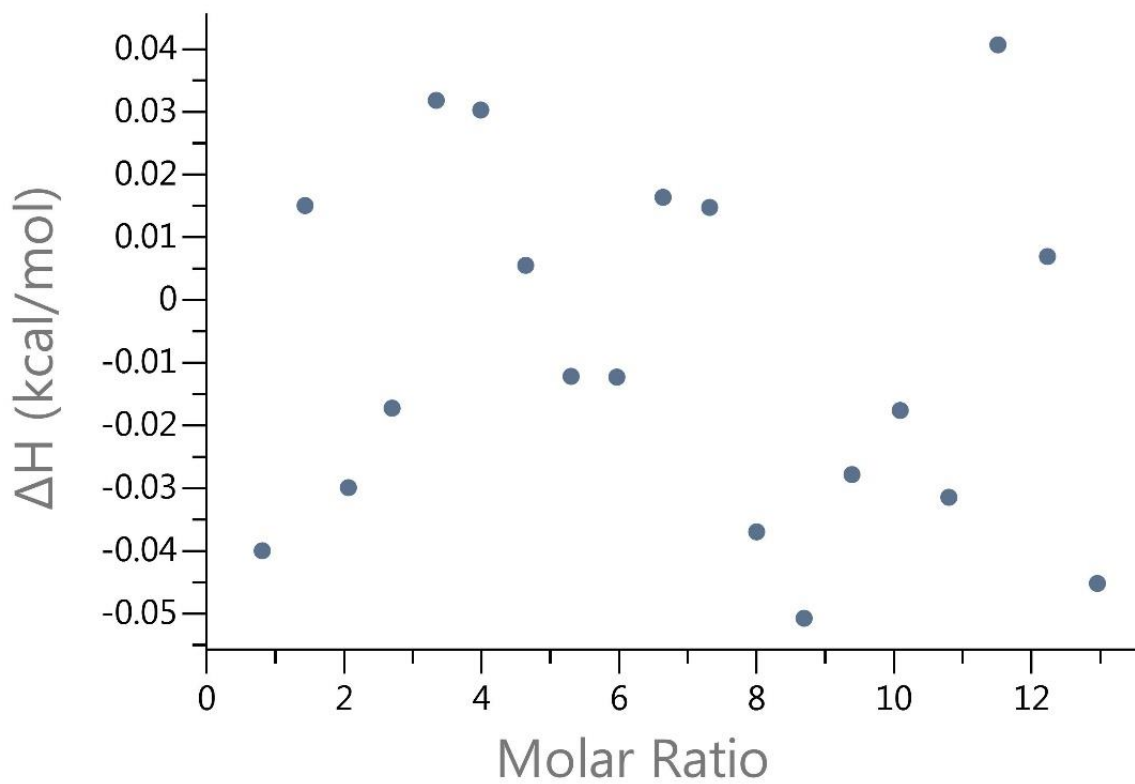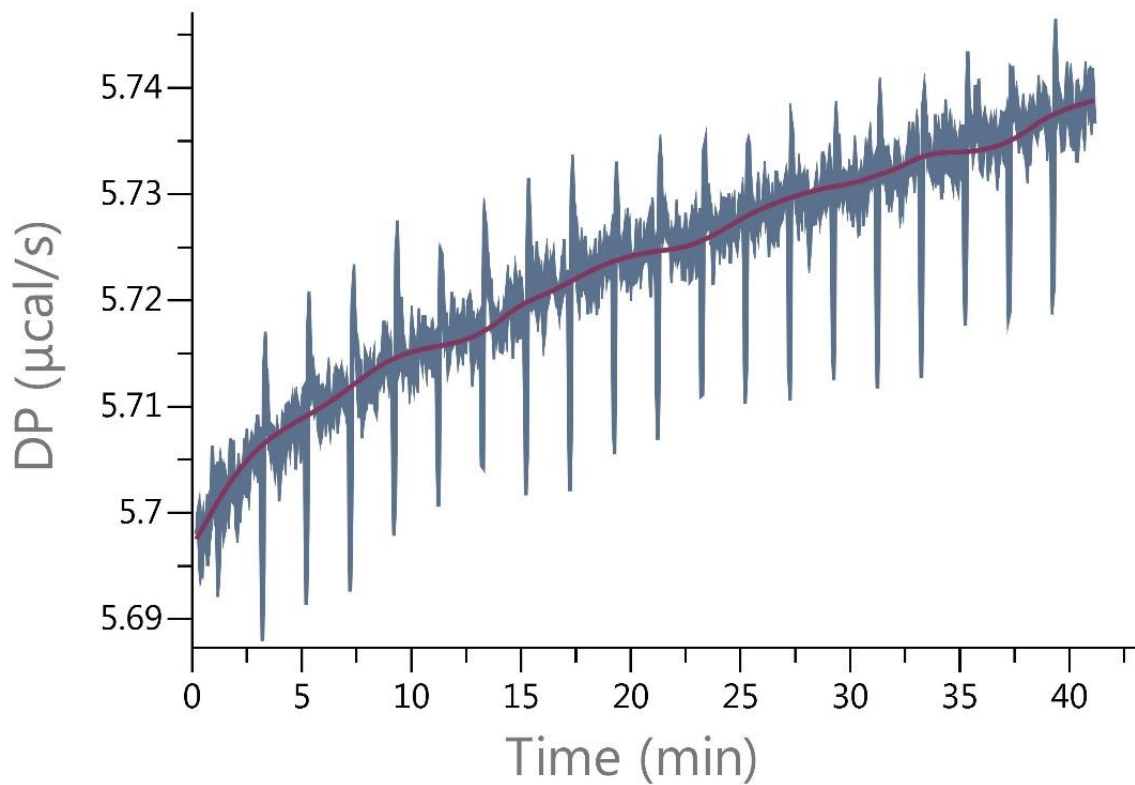
*At 1 mM*





No binding observed.
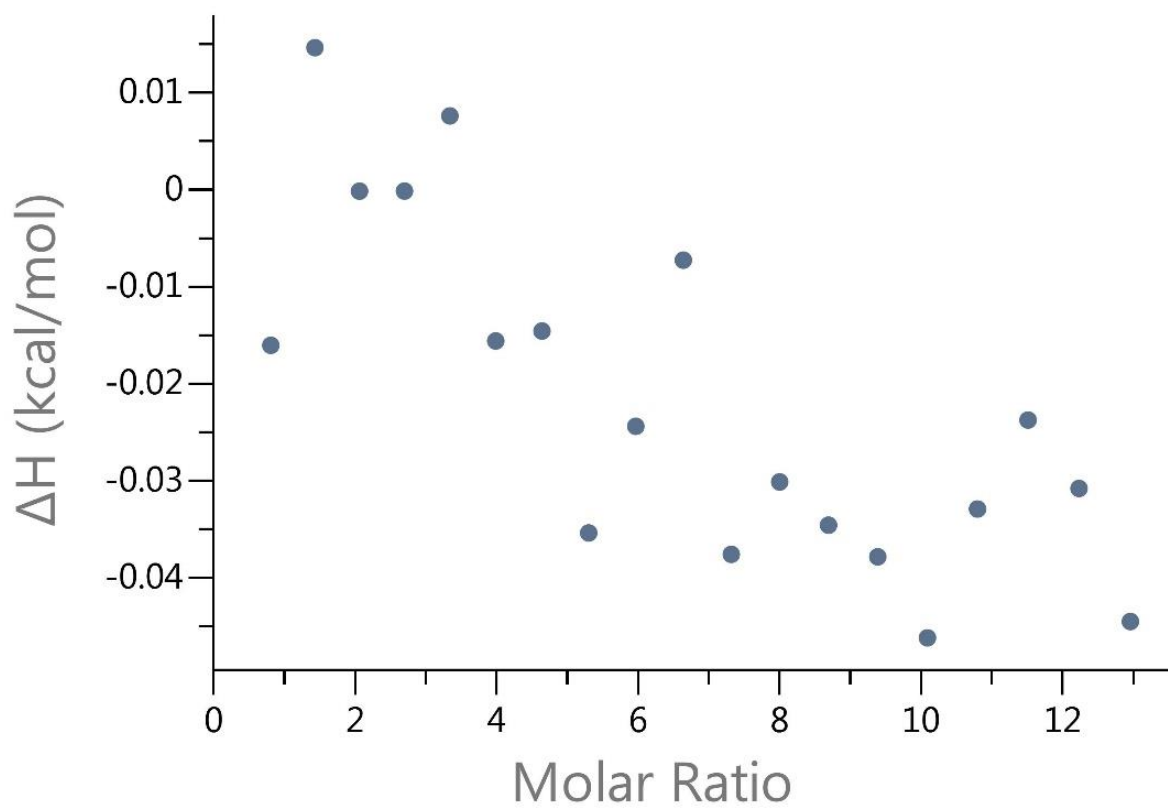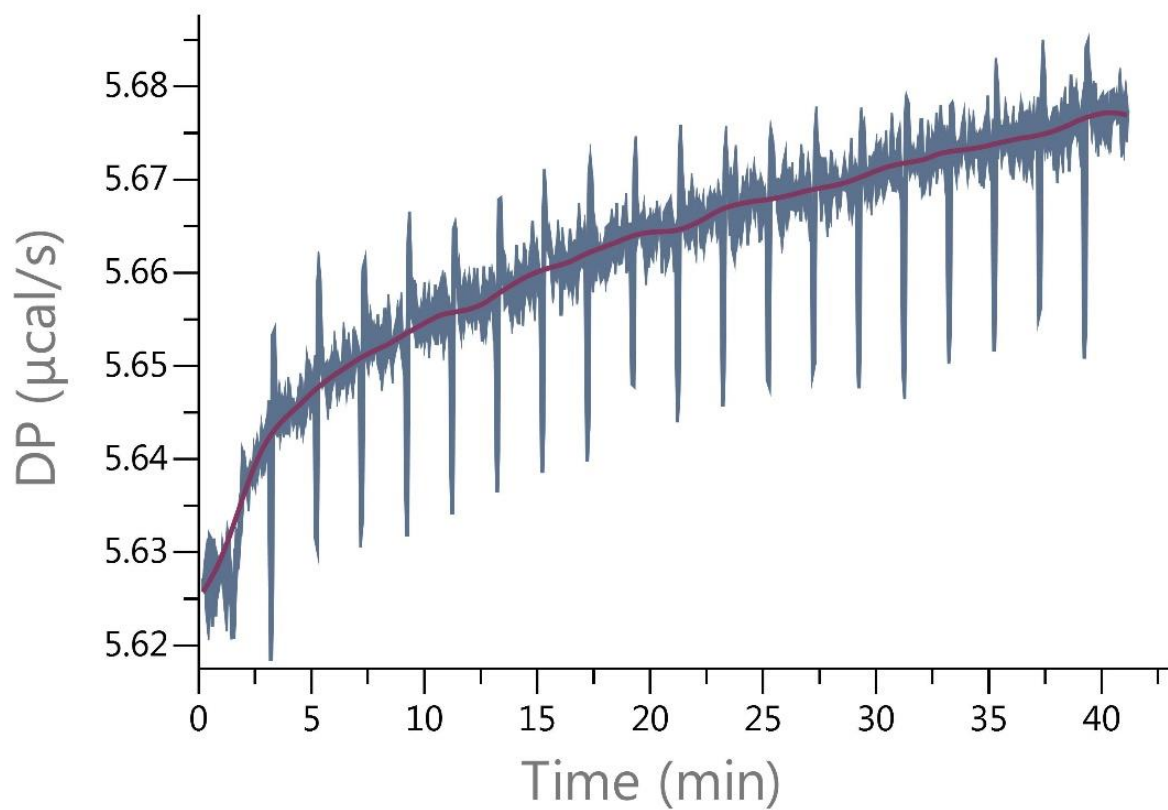
No binding observed.

**11.4.11 ITC measurement – HPβCD**
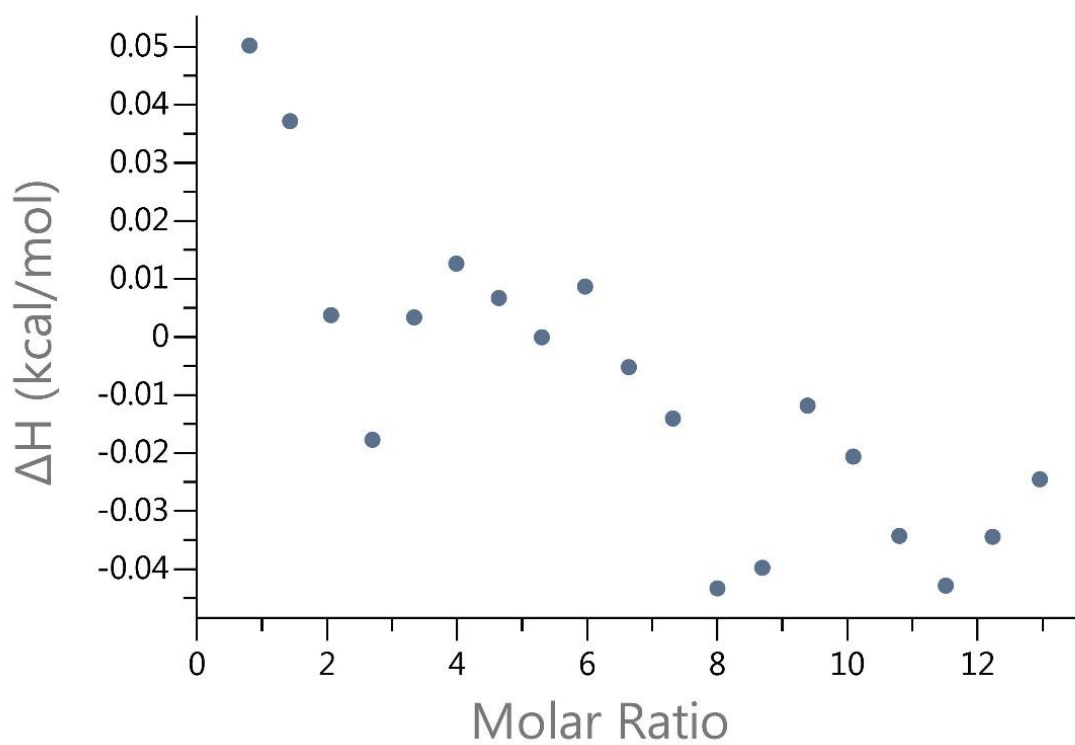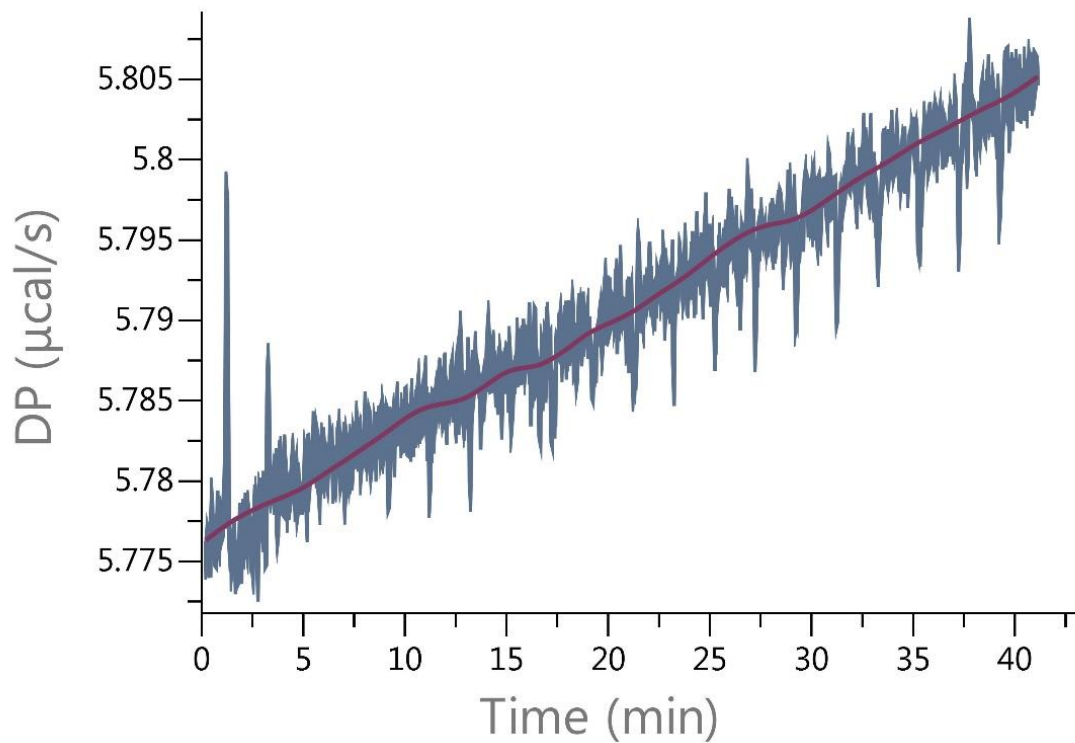
*At 1 mM*



No binding observed.
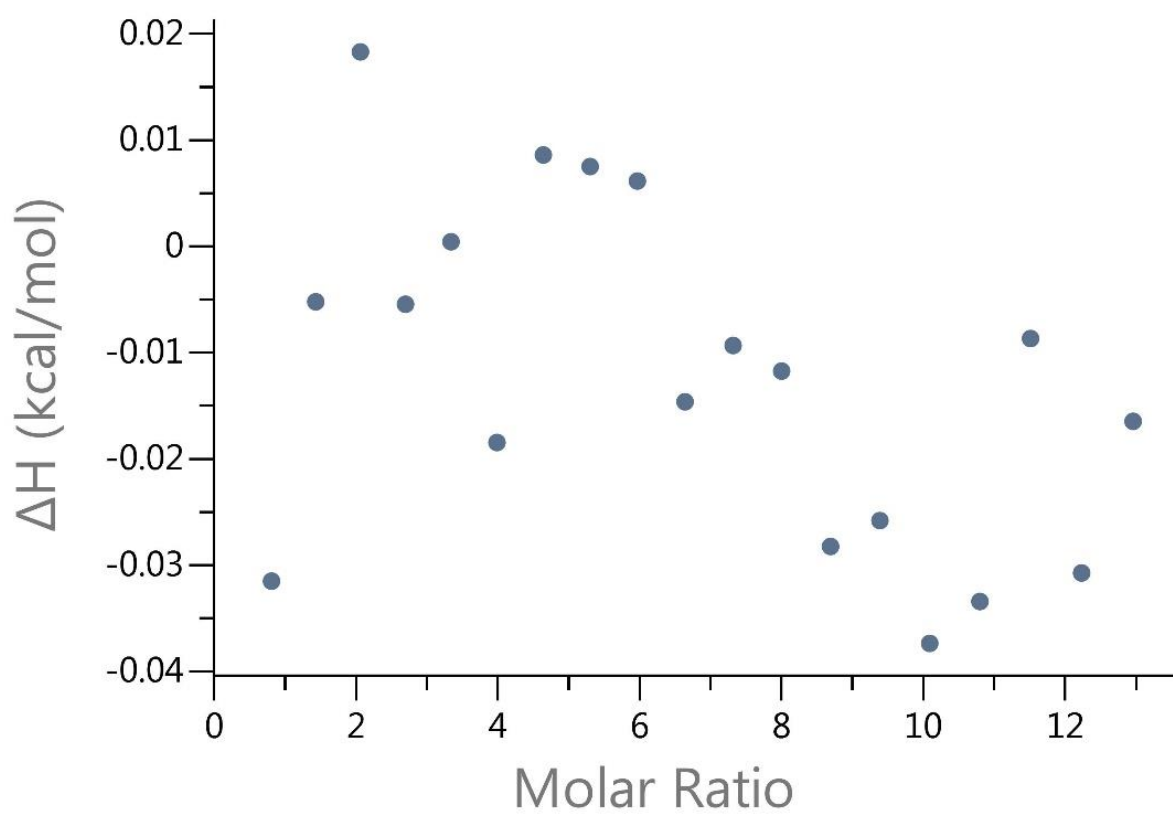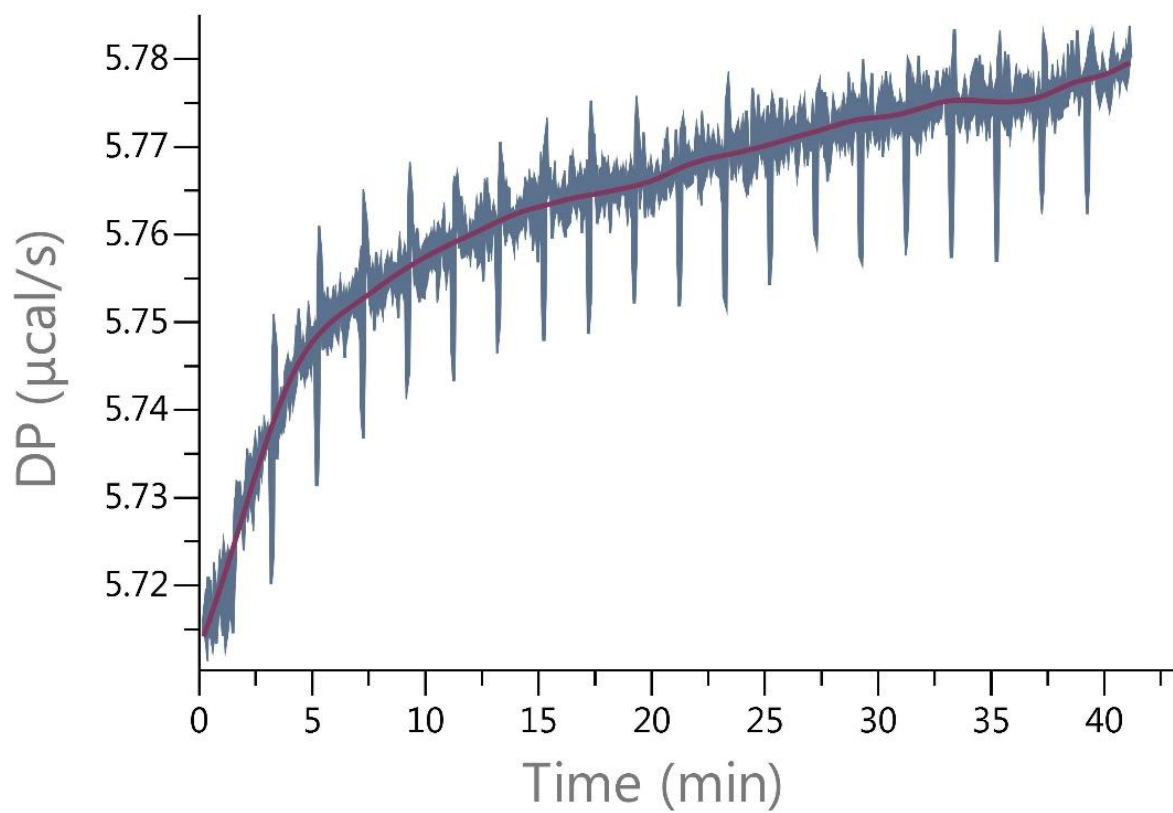
No binding observed.

**11.4.12 ITC measurement - SBEβCD**

*At 1 mM*





MB11SE1
Model: One Set of Sites
[Cell] (M) = 16.0e-6
[Syr] (M) = 1.00e-3
N (sites) = 7.80 ± 2.62
KD (M) = 170e-6 ± 506e-6
ΔH (kcal/mol) = -1.05 ± 2.35
Offset (kcal/mol) = -0.159 ± 0.241
ΔG (kcal/mol) = -5.14
-TΔS (kcal/mol) = -4.09
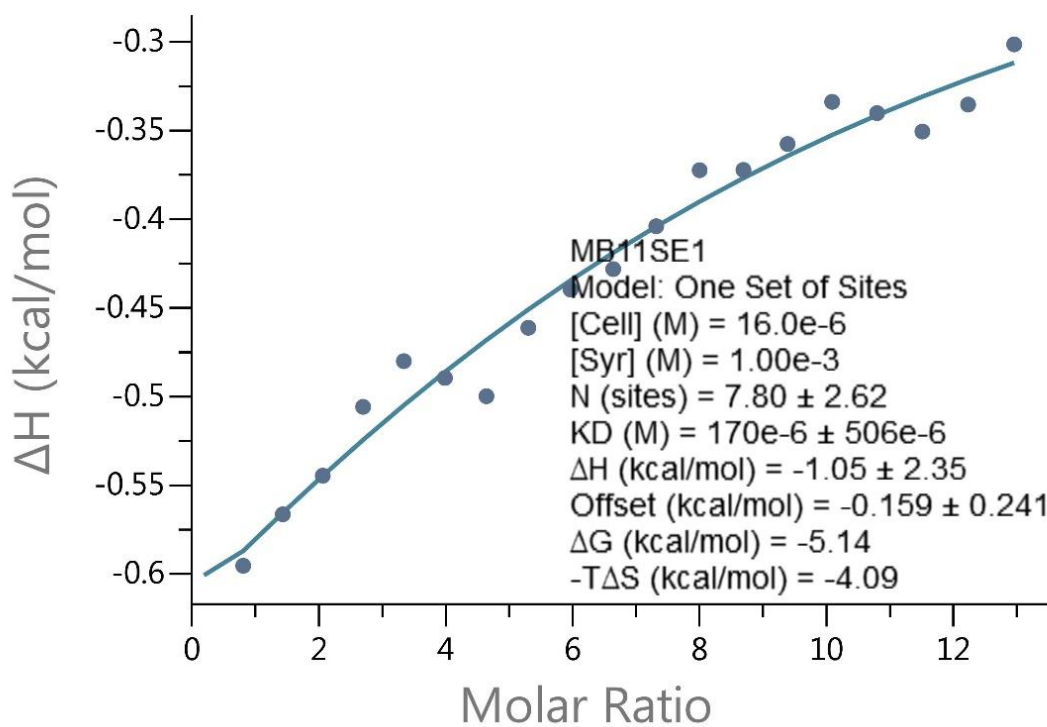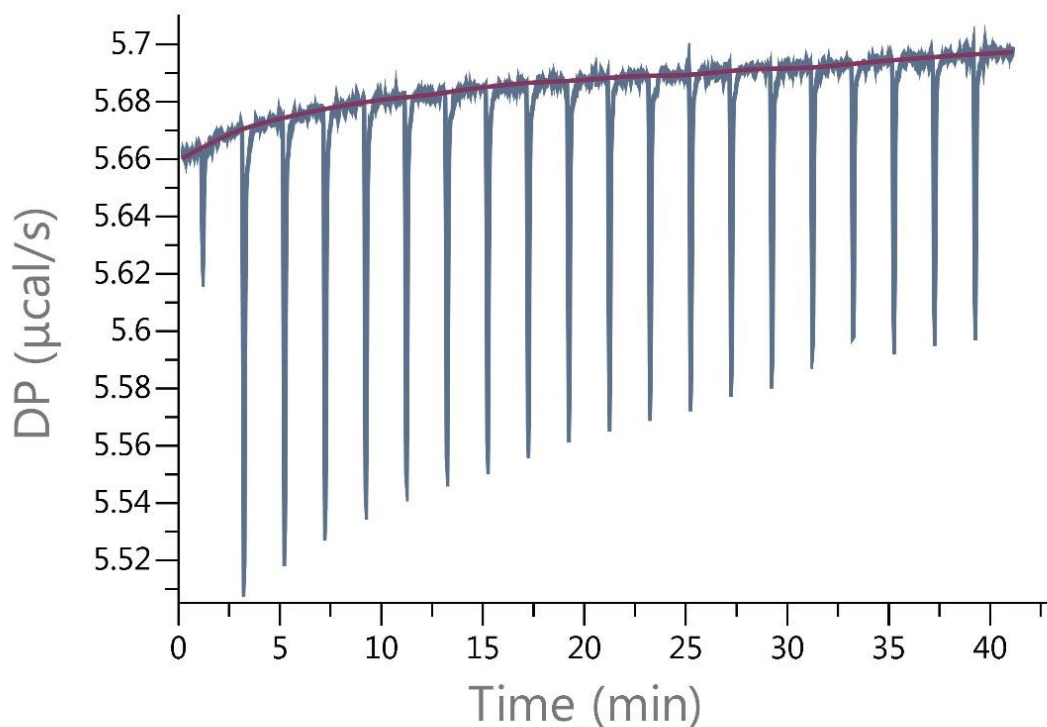
Values reported:

$K_D = 170 \times 10^{-6} \pm 506 \times 10^{-6}$ M

$K_A = 5882$ M$^{-1}$

Reduced $\chi^2 = 4.09 \times 10^{-4}$ Kcal/mol$^2$
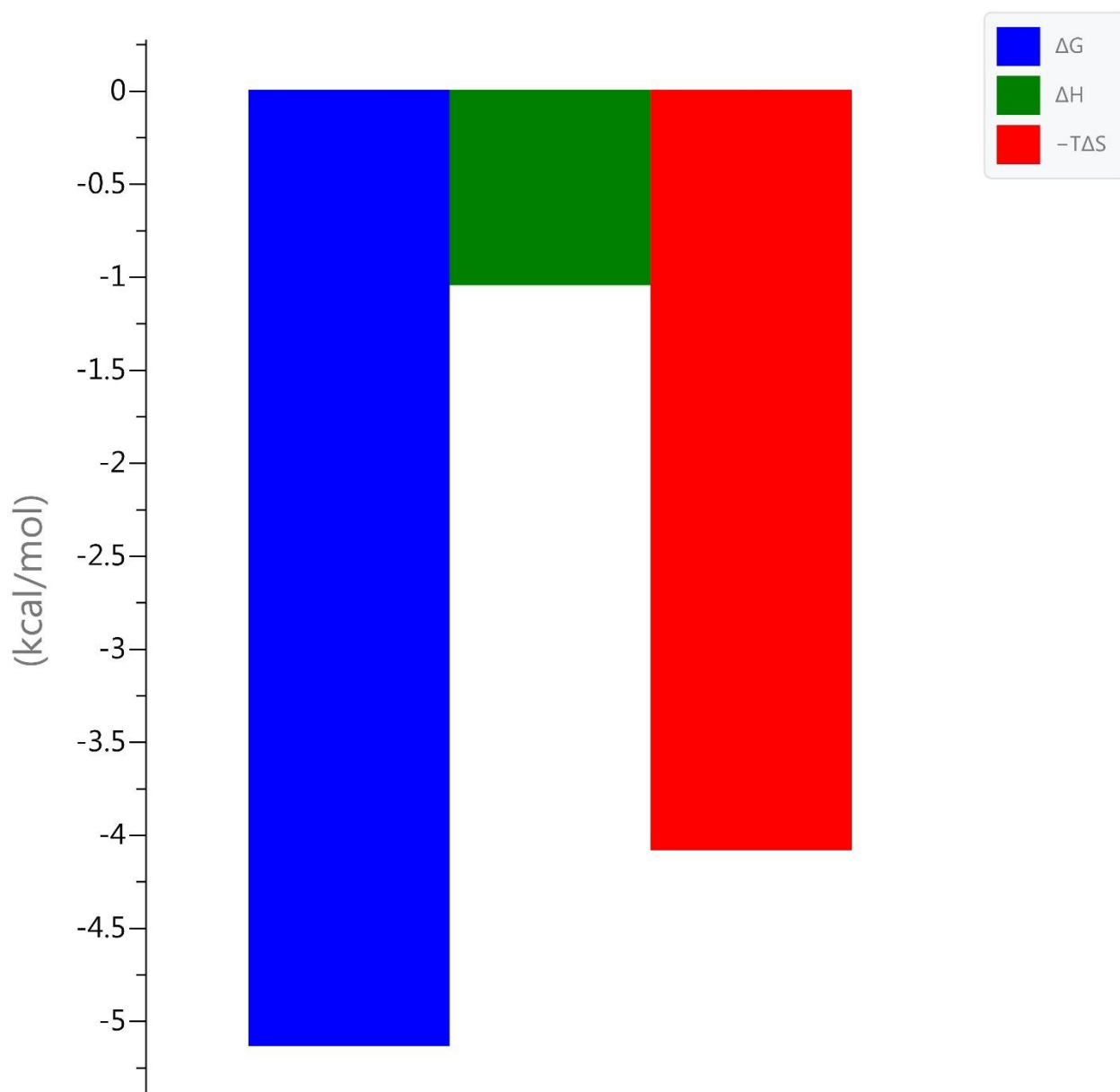
Reported values:

ΔH= -1.05± 2.35 Kcal/mol

ΔG= -4.97 Kcal/mol

-TΔS= -5.14 Kcal/mol

MB11SE1
Model: One Set of Sites
[Cell] (M) = 16.0e-6
[Syr] (M) = 1.00e-3
N (sites) = 1.00
KD (M) = 703e-6 ± 415e-6
ΔH (kcal/mol) = -24.3 ± 17.9
Offset (kcal/mol) = -6.8e-2 ± 9.8e-2
ΔG (kcal/mol) = -4.30
-TΔS (kcal/mol) = 20.0
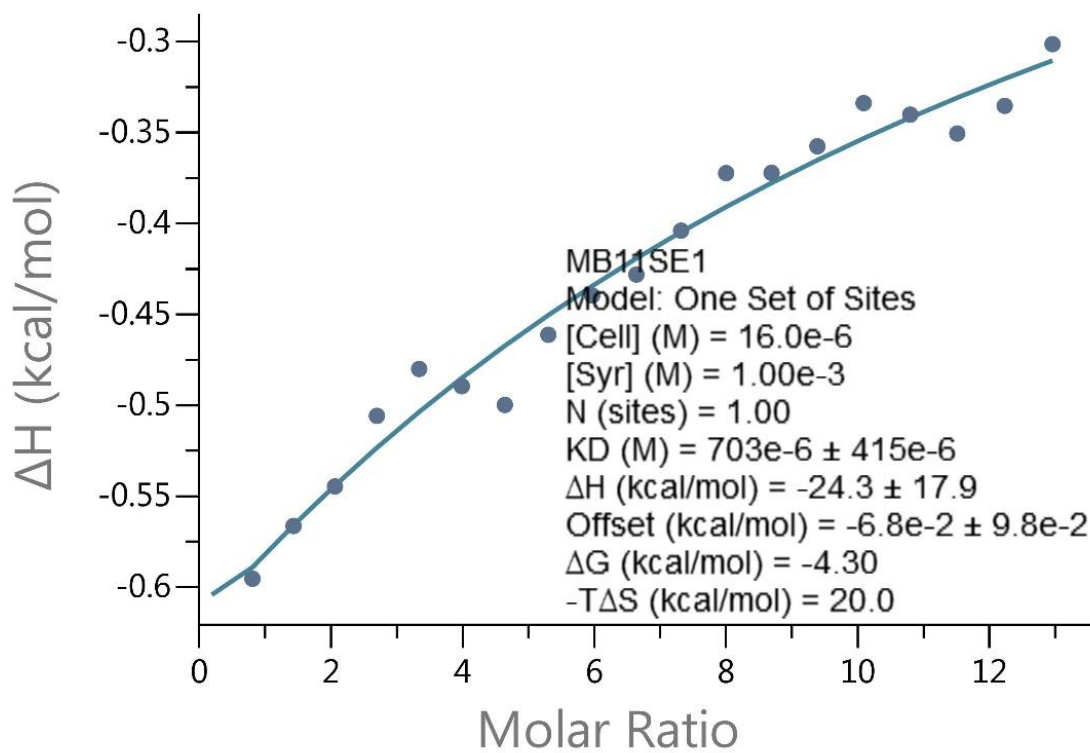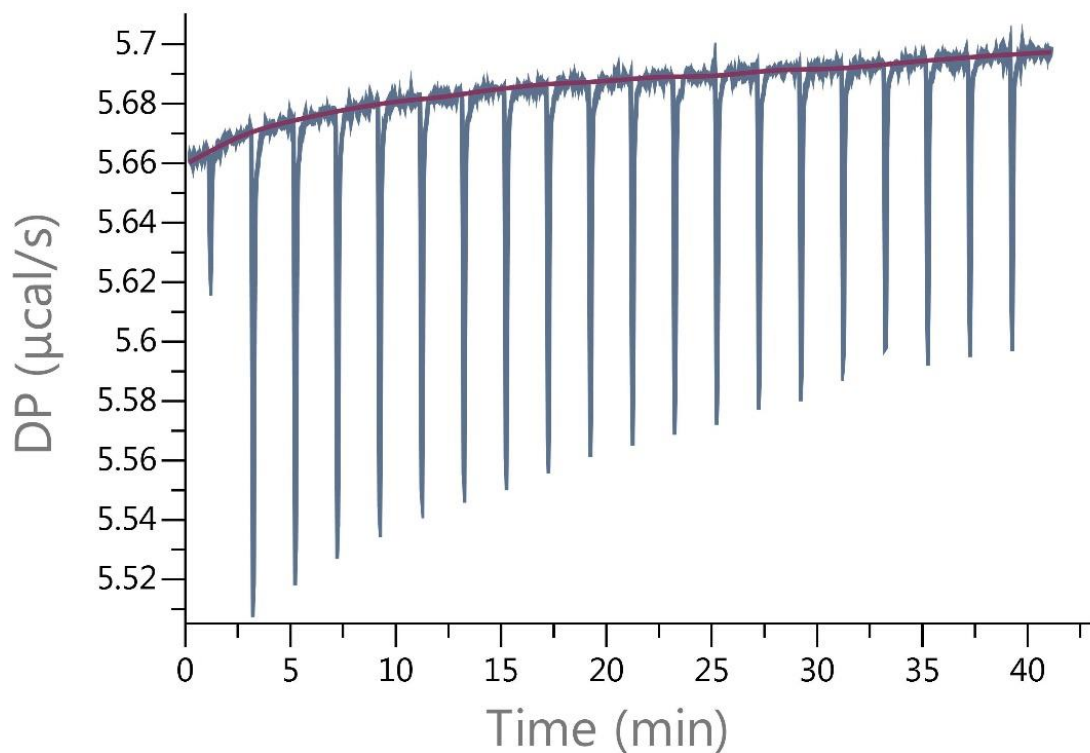
Reported values:
$K_D$= 703x10$^{-6}$ ±415x10$^{-6}$ M
$K_A$= 1422 M$^{-1}$
Reduced $\chi^2$= 2.3x10$^{-4}$ Kcal/mol$^2$
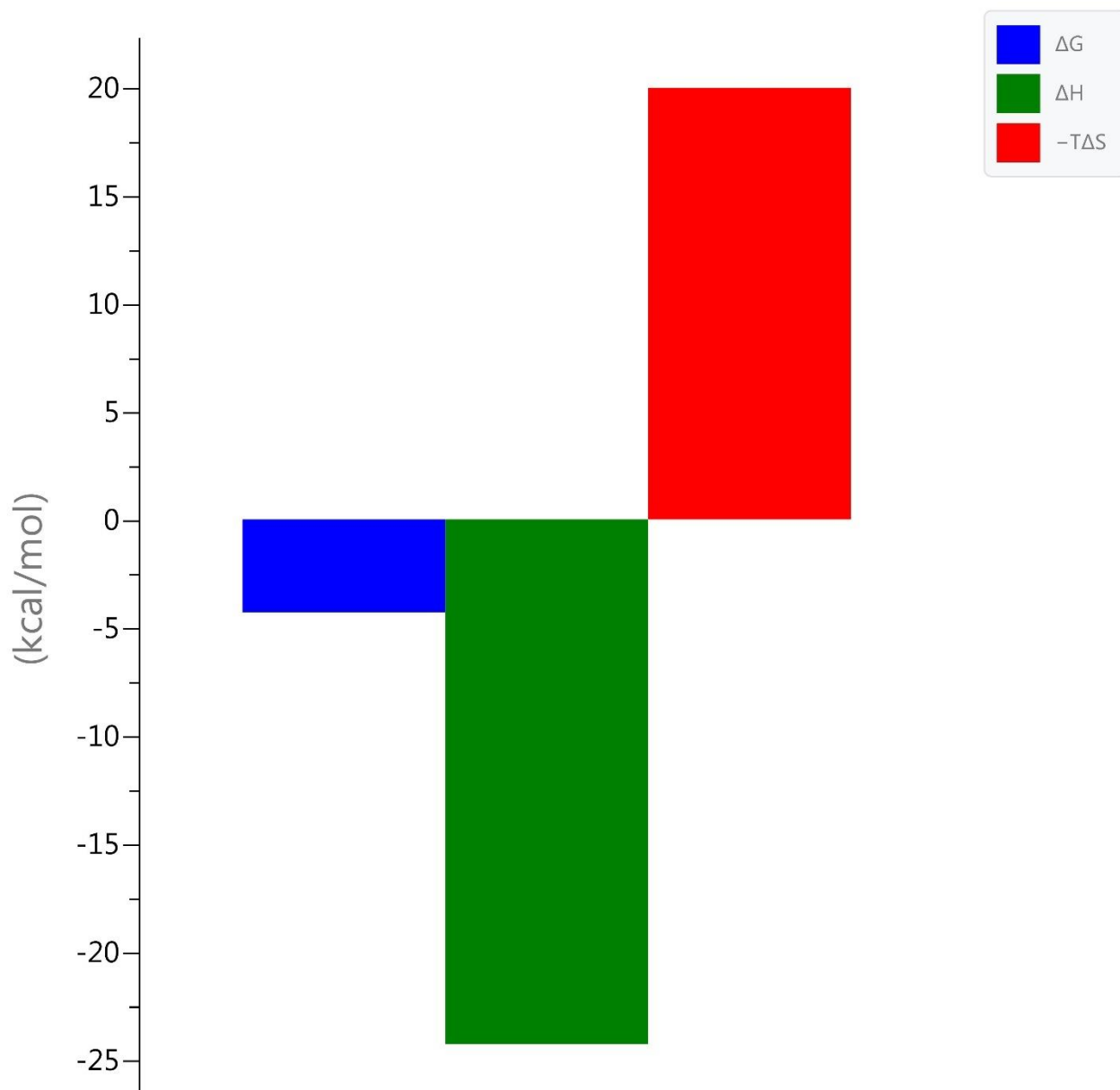
Reported values:
ΔH= -24.3± 17.9 Kcal/mol
ΔG= -4.43 Kcal/mol
-TΔS= 20 Kcal/mol
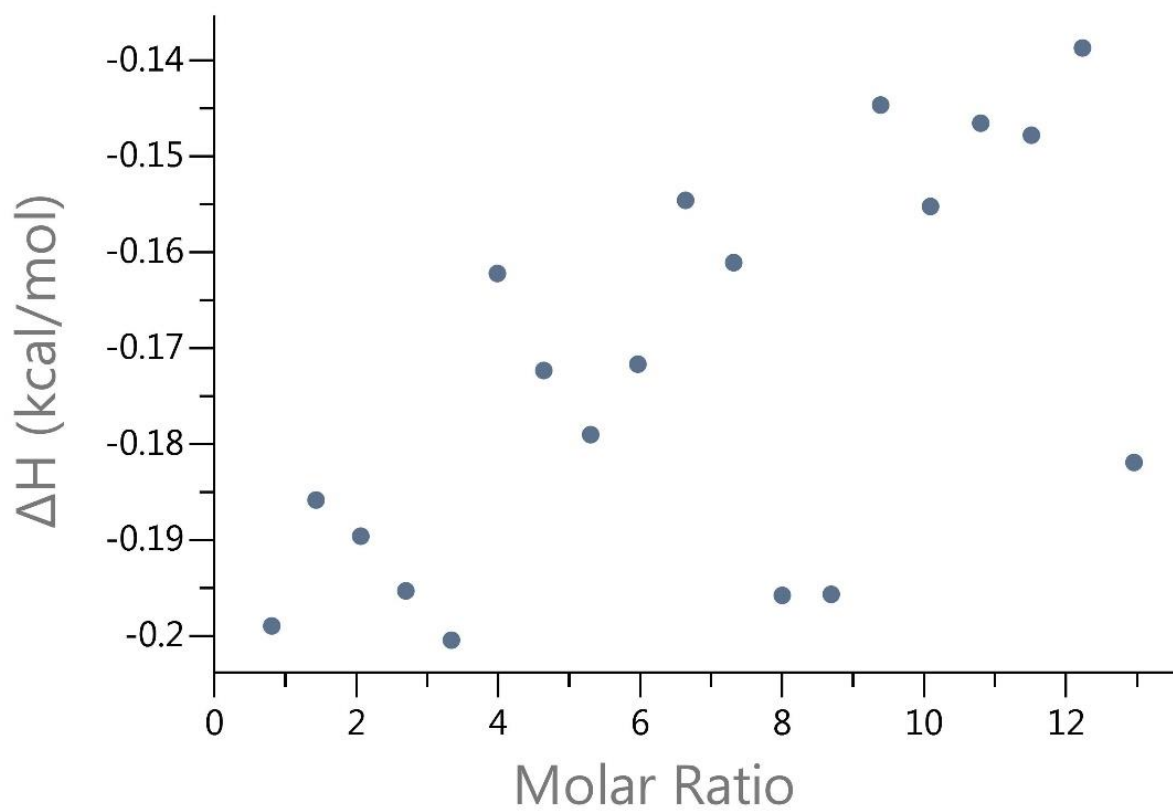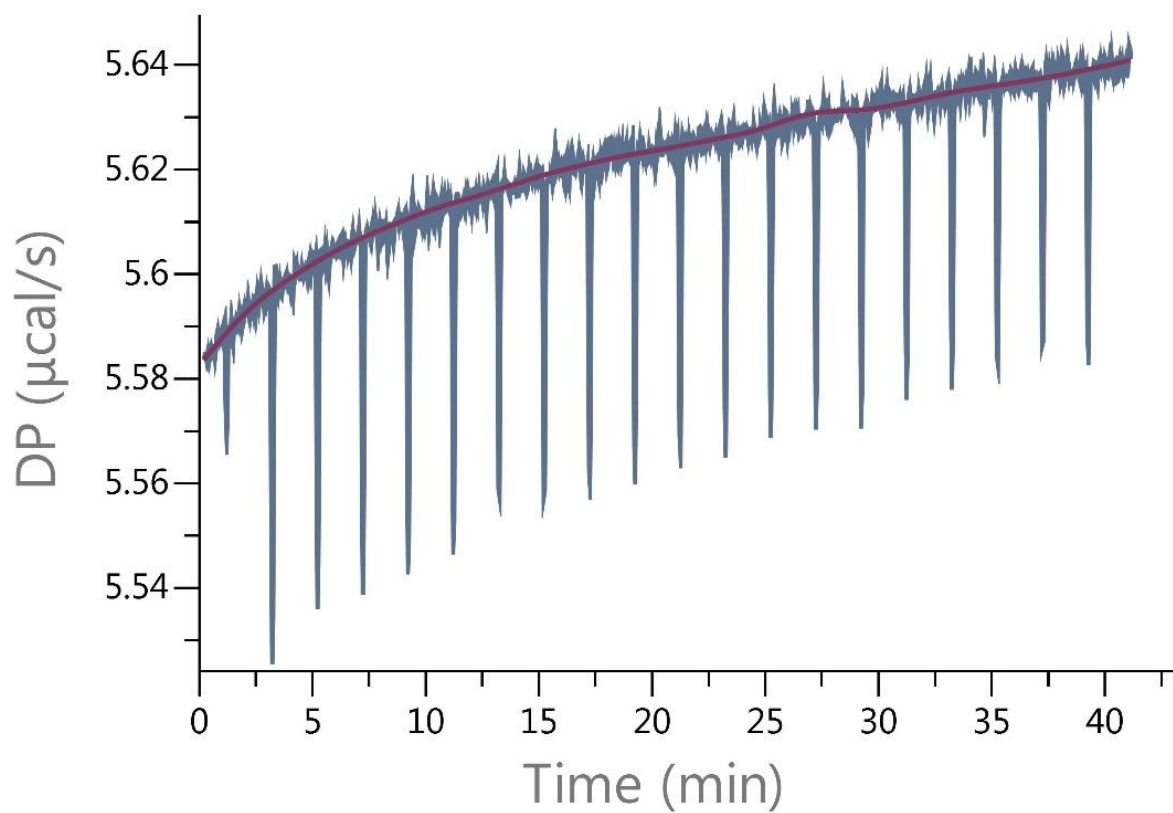
No binding observed.

**11.4.13 ITC measurement – DβCD**

*At 1 mM*
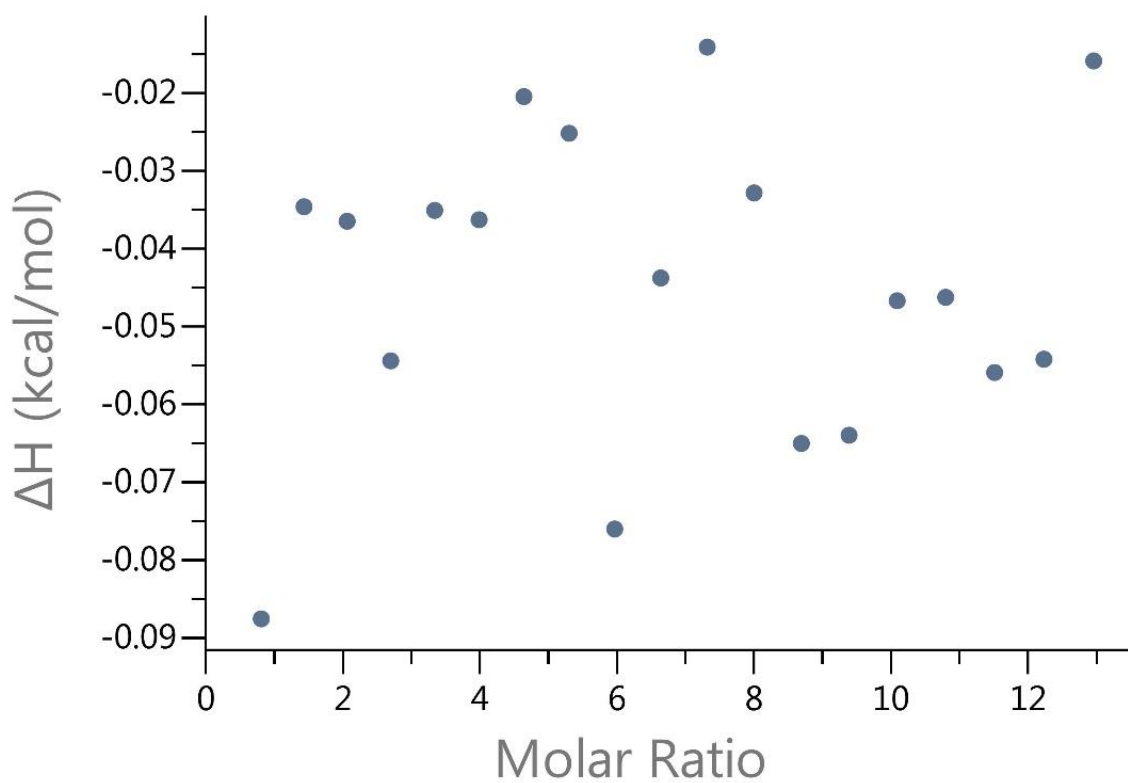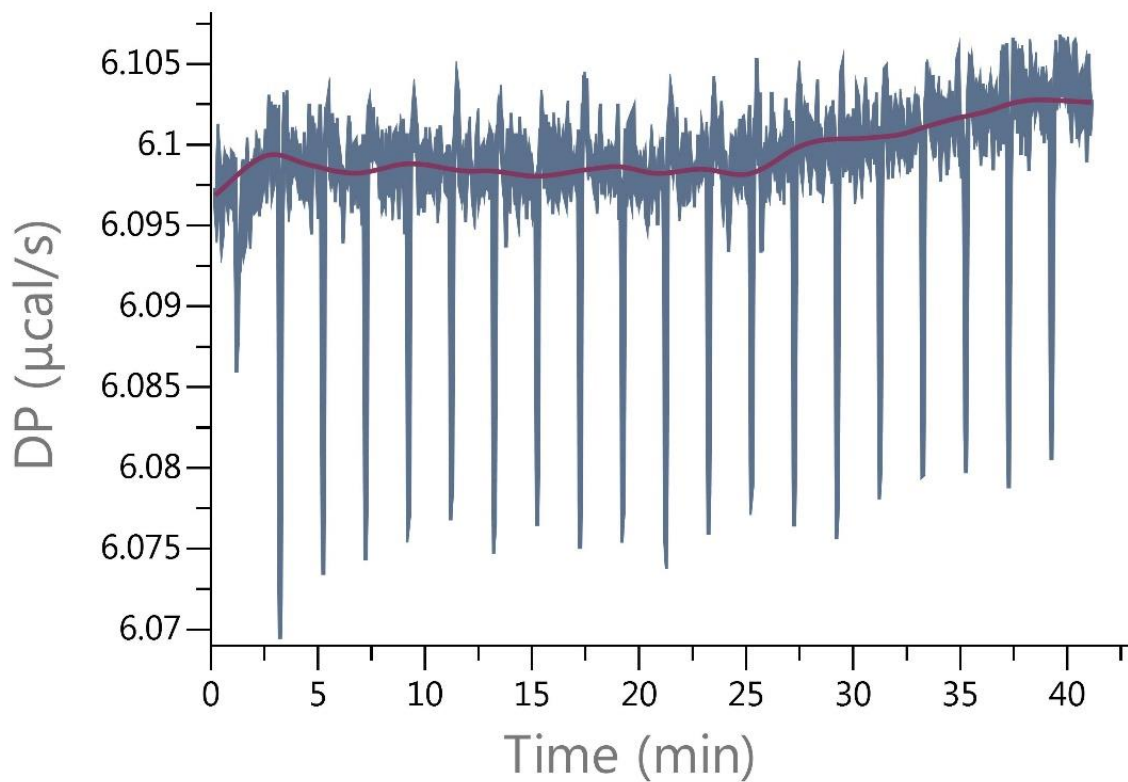


No binding observed.
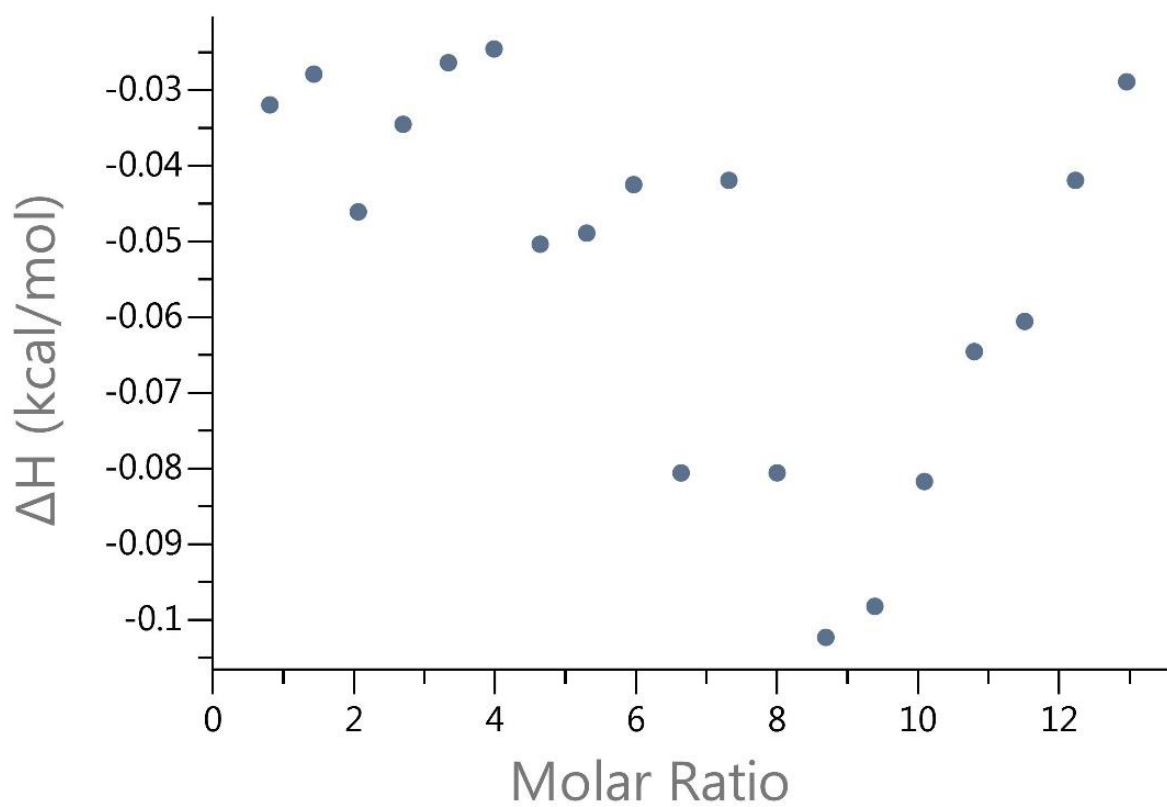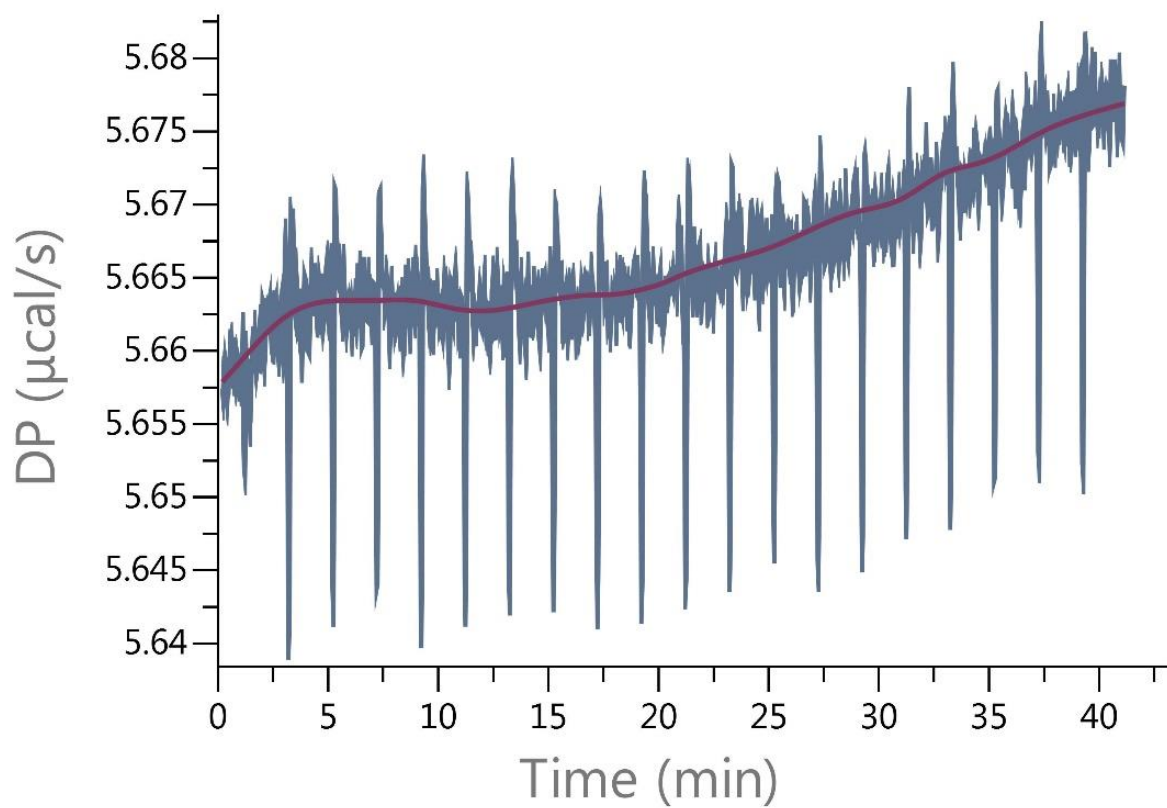
No binding observed.

## 11.5 3-(((3s,5s,7s)-adamantan-1-yl)disulfaneyl)propanehydrazine (2)
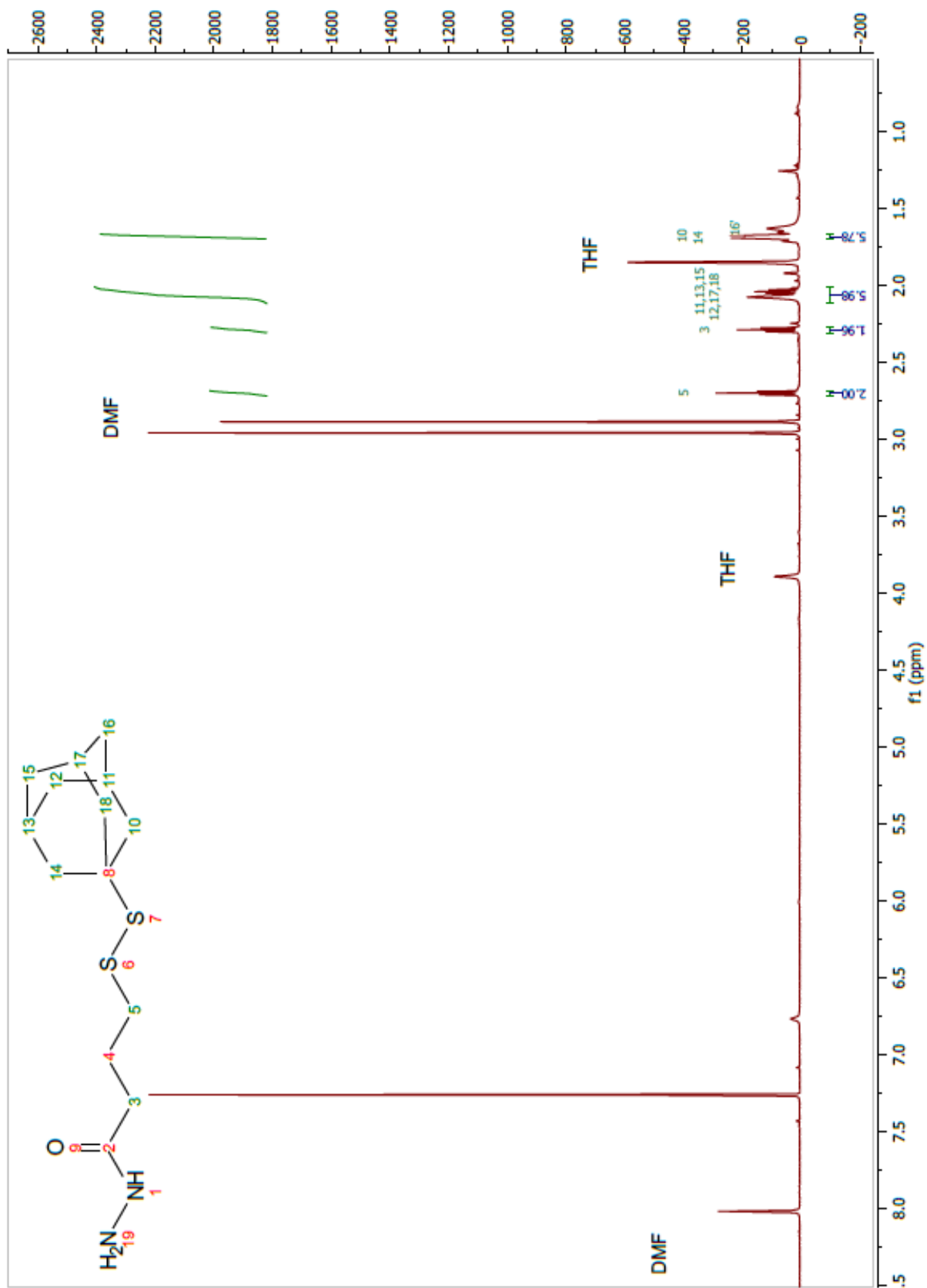


$^1$H NMR (CDCl$_3$): δ 2.70 (2H, t, $J$=6.69 Hz), 2.29 (2H t, $J$=7.26 Hz), 2.05 (m) 1.69 (m).

## 11.6 4-(((1s,3R)-adamantan-1-yl)disulfaneyl)-N-((E(-1((2S,4S)-4-(((2R,4S,5R,6S)-1-amino-5-hydroxy-6-methyltetrahydro-2*H*-pyran-2-yl)oxy)-2,5,12-trihydroxy-7-methyoxy-6,11-dioxo-1,2,3,4,6,11-hexalhydrotetracen-2-yl)-2-hydroxyethylidene)butanehydrazide (1)

### 11.6.1 Reaction A

*11.6.1.1 Before purification*



$^1$H NMR ((CD$_3$)$_2$SO$_2$): δ 7.93 (m) 7.69-7.65 (m), 5.45 (m) 5.30 (m), 4.96 (m), 4.87 (m), 4.00 (s), 3.57 (m), 3.03-2.92 (m), 2.18-1.53 (m), 1.16 (m).

*11.6.1.2 Purification*

**REVELERIS® PREP**

Method Name:
Run Name: MFB/2017-03-22_13-28-01mb09
Run Date: 2017-03-22 13:37

Column: Reveleris® C18 12g
Flow Rate: 30 mL/min
Equilibration: 6.0 CV
Run Length: 28.1 CV
Mode: Flash Liquid

Solvent A: Water
Solvent B: Methanol
Solvent C: Empty
Solvent D: Empty
Slope Detection: Off

UV Threshold: 0.02 AU
UV Sensitivity: Low
UV1 Wavelength: 254 nm
UV2 Wavelength: 265 nm
UV3 Wavelength: 550 nm

ELSD Threshold: 20 mV
ELSD Sensitivity: Low
Collection: Collect Peaks
Per-Vial Volume: 7 mL
Non-Peak Volume: 8.5 mL
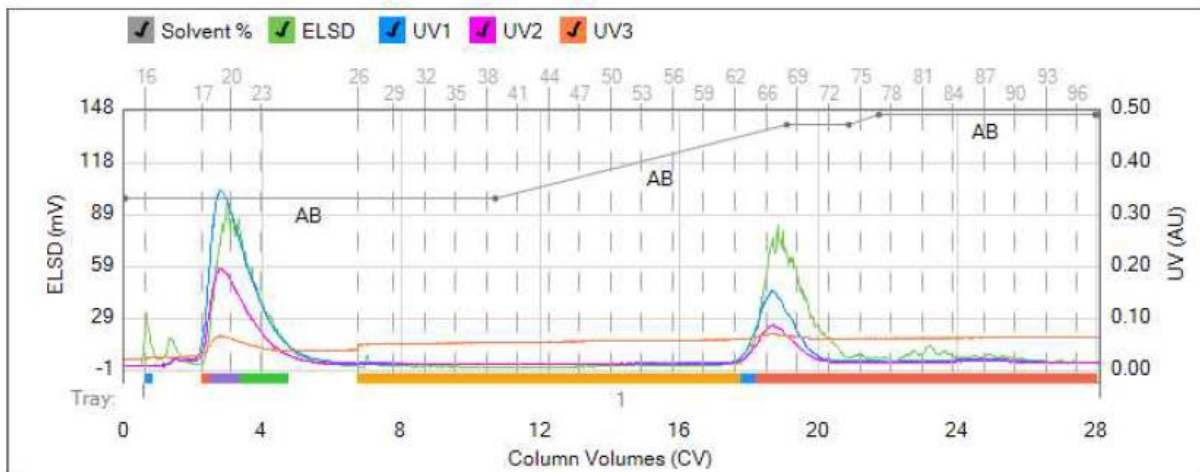


1 - 4019



**Gradient Table**

|   | CV | Solvents | % 2nd |
|---|------|----------|-------|
| 1 | 0.0  | AB | 66 |
| 2 | 10.7 | AB | 66 |
| 3 | 8.4  | AB | 95 |
| 4 | 1.8  | AB | 95 |
| 5 | 0.9  | AB | 99 |
| 6 | 6.3  | AB | 99 |
| 7 | 6.3  | AB | 99 |

**Vial Mapping Table**

| Peak # | Start Tray:Vial | End Tray:Vial |
|--------|-----------------|---------------|
| 1 | 1:16 | 1:16 |
| 2 | 1:17 | 1:17 |
| 3 | 1:18 | 1:20 |
| 4 | 1:21 | 1:25 |
| 5 | 1:26 | 1:62 |
| 6 | 1:63 | 1:64 |
| 7 | 1:65 | 1:98 |
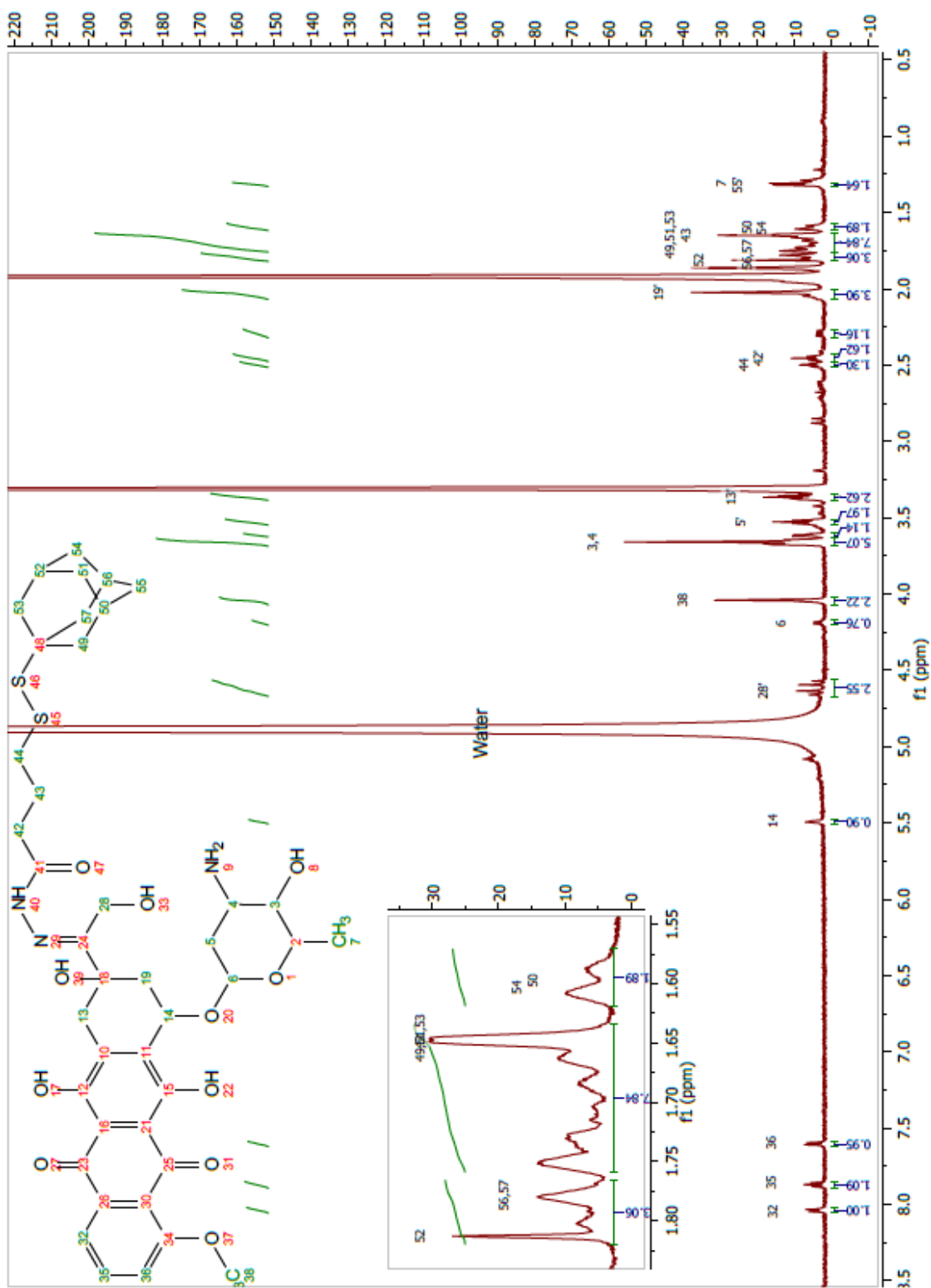
^{1}H NMR (CD₃OD): δ 8.04 (2H, d, $J$=8.64 Hz), 7.87 (2H, t, $J$=8.13 Hz), 7.60 (2H, d, $J$=8.64 Hz), 5.49 (1H, m), 4.62 (2H, dd, $J$=14.12, 23.39 Hz), 4.19 (1H, d, $J$=7.06 Hz), 4.04 (3H, s) 3.66 (1H, m) 3.62 (1H, m), 3.53 (1H, m) 3.37 (1H, m), 2.50 (2H, t, $J$=6.80 Hz), 2.45 (2h, t, $J$=7.38 Hz), 2.29 (2H, m) 2.02 (4H, m), 1.80 (6H, m) 1.76-1.64 (5H, m), 1.59 (2H, m), 1.31 (3H, d, $J$=6.5 Hz).
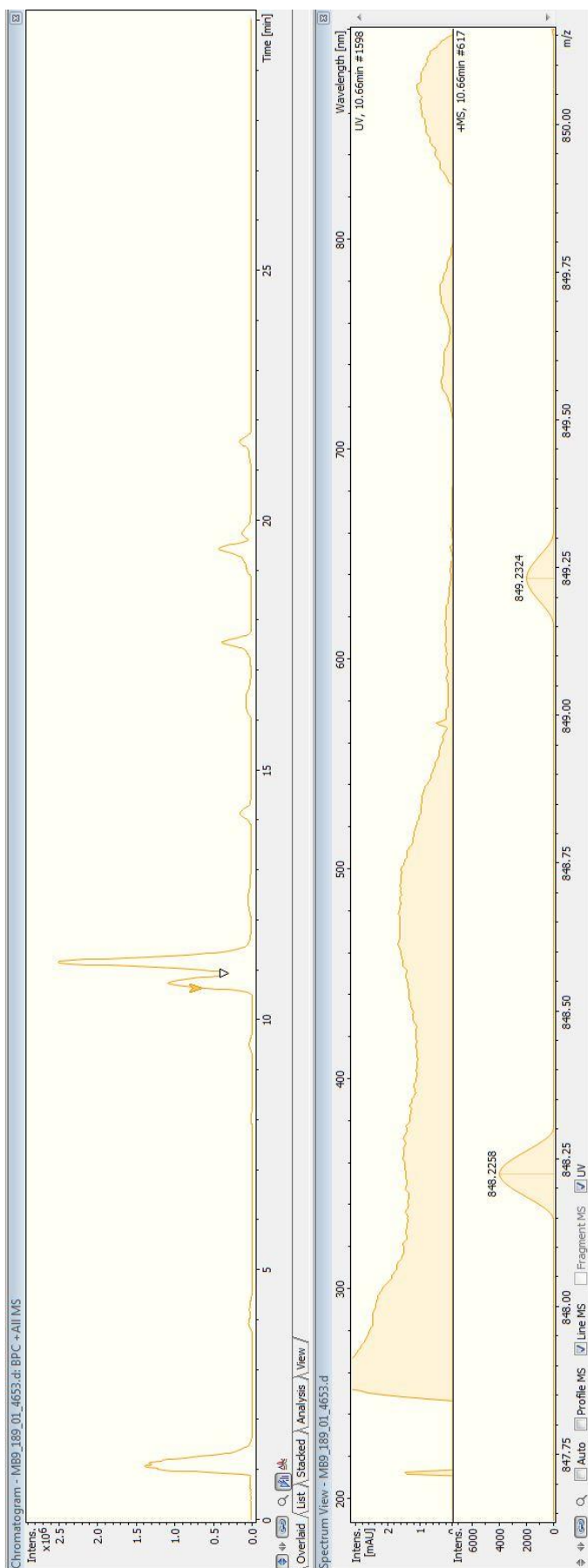
LC-MS: m/z = 848.2258 [M+Na$^+$], calc. for. (C$_{41}$H$_{51}$N$_3$O$_{11}$S$_2$ Na$^+$): m/z: 848.2857

Deviation of 0.0599 Da.

MB09B1
Model: One Set of Sites
[Cell] (M) = 16.0e-6
[Syr] (M) = 1.00e-3
N (sites) = 1.6e-2 ± 0.614
KD (M) = 33.9e-6 ± 11.2e-6
ΔH (kcal/mol) = -80.0 ± 3140
Offset (kcal/mol) = -1.9e-2 ± 5.9e-3
ΔG (kcal/mol) = -6.10
-TΔS (kcal/mol) = 73.9
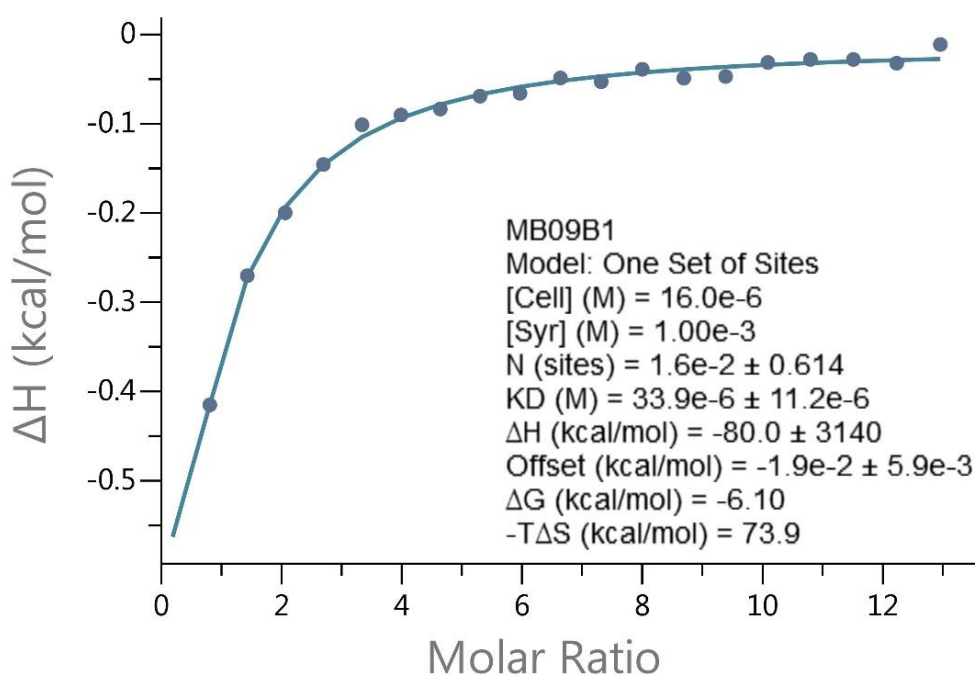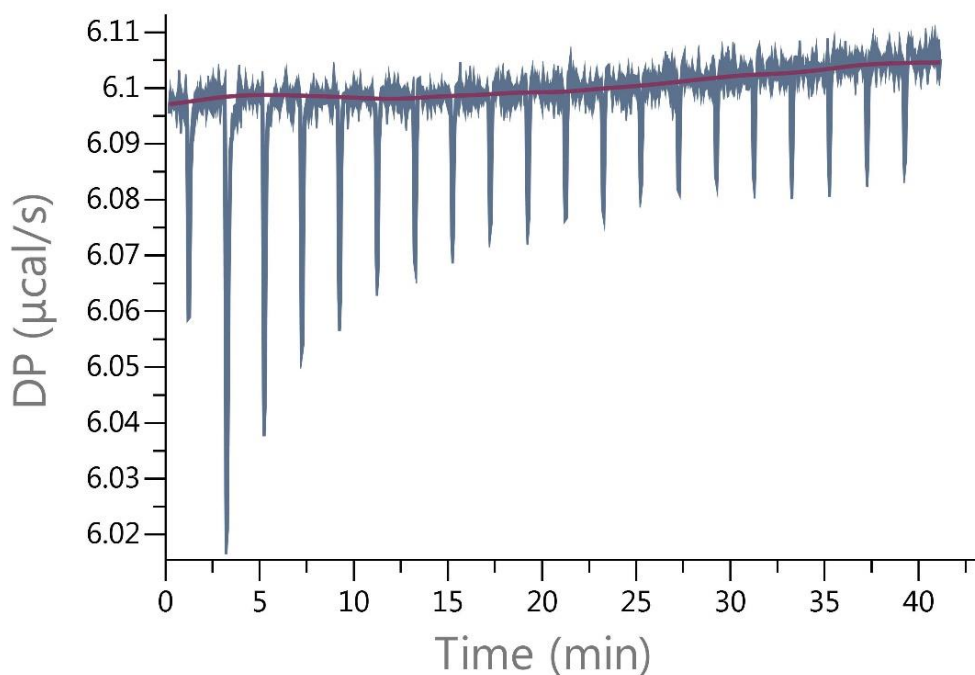
Values reported:

$K_D$=33.9x10$^{-6}$ ± 11.2x10$^{-6}$ M

$K_A$=29499 M$^{-1}$

ΔH= -80.0 ± 3140 Kcal/mol

ΔG= -6.10 Kcal/mol

-TΔS= 73.9 Kcal/mol

Reduced $\chi^2$=6.0x10$^{-5}$ Kcal/mol$^2$

MB09B1
Model: One Set of Sites
[Cell] (M) = 16.0e-6
[Syr] (M) = 1.00e-3
N (sites) = 1.00
KD (M) = 17.1e-6 ± 1.94e-6
$\Delta$H (kcal/mol) = -1.02 ± 5.5e-2
Offset (kcal/mol) = -2.8e-2 ± 3.9e-3
$\Delta$G (kcal/mol) = -6.50
-T$\Delta$S (kcal/mol) = -5.49
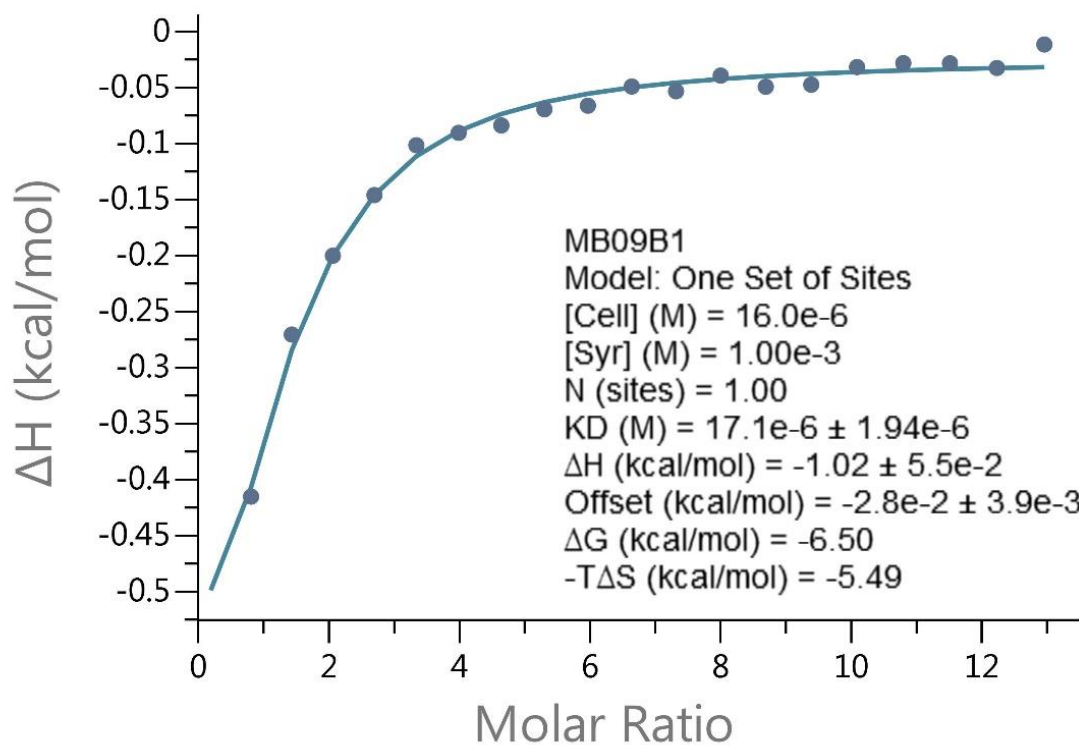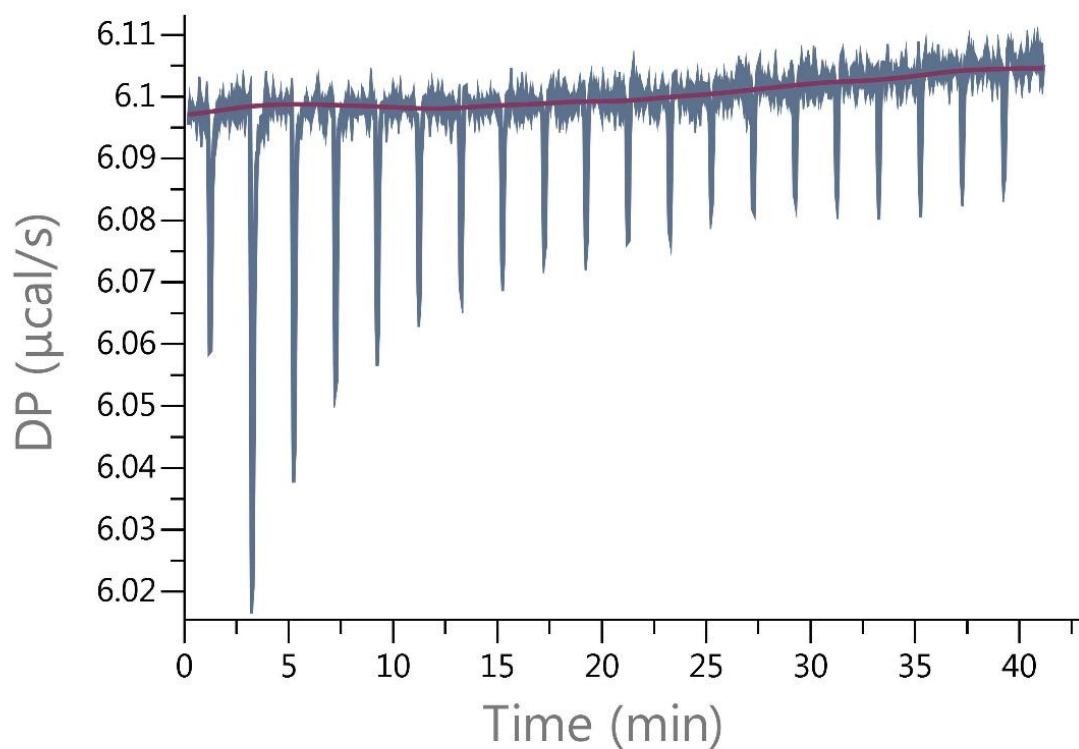
Values reported:
$K_D$= 17.1x$10^{-6}$ ±1.94x$10^{-6}$ M
$K_A$= 58480 $M^{-1}$
Reduced $\chi^2$= 8.6x$10^{-5}$ Kcal/$mol^2$
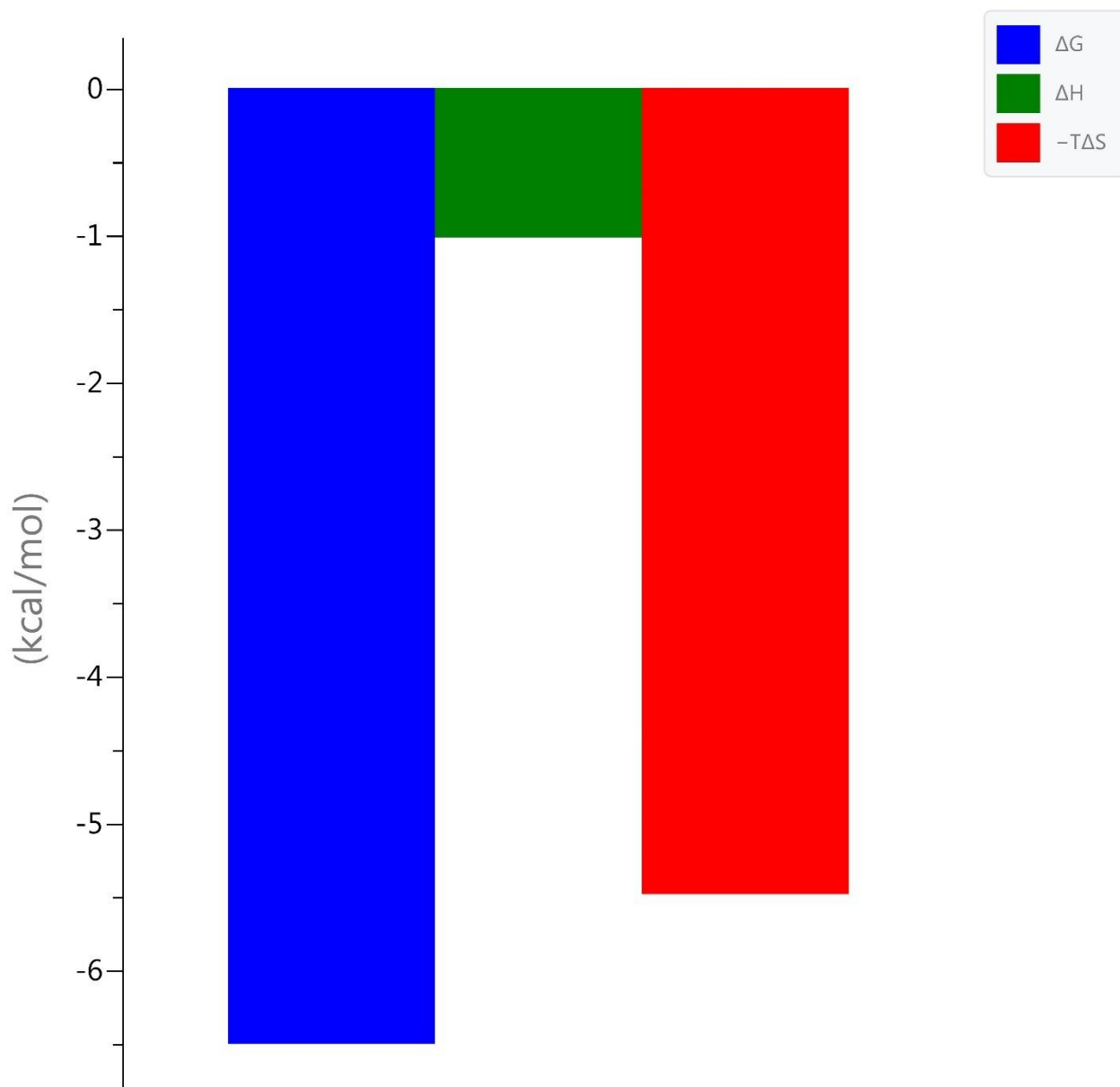
Values reported:

$\Delta H = -1.02 \pm 5.5 \times 10^{-2}$ Kcal/mol

$\Delta G = -6.50$ Kcal/mol

$-T\Delta S = -5.49$ Kcal/mol

No binding observed.

MB09W7
Model: One Set of Sites
[Cell] (M) = 16.0e-6
[Syr] (M) = 1.00e-3
N (sites) = 6.7e-3 ± 1.70
KD (M) = 27.4e-6 ± 28.1e-6
ΔH (kcal/mol) = -80.0 ± 2.0e4
Offset (kcal/mol) = -4.5e-2 ± 8.1e-3
ΔG (kcal/mol) = -6.22
-TΔS (kcal/mol) = 73.8
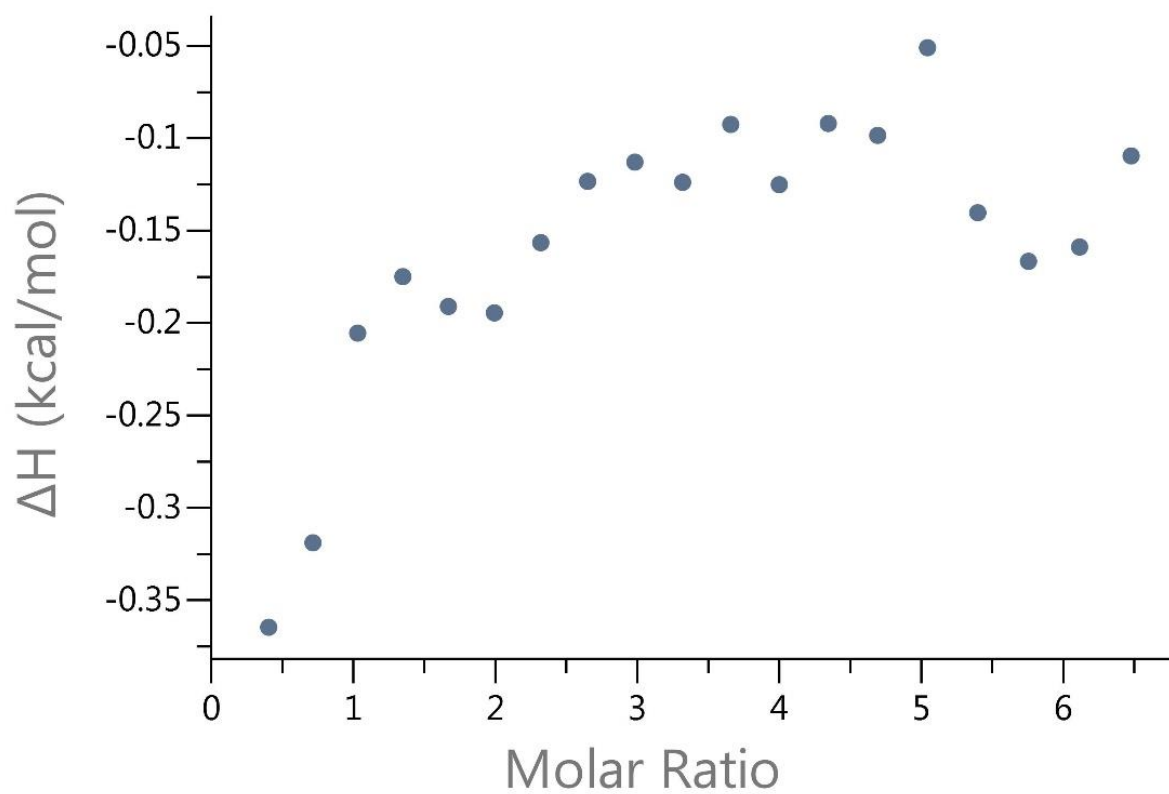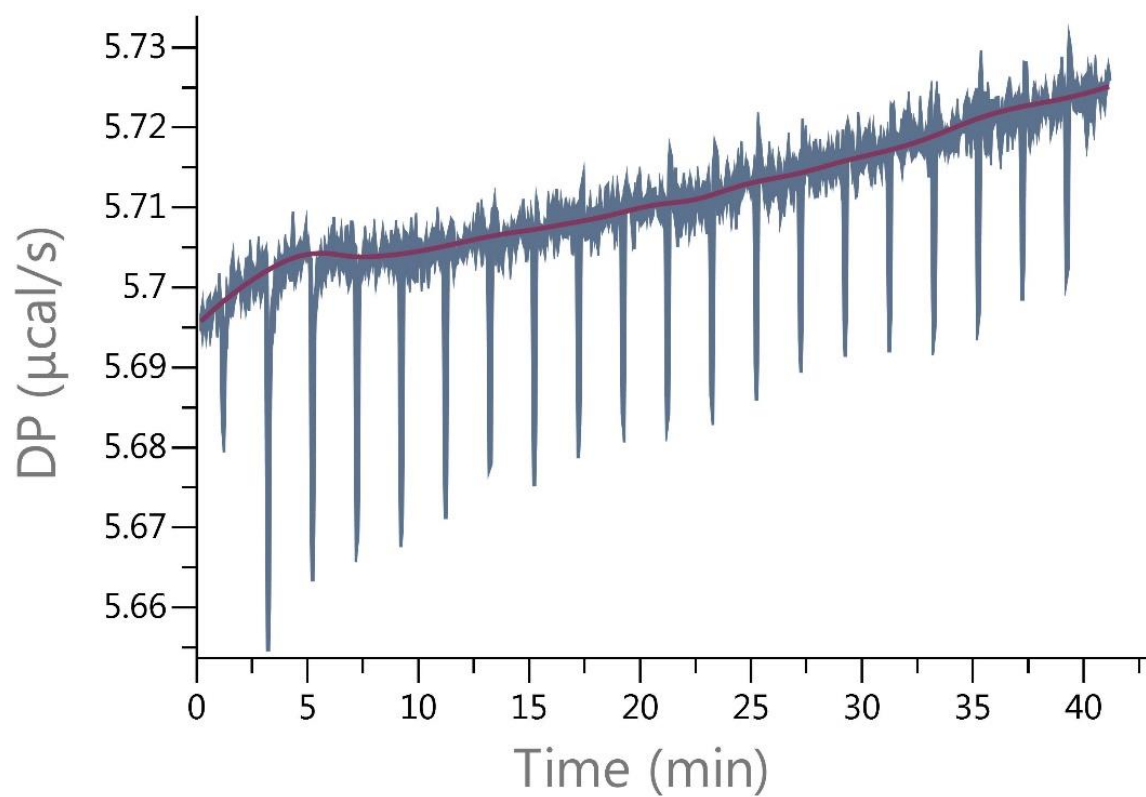
Values reported:

$K_D = 27.4 \times 10^{-6} \pm 28.1 \times 10^{-6}$ M

$K_A = 36496$ M$^{-1}$

$\Delta H = -80.0 \pm 2.0 \times 10^{4}$ Kcal/mol

$\Delta G = -6.22$ Kcal/mol

$-T\Delta S = 73.8$ Kcal/mol

$\chi^2 = 1.5 \times 10^{-4}$ Kcal/mol$^2$

*At 1 mM with n=1*



MB09W7
Model: One Set of Sites
[Cell] (M) = 16.0e-6
[Syr] (M) = 1.00e-3
N (sites) = 1.00
KD (M) = 11.8e-6 ± 4.05e-6
ΔH (kcal/mol) = -0.424 ± 6.0e-2
Offset (kcal/mol) = -5.0e-2 ± 4.8e-3
ΔG (kcal/mol) = -6.72
-TΔS (kcal/mol) = -6.30
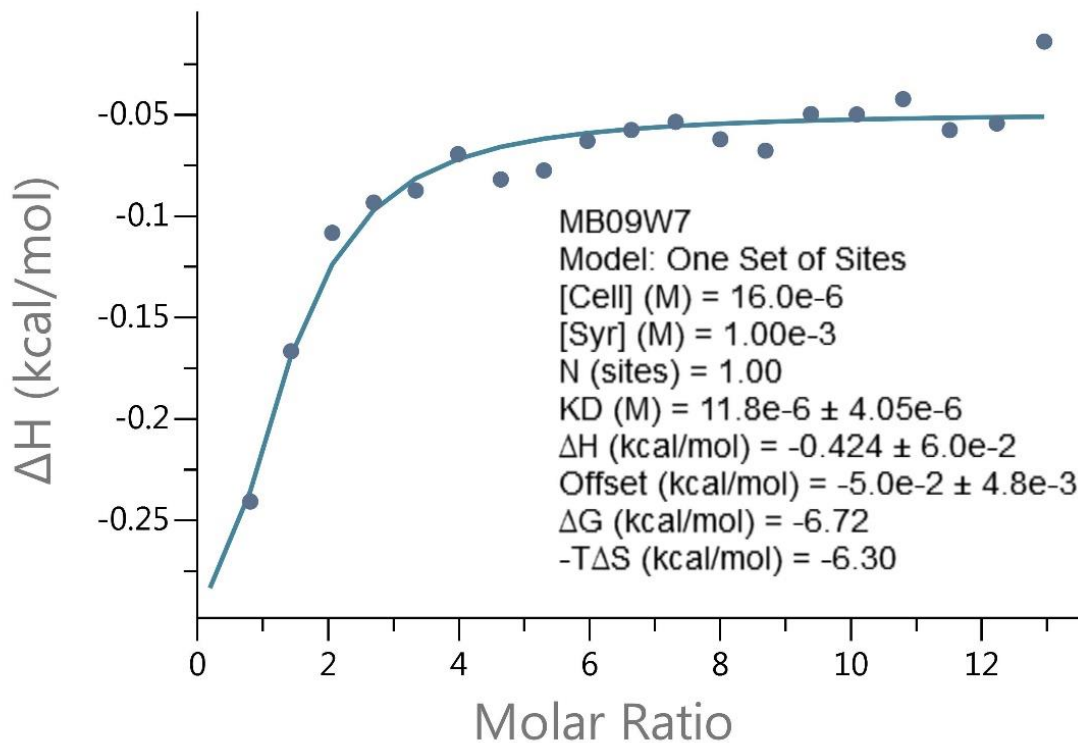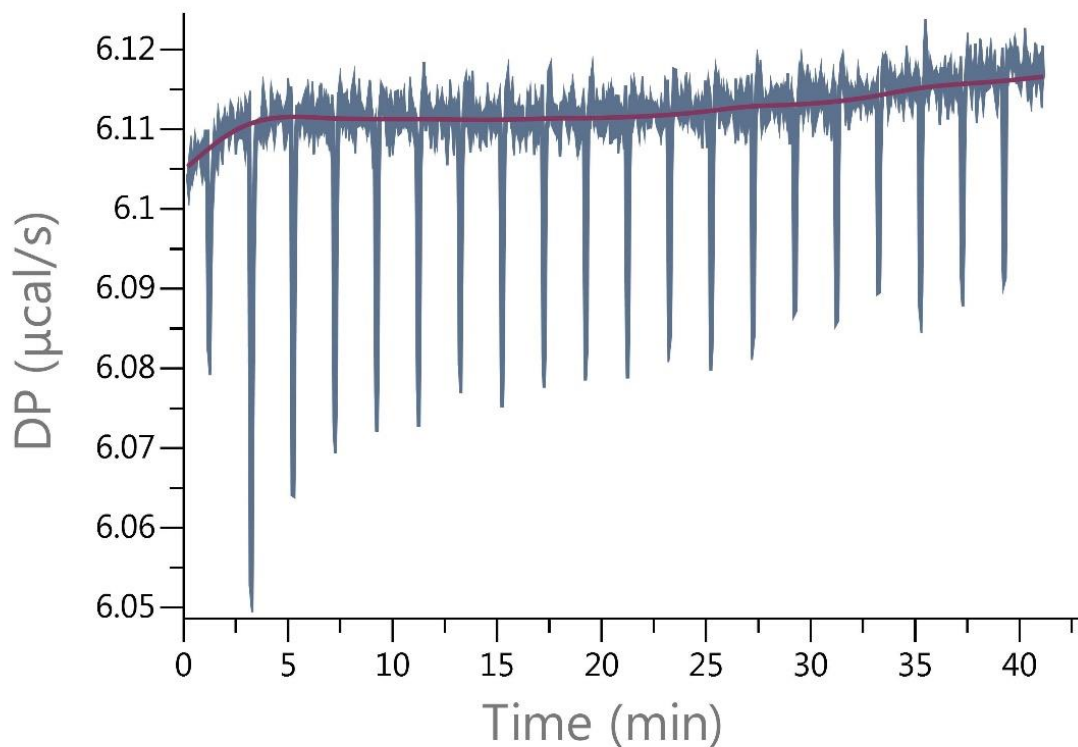
Values reported:
$K_D$= 11.8x$10^{-6}$ ±4.05x$10^{-6}$ M
$K_A$= 84746 $M^{-1}$
Reduced $\chi^2$= 1.7x$10^{-4}$ Kcal/$mol^2$

Values reported:
ΔH= -0.424± 0.06 Kcal/mol
ΔG= -6.72 Kcal/mol
-TΔS= -6.30 Kcal/mol

No binding observed.

138
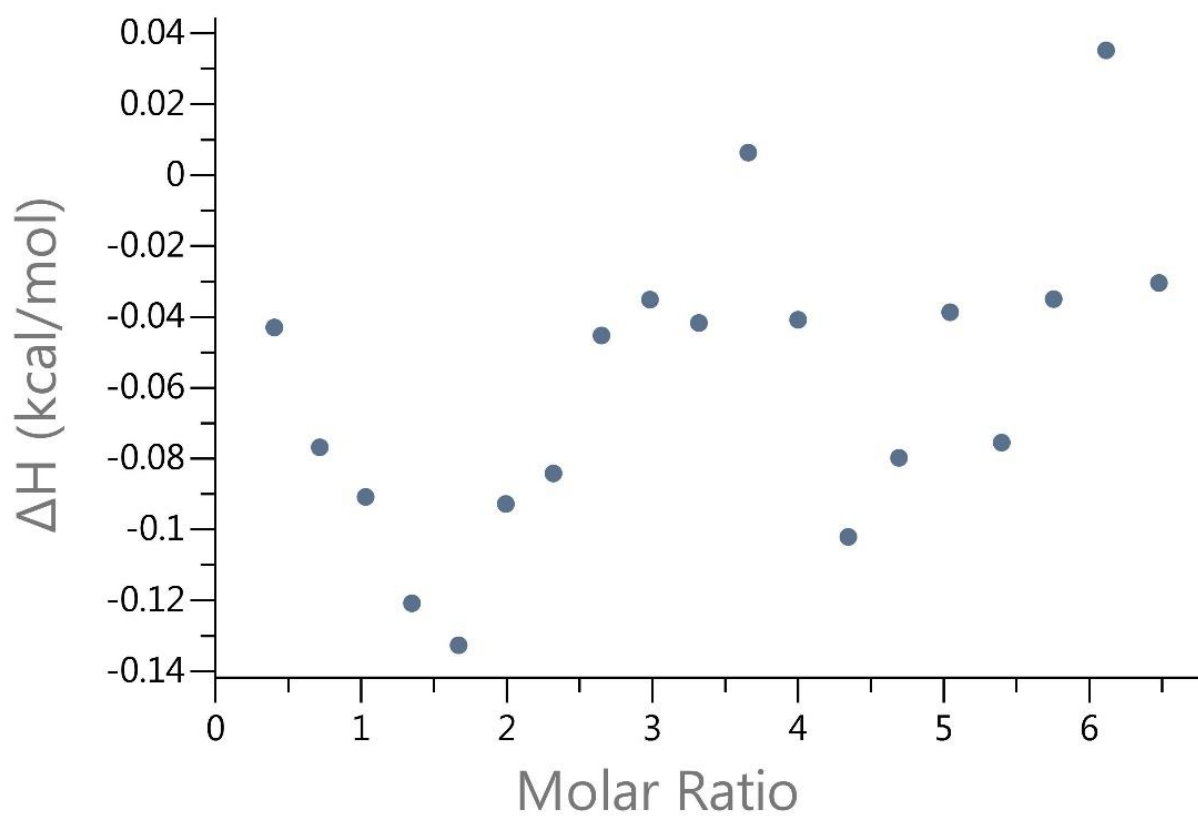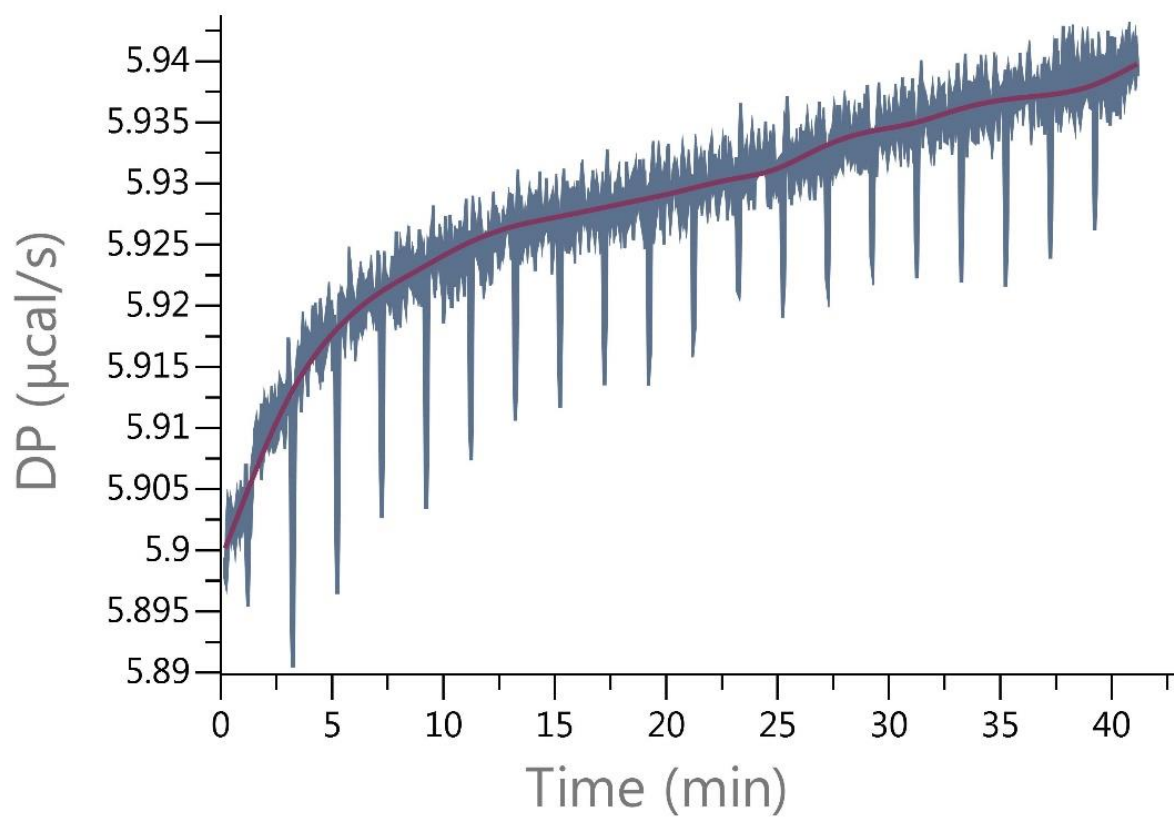
*11.6.1.7 ITC measurement – HPβCD*
*At 1 mM*
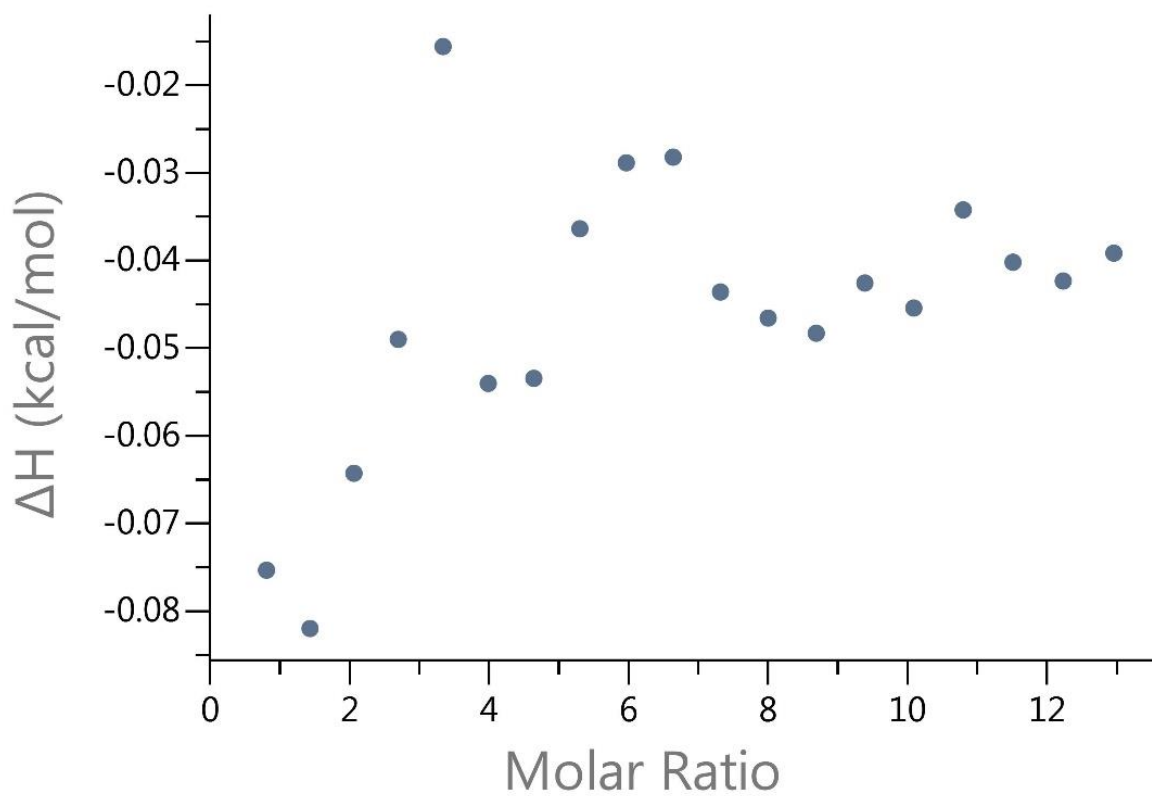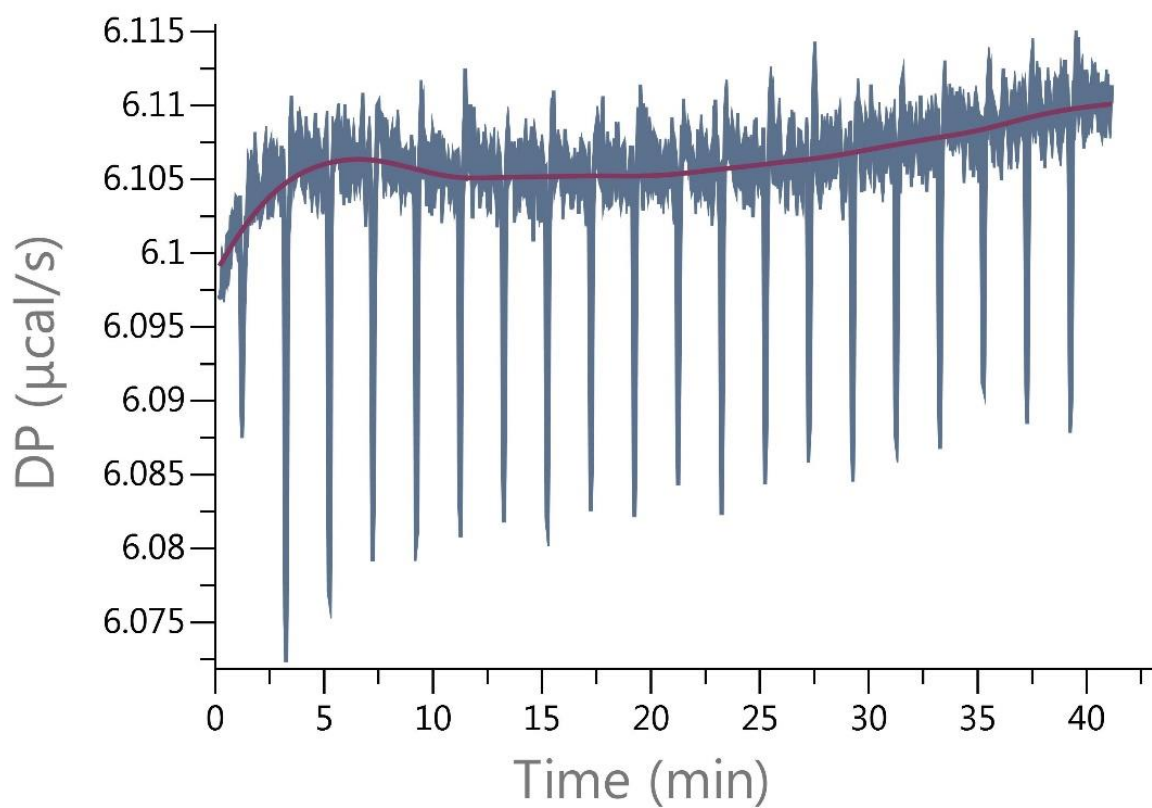


No binding observed.

*At 0.5 mM*



No binding observed.

MB09SE1
Model: One Set of Sites
[Cell] (M) = 16.0e-6
[Syr] (M) = 1.00e-3
N (sites) = 0.206 ± 17.6
KD (M) = 292e-6 ± 657e-6
$\Delta H$ (kcal/mol) = -50.8 ± 4340
Offset (kcal/mol) = -0.175 ± 0.122
$\Delta G$ (kcal/mol) = -4.82
$-T\Delta S$ (kcal/mol) = 45.9
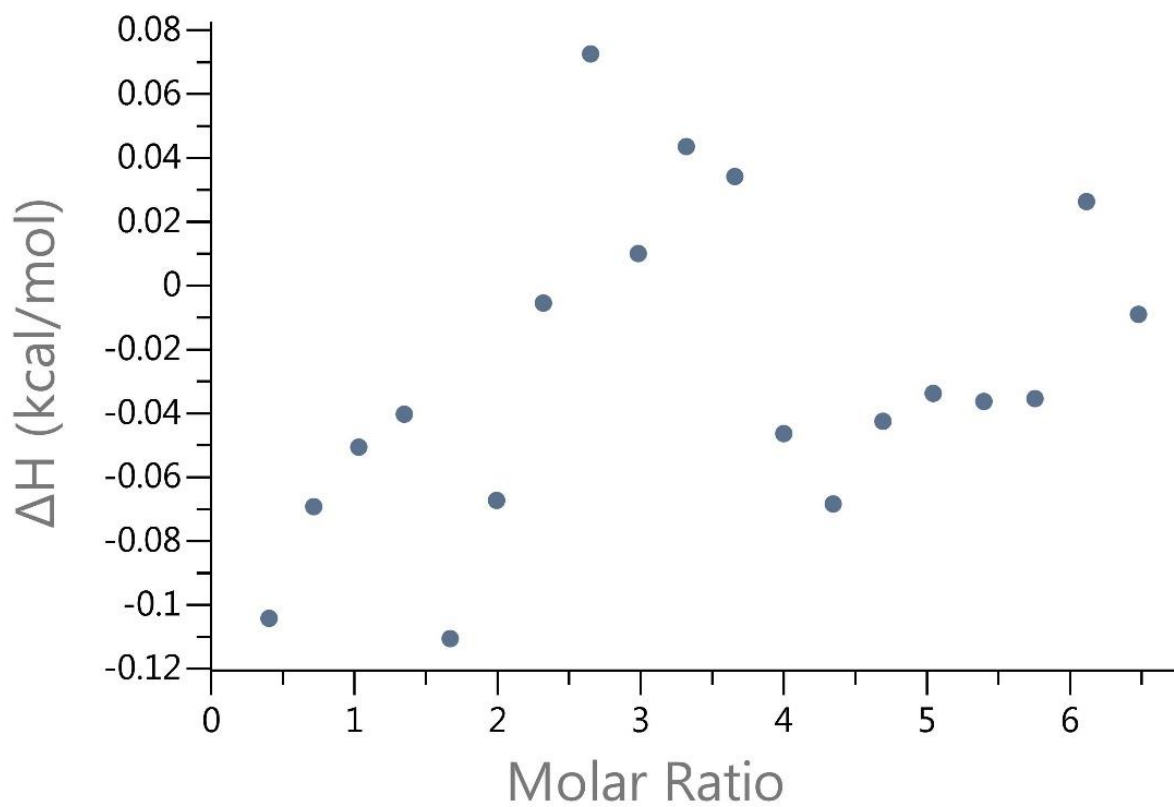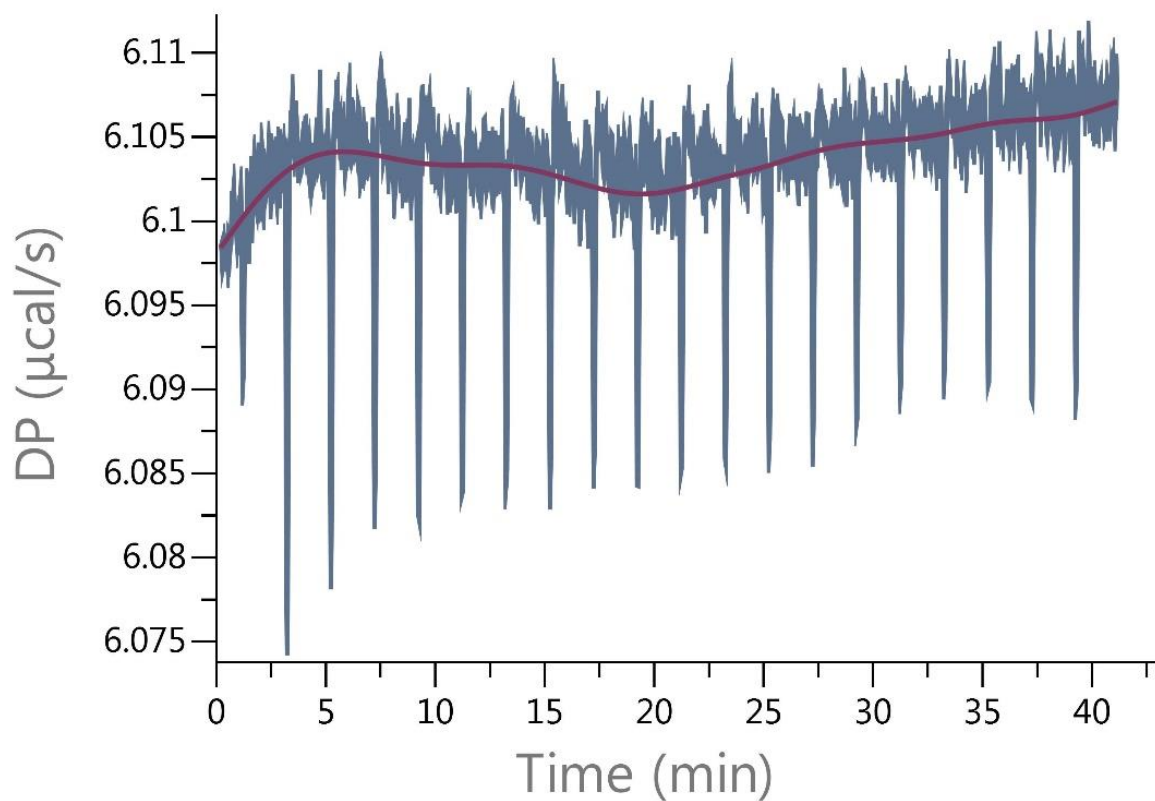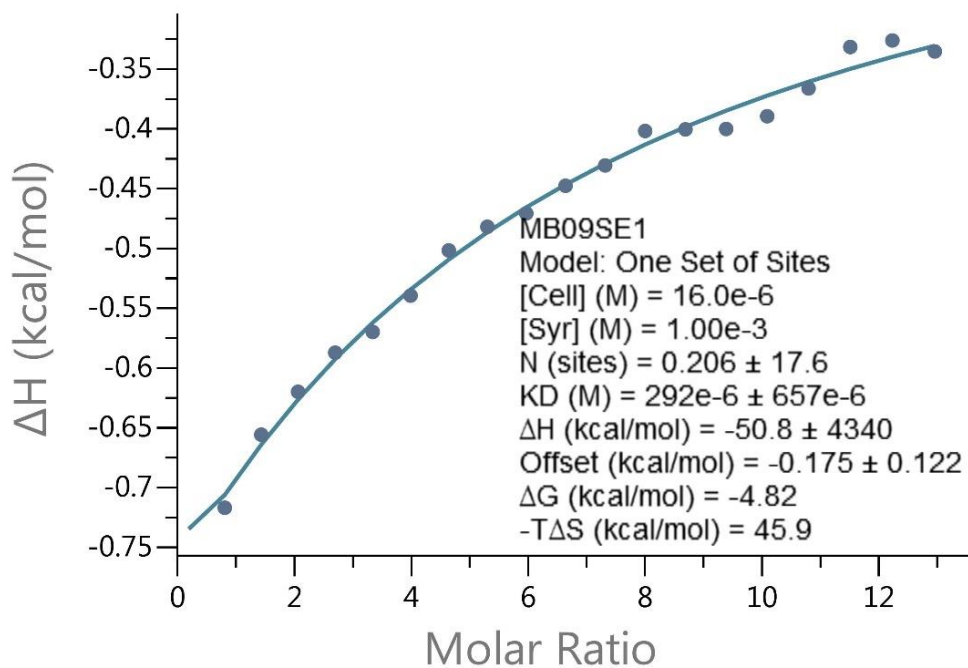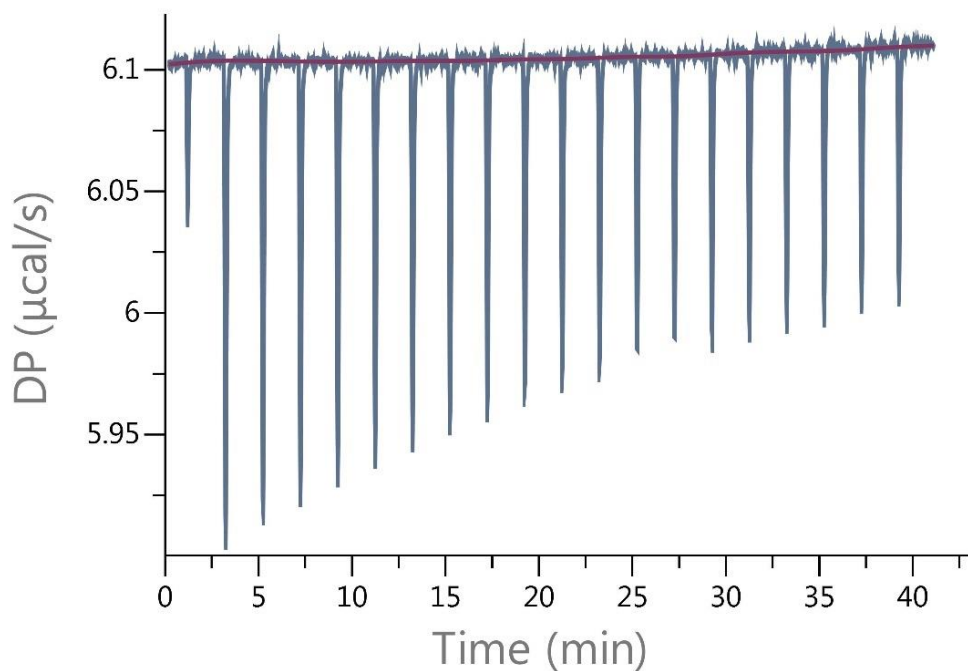
Values reported:

$K_D$=292x10$^{-6}$ ± 675x10$^{-6}$ M

$K_A$= 3452 M$^{-1}$

$\Delta H$= -50.8 ± 4340 Kcal/mol

$\Delta G$= -4.82 Kcal/mol

$-T\Delta S$= 45.9 Kcal/mol

Reduced $\chi^2$=1.1x10$^{-4}$ Kcal/mol$^2$

*At 1 mM with n=1*



MB09SE1
Model: One Set of Sites
[Cell] (M) = 16.0e-6
[Syr] (M) = 1.00e-3
N (sites) = 1.00
KD (M) = 263e-6 ± 44.3e-6
ΔH (kcal/mol) = -9.79 ± 1.89
Offset (kcal/mol) = -0.180 ± 2.8e-2
ΔG (kcal/mol) = -4.88
-TΔS (kcal/mol) = 4.90
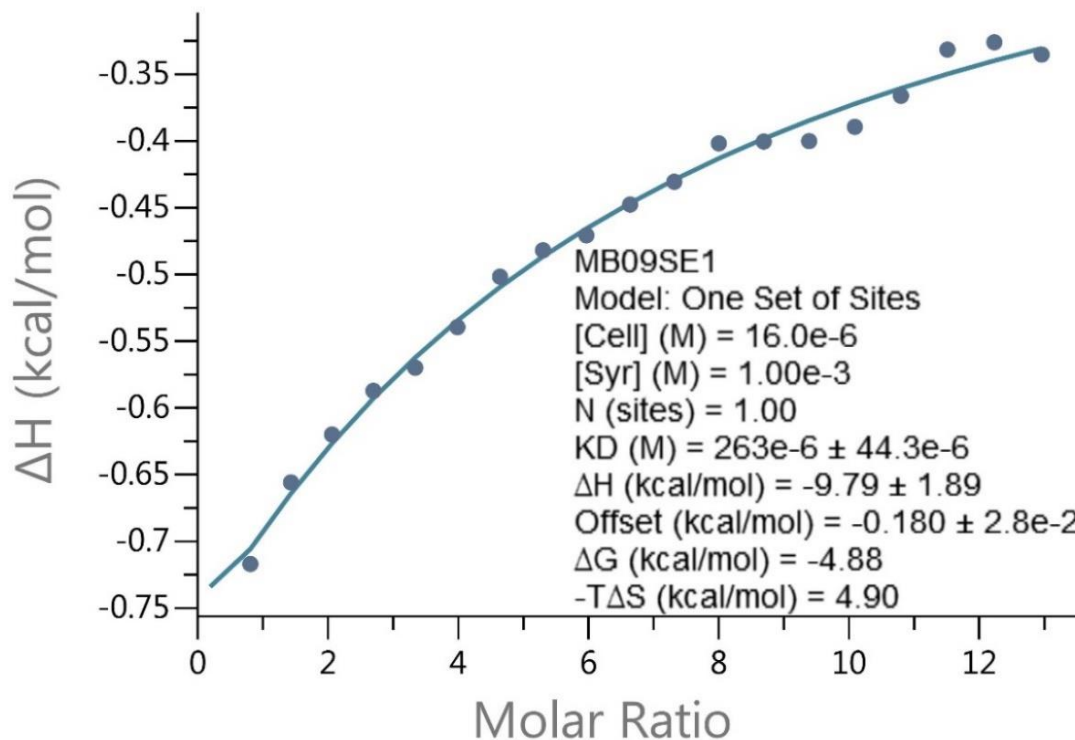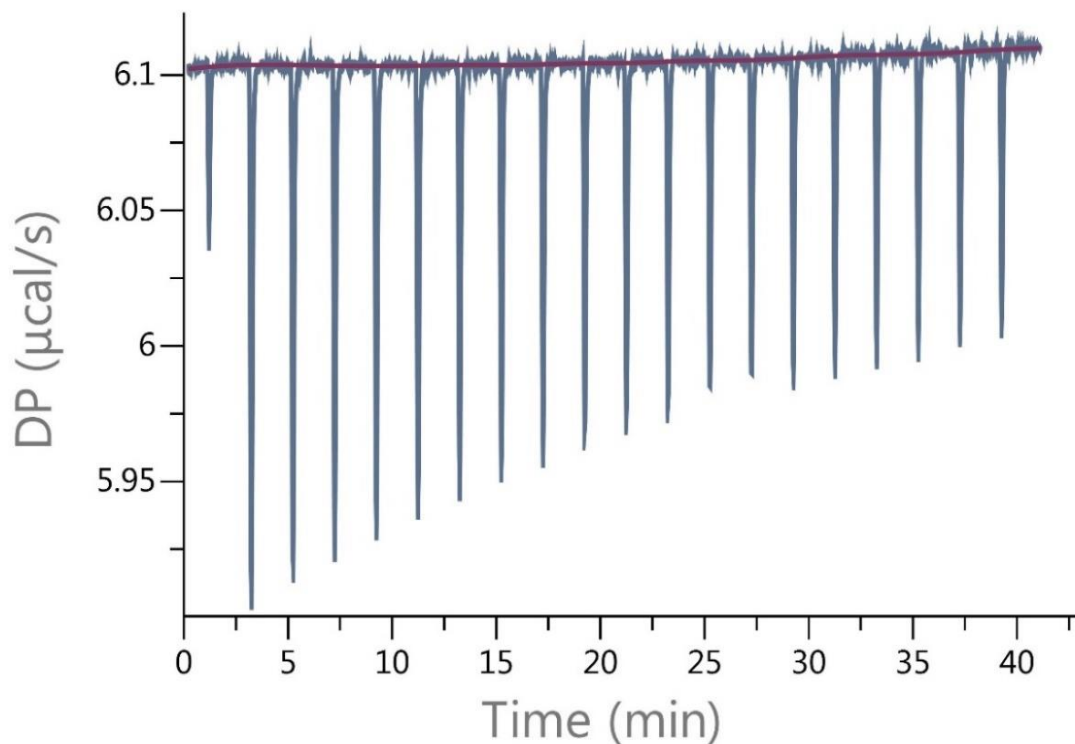
Values reported:

$K_D$= 263x10$^{-6}$ ±44.3x10$^{-6}$ M

$K_A$= 3802 M$^{-1}$

Reduced $\chi^2$= 1.1x10$^{-4}$ Kcal/mol$^2$
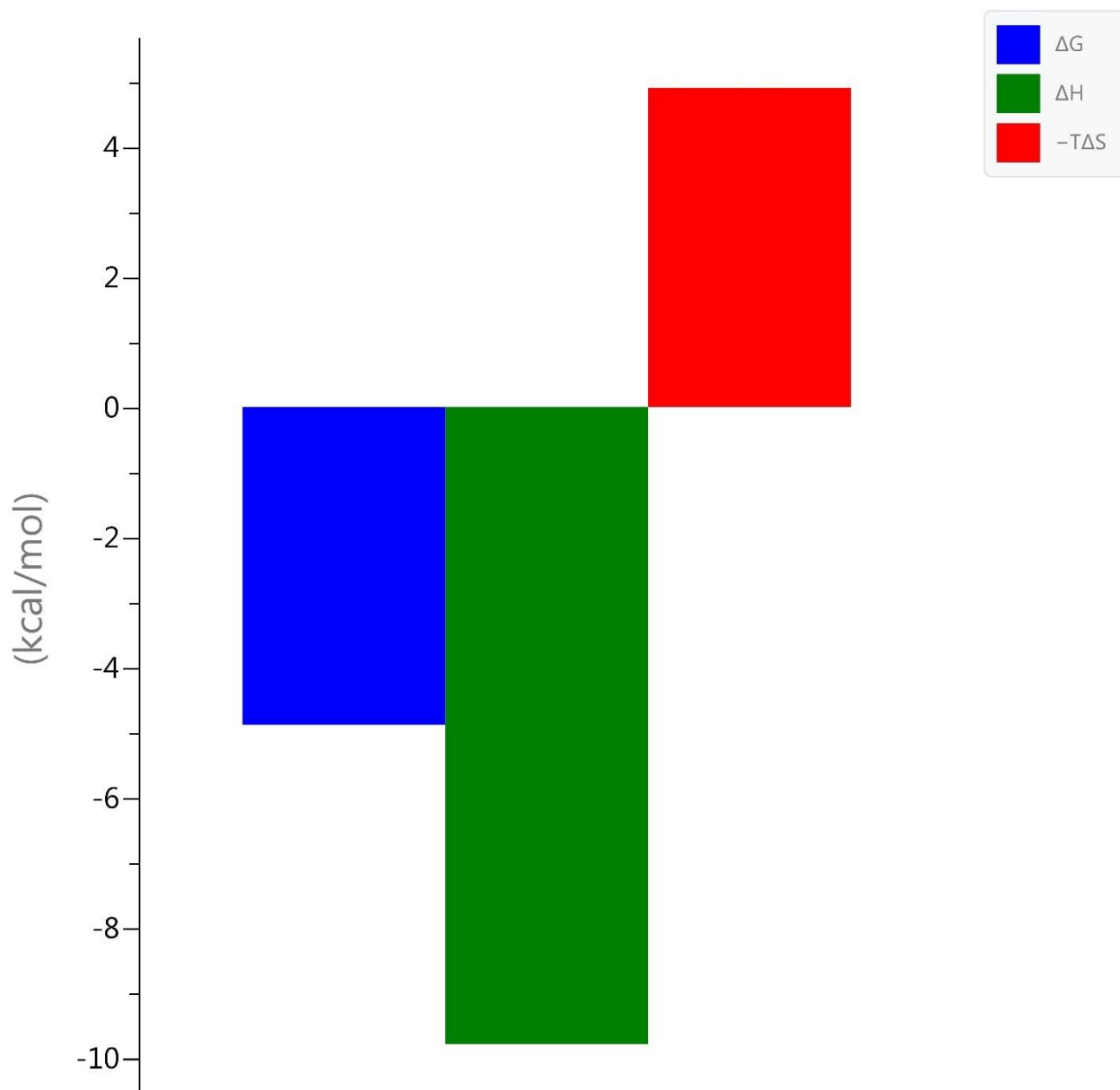
Values reported:
ΔH= -9.79± 1.89 Kcal/mol
ΔG= -4.88 Kcal/mol
-TΔS= 4.90 Kcal/mol

*At 0.5 mM*
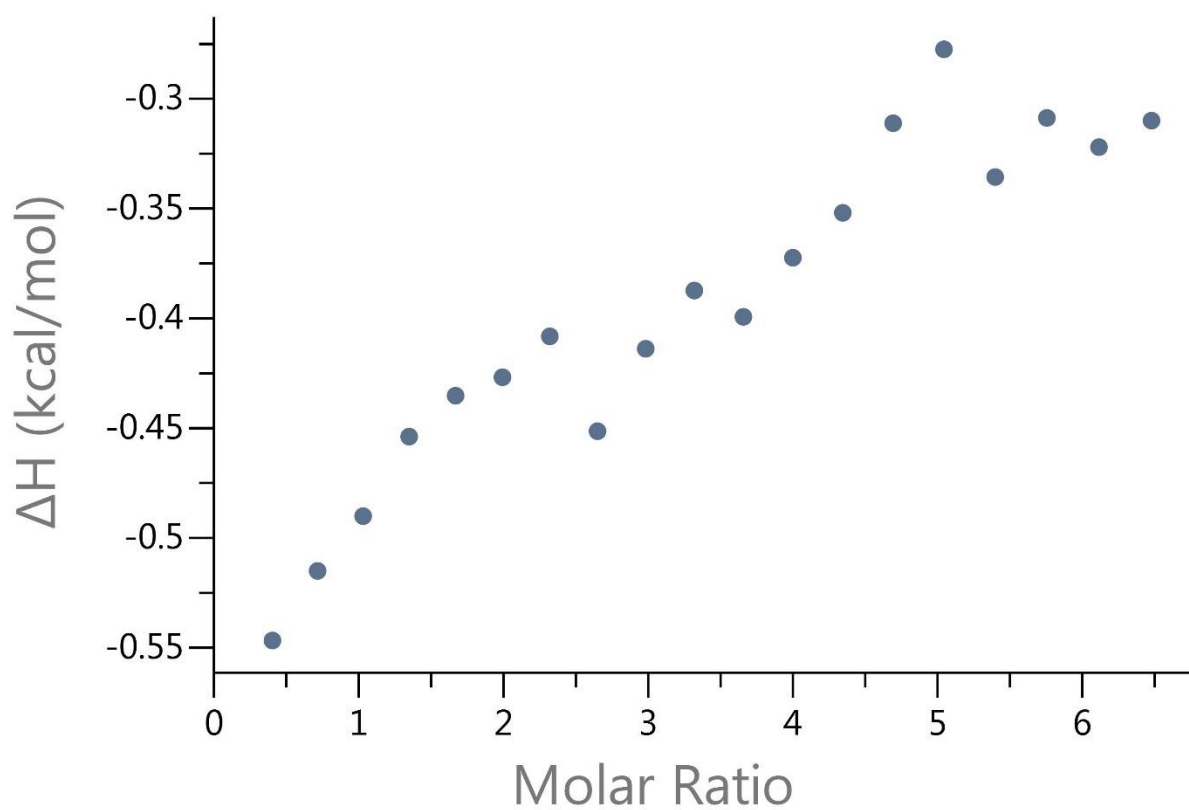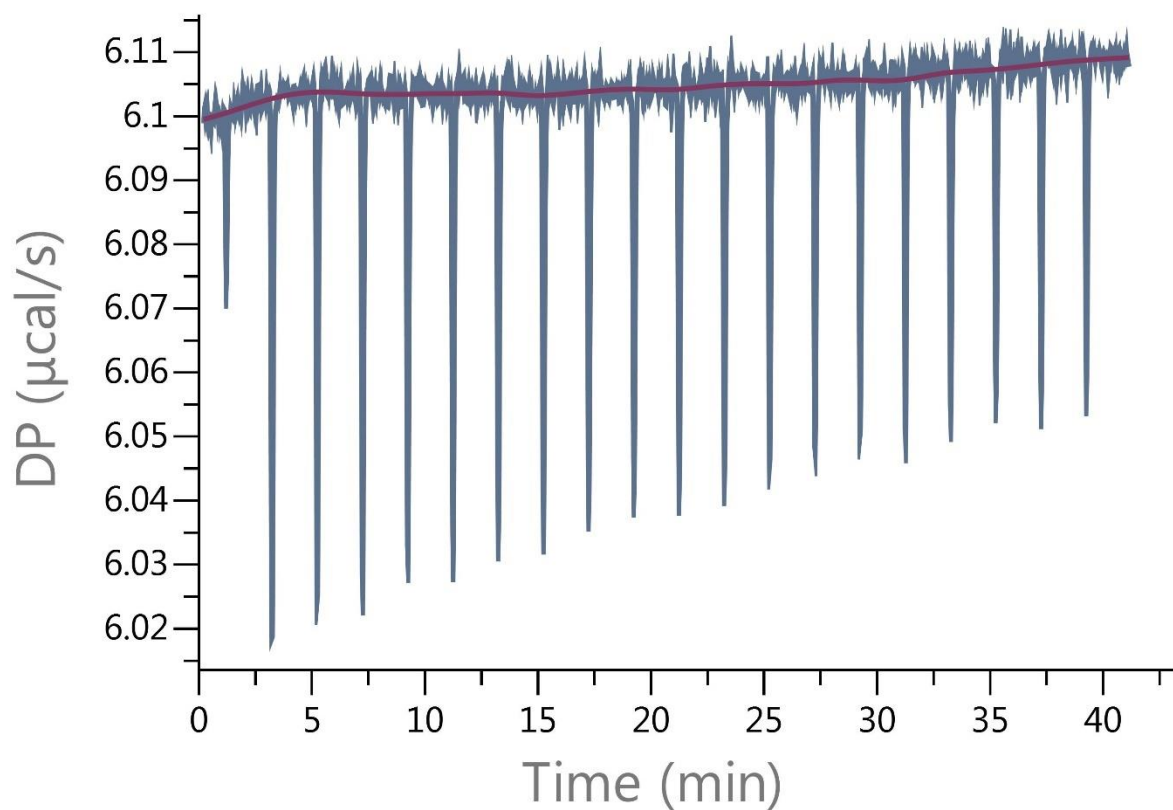


No binding observed.
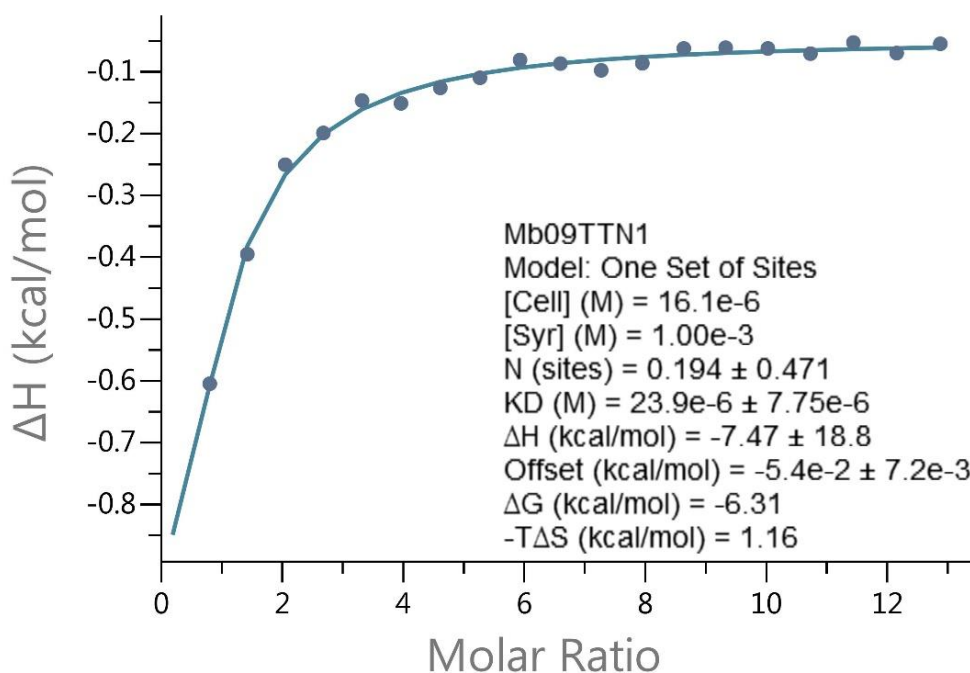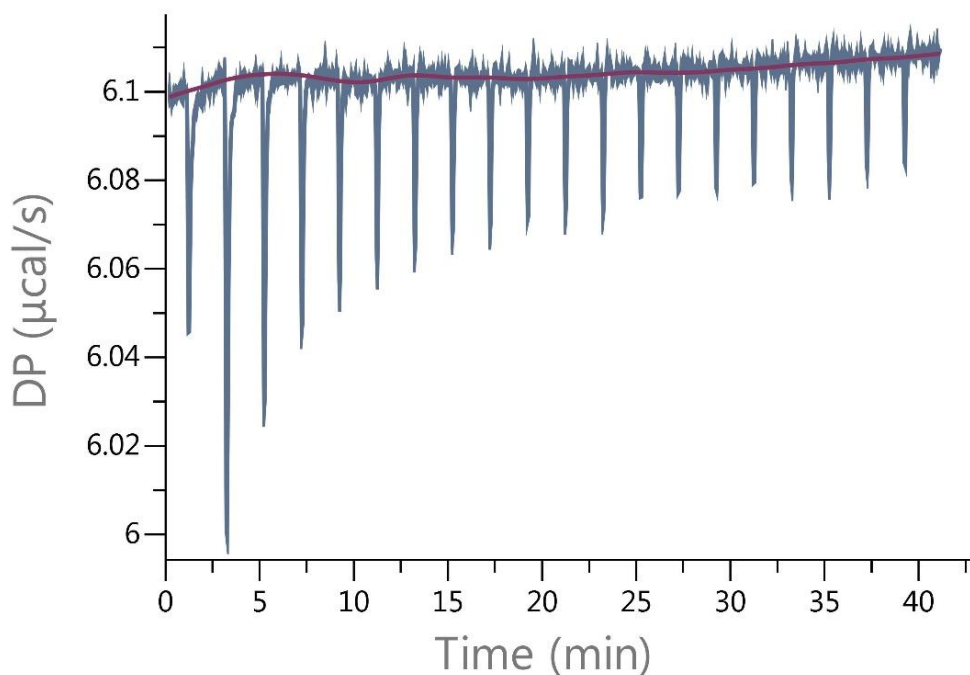
Values reported:

$K_D$: $23.9 \times 10^{-6} \pm 7.75 \times 10^{-6}$ M

$K_A$= 41841 $M^{-1}$

$\Delta H$= -7.47±18.8 Kcal/mol

$\Delta G$= -6.31 Kcal/mol

-T$\Delta S$= 1.16 Kcal/mol

Reduced $\chi^2$=$1.4 \times 10^{-4}$ Kcal/mol

*At 1 mM with n=1*



Mb09TTN1
Model: One Set of Sites
[Cell] (M) = 16.0e-6
[Syr] (M) = 1.00e-3
N (sites) = 1.00
KD (M) = 11.5e-6 ± 1.50e-6
$\Delta$H (kcal/mol) = -1.20 ± 6.4e-2
Offset (kcal/mol) = -6.5e-2 ± 5.2e-3
$\Delta$G (kcal/mol) = -6.74
-T$\Delta$S (kcal/mol) = -5.54
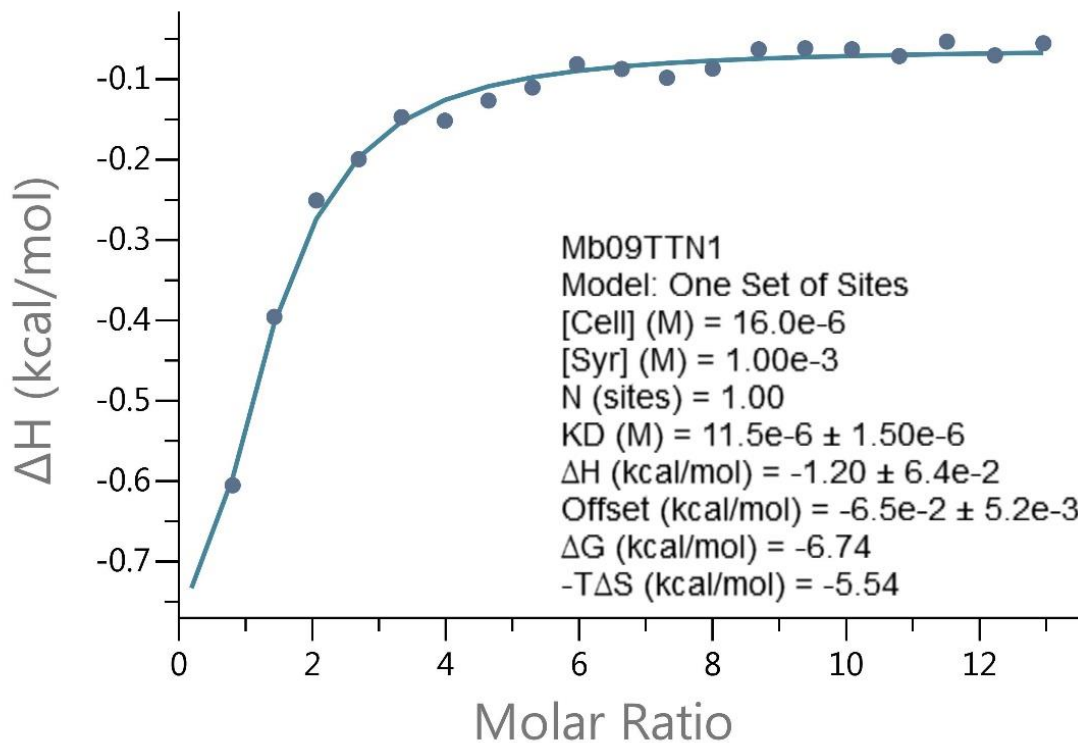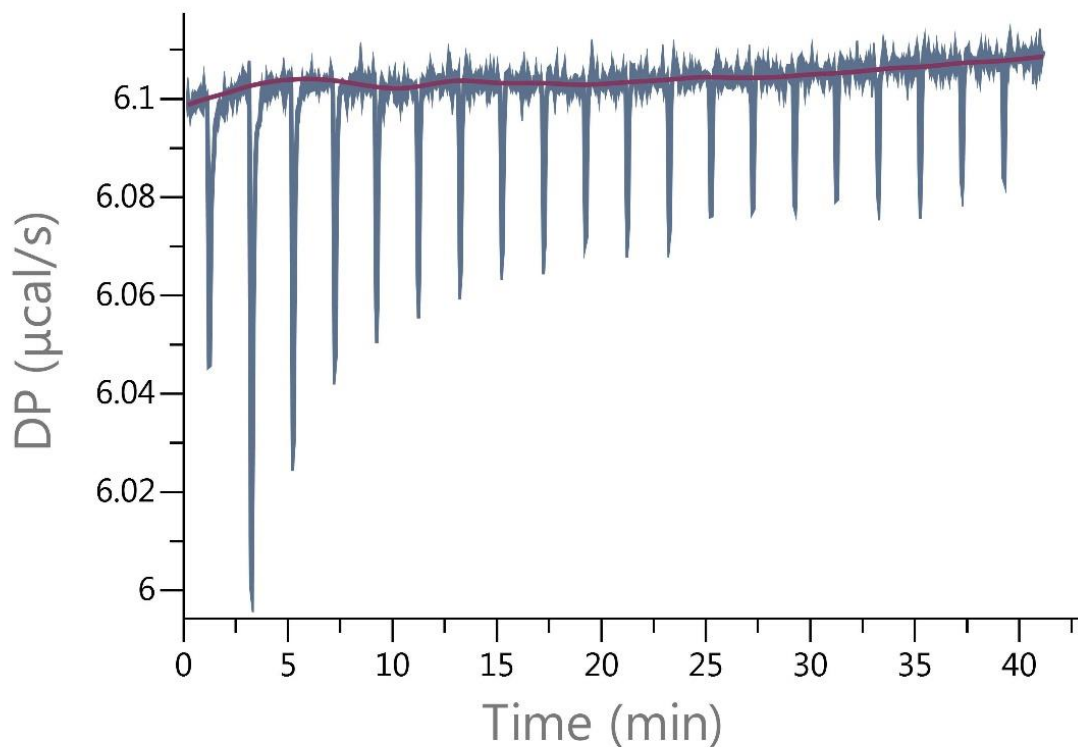
Values reported:

$K_D = 11.5 \times 10^{-6} \pm 1.50 \times 10^{-6}$ M

$K_A = 86957$ M$^{-1}$

Reduced $\chi^2 = 1.94 \times 10^{-4}$ Kcal/mol$^2$

Values reported:

ΔH= -1.20± 0.064 Kcal/mol

ΔG= -6.74 Kcal/mol

-TΔS= -5.54 Kcal/mol

MB09TTN0
Model: One Set of Sites
[Cell] (M) = 16.0e-6
[Syr] (M) = 500e-6
N (sites) = 1.2e-2 ± 0.699
KD (M) = 15.5e-6 ± 12.2e-6
$\Delta$H (kcal/mol) = -80.0 ± 4650
Offset (kcal/mol) = -8.7e-2 ± 2.2e-2
$\Delta$G (kcal/mol) = -6.56
-T$\Delta$S (kcal/mol) = 73.4
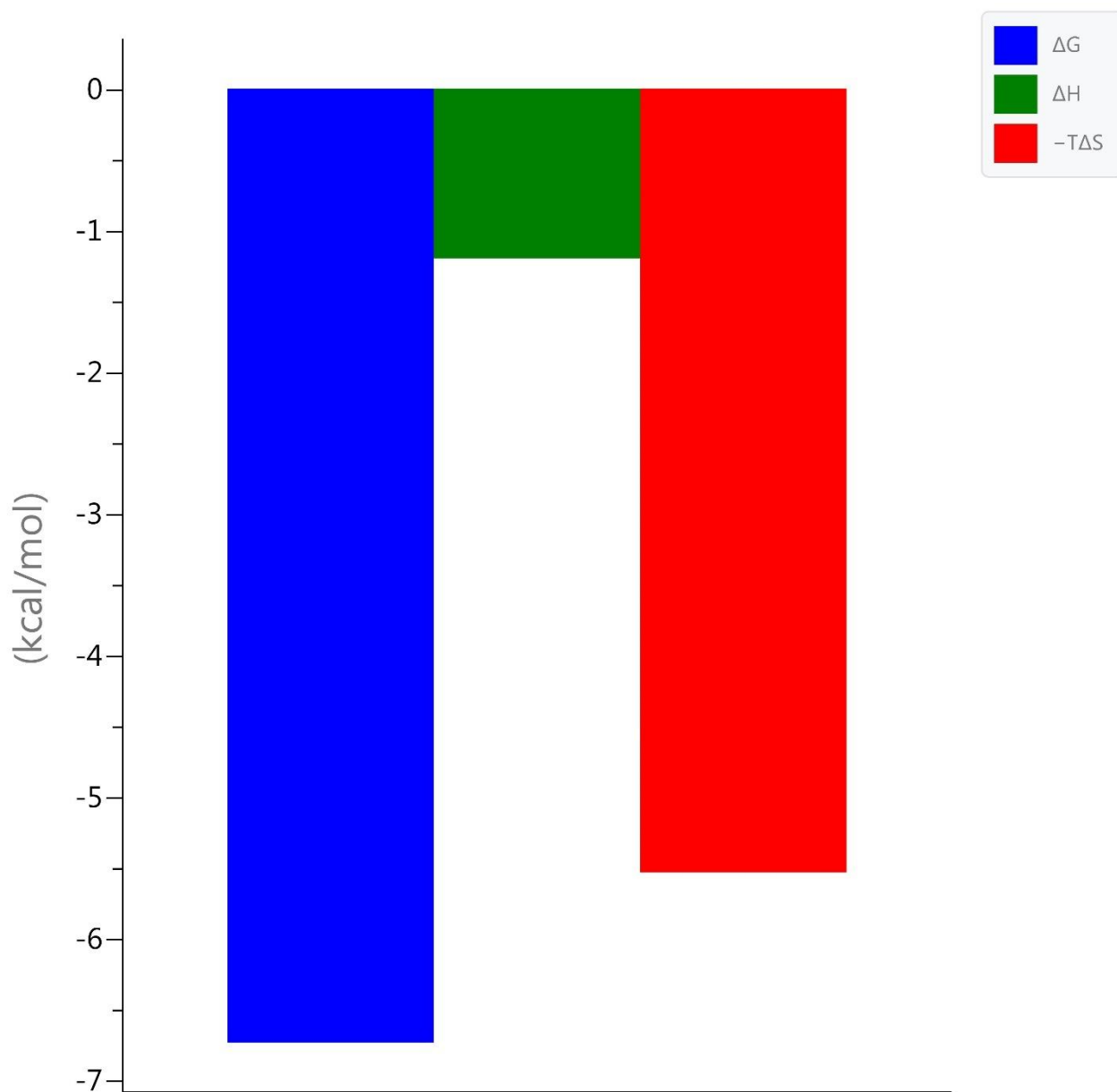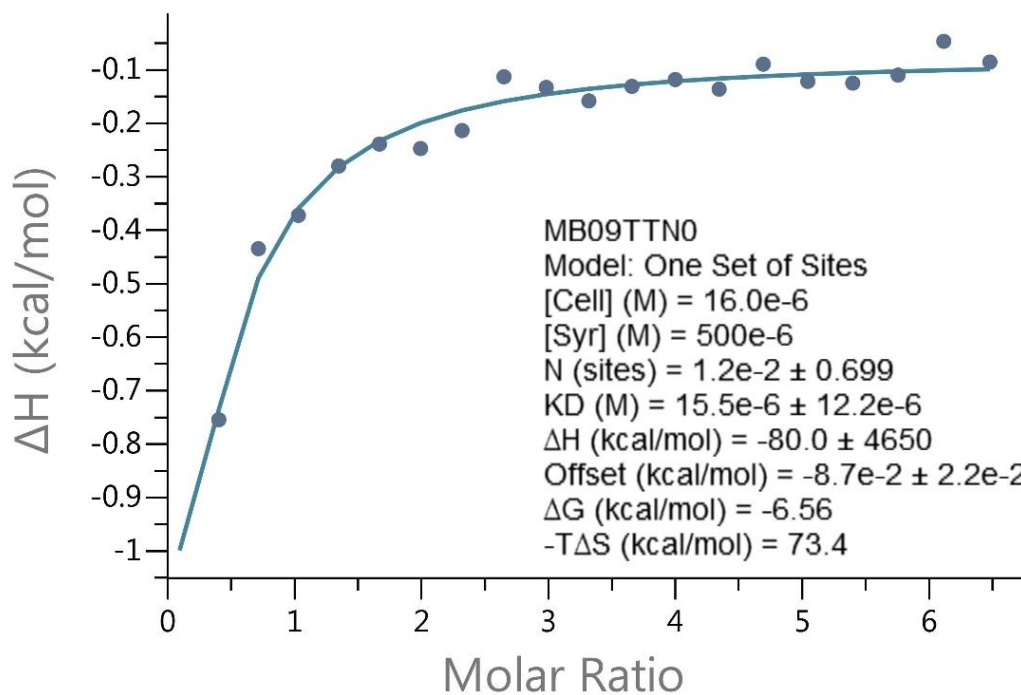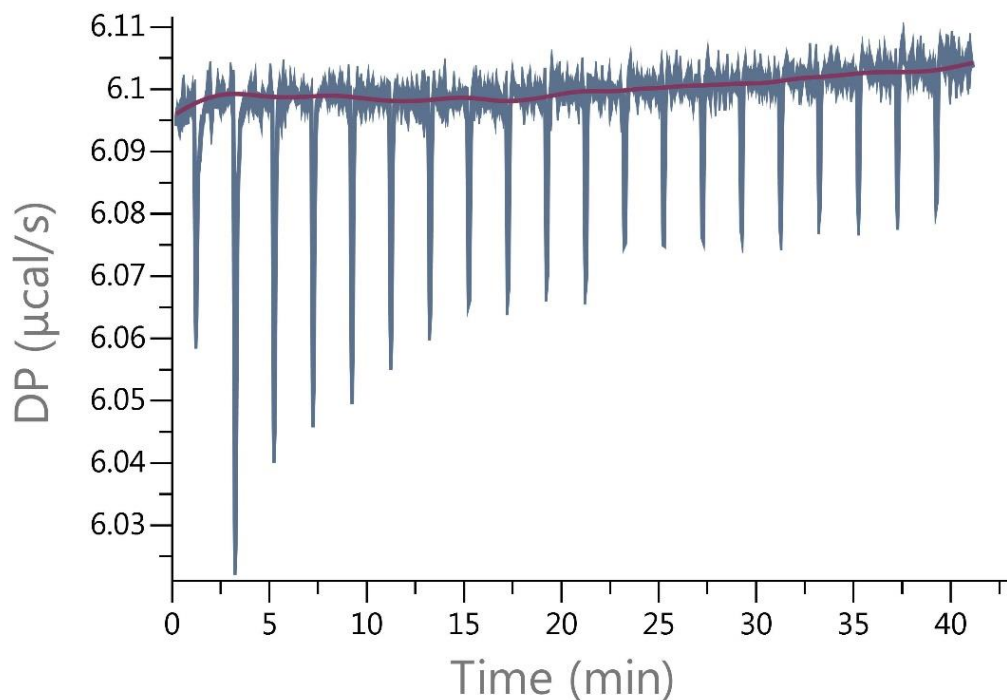
Values reported:
$K_D = 15.5 \times 10^{-6} \pm 12.2 \times 10^{-6}$ M
$K_A = 64516$ M$^{-1}$
$\Delta H = -80.0 \pm 4650$ Kcal/mol
$\Delta G = -6.56$ Kcal/mol
$-T\Delta S = 73.4$ Kcal/mol
Reduced $\chi^2 = 9.8 \times 10^{-4}$ Kcal/mol$^2$

*At 0.5 mM with n=1*



MB09TTN0
Model: One Set of Sites
[Cell] (M) = 16.0e-6
[Syr] (M) = 500e-6
N (sites) = 1.00
KD (M) = 6.22e-6 ± 3.70e-6
ΔH (kcal/mol) = –0.852 ± 0.187
Offset (kcal/mol) = –8.8e-2 ± 2.5e-2
ΔG (kcal/mol) = –7.10
-TΔS (kcal/mol) = –6.25
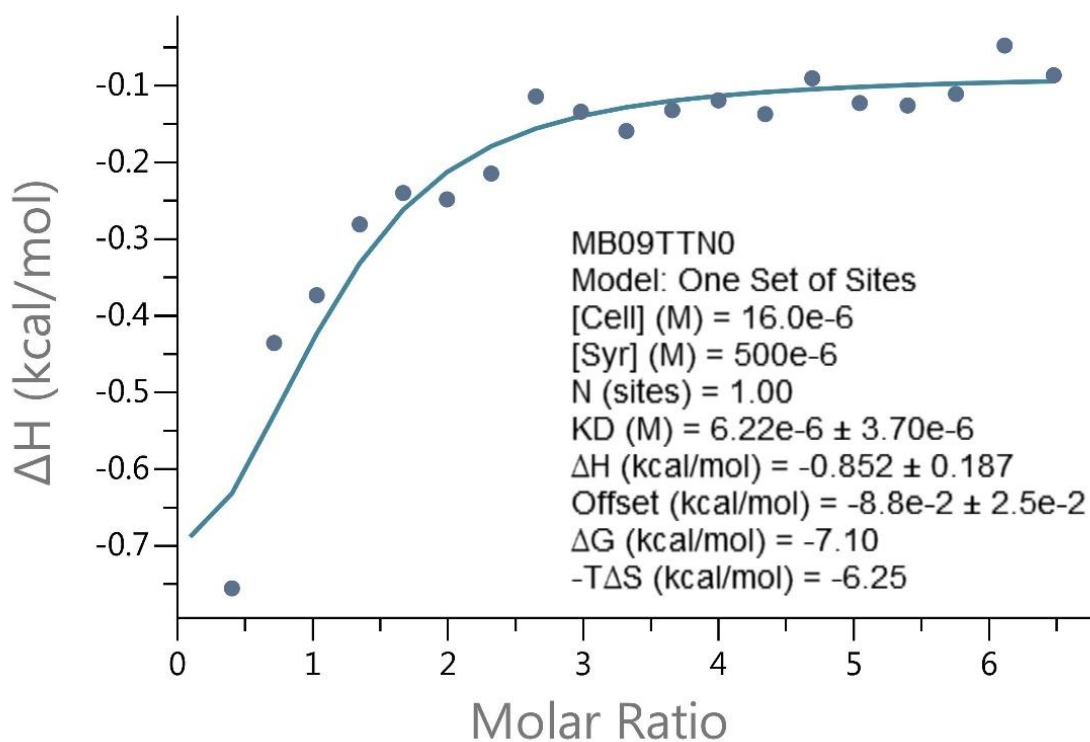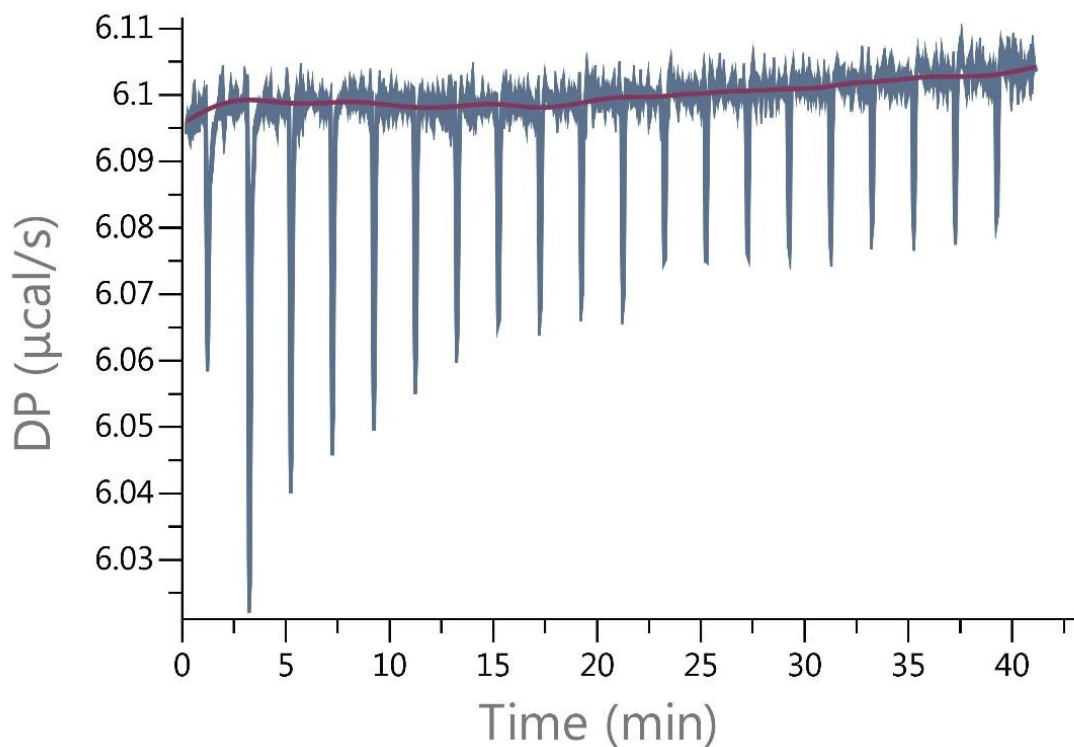
Values reported:
$K_D$= 6.22x10$^{-6}$ ±3.70x10$^{-6}$ M
$K_A$= 160772 M$^{-1}$
Reduced $\chi^2$= 2.5x10$^{-3}$ Kcal/mol$^2$
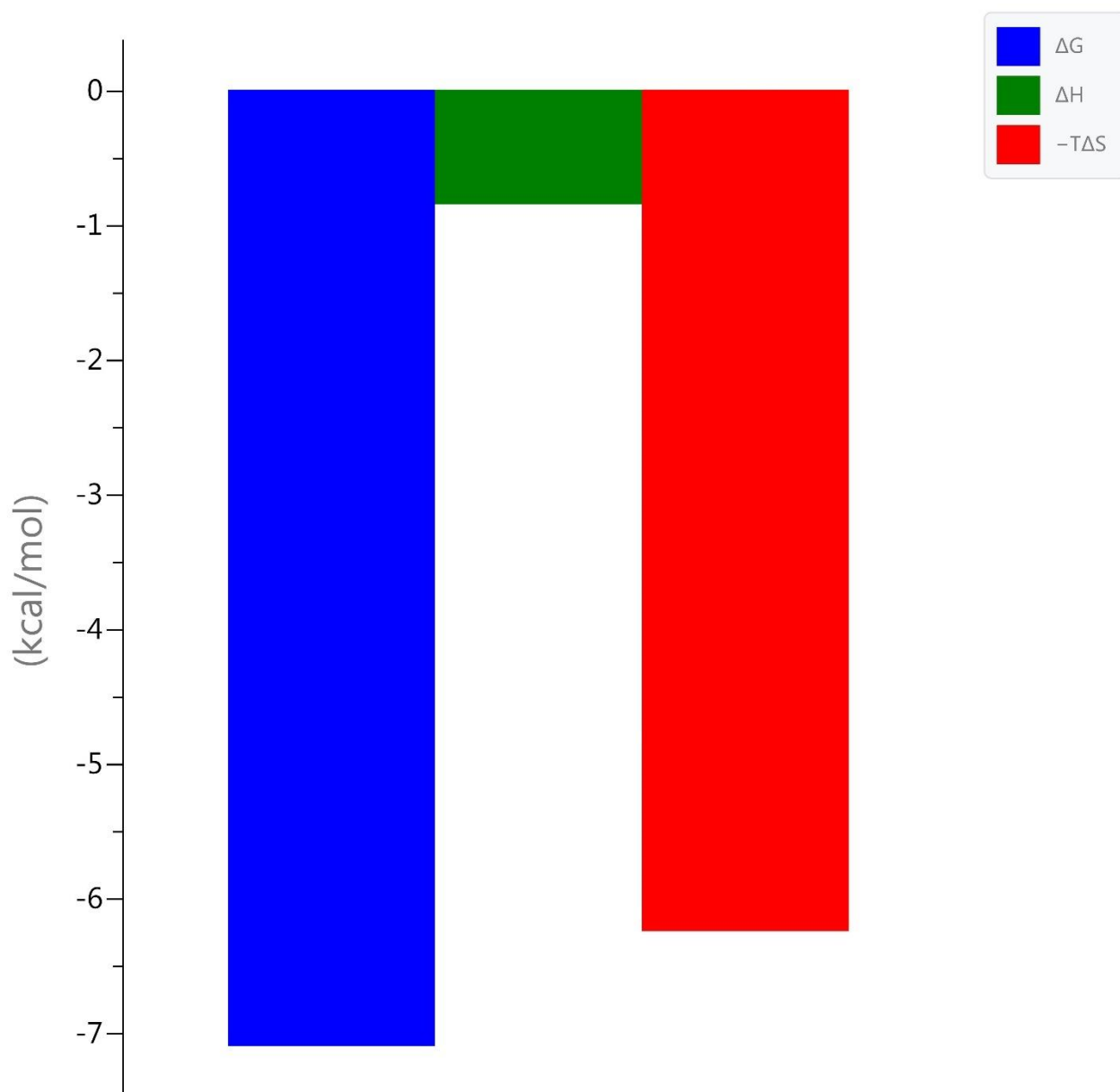
Values reported:

ΔH= -0.852± 0.187 Kcal/mol

ΔG= -7.10 Kcal/mol

-TΔS= -6.25 Kcal/mol

## 11.6.2 Reaction B

### 11.6.2.1 Purification attempts
### First attempt

**Method Name:**
**Run Name: 2017-04-25_11-58-36mb09b**
**Run Date: 2017-04-25 12:16**

Column: Reveleris® C18 12g
Flow Rate: 30 mL/min
Equilibration: 0.1 CV
Run Length: 20.0 CV
Air Purge Time: 0 min

Slope Detection: Off
ELSD Threshold: 5 mV
UV Threshold: 0.02 AU
UV1 Wavelength: 254 nm
UV2 Wavelength: 280 nm

Collection Mode: Collect Peaks
Per-Vial Volume: 10 mL
Non-Peaks: 25 mL
Injection Type: Manual

ELSD Carrier: Iso-propanol
Solvent A: Water
Solvent B: Methanol
Solvent C: <No solvent chosen
Solvent D: <No solvent chosen
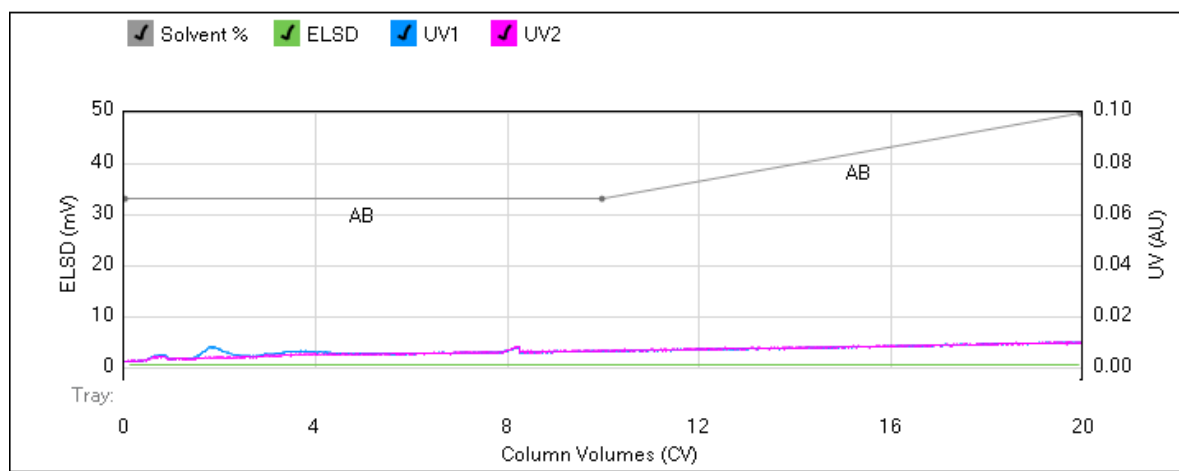


**Gradient Table**

|   | CV | Solvents | % 2nd |
|---|------|----------|-------|
| 1 | 0.0  | AB       | 66    |
| 2 | 10.0 | AB       | 66    |
| 3 | 10.0 | AB       | 100   |

**Vial Mapping Table**

| Peak # | Start Tray:Vial | End Tray:Vial |
|--------|-----------------|---------------|

*Second attempt*

**Method Name:**
**Run Name: 2017-04-25_13-10-19mb09b2**
**Run Date: 2017-04-25 13:14**

Column: Reveleris® C18 12g
Flow Rate: 30 mL/min
Equilibration: 0.1 CV
Run Length: 25.0 CV
Air Purge Time: 0 min

Slope Detection: Off
ELSD Threshold: 5 mV
UV Threshold: 0.02 AU
UV1 Wavelength: 254 nm
UV2 Wavelength: 280 nm

Collection Mode: Collect Peaks
Per-Vial Volume: 10 mL
Non-Peaks: 25 mL
Injection Type: Manual

ELSD Carrier: Iso-propanol
Solvent A: Water
Solvent B: Methanol
Solvent C: <No solvent chosen
Solvent D: <No solvent chosen
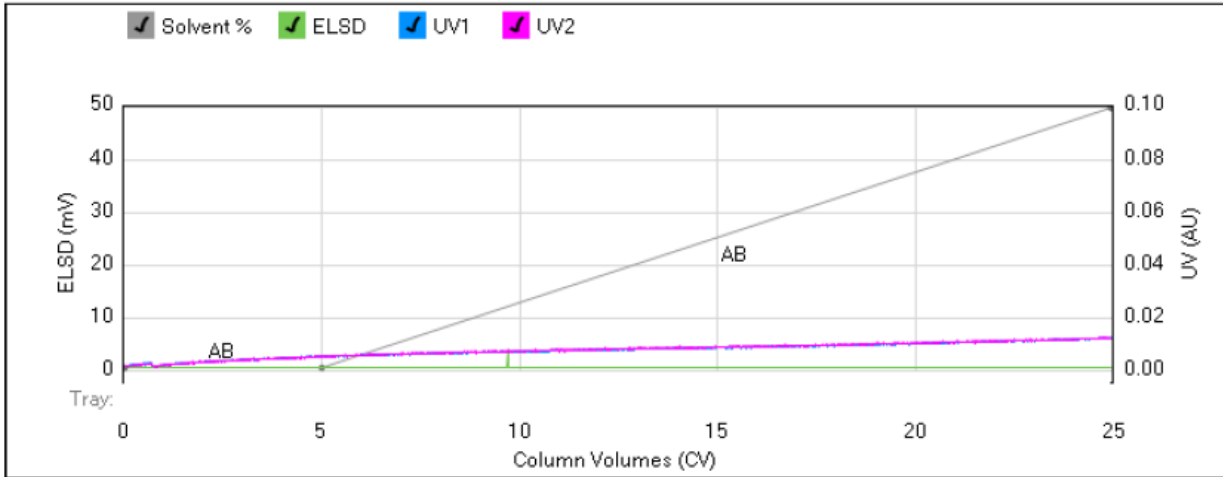


Gradient Table

|   | CV | Solvents | % 2nd |
|---|------|----------|-------|
| 1 | 0.0  | AB       | 0     |
| 2 | 5.0  | AB       | 0     |
| 3 | 20.0 | AB       | 100   |

Vial Mapping Table

| Peak # | Start Tray:Vial | End Tray:Vial |
|--------|-----------------|---------------|

*Third attempt*

**Method Name:**
**Run Name: 2017-04-25_13-47-36mb092c**
**Run Date: 2017-04-25 13:51**

REVELERIS™
Flash Chromatography System

Column: Reveleris® C18 12g
Flow Rate: 30 mL/min
Equilibration: 1.0 CV
Run Length: 20.0 CV
Air Purge Time: 0 min

Slope Detection: Off
ELSD Threshold: 5 mV
UV Threshold: 0.02 AU
UV1 Wavelength: 254 nm
UV2 Wavelength: 280 nm

Collection Mode: Collect Peaks
Per-Vial Volume: 10 mL
Non-Peaks: 25 mL
Injection Type: Manual

ELSD Carrier: Iso-propanol
Solvent A: Water
Solvent B: Methanol
Solvent C: <No solvent chosen
Solvent D: <No solvent chosen



Gradient Table

|   | CV   | Solvents | % 2nd |
|---|------|----------|-------|
| 1 | 0.0  | AB       | 66    |
| 2 | 10.0 | AB       | 66    |
| 3 | 10.0 | AB       | 100   |

Vial Mapping Table

| Peak # | Start Tray:Vial | End Tray:Vial |
|--------|-----------------|---------------|

*Fourth attempt*



**Method Name:**
**Run Name: 2017-04-26_09-41-00mb09b3**
**Run Date: 2017-04-26 09:45**

Column: Reveleris® C18 12g
Flow Rate: 30 mL/min
Equilibration: 1.0 CV
Run Length: 24.0 CV
Air Purge Time: 0 min

Slope Detection: Off
ELSD Threshold: 5 mV
UV Threshold: 0.02 AU
UV1 Wavelength: 254 nm
UV2 Wavelength: 280 nm

Collection Mode: Collect Peaks
Per-Vial Volume: 10 mL
Non-Peaks: 25 mL
Injection Type: Manual

ELSD Carrier: Iso-propanol
Solvent A: Water
Solvent B: Acetonitrile
Solvent C: <No solvent chosen
Solvent D: <No solvent chosen
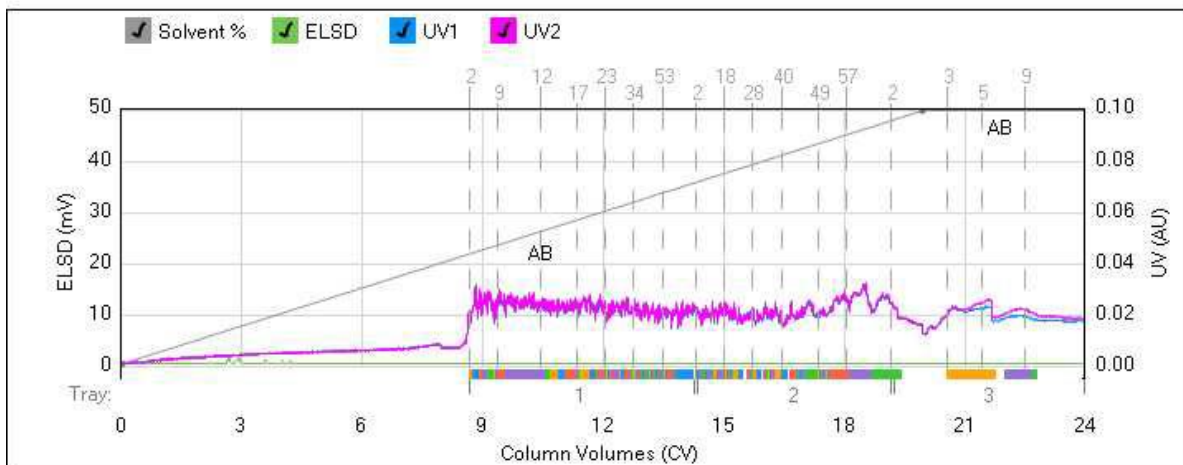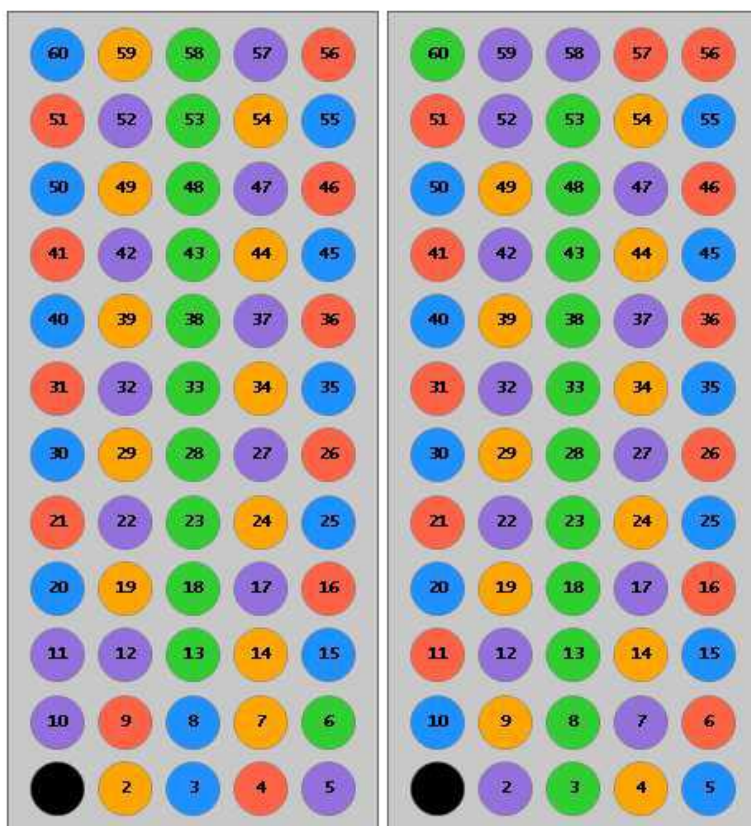
Gradient Table

| | CV | Solvents | % 2nd |
|---|---|---|---|
| 1 | 0.0 | AB | 0 |
| 2 | 20.0 | AB | 100 |
| 3 | 6.3 | AB | 100 |

Vial Mapping Table

| Peak # | Start Tray:Vial | End Tray:Vial |
|---|---|---|
| 1 | 1:2 | 1:2 |
| 2 | 1:3 | 1:3 |
| 3 | 1:4 | 1:4 |
| 4 | 1:5 | 1:5 |
| 5 | 1:6 | 1:6 |
| 6 | 1:7 | 1:7 |
| 7 | 1:8 | 1:8 |
| 8 | 1:9 | 1:9 |
| 9 | 1:10 | 1:12 |
| 10 | 1:13 | 1:13 |
| 11 | 1:14 | 1:14 |
| 12 | 1:15 | 1:15 |
| 13 | 1:16 | 1:16 |
| 14 | 1:17 | 1:17 |
| 15 | 1:18 | 1:18 |
| 16 | 1:19 | 1:19 |
| 17 | 1:20 | 1:20 |
| 18 | 1:21 | 1:21 |
| 19 | 1:22 | 1:22 |
| 20 | 1:23 | 1:23 |
| 21 | 1:24 | 1:24 |
| 22 | 1:25 | 1:25 |

Page 1

154

## REVELERIS™
Flash Chromatography System

### 3 - DCD9
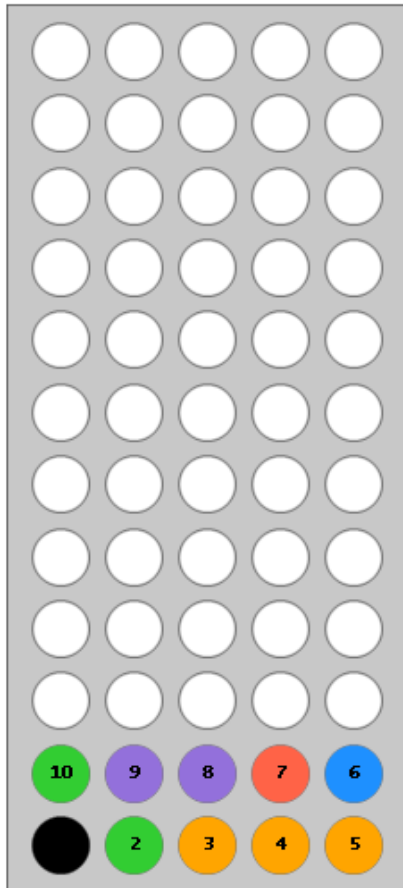


Vial Mapping Table

| Peak # | Start Tray:Vial | End Tray:Vial |
|---|---|---|
| 23 | 1:26 | 1:26 |
| 24 | 1:27 | 1:27 |
| 25 | 1:28 | 1:28 |
| 26 | 1:29 | 1:29 |
| 27 | 1:30 | 1:30 |
| 28 | 1:31 | 1:31 |
| 29 | 1:32 | 1:32 |
| 30 | 1:33 | 1:33 |
| 31 | 1:34 | 1:34 |
| 32 | 1:35 | 1:35 |
| 33 | 1:36 | 1:36 |
| 34 | 1:37 | 1:37 |
| 35 | 1:38 | 1:38 |
| 36 | 1:39 | 1:39 |
| 37 | 1:40 | 1:40 |
| 38 | 1:41 | 1:41 |
| 39 | 1:42 | 1:42 |
| 40 | 1:43 | 1:43 |
| 41 | 1:44 | 1:44 |
| 42 | 1:45 | 1:45 |
| 43 | 1:46 | 1:46 |
| 44 | 1:47 | 1:47 |
| 45 | 1:48 | 1:48 |
| 46 | 1:49 | 1:49 |
| 47 | 1:50 | 1:50 |
| 48 | 1:51 | 1:51 |
| 49 | 1:52 | 1:52 |
| 50 | 1:53 | 1:53 |
| 51 | 1:54 | 1:54 |
| 52 | 1:55 | 1:55 |
| 53 | 1:56 | 1:56 |
| 54 | 1:57 | 1:57 |
| 55 | 1:58 | 1:58 |
| 56 | 1:59 | 1:59 |
| 57 | 1:60 | 1:60 |
| 58 | 2:2 | 2:2 |
| 59 | 2:3 | 2:3 |
| 60 | 2:4 | 2:4 |
| 61 | 2:5 | 2:5 |
| 62 | 2:6 | 2:6 |
| 63 | 2:7 | 2:7 |
| 64 | 2:8 | 2:8 |
| 65 | 2:9 | 2:9 |
| 66 | 2:10 | 2:10 |
| 67 | 2:11 | 2:11 |
| 68 | 2:12 | 2:12 |
| 69 | 2:13 | 2:13 |
| 70 | 2:14 | 2:14 |
| 71 | 2:15 | 2:15 |
| 72 | 2:16 | 2:16 |
| 73 | 2:17 | 2:17 |
| 74 | 2:18 | 2:18 |
| 75 | 2:19 | 2:19 |

*Fifth attempt*

**Method Name:**
**Run Name: 2017-04-26_10-13-19mb094**
**Run Date: 2017-04-26 10:17**

Column: Reveleris® C18 12g
Flow Rate: 30 mL/min
Equilibration: 1.0 CV
Run Length: 20.0 CV
Air Purge Time: 0 min

Slope Detection: Off
ELSD Threshold: 5 mV
UV Threshold: 0.02 AU
UV1 Wavelength: 254 nm
UV2 Wavelength: 280 nm

Collection Mode: Collect Peaks
Per-Vial Volume: 25 mL
Non-Peaks: 25 mL
Injection Type: Manual

ELSD Carrier: Iso-propanol
Solvent A: Methanol
Solvent B: Acetonitrile
Solvent C: <No solvent chosen
Solvent D: <No solvent chosen
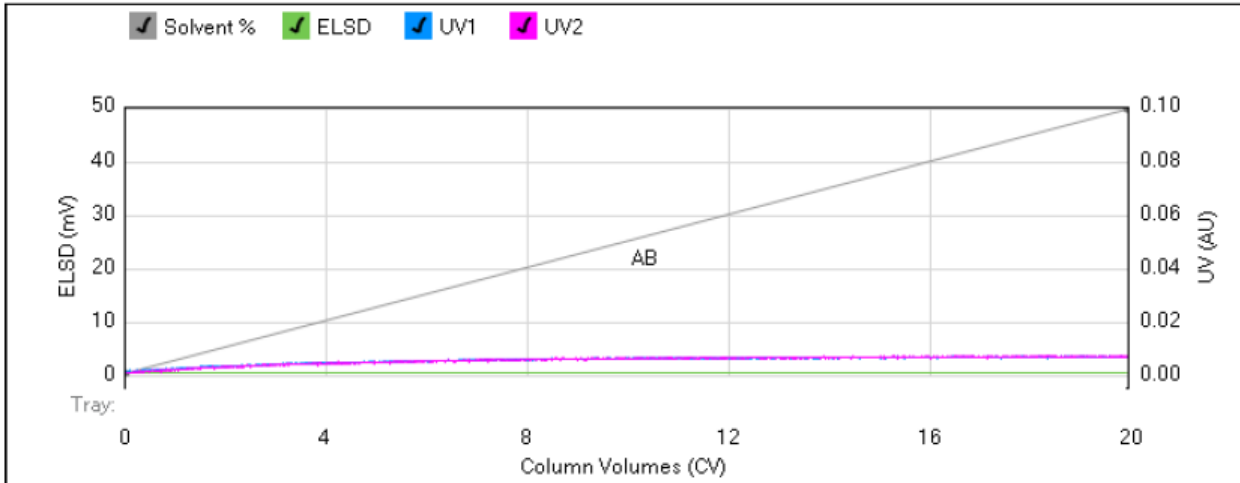


Gradient Table

|   | CV | Solvents | % 2nd |
|---|------|----------|-------|
| 1 | 0.0  | AB       | 0     |
| 2 | 20.0 | AB       | 100   |

Vial Mapping Table

| Peak # | Start Tray:Vial | End Tray:Vial |
|--------|-----------------|---------------|

### 11.6.3 Reaction C

*11.6.3.1 Purification*

**REVELERIS® PREP**

**Method Name:**
Run Name: MFB/2017-04-28_10-05-01 mb09a
Run Date: 2017-04-28 10:18

Column: Reveleris® Silica 40g
Flow Rate: 40 mL/min
Equilibration: 7.1 min
Run Length: 41.3 min
Mode: Flash Dry

Solvent A: Methylene chloride
Solvent B: Methanol
Solvent C: Empty
Solvent D: Empty
Slope Detection: Off

UV Threshold: 0.05 AU
UV Sensitivity: Low
UV1 Wavelength: 254 nm
UV2 Wavelength: 265 nm
UV3 Wavelength: 280 nm

ELSD Threshold: 20 mV
ELSD Sensitivity: Low
Collection: Collect Peaks
Per-Vial Volume: 25 mL
Non-Peak Volume: 25 mL



1 - DCD9



**Gradient Table**

|    | Min  | Solvents | % 2nd |
|----|------|----------|-------|
| 1  | 0.0  | AB       | 0     |
| 2  | 26.4 | AB       | 18    |
| 3  | 2.2  | AB       | 35    |
| 4  | 0.8  | AB       | 35    |
| 5  | 0.0  | AB       | 35    |
| 6  | 0.1  | AB       | 35    |
| 7  | 0.4  | AB       | 39    |
| 8  | 0.1  | AB       | 39    |
| 9  | 0.6  | AB       | 41    |
| 10 | 1.5  | AB       | 41    |
| 11 | 4.3  | AB       | 61    |
| 12 | 0.1  | AB       | 61    |
| 13 | 5.0  | AB       | 100   |

**Vial Mapping Table**

| Peak # | Start Tray:Vial | End Tray:Vial |
|--------|-----------------|---------------|
| 1      | 1:2             | 1:3           |
| 2      | 1:4             | 1:5           |
| 3      | 1:6             | 1:6           |
| 4      | 1:7             | 1:7           |
| 5      | 1:8             | 1:9           |
| 6      | 1:10            | 1:10          |
| 7      | 1:11            | 1:11          |
| 8      | 1:12            | 1:16          |
| 9      | 1:17            | 1:17          |
| 10     | 1:18            | 1:18          |
| 11     | 1:19            | 1:19          |

Page 1
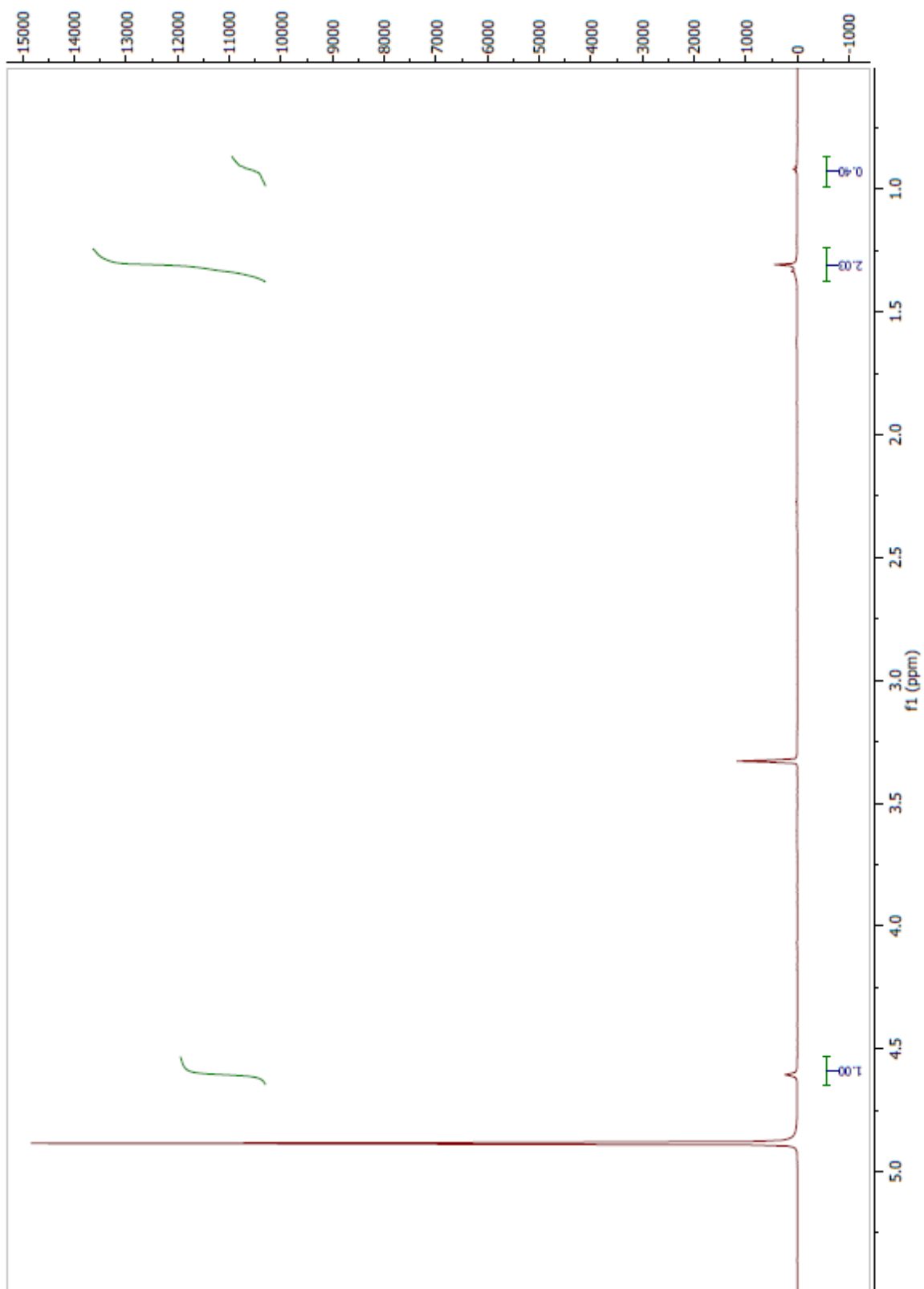
¹H NMR (CD₃OD): δ 4.60 (2H, s), 1.32 (4H, m), 0.92 (1H, t, *J*=7.74 Hz).
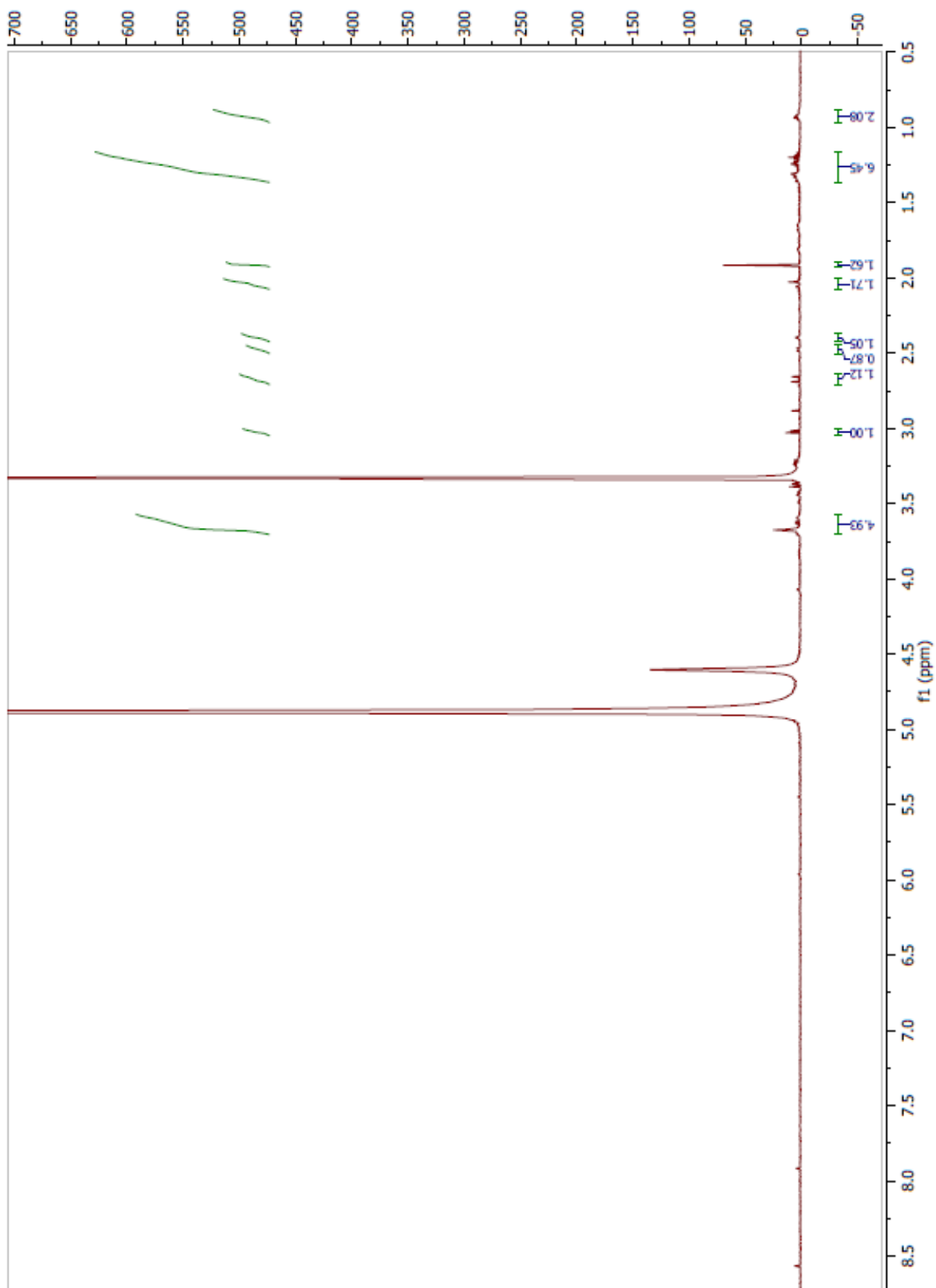
¹H NMR (CD₃OD): δ 3.67 (4H, m), 3.02 (1H, d, *J*= 7.66 Hz), 2.67 (1H, m), 2.48 (1H, d, *J*= 11.68 Hz), 2.39 (1H, m), 2.04 (2H, m), 1.92 (1H, s), 1.38-1.16 (6H, m), 0.93 (2H, m)

## 11.7 N-Adamantanoylglycine (6)
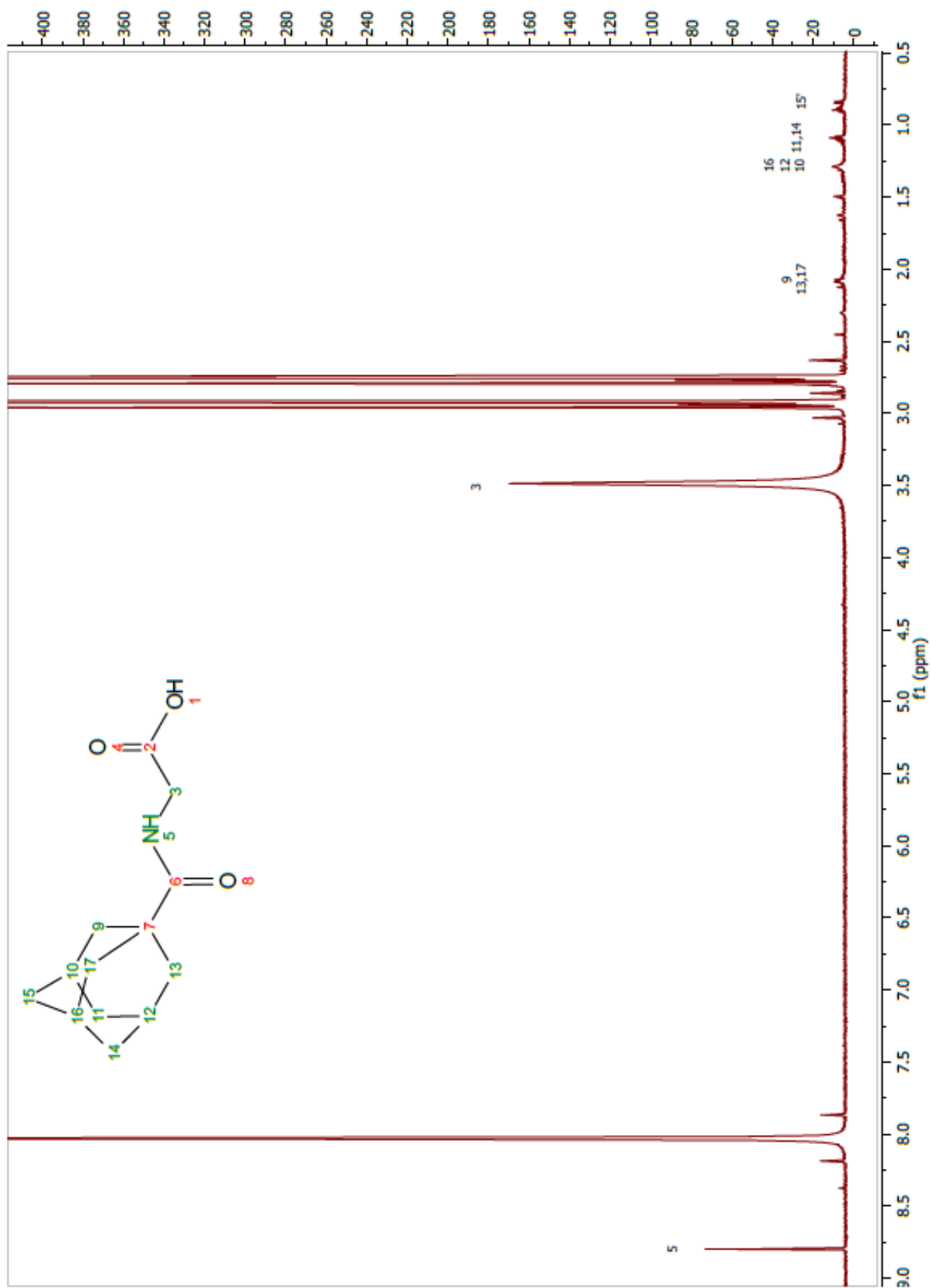


$^1$H NMR (DMF-d7): δ 8.79 (m), 3.49 (m), 2.08 (m), 1,28 (m), 1.09 (m), 0.89 (m).

## 11.8 3′-O-(tert-Butoxycarbonyl) gemcitabine (10)
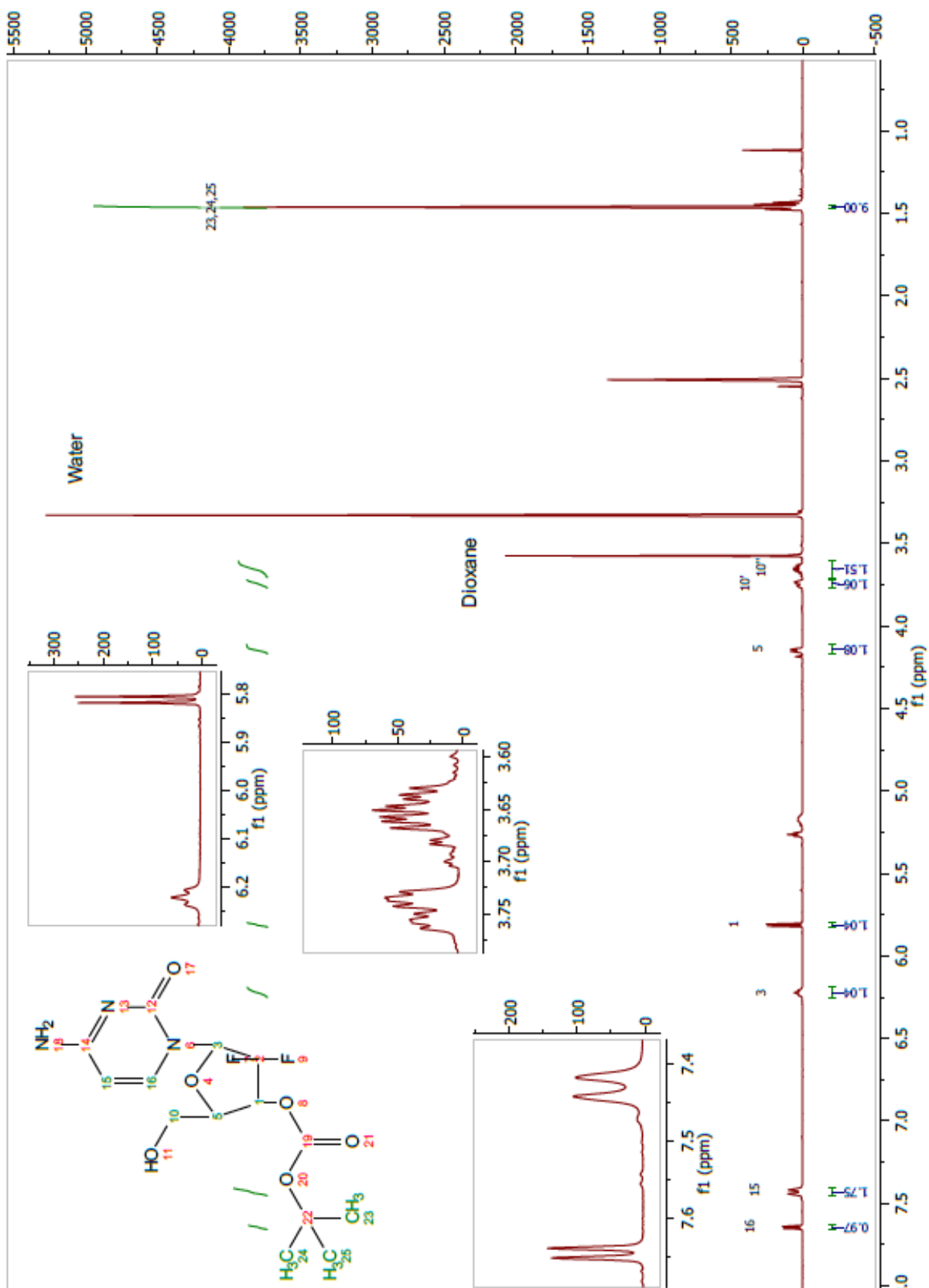


$^1$H NMR ((CD$_3$)SO$_2$): δ 7.64 (1H, d, J=7.43 Hz), 7.43 (1H, d, J=13.86 Hz), 6.22 (1H, t, J=9.41 Hz), 5.81 (1H, d, J=7.43 Hz), 4.15 (1H, m) 3.74 (1H, m) 3.65 (1H, m), 1.45 (9H, s).

## 11.9 (5-(4-(4-(((1S,3s)-adamantan-1-yl)disulfaneyl)butanamido)-2-oxopyrimidin-1(2H)-yl)-4,4-difluoro-2-(hydroxymethyl)tetrahydrofuran-3-yl *tert* butylcarbonate (12)

### 11.9.1 Before purification
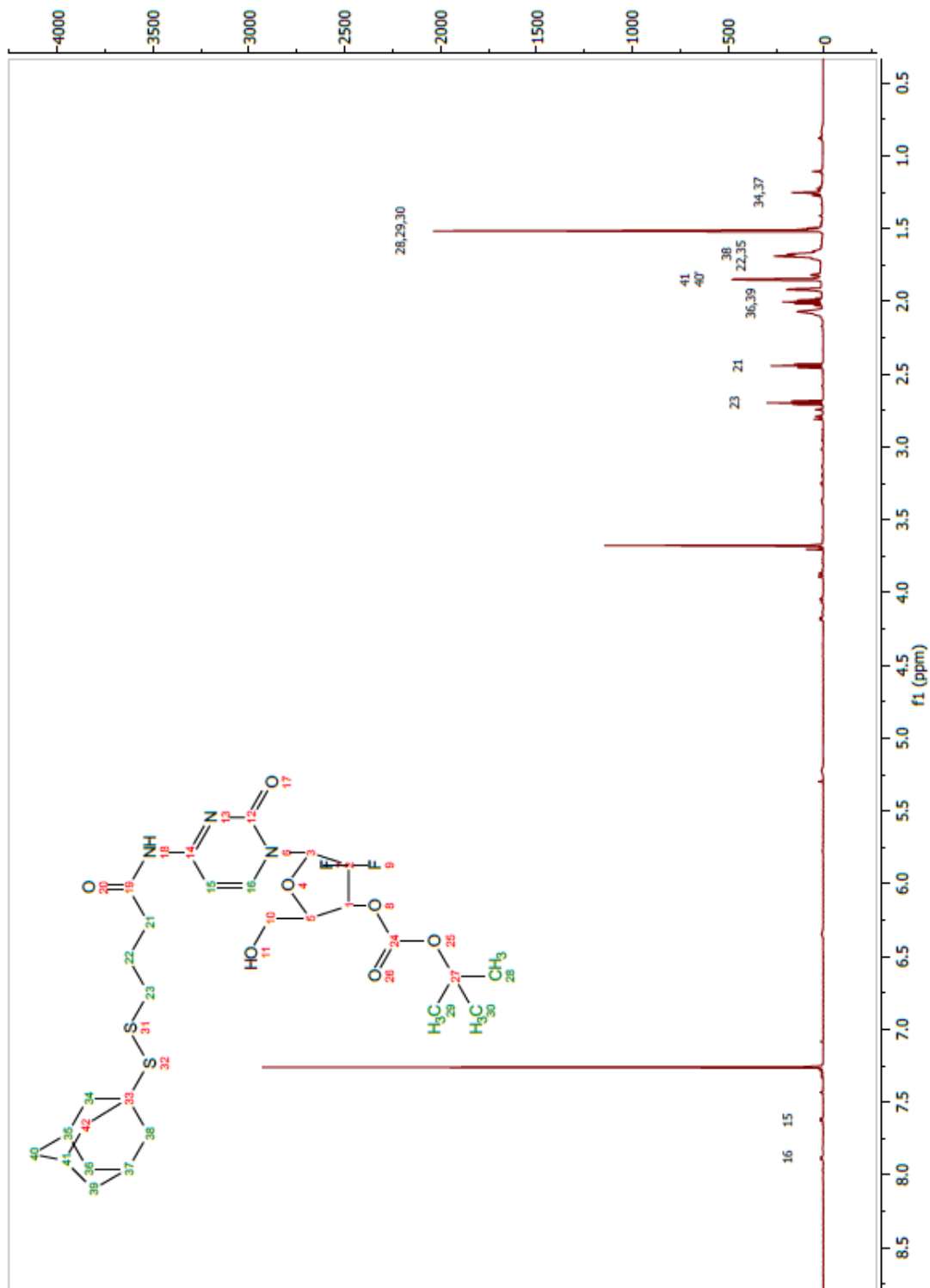


$^1$H NMR (CDCl$_3$): δ 7.89 (d, *J*=7.47 Hz), 7.78 (d, *J*=8.18 Hz), 6.35 (m), 5.30 (m), 2.70 (t, *J*=7.29 Hz), 2.44 (t, *J*=6.81 Hz), 2.10-1.91 (m), 1.69 (m), 1.52 (s) 1.25 (m).

## 11.9.2 Purification

**REVELERIS® PREP**

Method Name:
Run Name: MFB/2017-05-02_08-45-10 mb10b
Run Date: 2017-05-02 08:56

Column: Reveleris® Silica 40g
Flow Rate: 40 mL/min
Equilibration: 7.1 min
Run Length: 45.0 min
Mode: Flash Liquid

Solvent A: Methylene chloride
Solvent B: Methanol
Solvent C: Empty
Solvent D: Empty
Slope Detection: Off

UV Threshold: 0.05 AU
UV Sensitivity: Low
UV1 Wavelength: 254 nm
UV2 Wavelength: 265 nm
UV3 Wavelength: 280 nm

ELSD Threshold: 20 mV
ELSD Sensitivity: Low
Collection: Collect Peaks
Per-Vial Volume: 25 mL
Non-Peak Volume: 25 mL
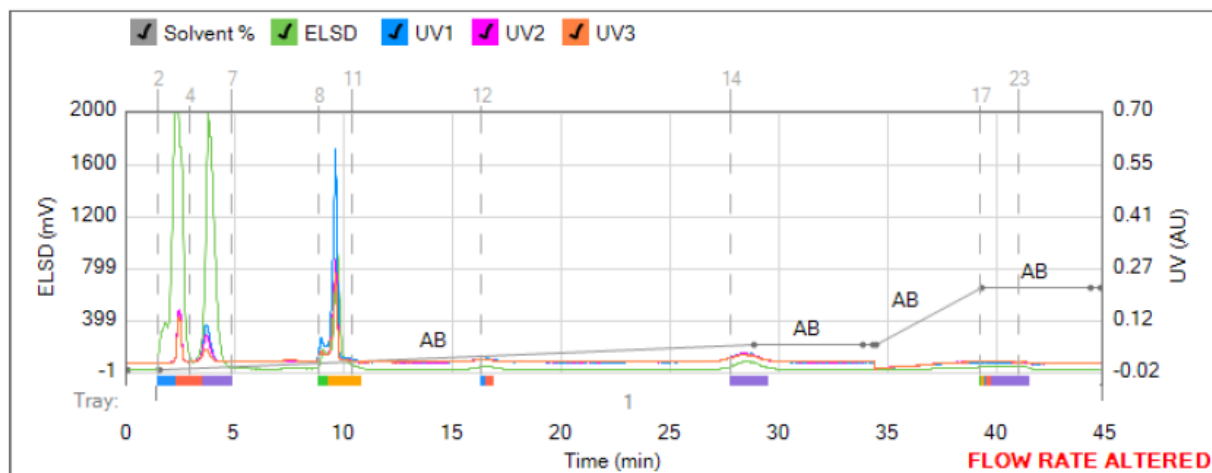


1 - DCD9
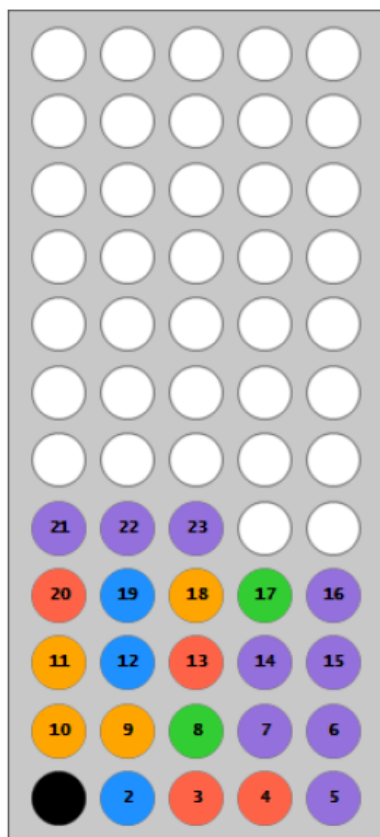


### Gradient Table

|   | Min | Solvents | % 2nd |
|---|-----|----------|-------|
| 1 | 0.0 | AB | 0 |
| 2 | 1.5 | AB | 0 |
| 3 | 27.6 | AB | 10 |
| 4 | 5.0 | AB | 10 |
| 5 | 0.5 | AB | 10 |
| 6 | 0.1 | AB | 10 |
| 7 | 4.9 | AB | 32 |
| 8 | 5.0 | AB | 32 |
| 9 | 0.5 | AB | 32 |

### Vial Mapping Table

| Peak # | Start Tray:Vial | End Tray:Vial |
|--------|-----------------|---------------|
| 1 | 1:2 | 1:2 |
| 2 | 1:3 | 1:4 |
| 3 | 1:5 | 1:7 |
| 4 | 1:8 | 1:8 |
| 5 | 1:9 | 1:11 |
| 6 | 1:12 | 1:12 |
| 7 | 1:13 | 1:13 |
| 8 | 1:14 | 1:16 |
| 9 | 1:17 | 1:17 |
| 10 | 1:18 | 1:18 |
| 11 | 1:19 | 1:19 |
| 12 | 1:20 | 1:20 |
| 13 | 1:21 | 1:23 |

Page 1

163

### 11.9.3 After purification

*$^1$H NMR fraction 2-4*
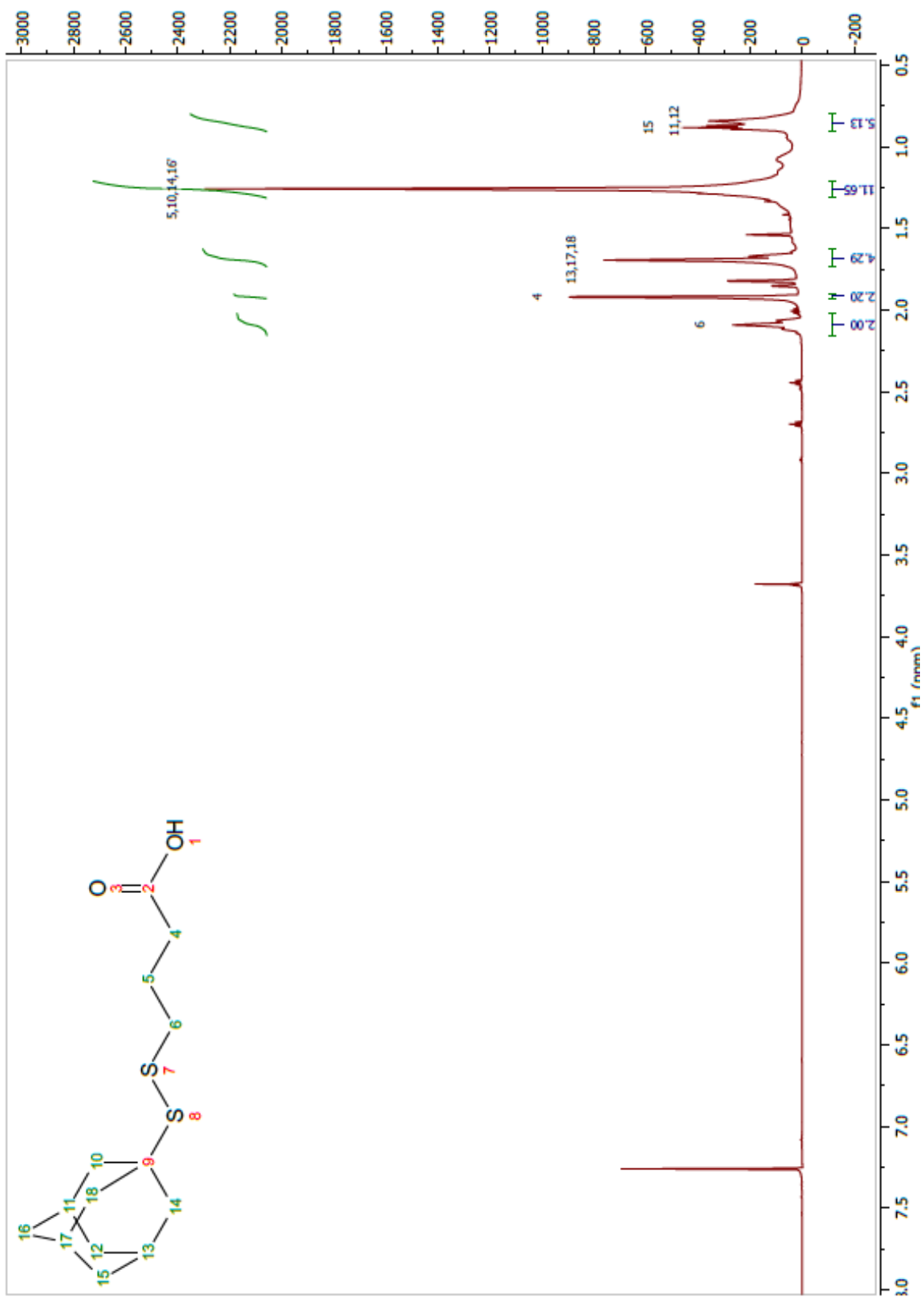


$^1$H NMR (CDCl$_3$): δ 2.09 (2H, m), 1.92 (2H, m), 1.72 (4H, m), 1.26 (8H, m), 0.86 (5H, m).

*¹H NMR fraction 5-7*
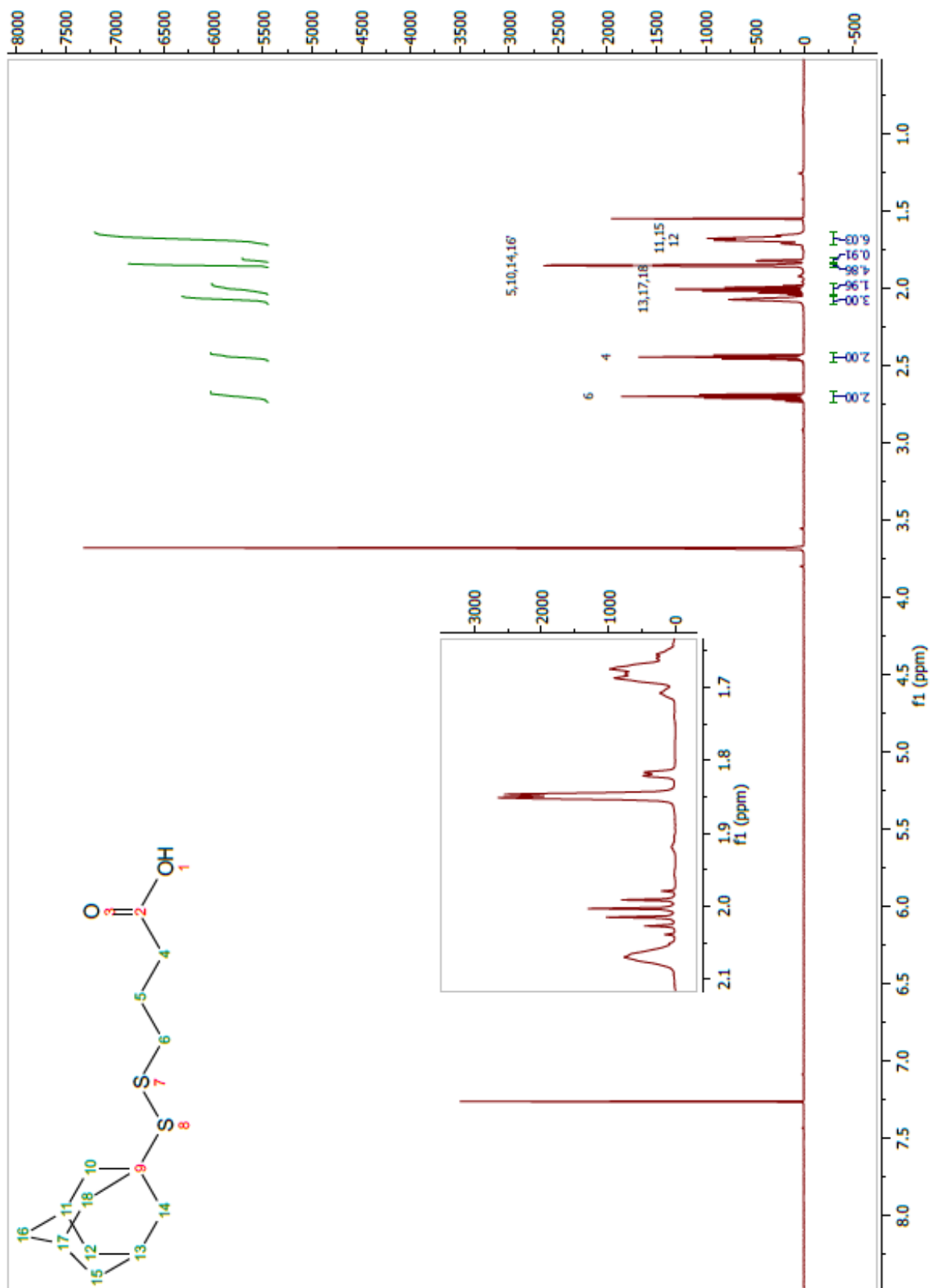


¹H NMR (CDCl₃): δ 2.70 (2H, m), 2.44 (2H, m), 2.07-2.00 (4H, m), 1.85 (8H, m), 1.82 (5H, m).
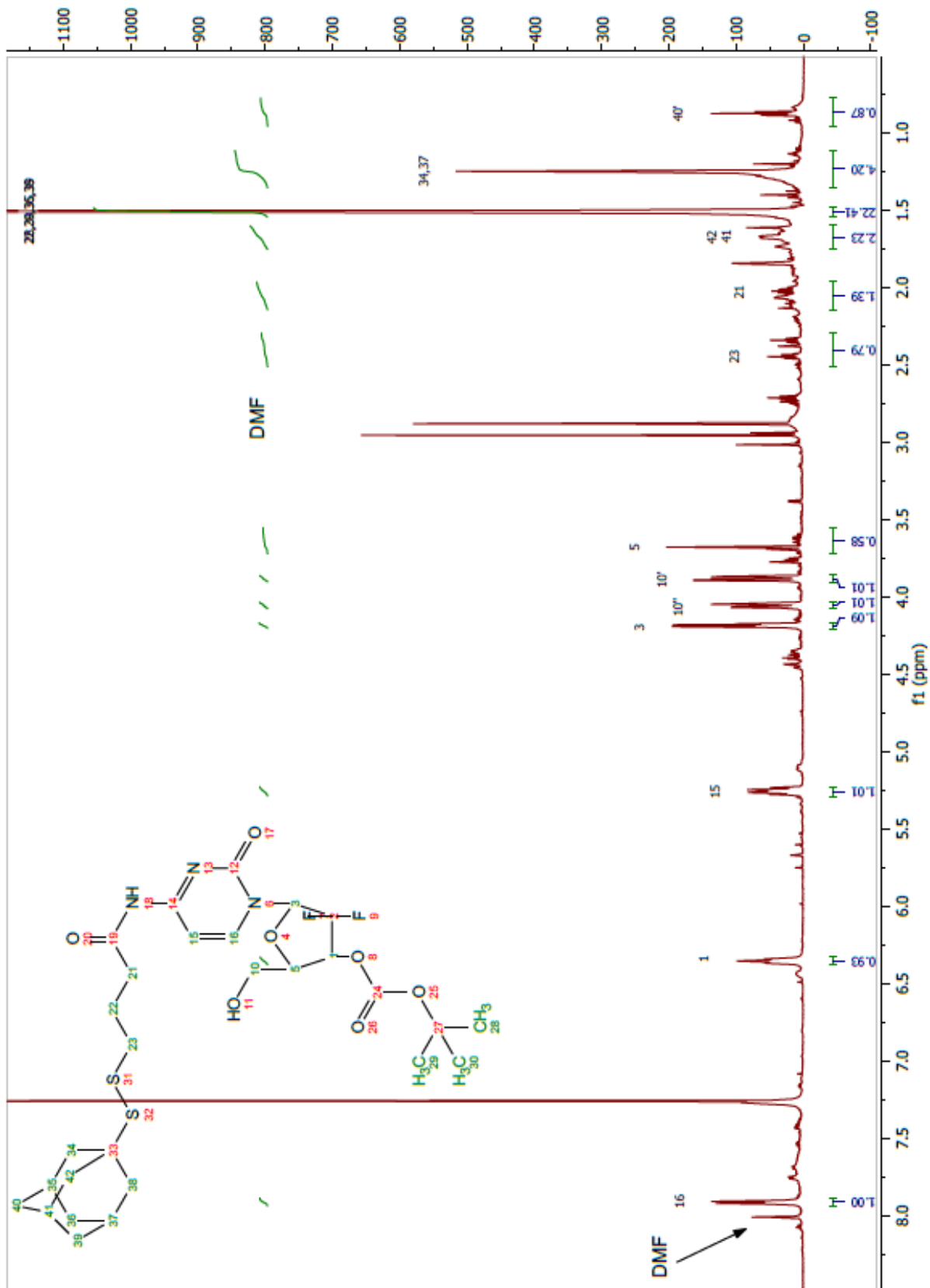
*^{1}H NMR (CDCl[3]): δ 7.91 (1H, d, *J*=7.26 Hz), 6.36 (1H, t, *J*=7.64 Hz), 5.26 (1H, m), 4.18 (1H, m), 3.88 (1H, dd, *J*=9.64, 3.03 Hz) 3.68 (1H, m), 2.38 (2H, m), 2.07 (2H, m), 1.65 (3H, m), 1.51 (18H, m), 1.26 (3H, m), 0.88 (2H, m).
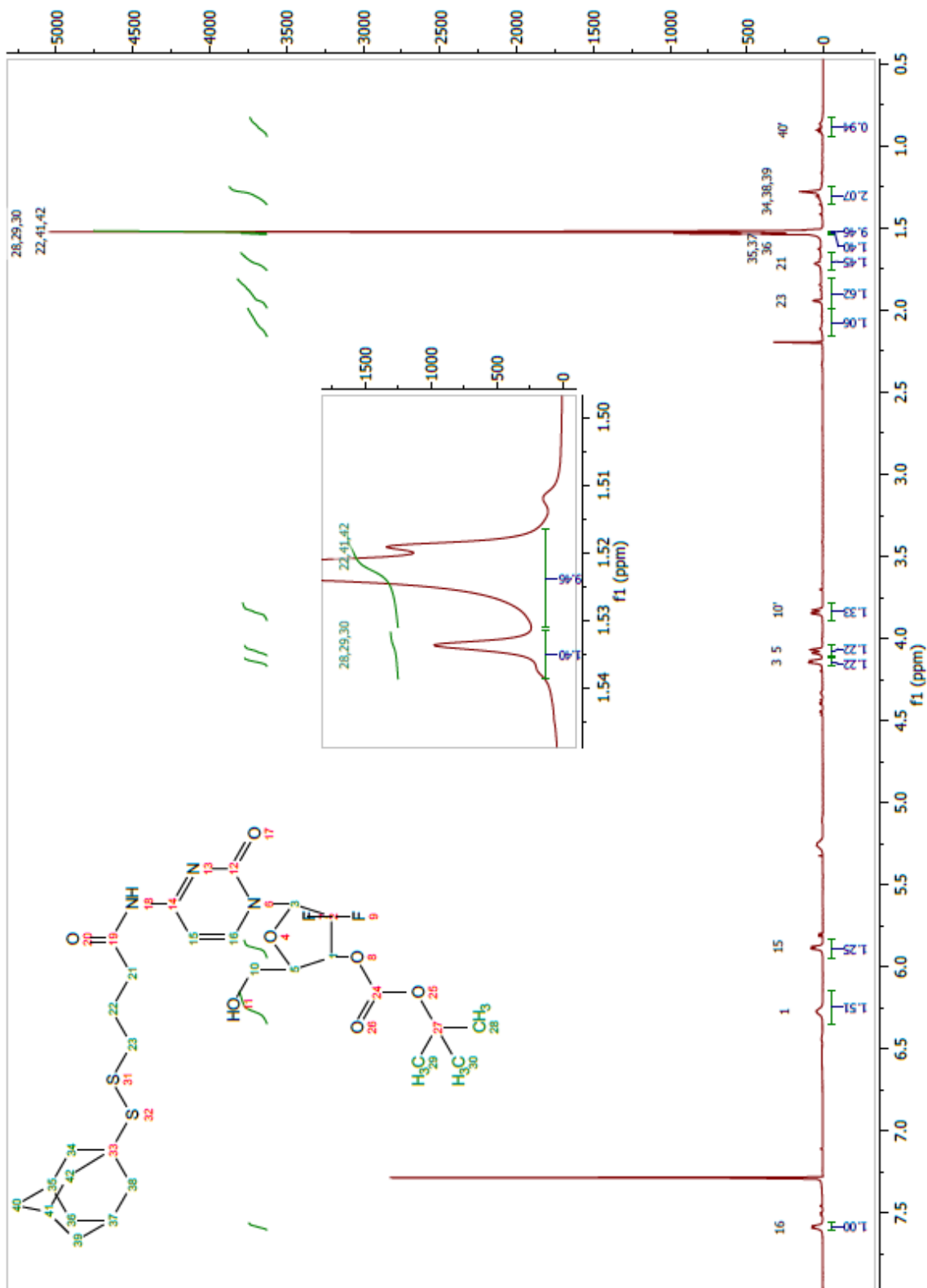
<sup>1</sup>H NMR (CDCl<sub>3</sub>): δ 7.58 (1H, d, *J*=9.20 Hz), 6.27 (1H, m), 5.89 (1H, d, *J*=8.26 Hz), 4.14 (1H, m), 4.08 (1H d, *J*=12.56) 3.84 (2H, dd, *J*=9.11, 2.83 Hz), 2.11 (2H, m), 1.92 (2H, m), 1.70 (3H, m), 1.53 (4H, m), 1.52 (14H, m), 1.28 (3H, m), 0.87 (2H, m).
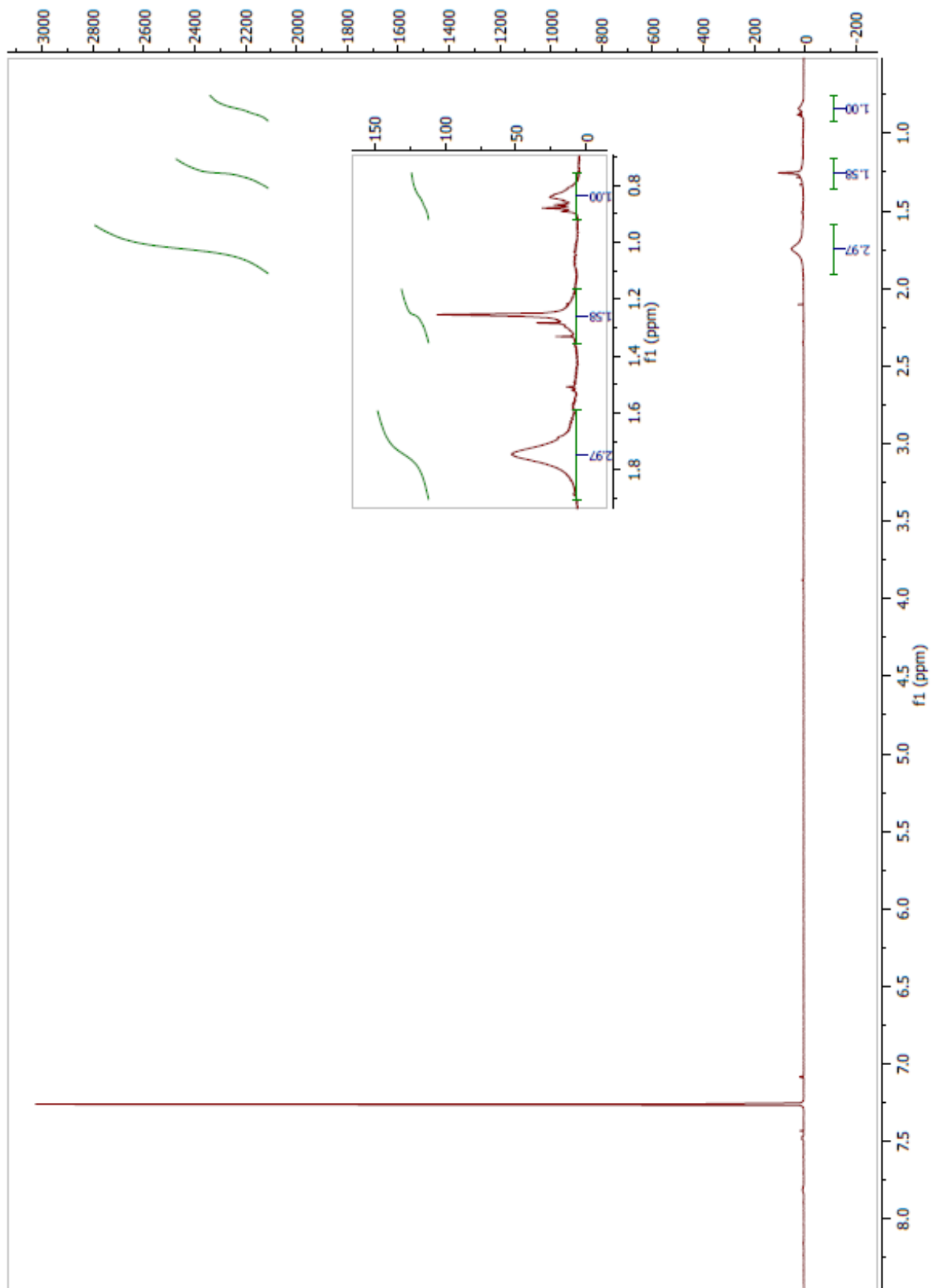
$^1$H NMR (CDCl$_3$): δ 1. 75 (3H, m), 1.27 (2H, m), 0.85 (1H, m).

## 11.10 4-(((1S,3s)-adamantan-1-yl)disulfaneyl)-N-(1-(2R,4R,5R)-3,3-difluoro-4-hydroxy-5-(hydroxymethyl)tetrahydrofuran-2-yl)-2oxo-1,2-dihydropyrimidin-4-yl)butanamide (8)

### 11.10.1 $^1$H NMR
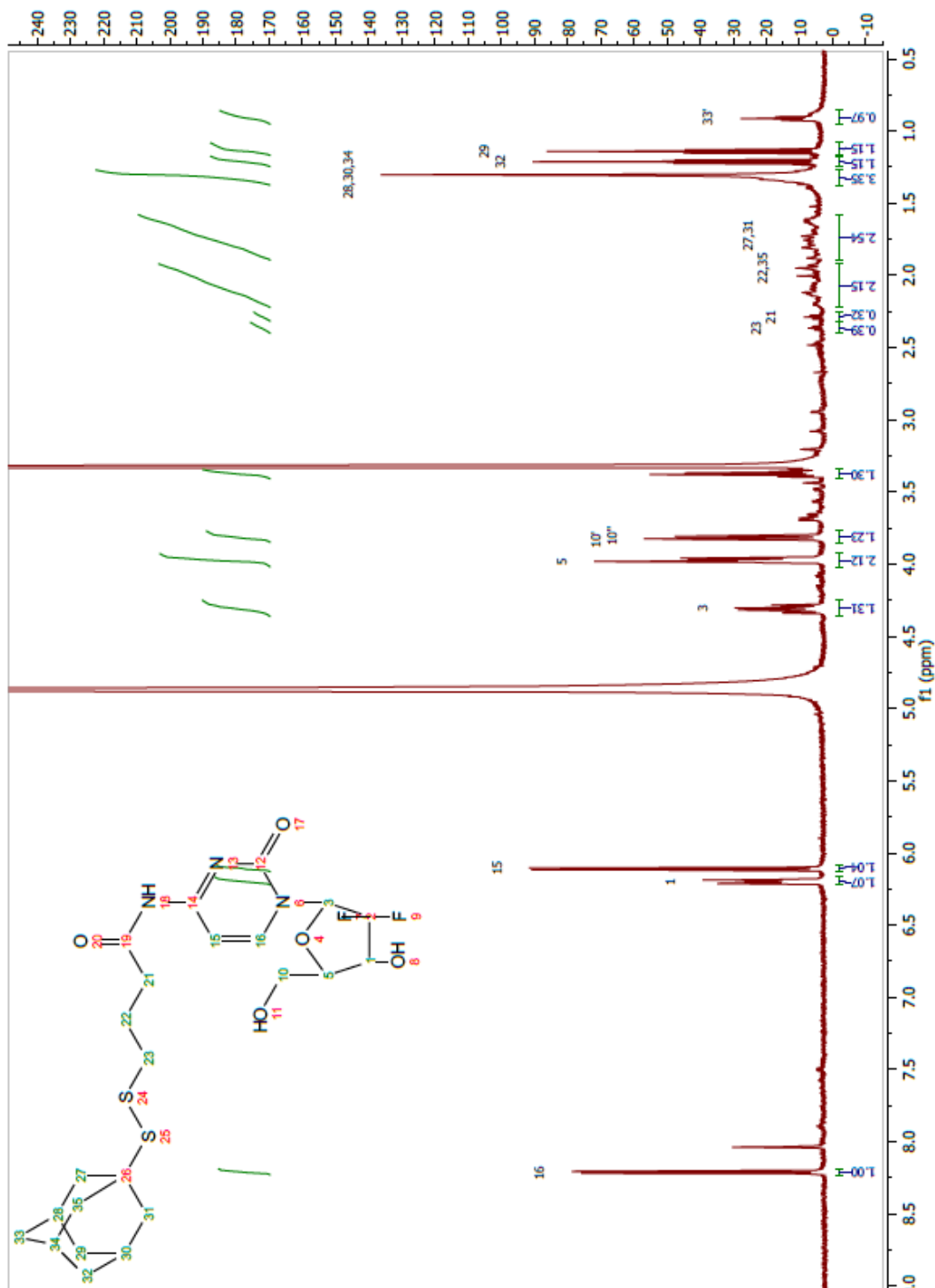


$^1$H NMR (CD$_3$OD): δ 8.21 (1H, d, J=7.82 Hz), 6.20 (1H, dd, J=4.94, 4.61 Hz), 6.11 (1H, d, J=7.82 Hz), 4.31 (1H, m), 3.98 (1H, m), 3.82 (2H, dd, J=9.62, 3.81 Hz), 2.37 (2H, t, J=7.31 Hz), 2.29 (2H, t, J=7.27 Hz), 1.31 (3H, m), 1.21 (2H, m), 1.14 (2H, t, J=7.34 Hz), 0.91 (2H, t, J=7.25 Hz).

## 11.10.2 LC-MS
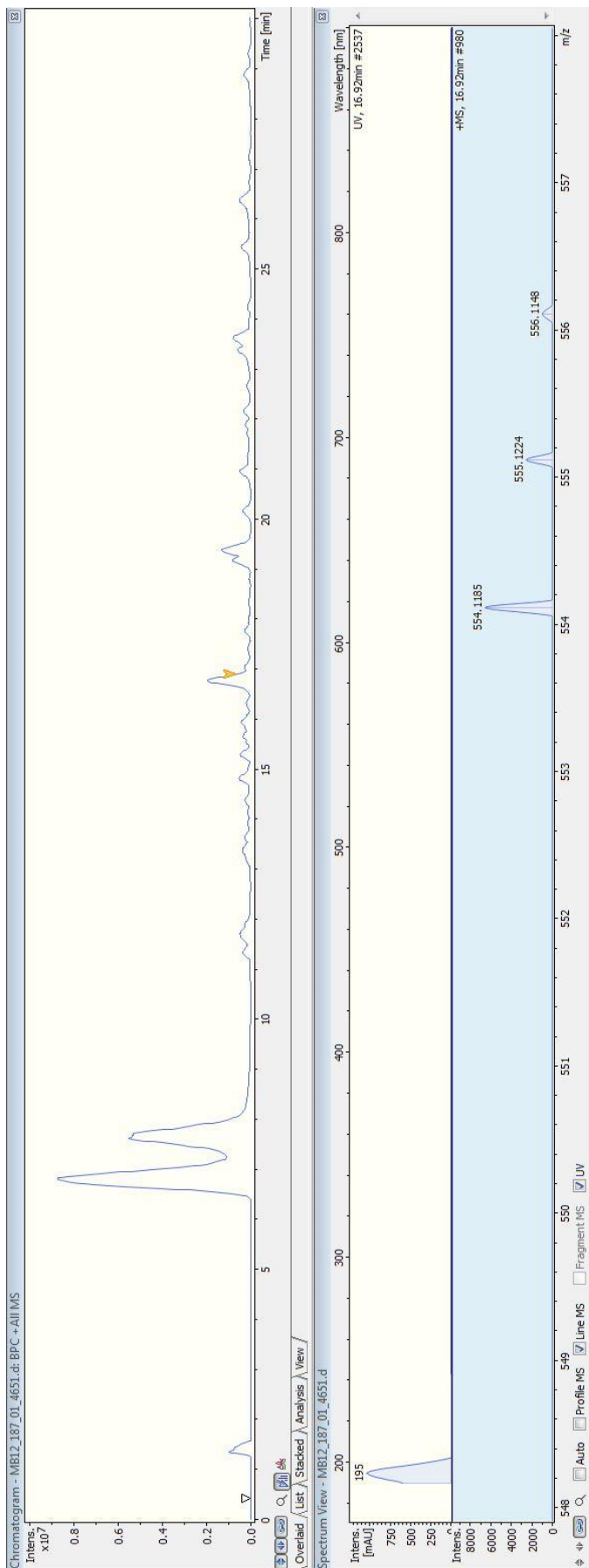


LC-MS: m/z =554.1185 [M+Na$^+$], calc. for.
(C$_{23}$H$_{31}$N$_3$O$_5$S$_2$ Na$^+$): m/z: 554.1565
Deviation of 0.0380Da.

### 10.11.3 ITC measurement - native β-CD
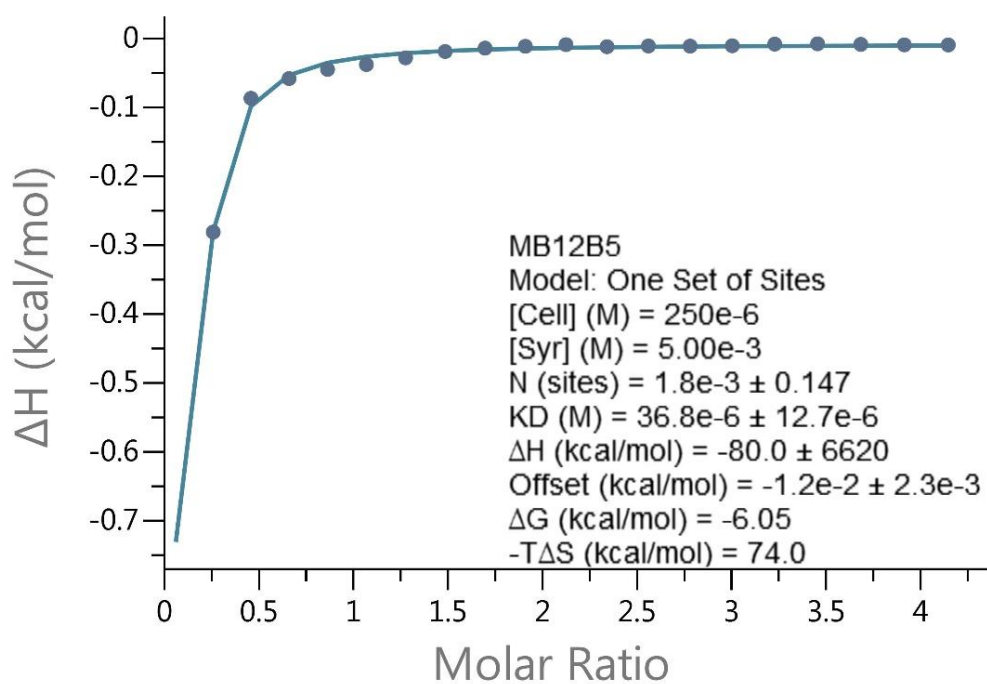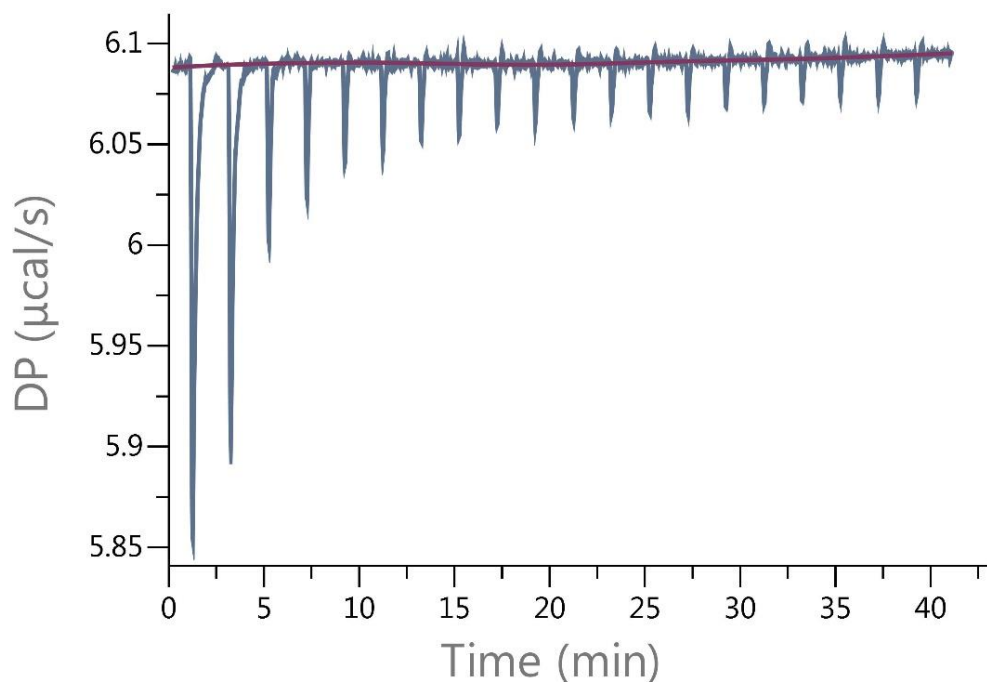
*At 5 mM*



MB12B5
Model: One Set of Sites
[Cell] (M) = 250e-6
[Syr] (M) = 5.00e-3
N (sites) = 1.8e-3 ± 0.147
KD (M) = 36.8e-6 ± 12.7e-6
ΔH (kcal/mol) = -80.0 ± 6620
Offset (kcal/mol) = -1.2e-2 ± 2.3e-3
ΔG (kcal/mol) = -6.05
-TΔS (kcal/mol) = 74.0

Binding observed. However, the initial peak is higher than first measurement. The solution was saturated to fast and the values are therefore unreliable.

Values reported:

$K_D = 36.8 \times 10^{-6} \pm 12.7 \times 10^{-6}$ M

$K_A = 27173$ M$^{-1}$

Reduced $\chi^2 = 3.3 \times 10^{-5}$ Kcal/mol$^2$
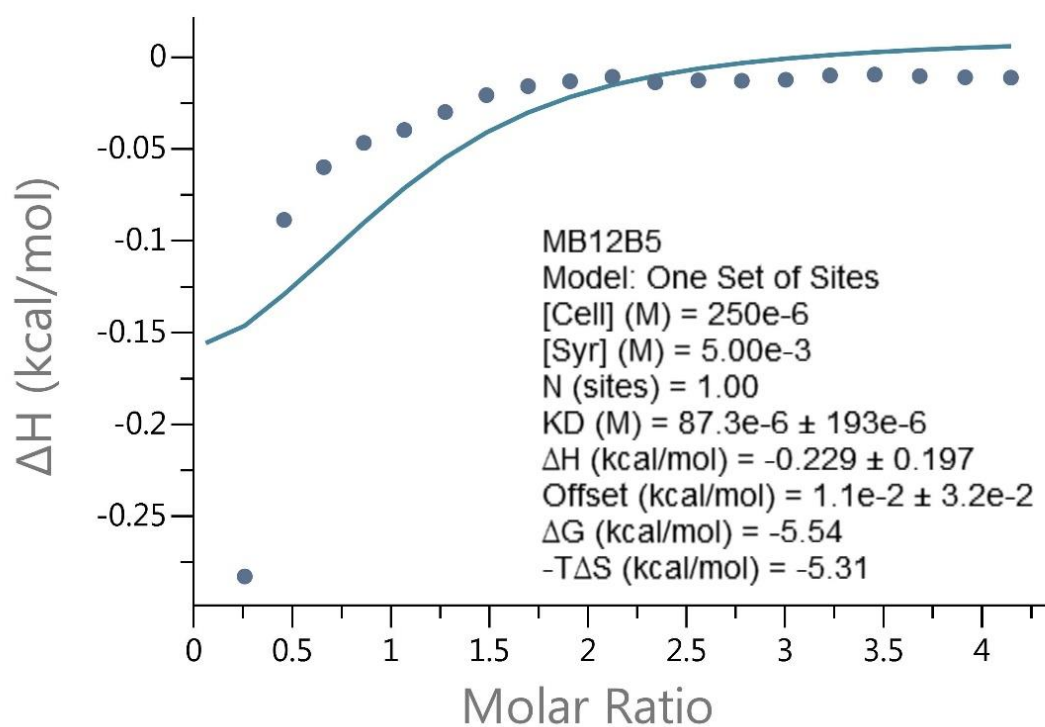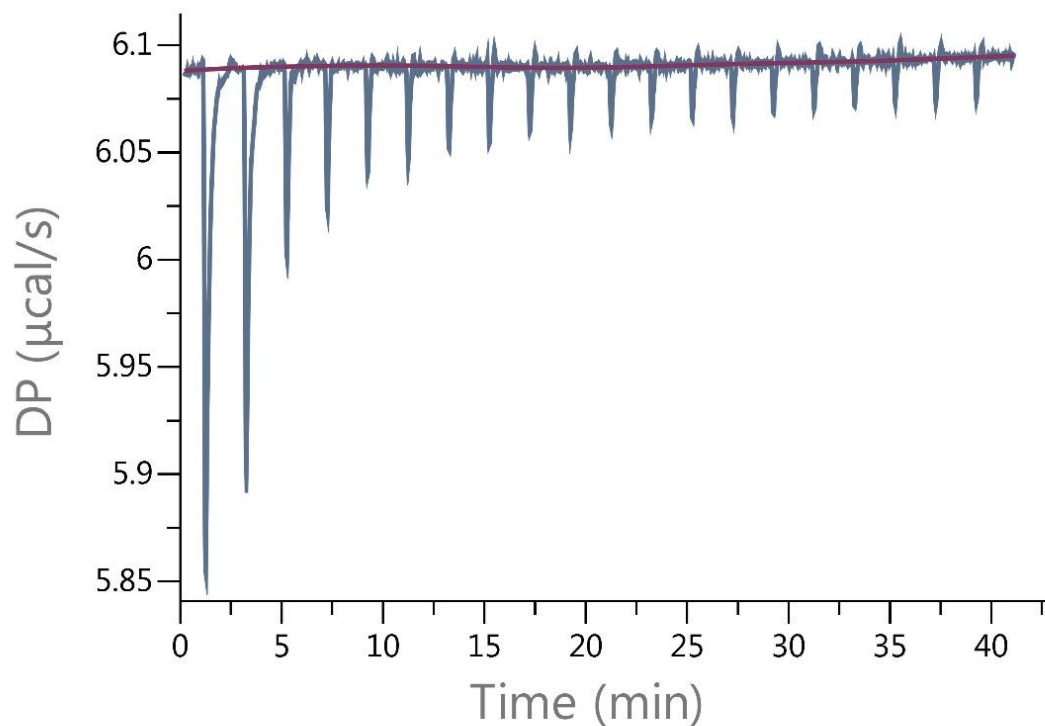
MB12B5
Model: One Set of Sites
[Cell] (M) = 250e-6
[Syr] (M) = 5.00e-3
N (sites) = 1.00
KD (M) = 87.3e-6 ± 193e-6
ΔH (kcal/mol) = –0.229 ± 0.197
Offset (kcal/mol) = 1.1e-2 ± 3.2e-2
ΔG (kcal/mol) = –5.54
–TΔS (kcal/mol) = –5.31

The values obtained from fixating n=1, has to be disregarded as the fit is not in line with the data points (systematic deviations).

Reduced $\chi^2$= 1.8x10$^{-3}$ Kcal/mol$^2$

MB12B2
Model: One Set of Sites
[Cell] (M) = 250e-6
[Syr] (M) = 2.00e-3
N (sites) = 1.8e-3 ± 3.3e-2
KD (M) = 20.0e-6 ± 4.23e-6
ΔH (kcal/mol) = -80.0 ± 1480
Offset (kcal/mol) = 6.7e-3 ± 3.4e-3
ΔG (kcal/mol) = -6.41
-TΔS (kcal/mol) = 73.6
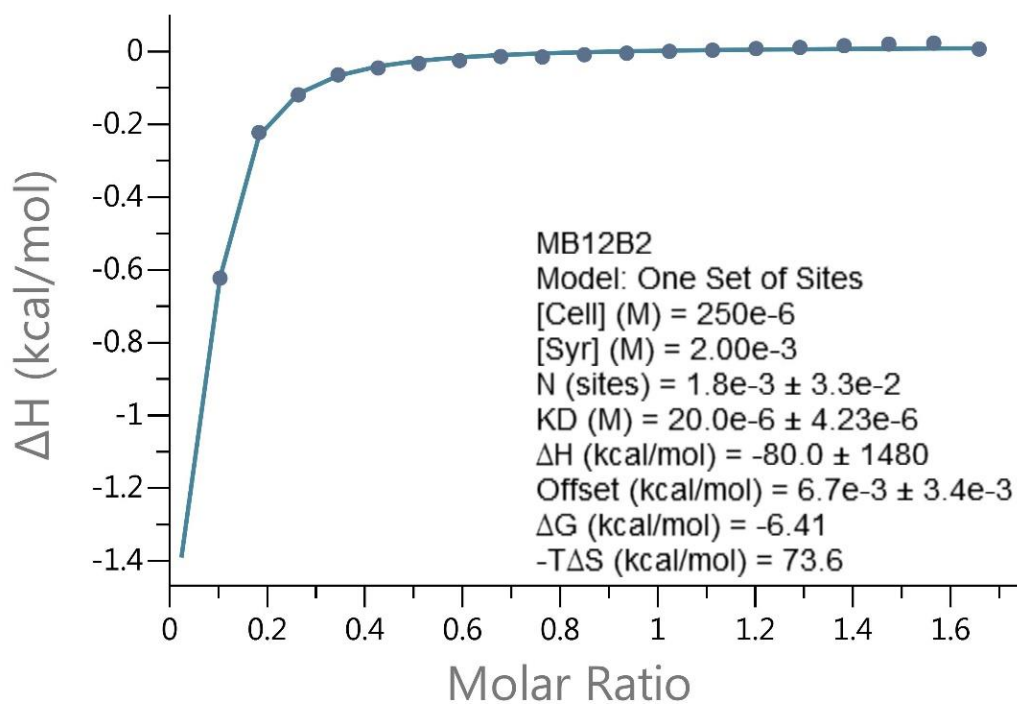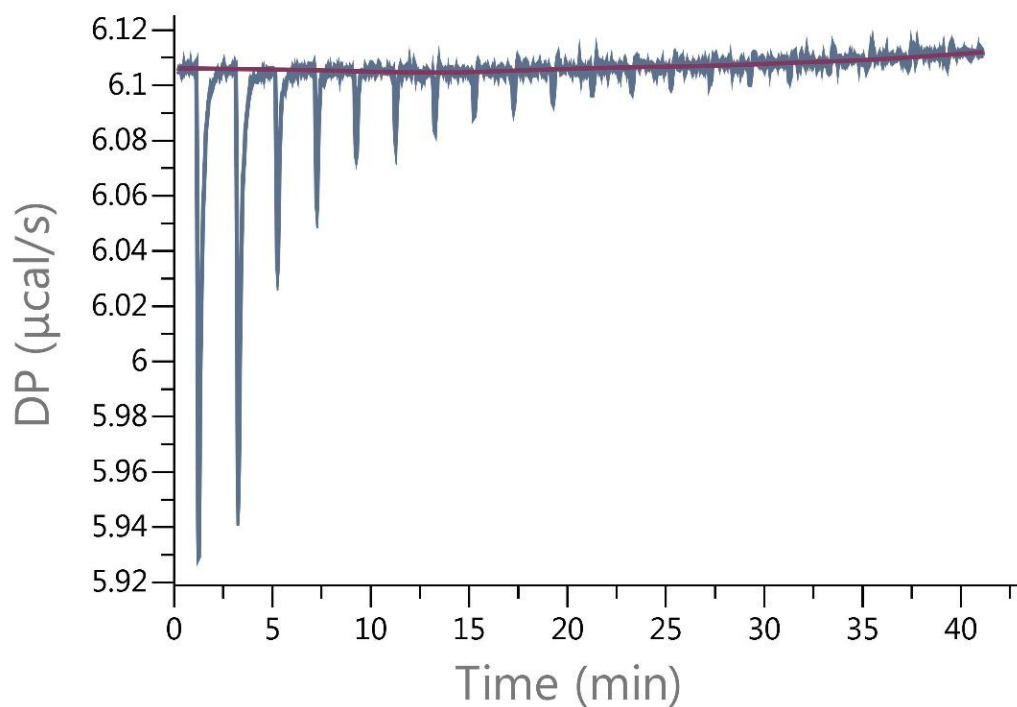
Binding observed. However, the initial peak is higher than first measurement. The solution was saturated to fast and the values are therefore unreliable.

Values reported:
$K_D = 20.0 \times 10^{-6} \pm 4.23 \times 10^{-6}$ M
$K_A = 50000$ M$^{-1}$
Reduced $\chi^2 = 6.4 \times 10^{-5}$ Kcal/mol$^2$
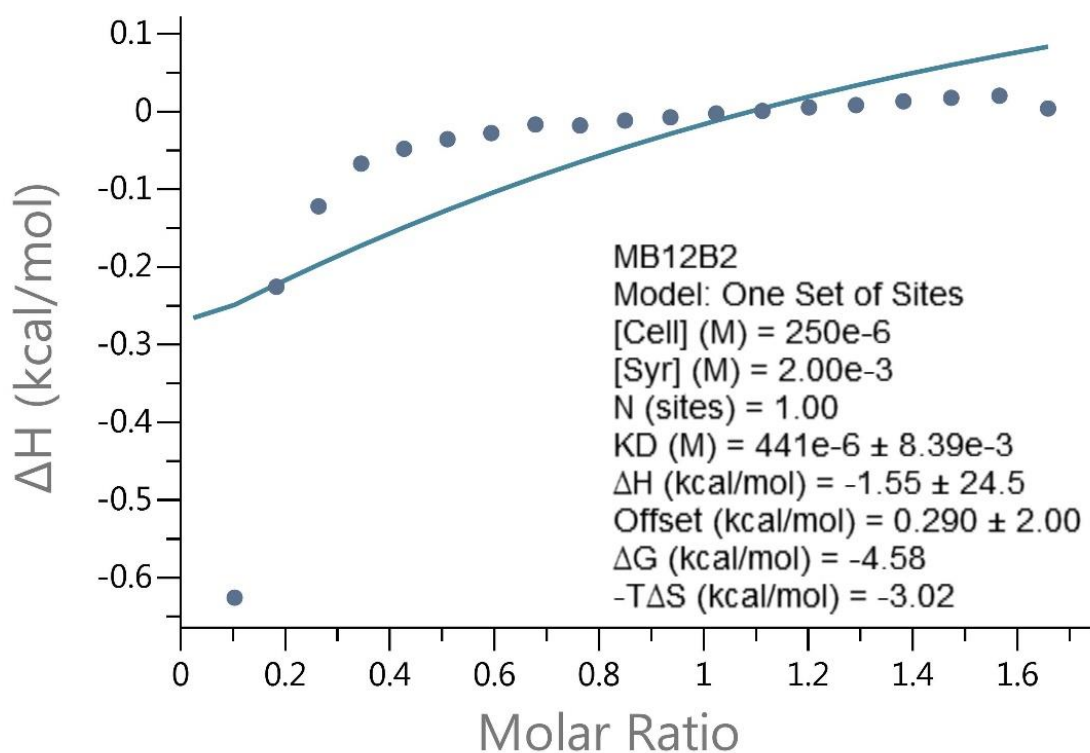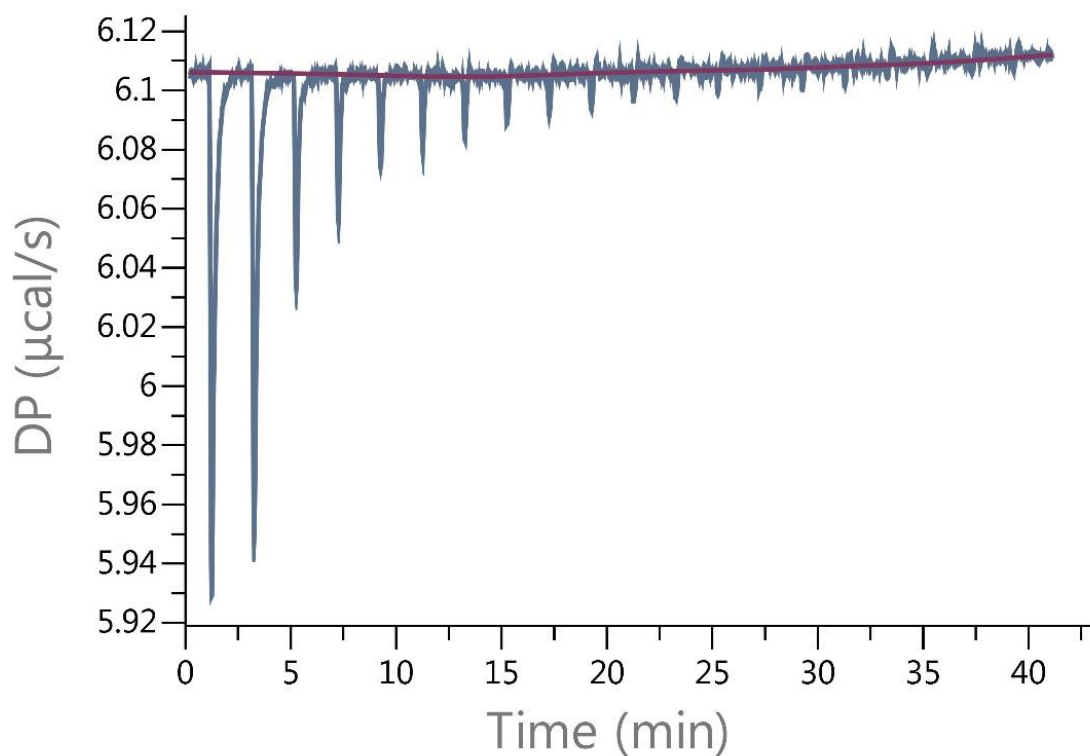
The values obtained from fixating n=1, has to be disregarded as the fit is not in line with the data points (systematic deviations).

Reduced $\chi^2$ = 1.3x10$^{-2}$ Kcal/mol$^2$

MB12B1
Model: One Set of Sites
[Cell] (M) = 251e-6
[Syr] (M) = 1.02e-3
N (sites) = 1.7e-3 ± 2.5e-2
KD (M) = 12.3e-6 ± 3.90e-6
ΔH (kcal/mol) = −80.0 ± 1190
Offset (kcal/mol) = 2.1e-2 ± 9.5e-3
ΔG (kcal/mol) = −6.70
−TΔS (kcal/mol) = 73.3
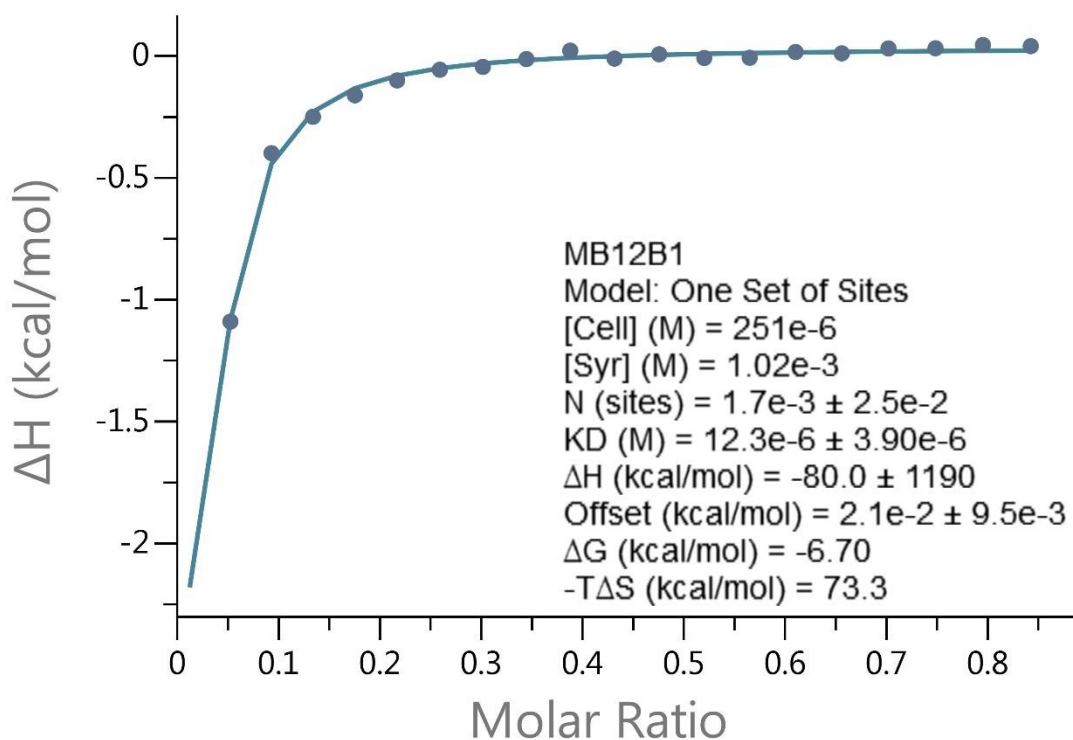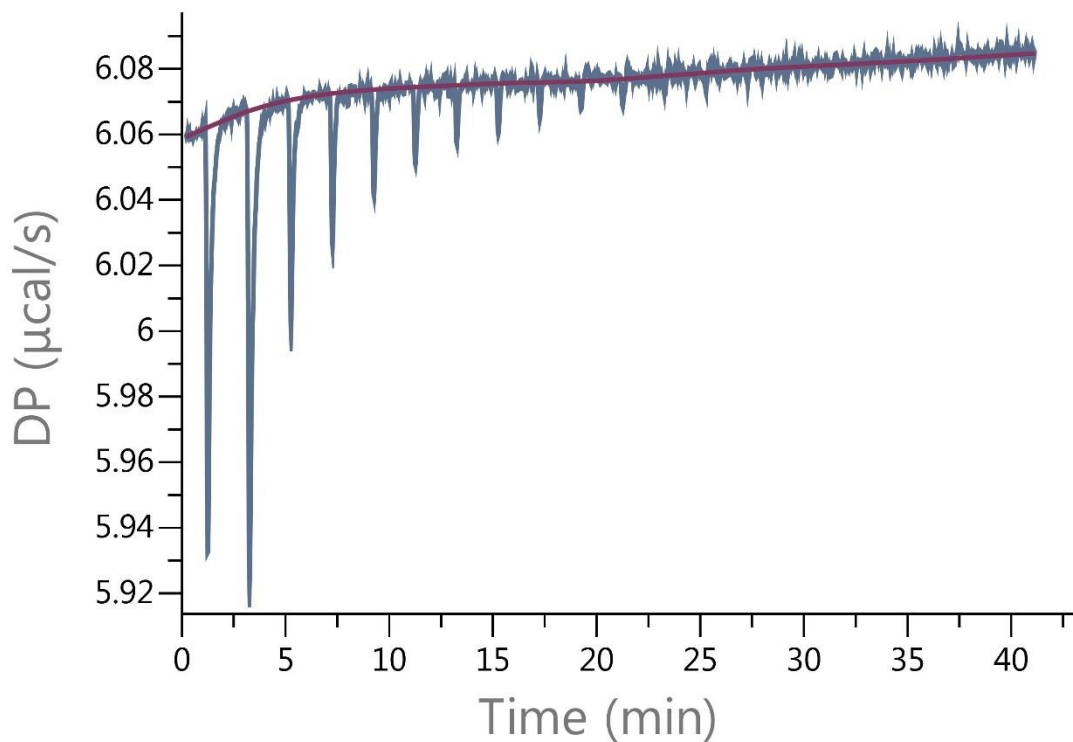
Values reported:

$K_D$= 12.3x$10^{-6}$ ±3.90x$10^{-6}$ M

$K_A$=81301 M$^{-1}$

Reduced $\chi^2$=4.5x$10^{-4}$ Kcal/mol$^2$
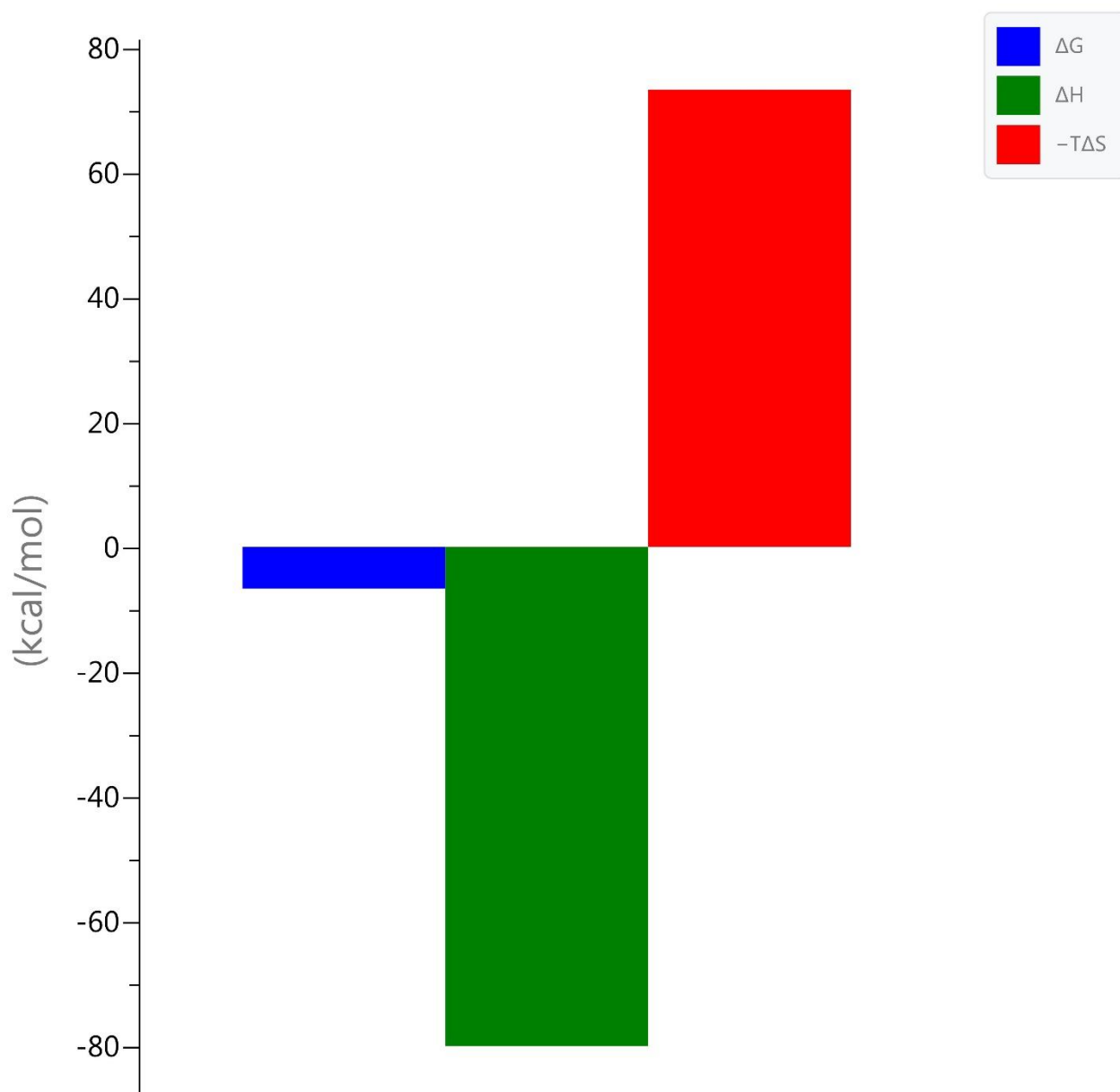
Reported Values:

ΔH= -80.0 ± 1190 Kcal/mol

ΔG= -6.70 Kcal/mol

-TΔS= 73.3 Kcal/mol

MB12B1
Model: One Set of Sites
[Cell] (M) = 251e-6
[Syr] (M) = 1.02e-3
N (sites) = 1.00
KD (M) = 1.00e-12 ± 133e-9
ΔH (kcal/mol) = -24.9 ± 22.3
Offset (kcal/mol) = 24.6 ± 22.3
ΔG (kcal/mol) = -16.4
-TΔS (kcal/mol) = 8.48
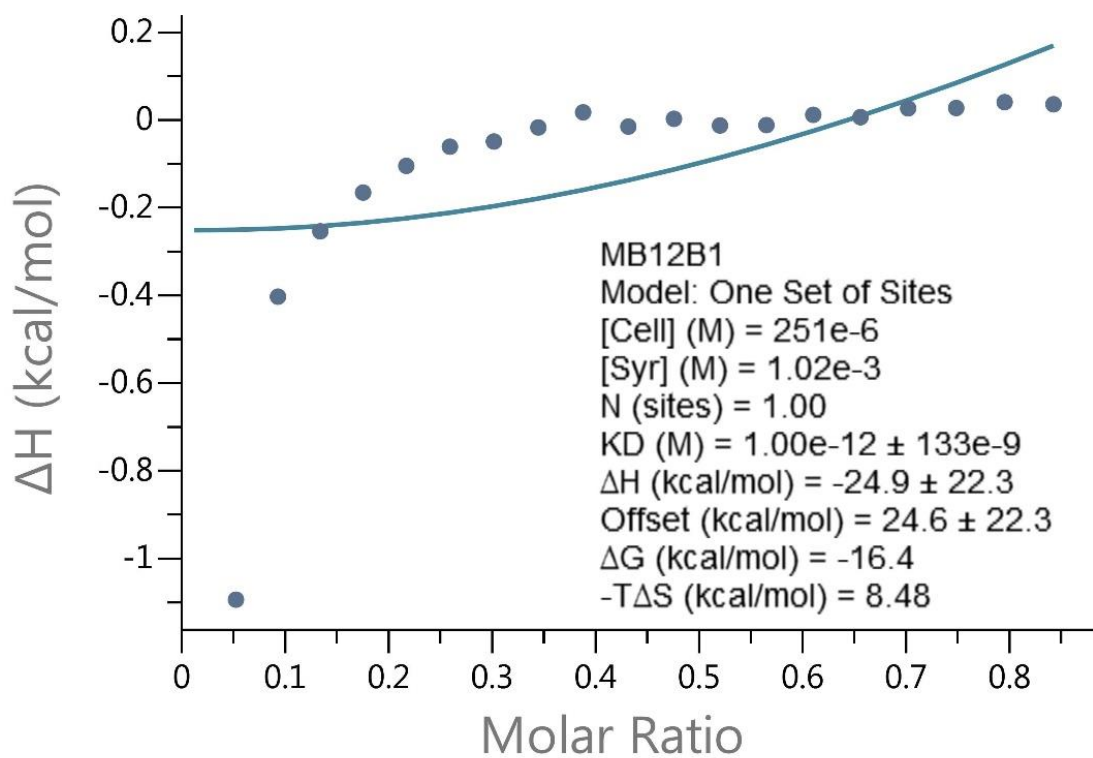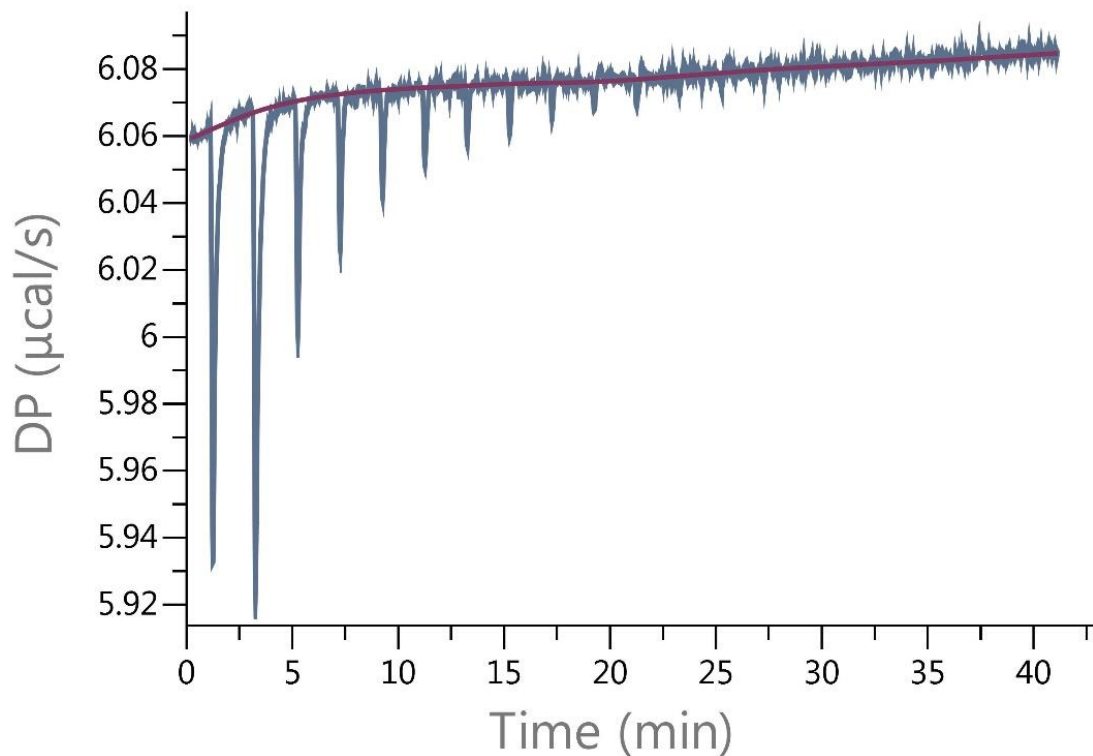
The values obtained from fixating n=1, has to be disregarded as the fit is not in line with the data points (systematic deviations).

Reduced $\chi^2$ = 5.8x10$^{-2}$ Kcal/mol$^2$

### 11.10.4 ITC measurement - MβCD

*At 5 mM*





MB12W75
Model: One Set of Sites
[Cell] (M) = 251e-6
[Syr] (M) = 4.94e-3
N (sites) = 1.2e-3 ± 0.210
KD (M) = 80.9e-6 ± 40.8e-6
ΔH (kcal/mol) = -80.0 ± 1.4e4
Offset (kcal/mol) = -3.7e-2 ± 2.3e-3
ΔG (kcal/mol) = -5.58
-TΔS (kcal/mol) = 74.4
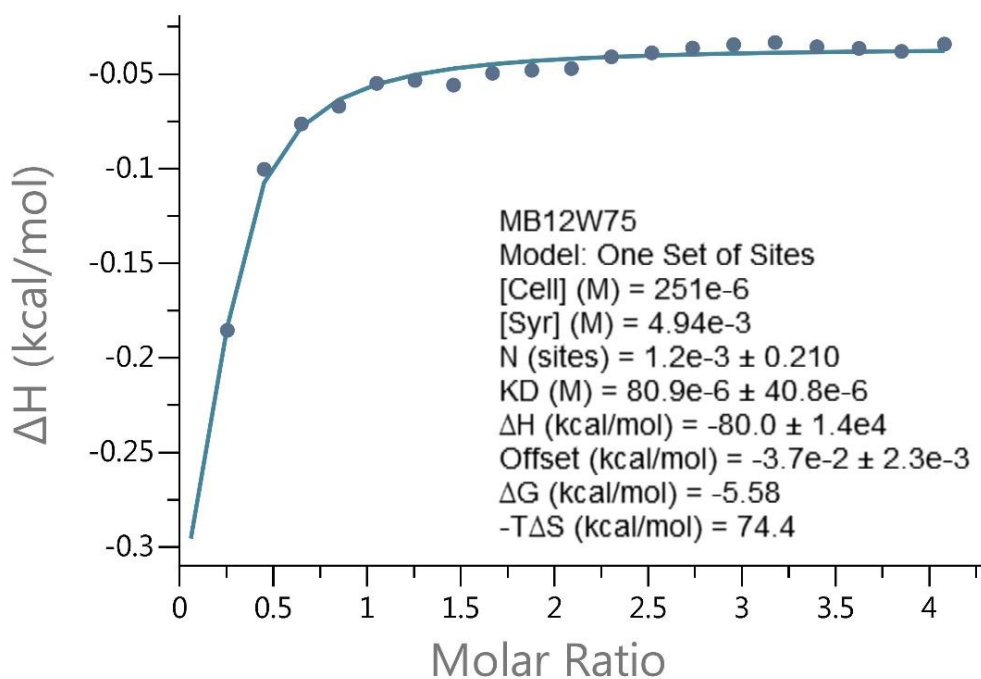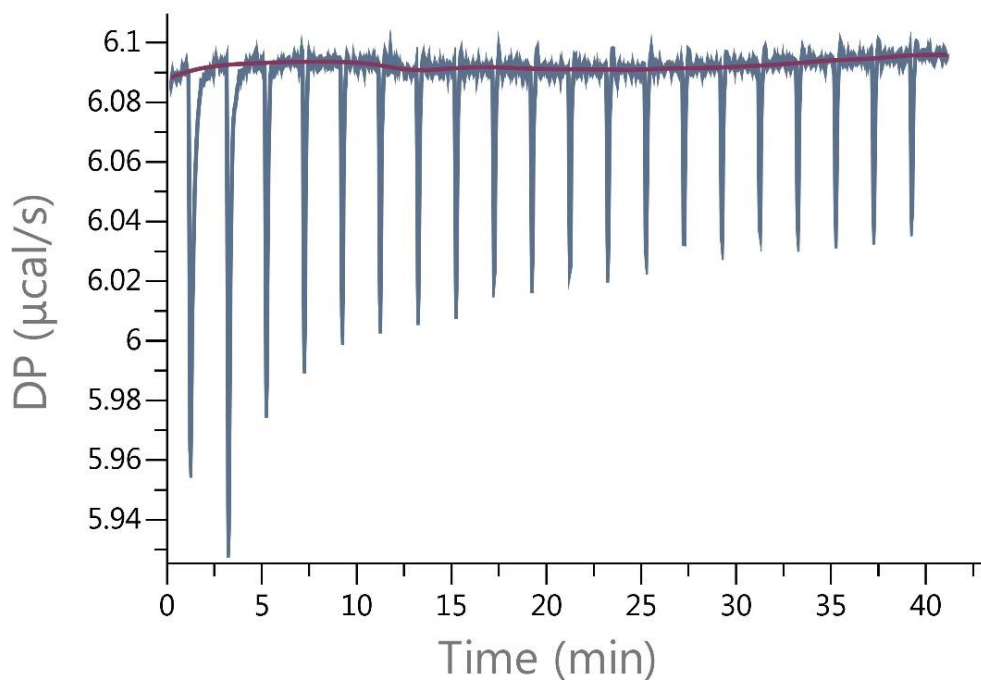
Binding observed. However, the initial peak is about the same height as first measurement. The solution was saturated to fast and the values are therefore unreliable.

Values reported:
$K_D$=80.9x$10^{-6}$ ± 40.8x$10^{-6}$ M
$K_A$=12361 M$^{-1}$
Reduced $\chi^2$= 2.1x$10^{-5}$ Kcal/mol$^2$
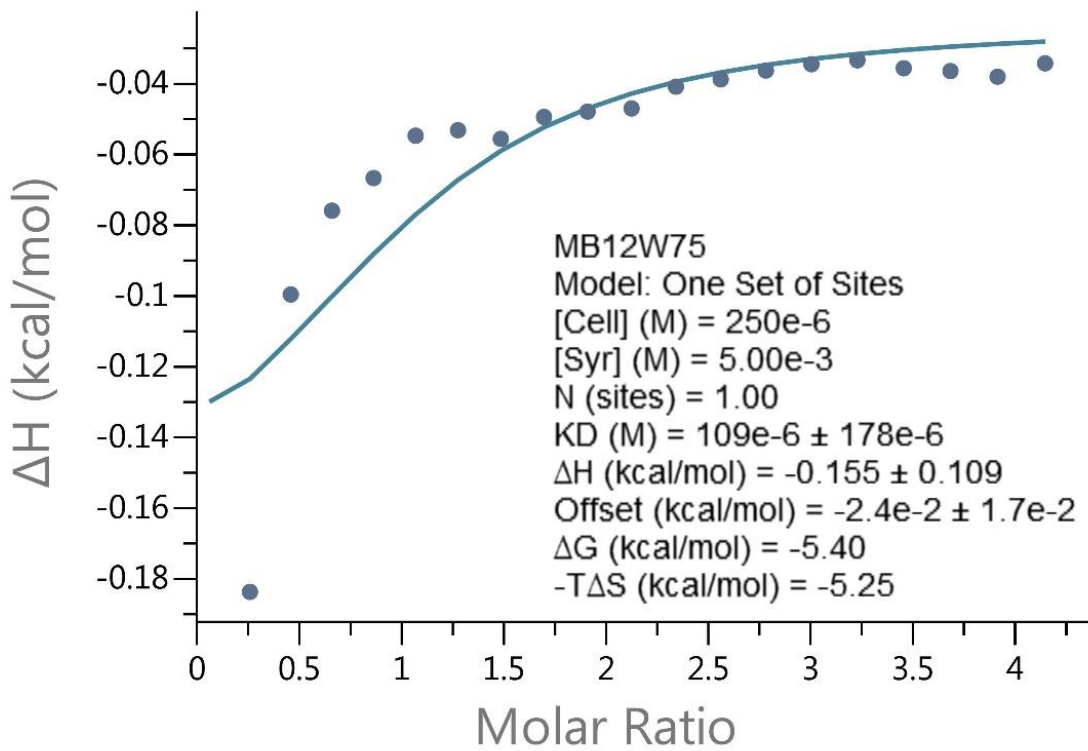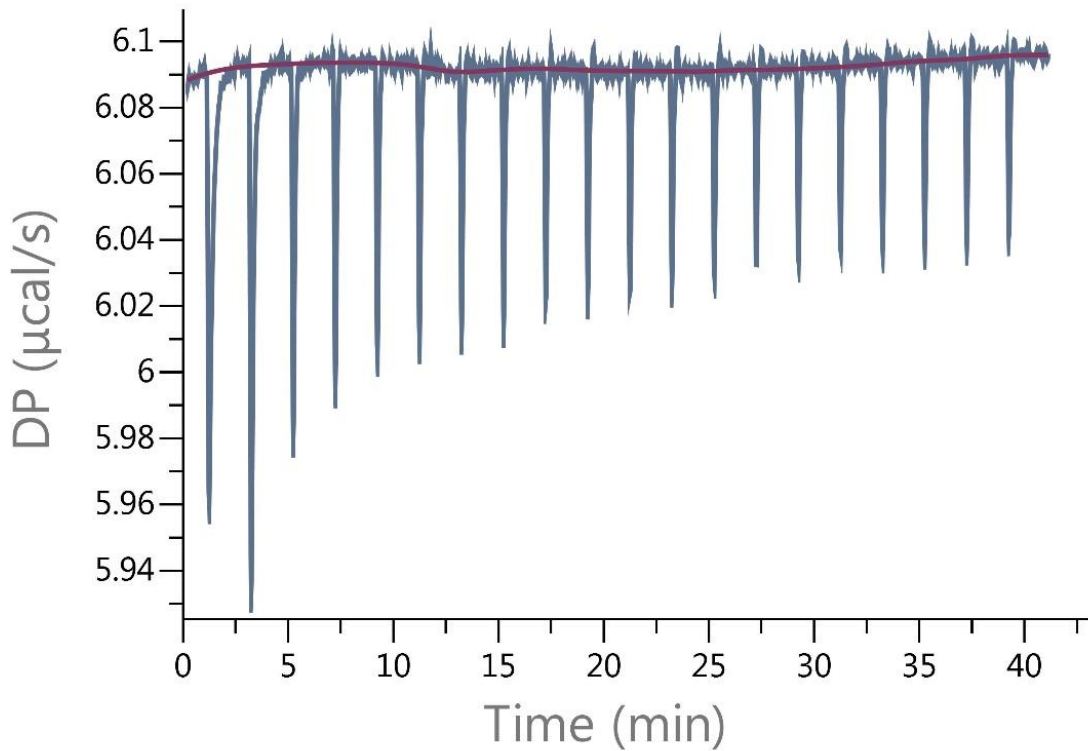
MB12W75
Model: One Set of Sites
[Cell] (M) = 250e-6
[Syr] (M) = 5.00e-3
N (sites) = 1.00
KD (M) = 109e-6 ± 178e-6
$\Delta H$ (kcal/mol) = -0.155 ± 0.109
Offset (kcal/mol) = -2.4e-2 ± 1.7e-2
$\Delta G$ (kcal/mol) = -5.40
-T$\Delta S$ (kcal/mol) = -5.25

The values obtained from fixating n=1, has to be disregarded as the fit is not in line with the data points (systematic deviations).

Reduced $\chi^2$= $3.6 \times 10^{-4}$ Kcal/mol$^2$

*At 2 mM*
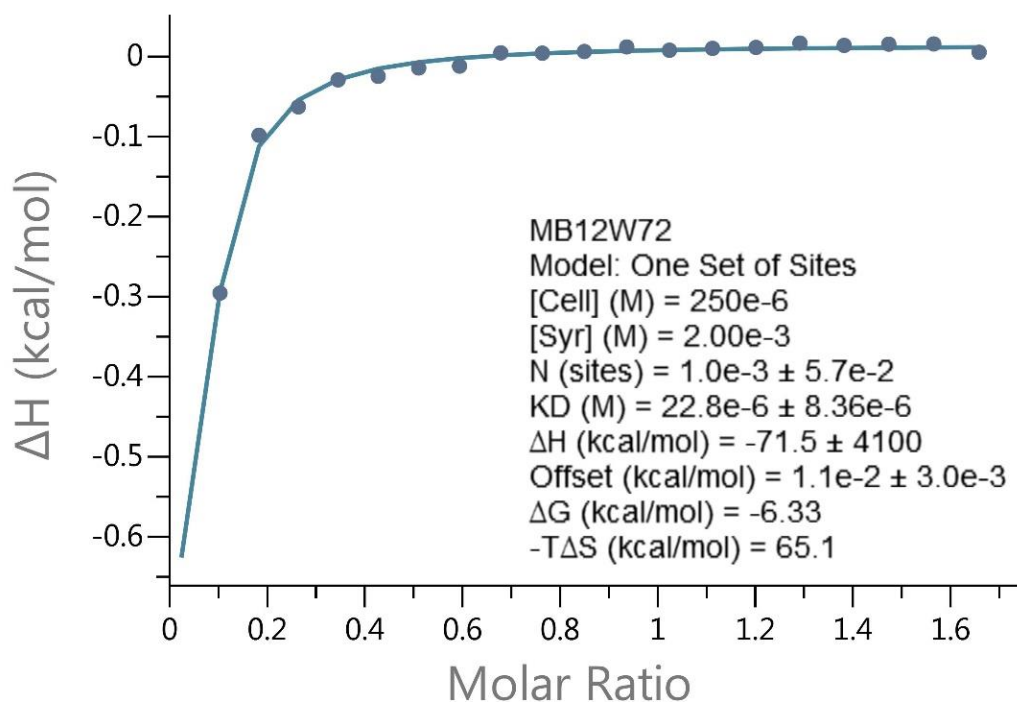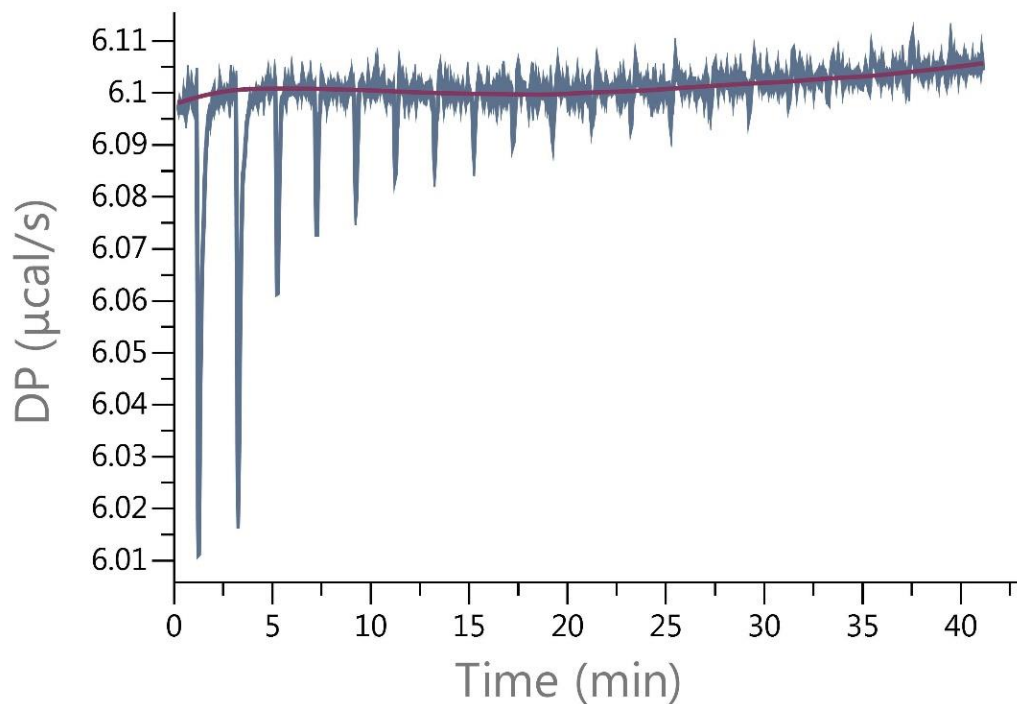




MB12W72
Model: One Set of Sites
[Cell] (M) = 250e-6
[Syr] (M) = 2.00e-3
N (sites) = 1.0e-3 ± 5.7e-2
KD (M) = 22.8e-6 ± 8.36e-6
ΔH (kcal/mol) = -71.5 ± 4100
Offset (kcal/mol) = 1.1e-2 ± 3.0e-3
ΔG (kcal/mol) = -6.33
-TΔS (kcal/mol) = 65.1

Binding observed. However, the initial peak is higher than first measurement. The solution was saturated to fast and the values are therefore unreliable.

Values reported:
$K_D = 22.8 \times 10^{-6} \pm 8.36 \times 10^{-6}$ M
$K_A = 43860$ M$^{-1}$
Reduced $\chi^2 = 4.6 \times 10^{-5}$ Kcal/mol$^2$
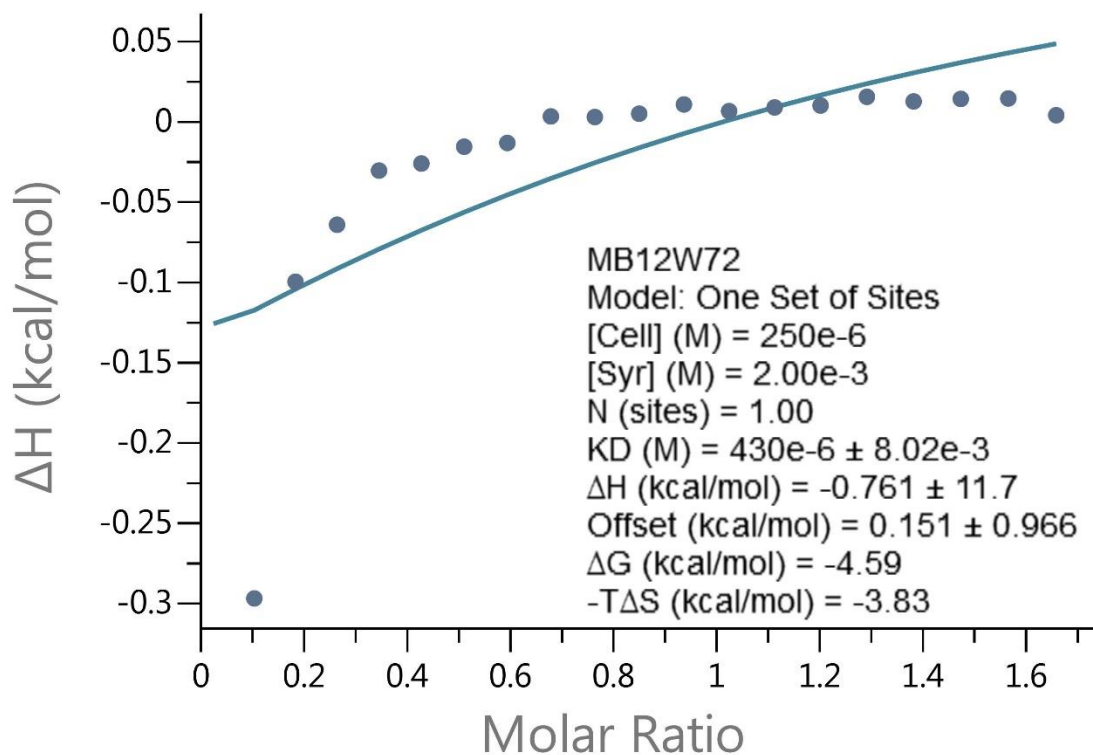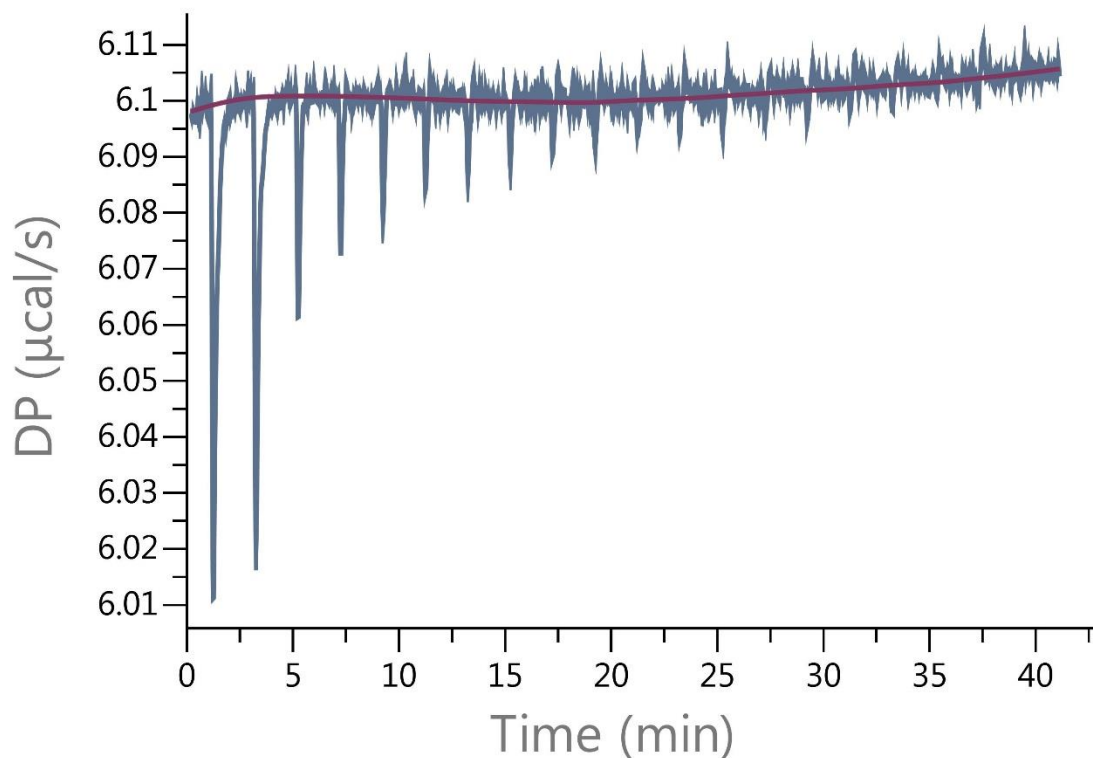
The values obtained from fixating n=1, has to be disregarded as the fit is not in line with the data points (systematic deviations).

Reduced $\chi^2$= 2.9x10$^{-3}$ Kcal/mol$^2$

MB12M1
Model: One Set of Sites
[Cell] (M) = 251e-6
[Syr] (M) = 1.00e-3
N (sites) = 1.0e-3 ± 4.8e-2
KD (M) = 8.08e-6 ± 4.91e-6
$\Delta H$ (kcal/mol) = –74.2 ± 3610
Offset (kcal/mol) = 4.6e-2 ± 1.0e-2
$\Delta G$ (kcal/mol) = –6.95
–T$\Delta S$ (kcal/mol) = 67.2
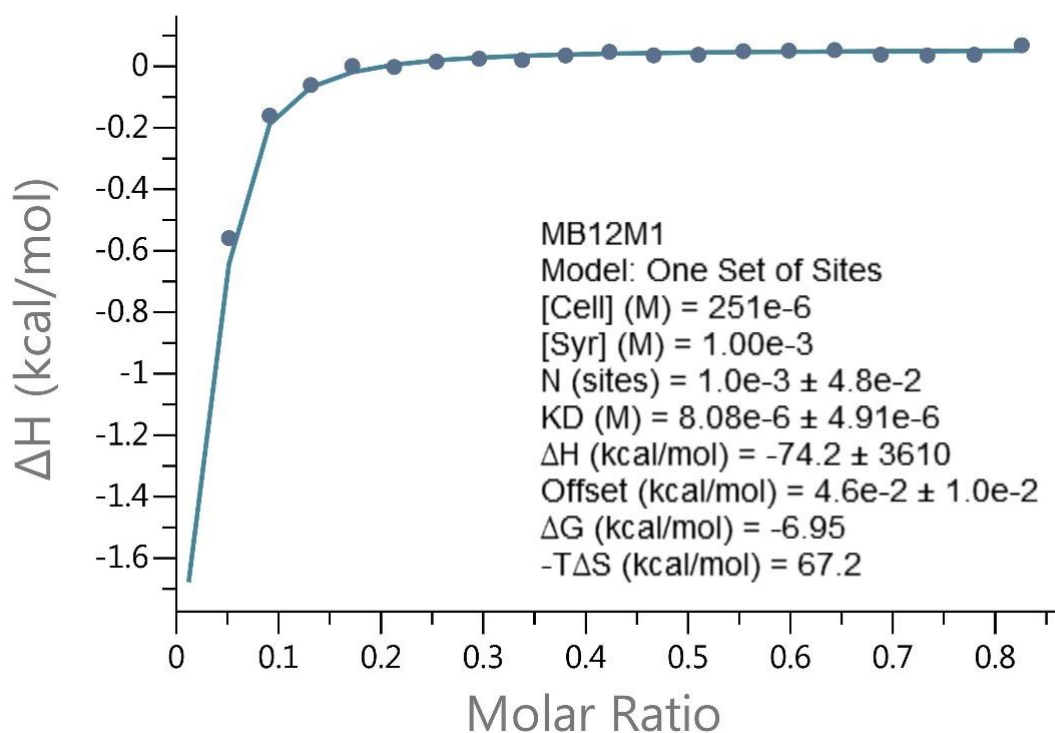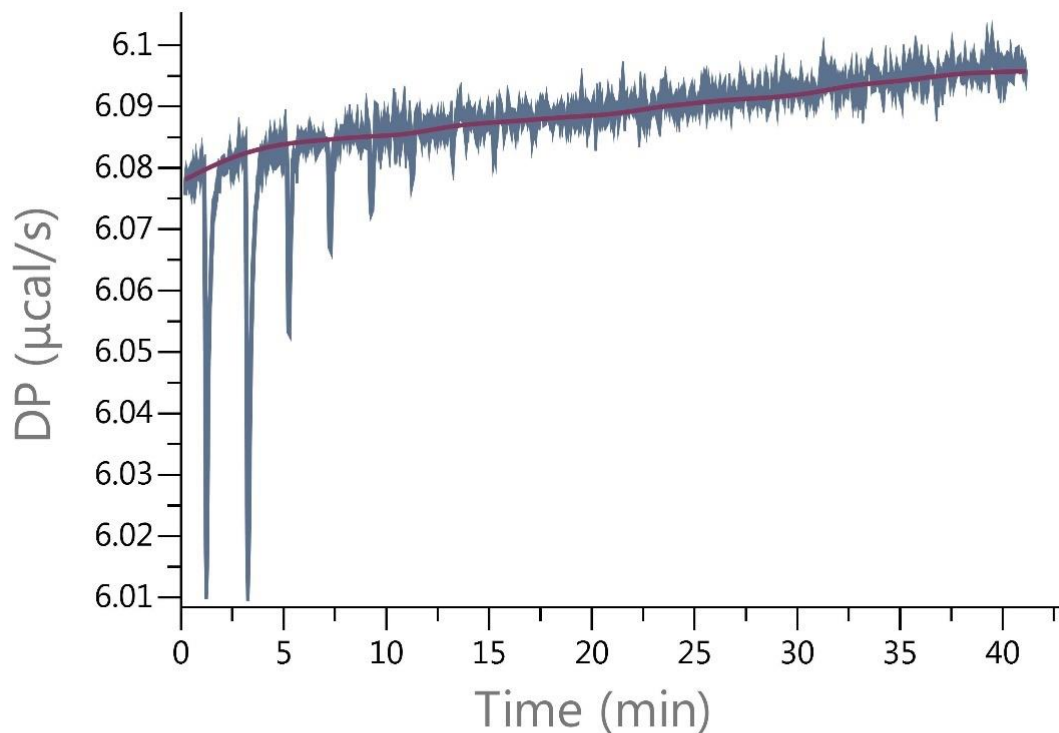
Values reported:
$K_D$= $8.08 \times 10^{-6}$ ±$4.91 \times 10^{-6}$ M
$K_A$=123762 M$^{-1}$
Reduced $\chi^2$=$6.4 \times 10^{-4}$ Kcal/mol$^2$
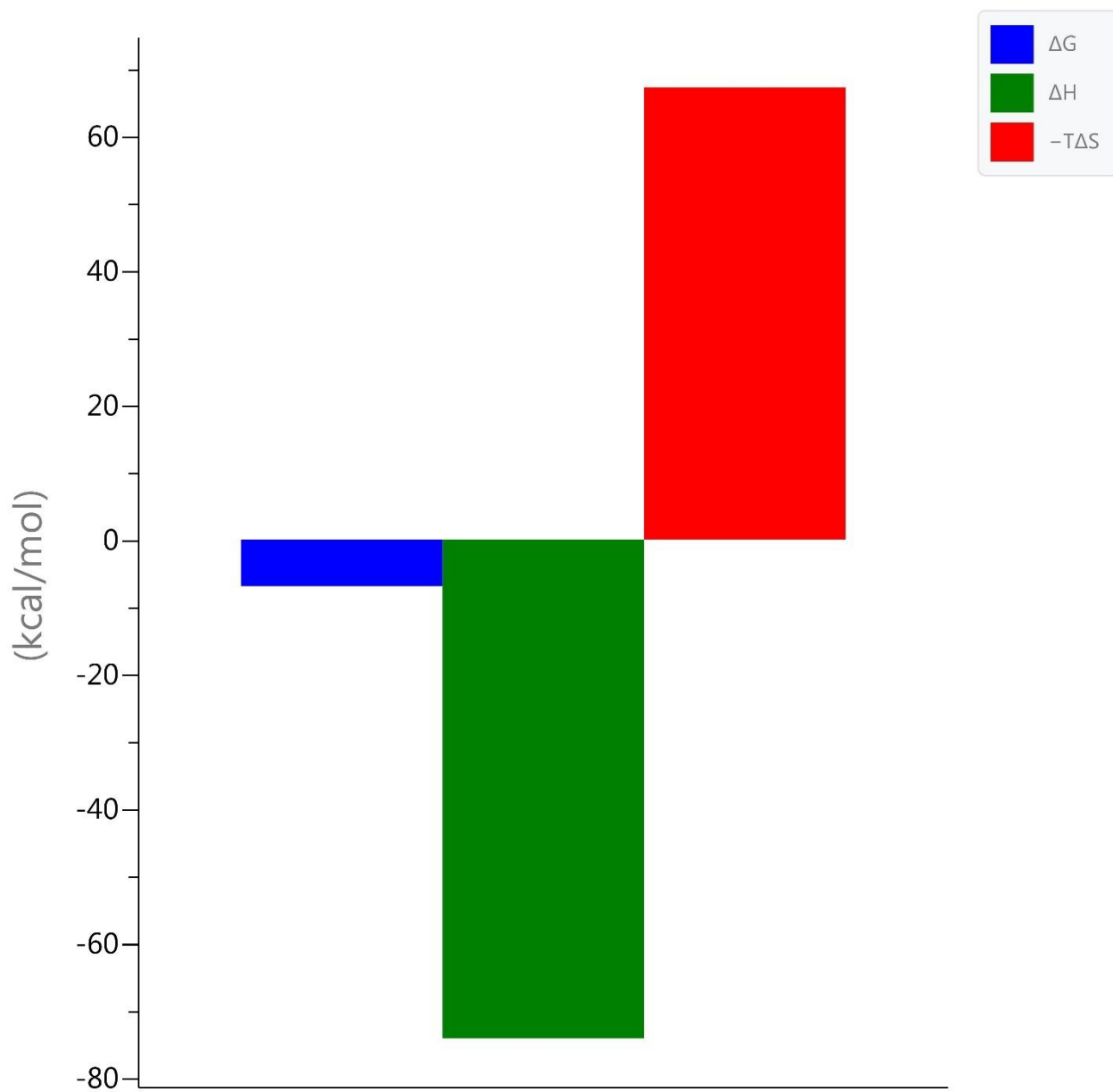
Reported Values:

$\Delta H = -74.2 \pm 3610$ Kcal/mol

$\Delta G = -6.95$ Kcal/mol

$-T\Delta S = 67.2$ Kcal/mol
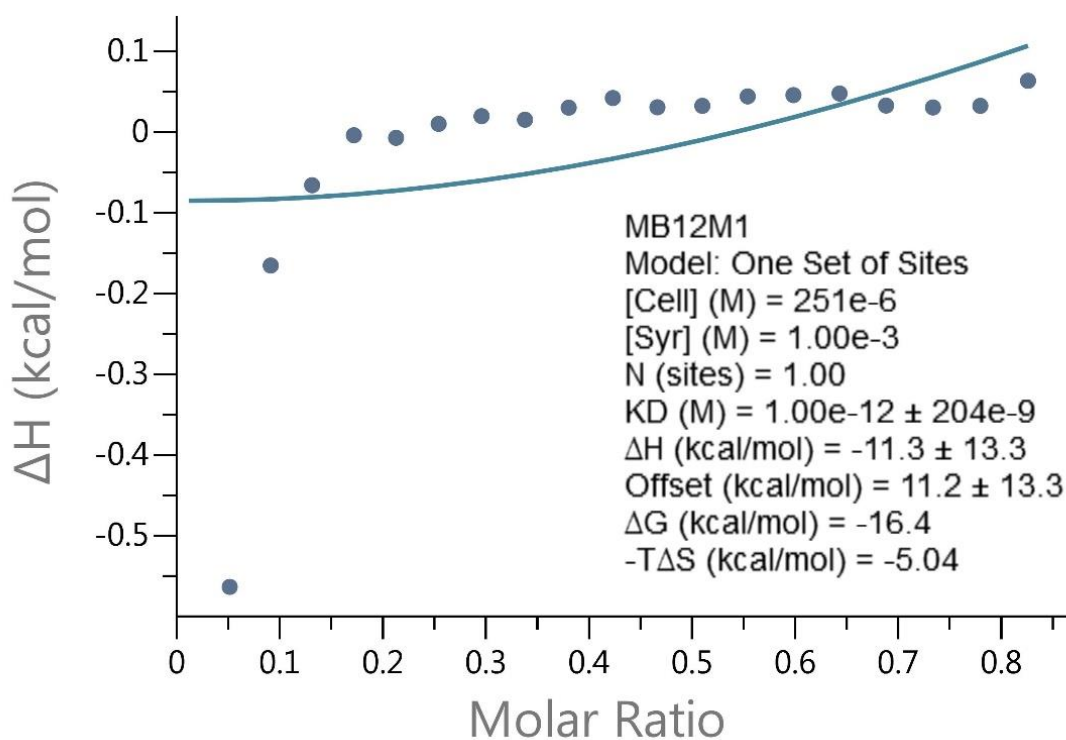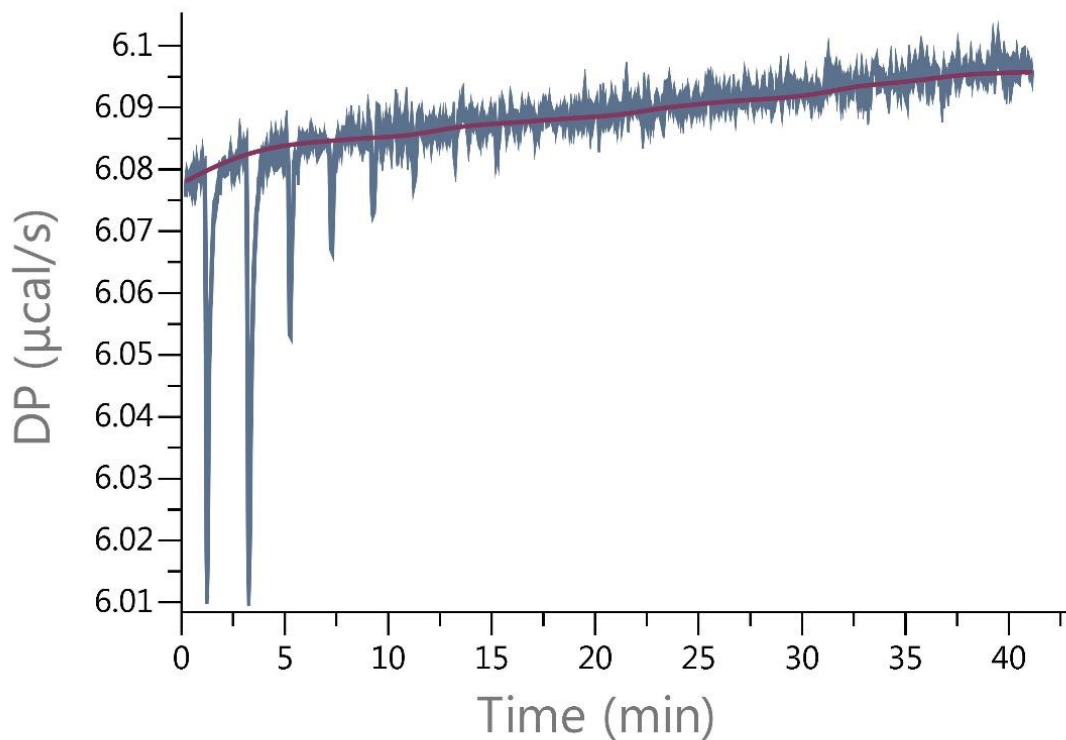
MB12M1
Model: One Set of Sites
[Cell] (M) = 251e-6
[Syr] (M) = 1.00e-3
N (sites) = 1.00
KD (M) = 1.00e-12 ± 204e-9
ΔH (kcal/mol) = -11.3 ± 13.3
Offset (kcal/mol) = 11.2 ± 13.3
ΔG (kcal/mol) = -16.4
-TΔS (kcal/mol) = -5.04

The values obtained from fixating n=1, has to be disregarded as the fit is not in line with the data points (systematic deviations).

Reduced $\chi^2$= 1.8x10$^{-2}$ Kcal/mol$^2$

## 11.10.5 ITC measurement – HPβCD

*At 5 mM*





MB12HP5
Model: One Set of Sites
[Cell] (M) = 250e-6
[Syr] (M) = 5.00e-3
N (sites) = 2.22 ± 0.577
KD (M) = 228e-6 ± 279e-6
ΔH (kcal/mol) = –0.253 ± 0.144
Offset (kcal/mol) = 9.4e-3 ± 4.2e-2
ΔG (kcal/mol) = –4.97
–TΔS (kcal/mol) = –4.71
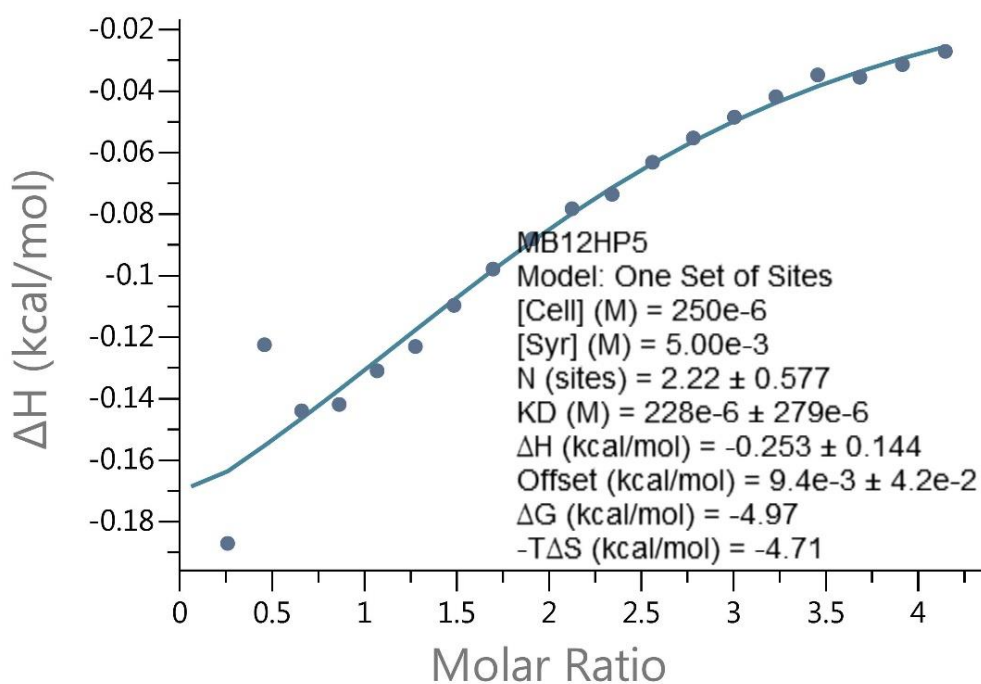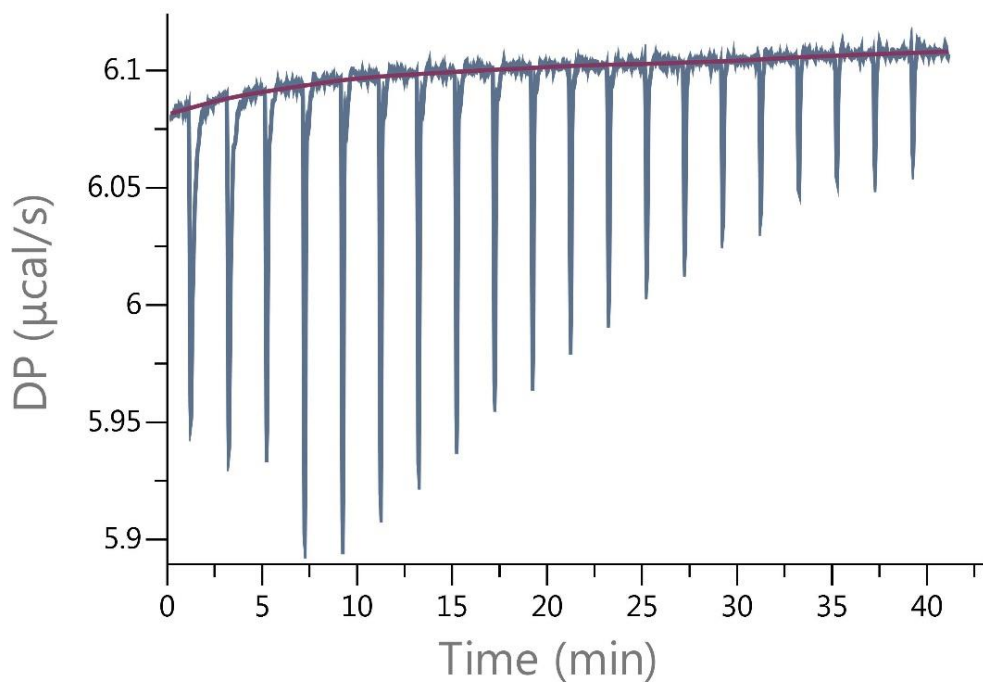
Binding observed. However, the initial measurements are not good. The values are therefore unreliable.

Values reported:
$K_D$= 228x10$^{-6}$ ±279x10$^{-6}$ M
$K_A$=4386 M$^{-1}$
Reduced $\chi^2$=1.2x10$^{-4}$ Kcal/mol$^2$
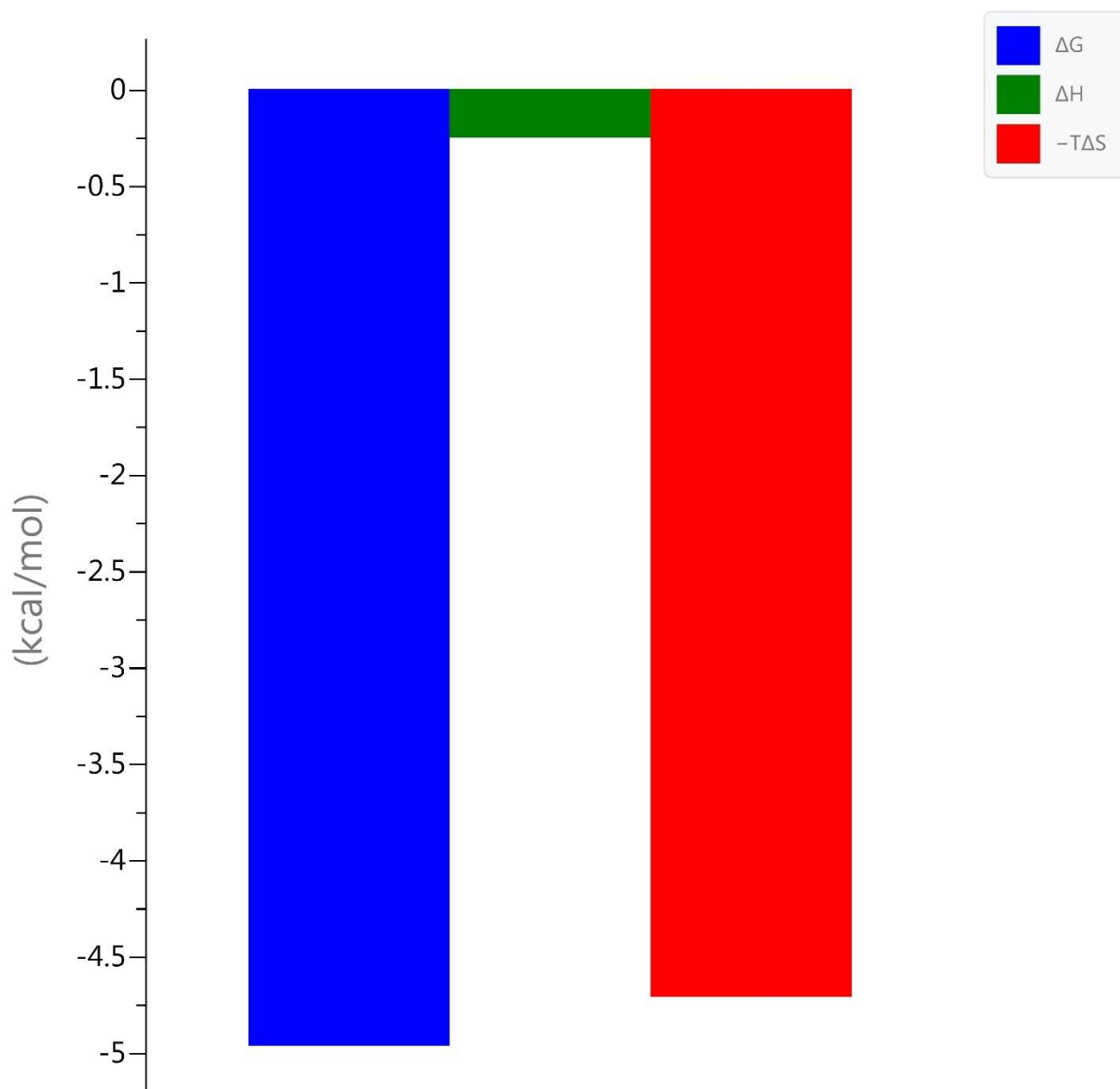
Values reported:

ΔH= -0.253±0.144 Kcal/mol

ΔG= -4.97 Kcal/mol

-TΔS= -4.71 Kcal/mol

*At 5 mM with n=1*



MB12HP5
Model: One Set of Sites
[Cell] (M) = 250e-6
[Syr] (M) = 5.00e-3
N (sites) = 1.00
KD (M) = 3.38e-3 ± 3.24e-3
ΔH (kcal/mol) = -4.18 ± 4.76
Offset (kcal/mol) = 0.110 ± 7.8e-2
ΔG (kcal/mol) = -3.37
-TΔS (kcal/mol) = 0.813
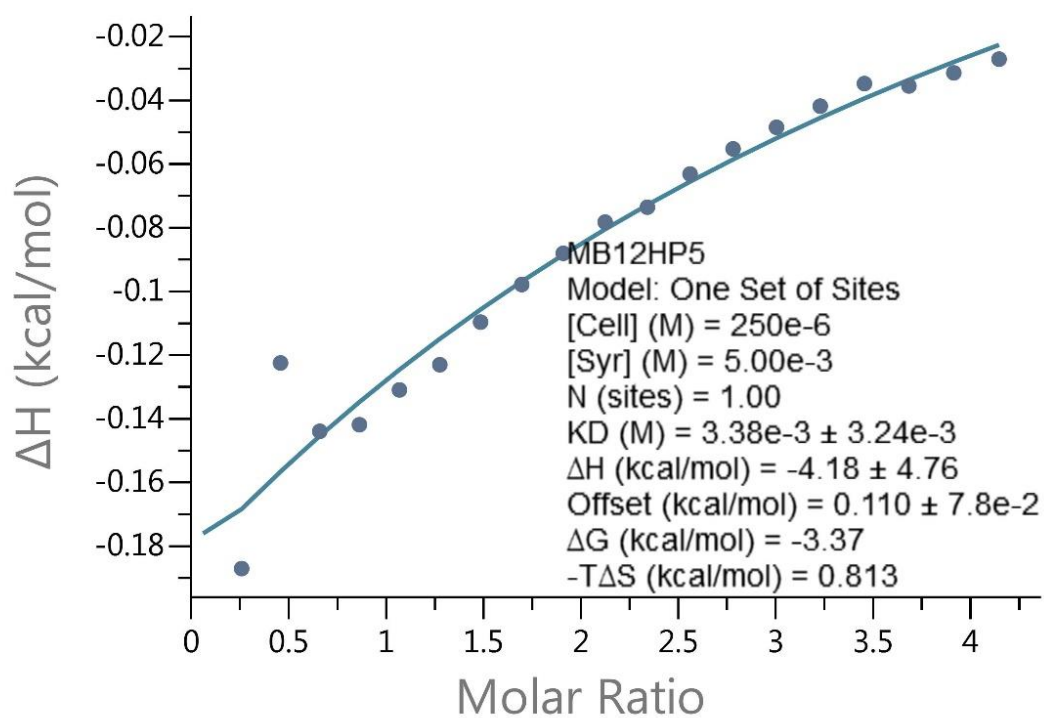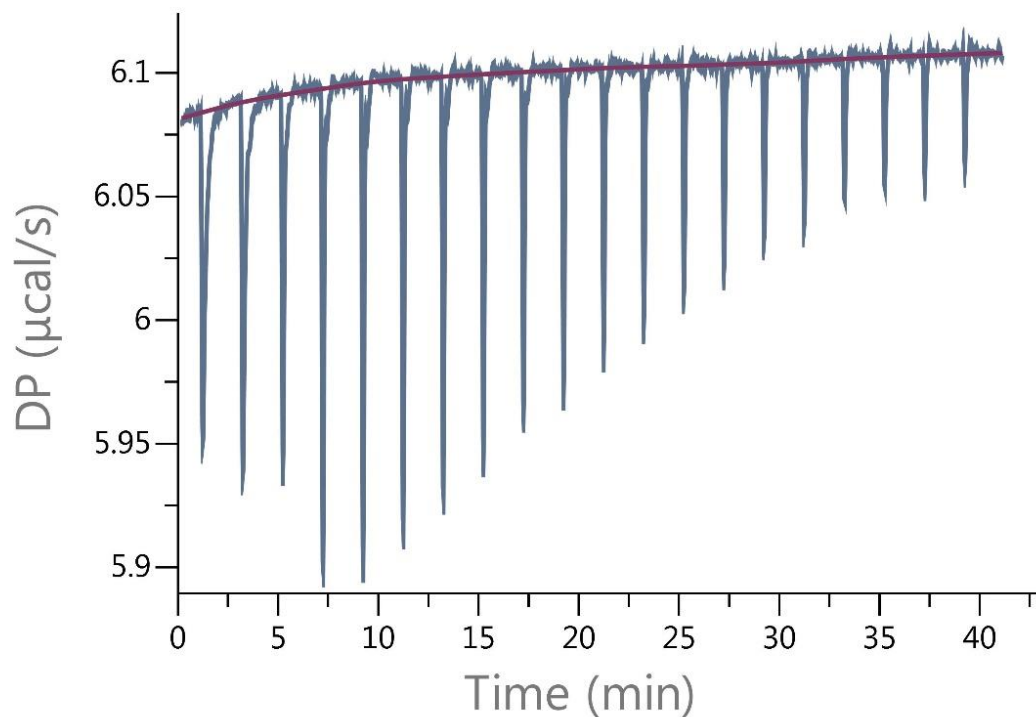
Values reported:

$K_D= 3.38 \times 10^{-3} \pm 3.24 \times 10^{-3}$ M

$K_A= 296\,M^{-1}$

Reduced $\chi^2= 1.1 \times 10^{-4}$ Kcal/mol$^2$
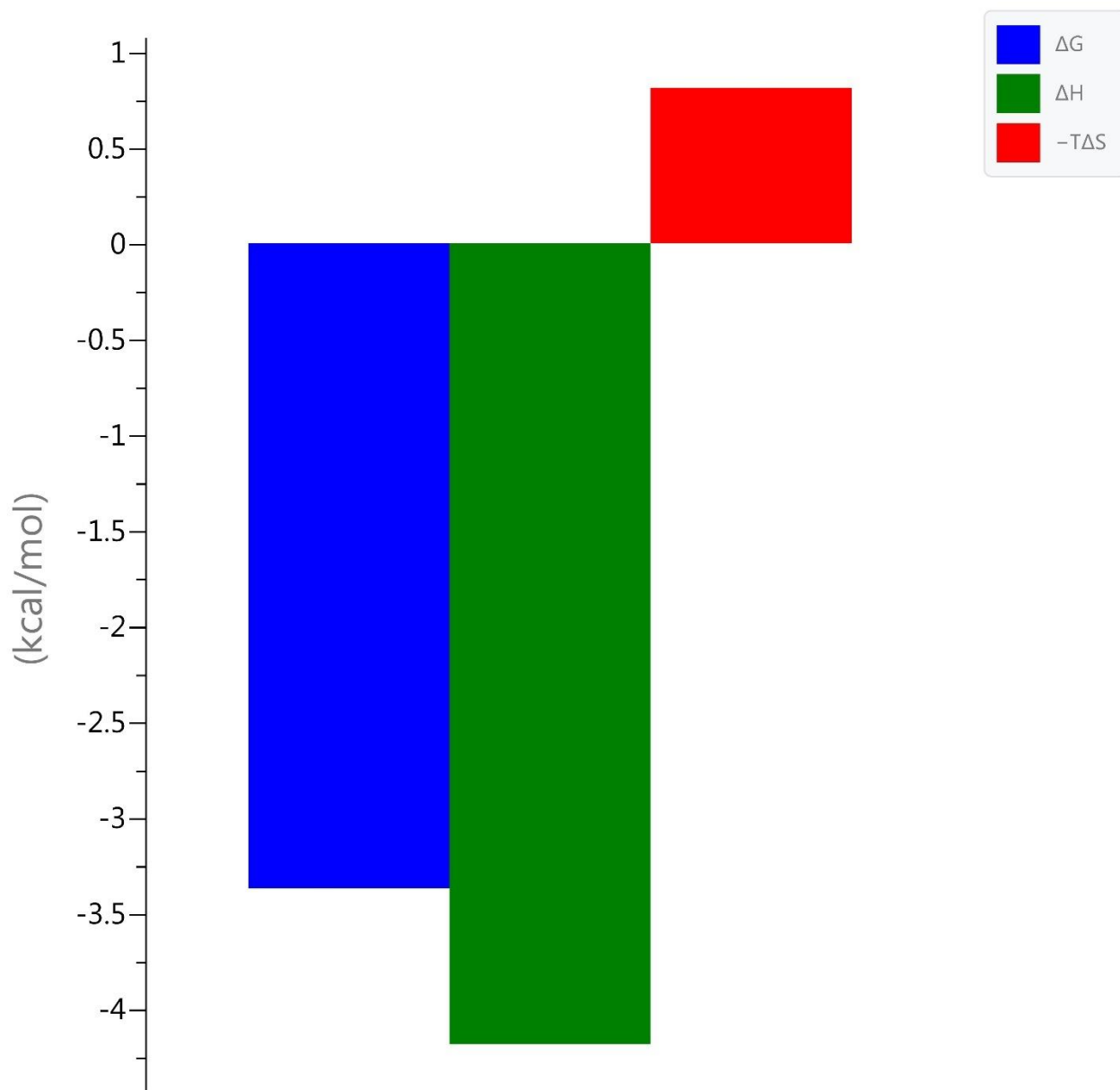
Values reported:
ΔH= -4.18± 4.76 Kcal/mol
ΔG= -3.37 Kcal/mol
-TΔS= 0.813 Kcal/mol

MB12HP2
Model: One Set of Sites
[Cell] (M) = 250e-6
[Syr] (M) = 2.00e-3
N (sites) = $1.1e-3 \pm 6.0e-2$
KD (M) = $25.1e-6 \pm 9.54e-6$
$\Delta H$ (kcal/mol) = $-80.0 \pm 4430$
Offset (kcal/mol) = $1.4e-2 \pm 3.8e-3$
$\Delta G$ (kcal/mol) = $-6.28$
$-T\Delta S$ (kcal/mol) = $73.7$
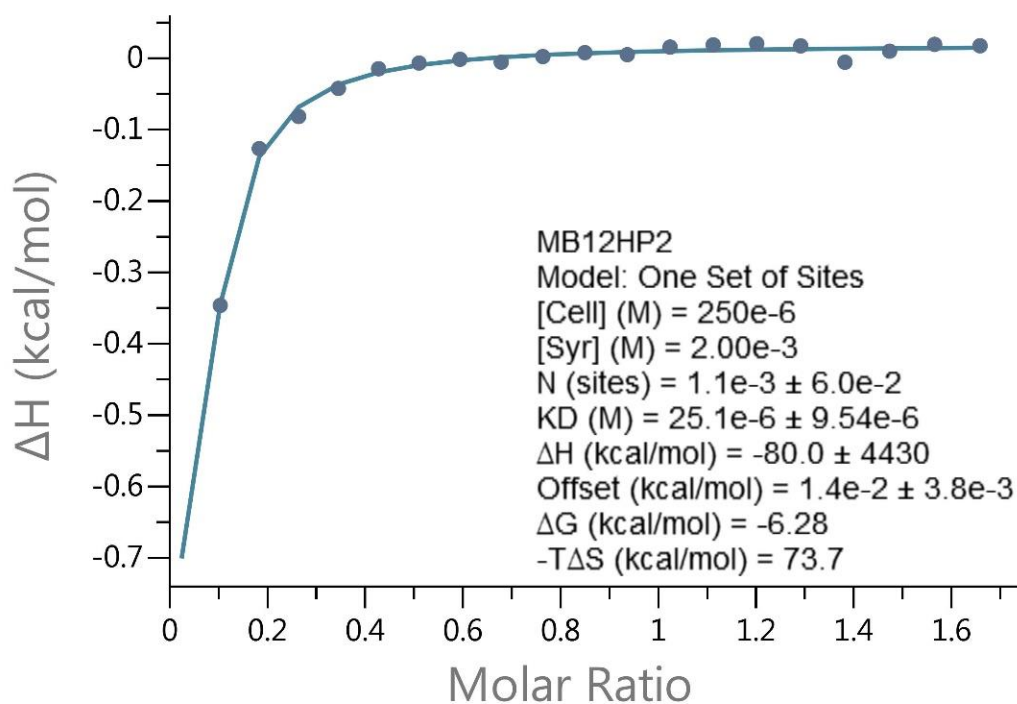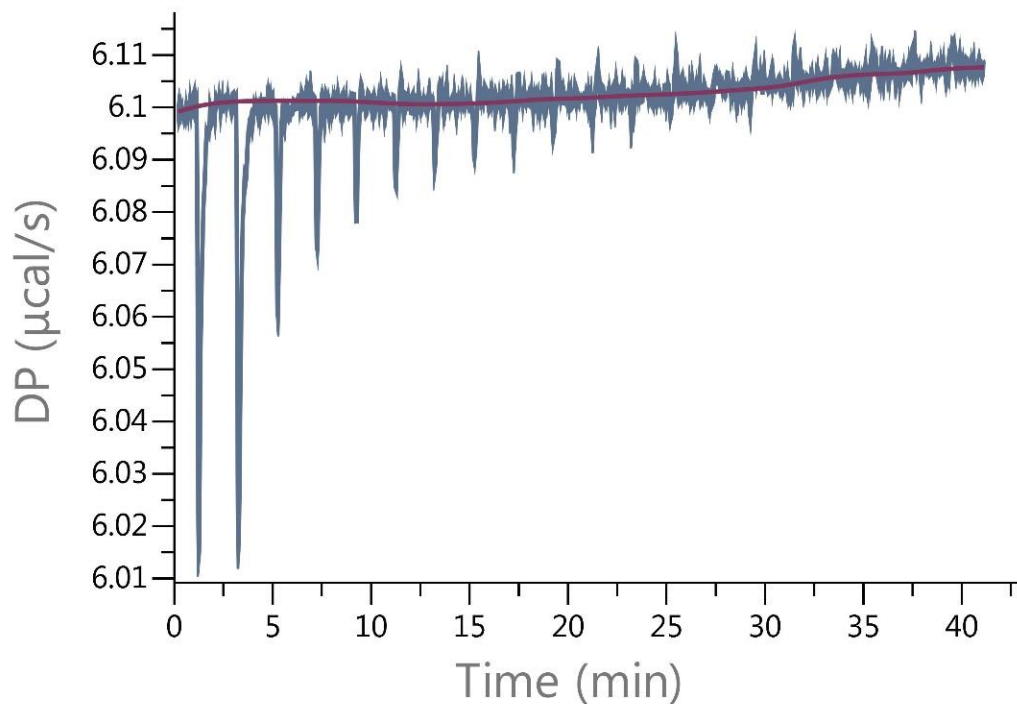
Binding observed. However, the initial peak is higher than first measurement. The solution was saturated to fast and the values are therefore unreliable.

Values reported:
$K_D$= $25.1 \times 10^{-6} \pm 9.54 \times 10^{-6}$ M
$K_A$=39841 M$^{-1}$
Reduced $\chi^2$=$6.9 \times 10^{-5}$ Kcal/mol$^2$

Reported values:

ΔH= -80 ± 4430 Kcal/mol

ΔG= -6.28 Kcal/mol

-TΔS= 73.7 Kcal/mol

MB12HP2
Model: One Set of Sites
[Cell] (M) = 250e-6
[Syr] (M) = 2.00e-3
N (sites) = 1.00
KD (M) = 433e-6 ± 8.09e-3
ΔH (kcal/mol) = -0.902 ± 13.9
Offset (kcal/mol) = 0.178 ± 1.15
ΔG (kcal/mol) = -4.59
-TΔS (kcal/mol) = -3.69
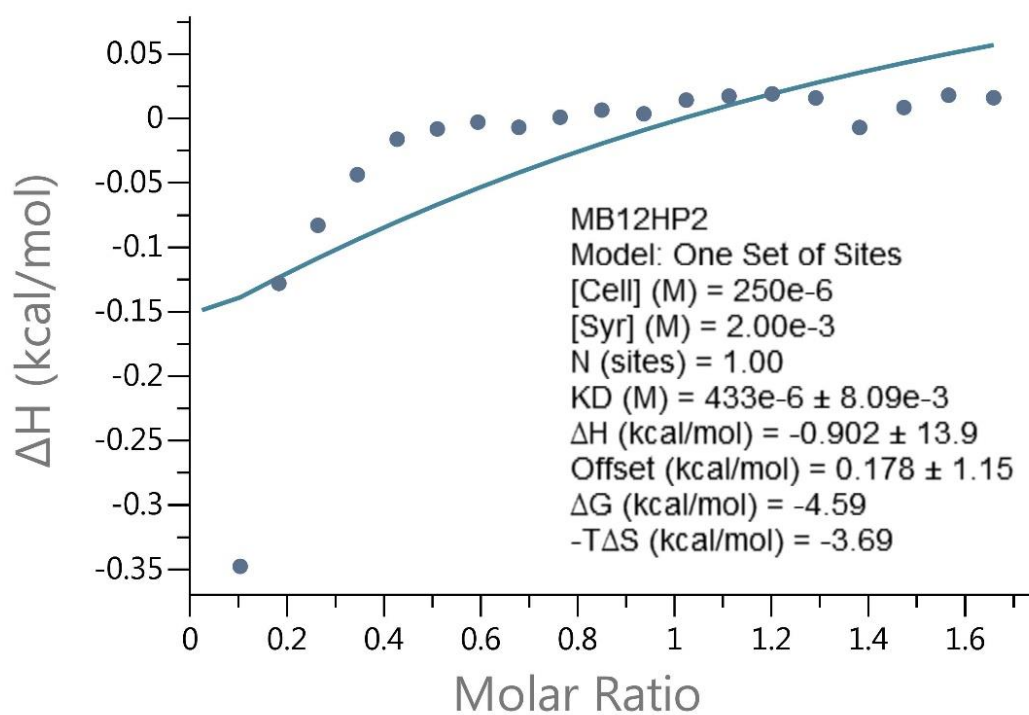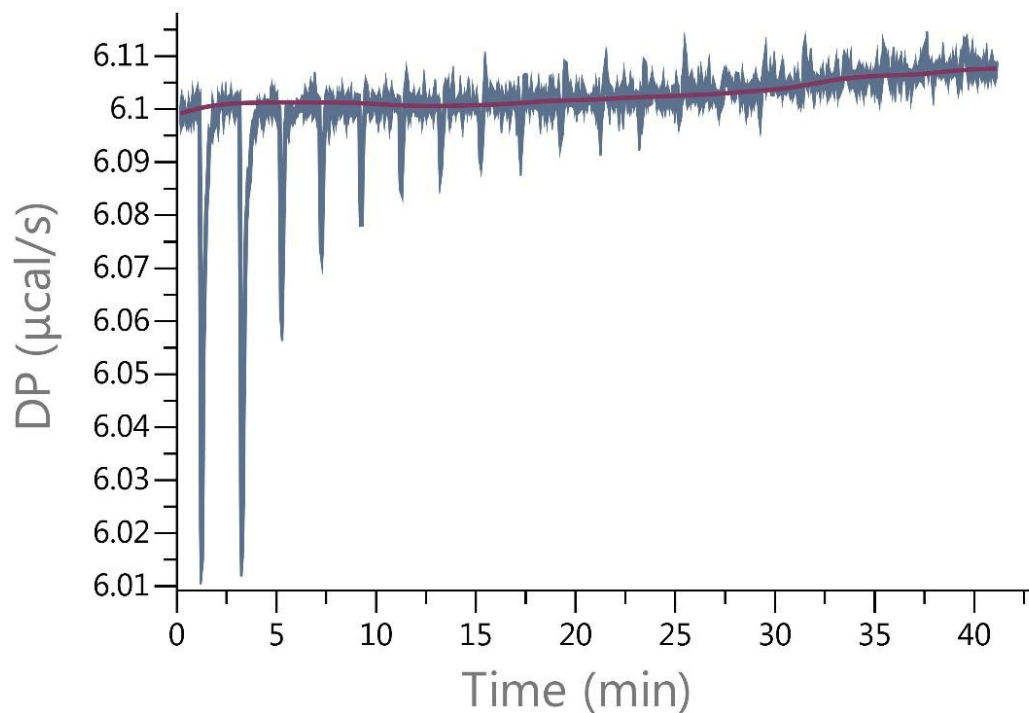
The values obtained from fixating n=1, has to be disregarded as the fit is not in line with the data points (systematic deviations).

Reduced $\chi^2$= 4.1x10$^{-3}$ Kcal/mol$^2$

**11.10.6 ITC measurement - SBEβCD**
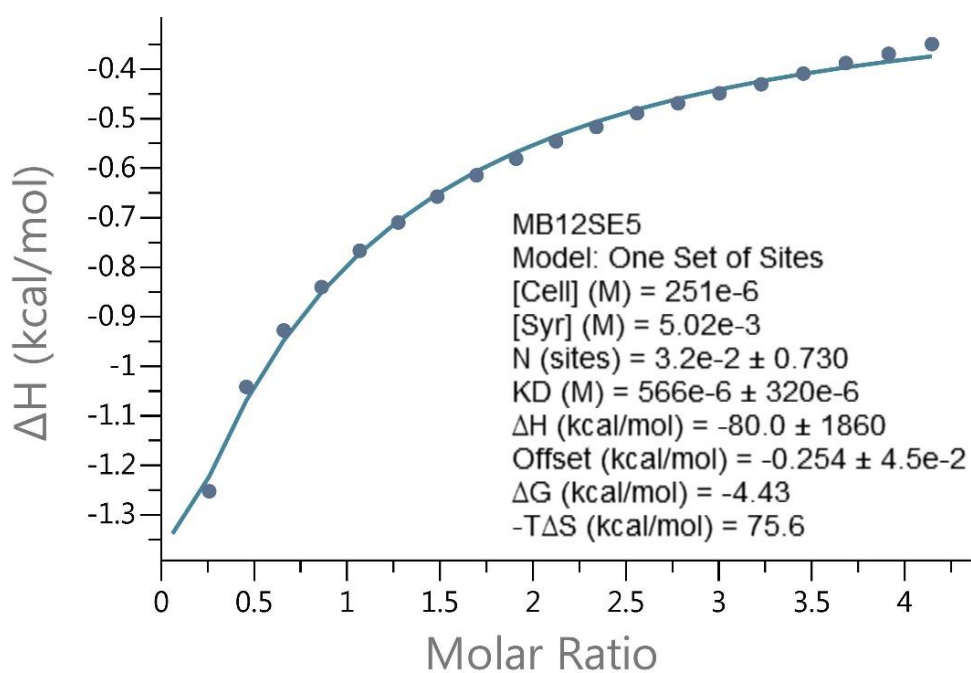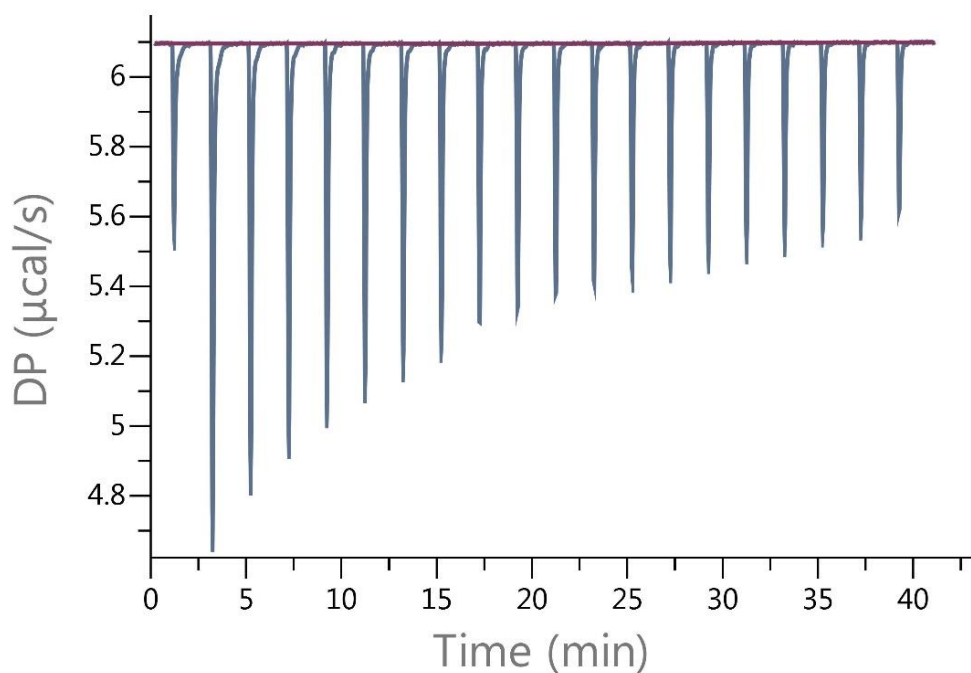
*At 5 mM*



Values reported:

$K_D$= 566x10$^{-6}$ ±320x10$^{-6}$ M

$K_A$= 1767 M$^{-1}$

ΔH= -80 ± 1860 Kcal/mol

ΔG= -4.43 Kcal/mol

-TΔS= 75.6 Kcal/mol

Reduced $\chi^2$= 1.2x10$^{-4}$ Kcal/mol$^2$

MB12SE5
Model: One Set of Sites
[Cell] (M) = 250e-6
[Syr] (M) = 5.00e-3
N (sites) = 1.00
KD (M) = 232e-6 ± 75.8e-6
$\Delta H$ (kcal/mol) = -1.85 ± 0.365
Offset (kcal/mol) = -0.289 ± 4.1e-2
$\Delta G$ (kcal/mol) = -4.96
$-T\Delta S$ (kcal/mol) = -3.11
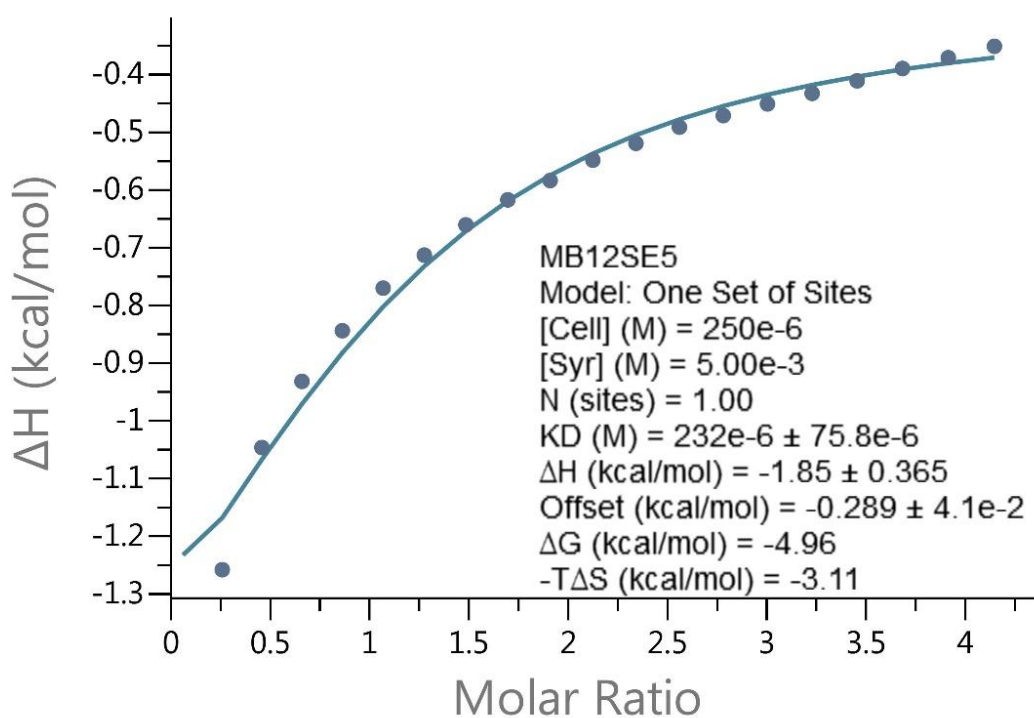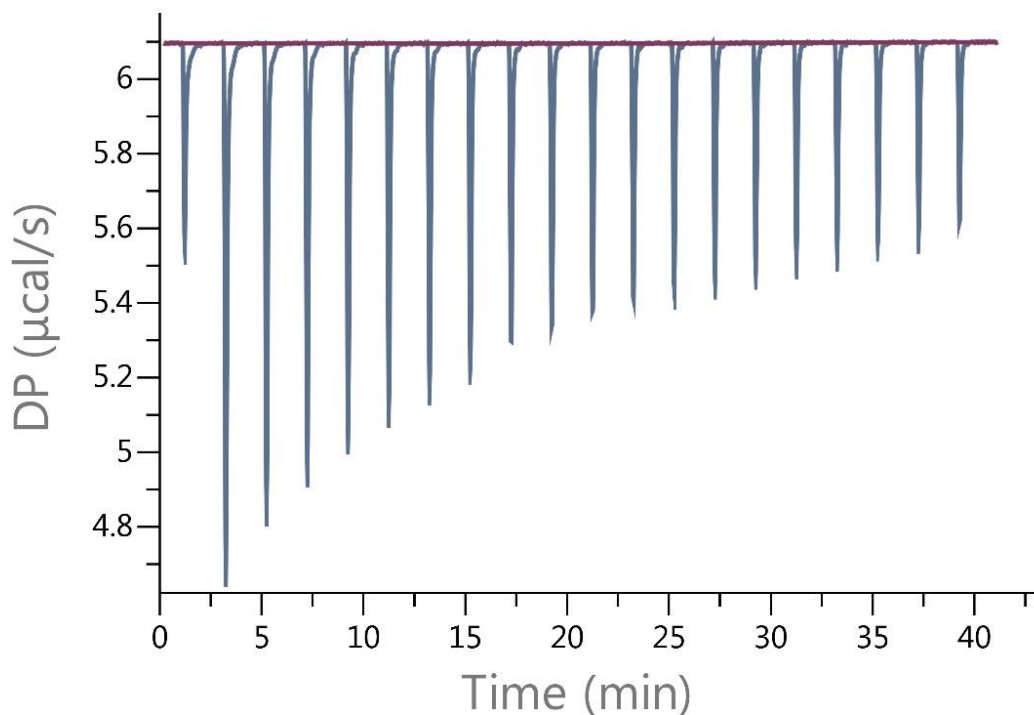
$K_D= 232 \times 10^{-6} \pm 75.8 \times 10^{-6}$ M

$K_A= 4310 \, M^{-1}$

$\Delta H= -1.85 \pm 0.365$ Kcal/mol

$\Delta G= -4.96$ Kcal/mol

$-T\Delta S= -3.11$ Kcal/mol

Reduced $\chi^2= 9.3 \times 10^{-4}$ Kcal/mol$^2$
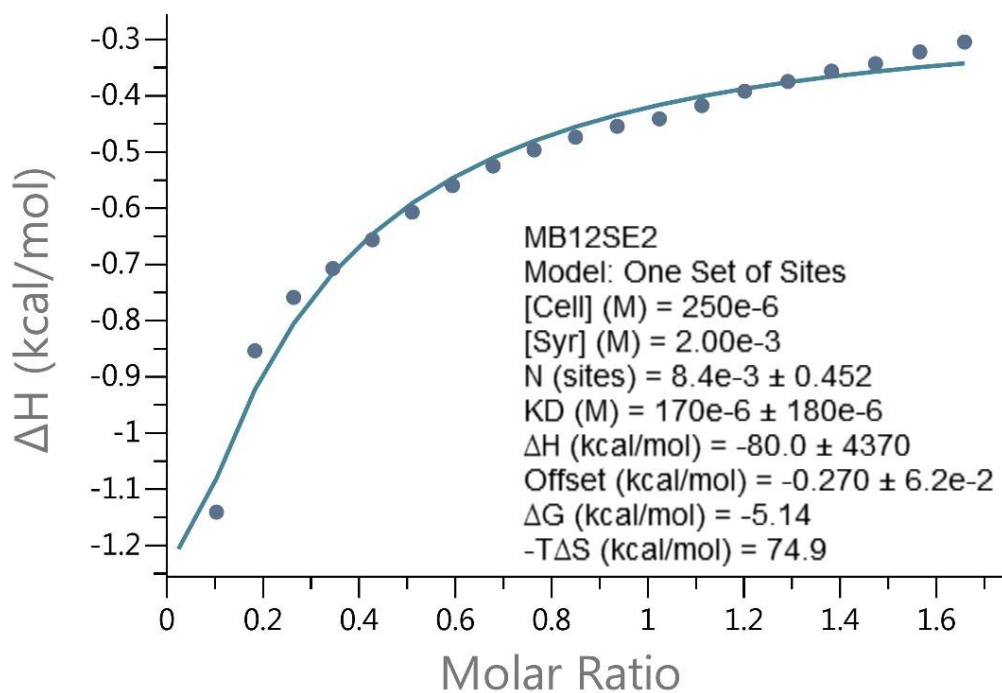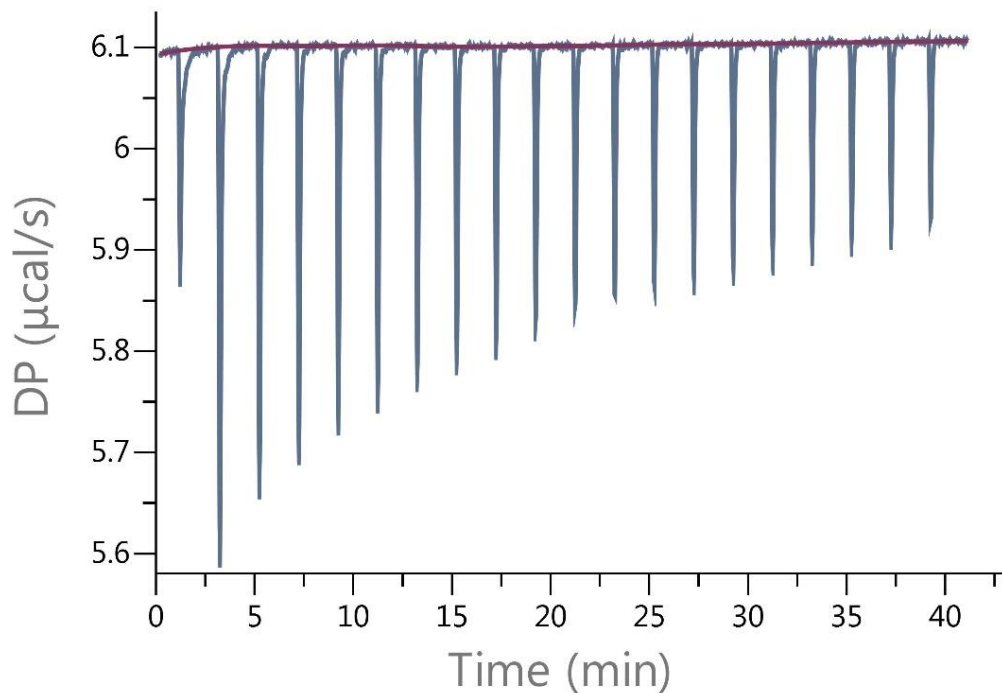
MB12SE2
Model: One Set of Sites
[Cell] (M) = 250e-6
[Syr] (M) = 2.00e-3
N (sites) = 8.4e-3 ± 0.452
KD (M) = 170e-6 ± 180e-6
ΔH (kcal/mol) = -80.0 ± 4370
Offset (kcal/mol) = -0.270 ± 6.2e-2
ΔG (kcal/mol) = -5.14
-TΔS (kcal/mol) = 74.9

Values reported:

$K_D$= 170x10$^{-6}$ ±180x10$^{-6}$ M

$K_A$=5882 M$^{-1}$

ΔH= -80 ± 4370 Kcal/mol

ΔG= -5.14 Kcal/mol

-TΔS= 74.9 Kcal/mol

Reduced $\chi^2$=1.1x10$^{-3}$ Kcal/mol$^2$

*At 2 mM with n=1*
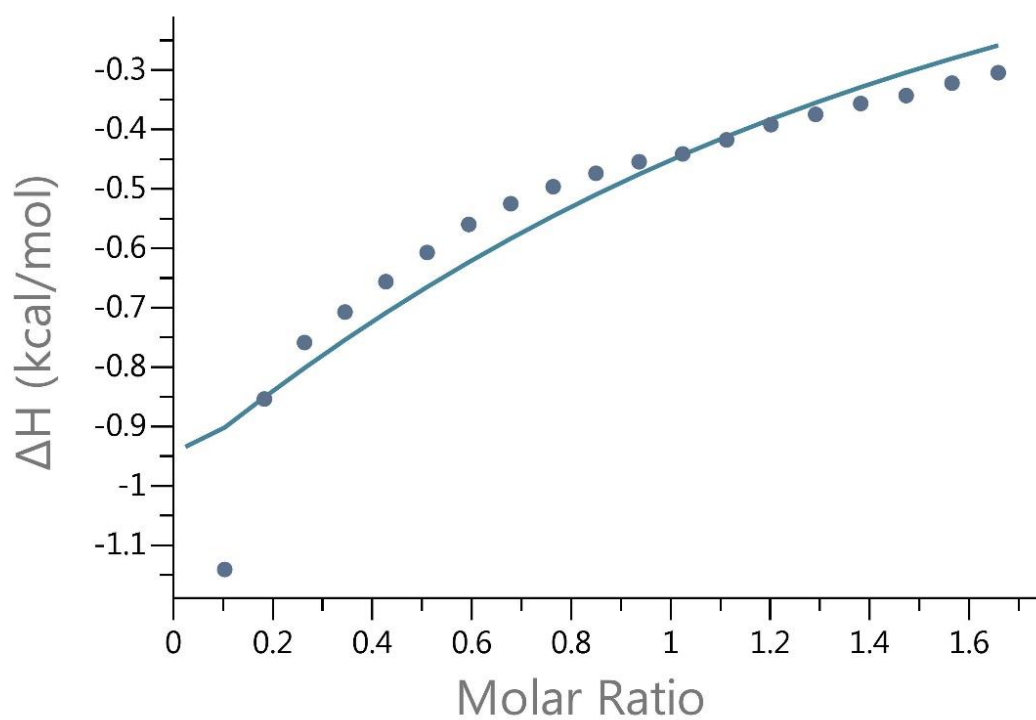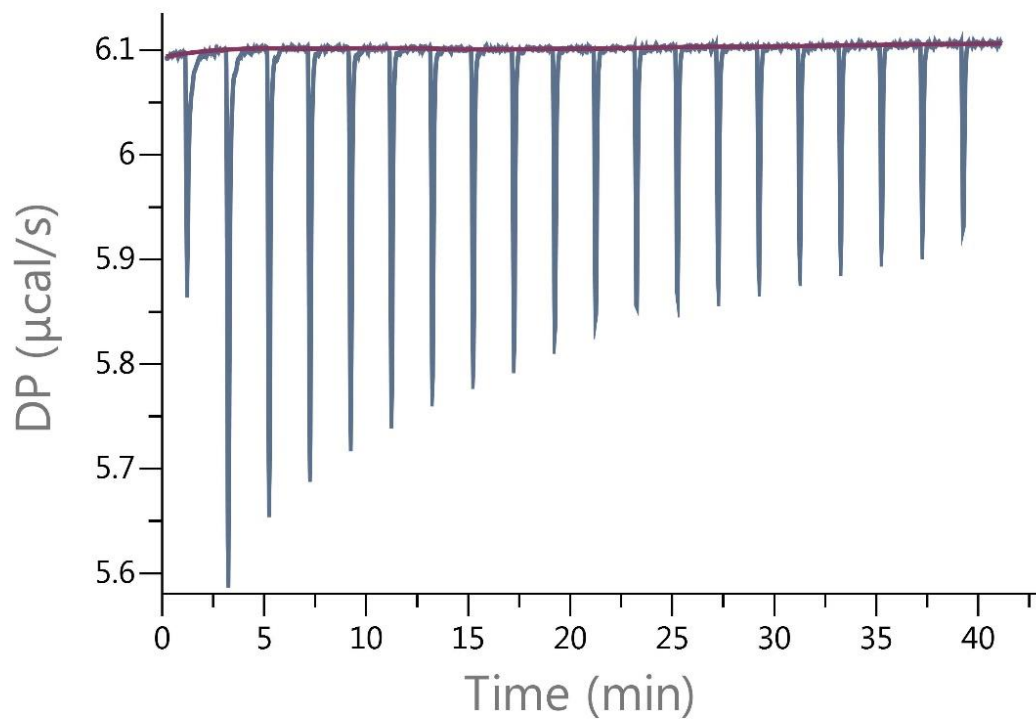


The values obtained from fixating n=1, has to be disregarded as the fit is not in line with the data points (systematic deviations).

Reduced $\chi^2$= 5.3x10$^{-3}$ Kcal/mol$^2$

MB12SBE1
Model: One Set of Sites
[Cell] (M) = 251e-6
[Syr] (M) = 1.00e-3
N (sites) = 2.3e-3 ± 0.104
KD (M) = 38.8e-6 ± 31.4e-6
ΔH (kcal/mol) = -80.0 ± 3640
Offset (kcal/mol) = -0.283 ± 3.3e-2
ΔG (kcal/mol) = -6.02
-TΔS (kcal/mol) = 74.0
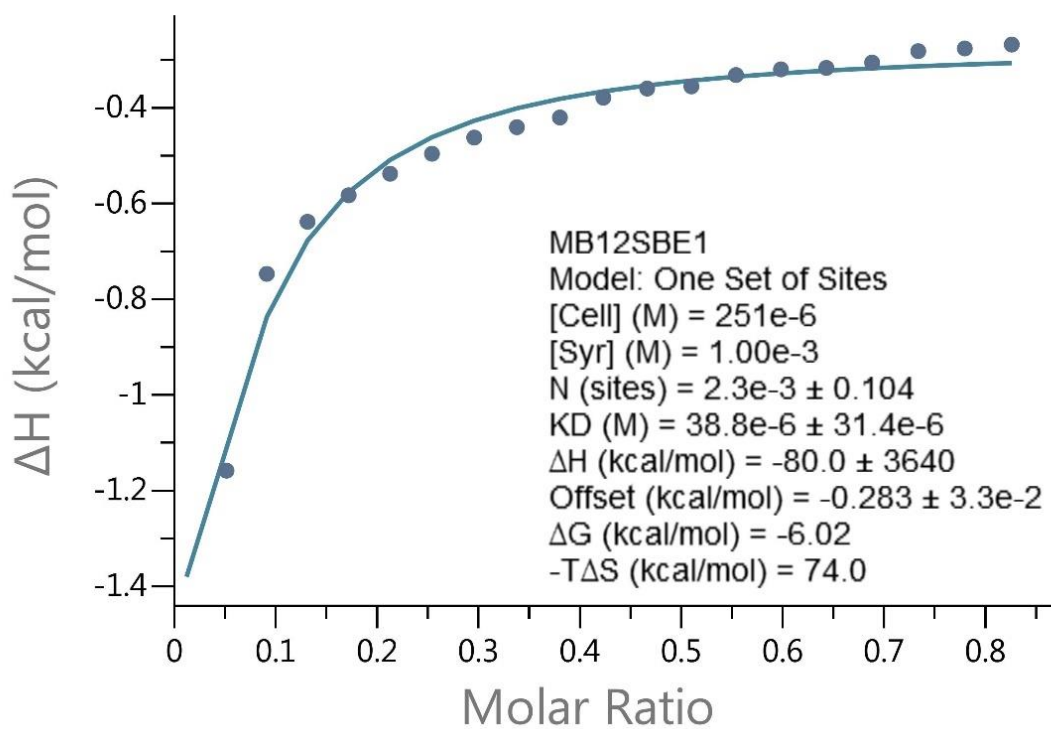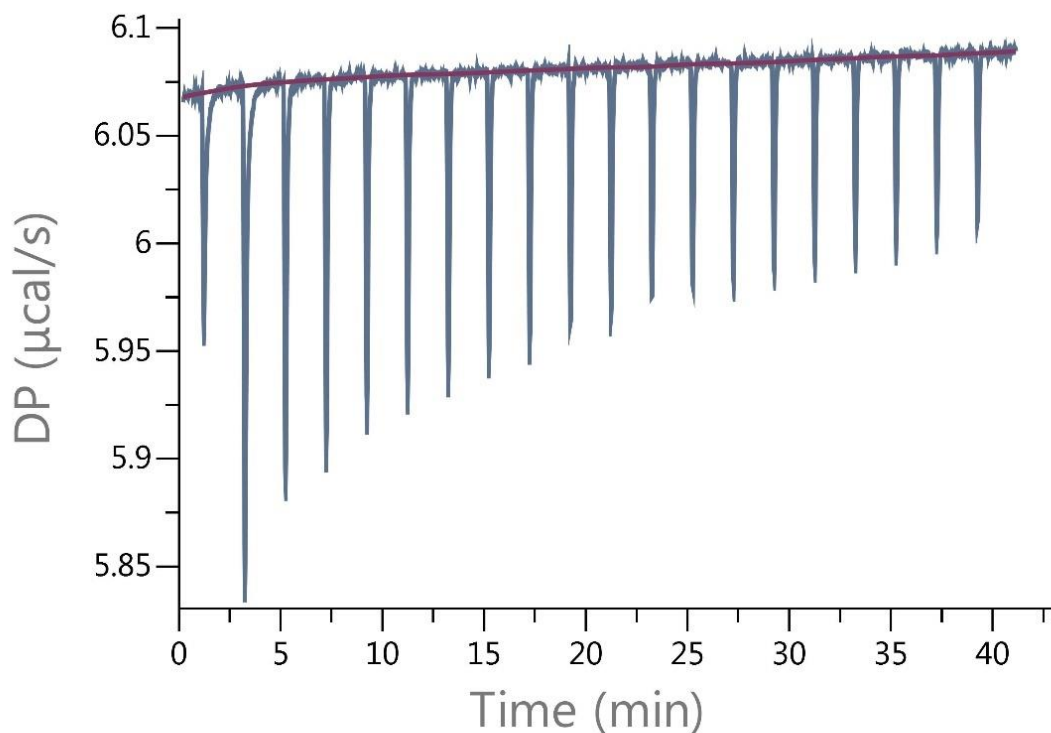
Values reported:
$K_D = 38.8 \times 10^{-6} \pm 31.4 \times 10^{-6}$
$K_A = 25773$ M$^{-1}$
Reduced $\chi^2 = 1.5 \times 10^{-3}$ Kcal/mol$^2$

Values reported:

ΔH= -80 ± 3640 Kcal/mol

ΔG= -6.02 Kcal/mol

-TΔS= 74.0 Kcal/mol

MB12SBE1
Model: One Set of Sites
[Cell] (M) = 251e-6
[Syr] (M) = 1.00e-3
N (sites) = 1.00
KD (M) = 691e-6 ± 32.5e-3
$\Delta$H (kcal/mol) = -5.34 ± 217
Offset (kcal/mol) = 0.607 ± 8.71
$\Delta$G (kcal/mol) = -4.31
-T$\Delta$S (kcal/mol) = 1.03
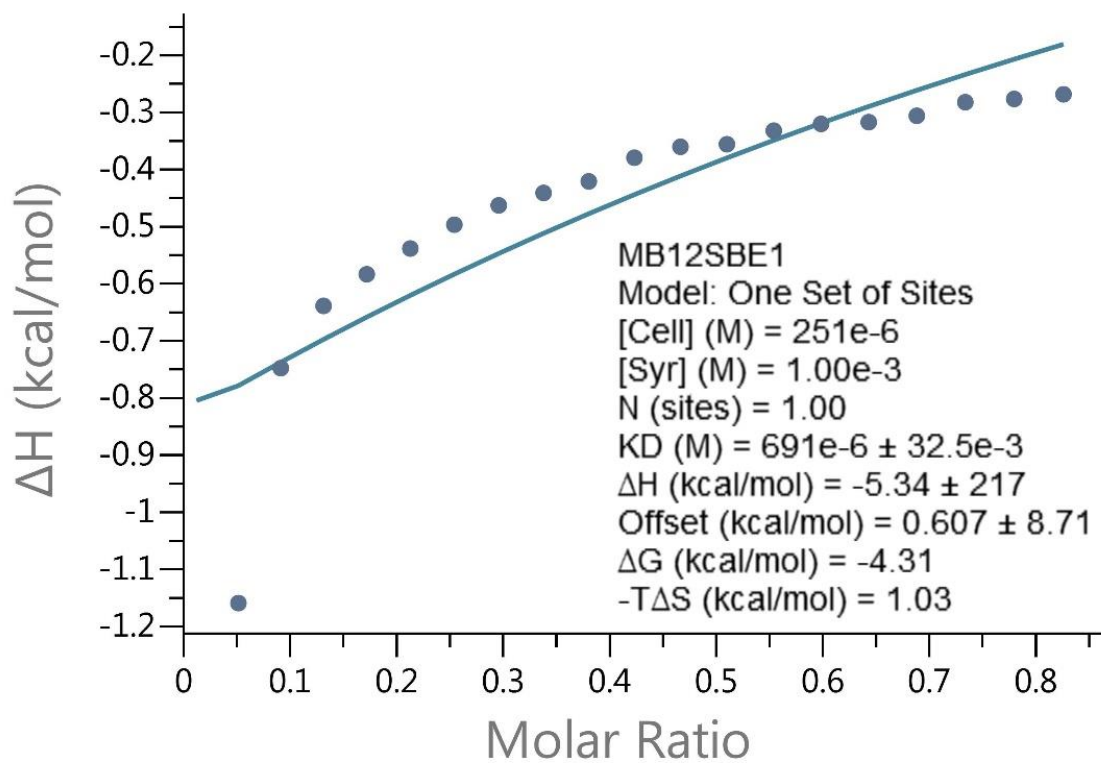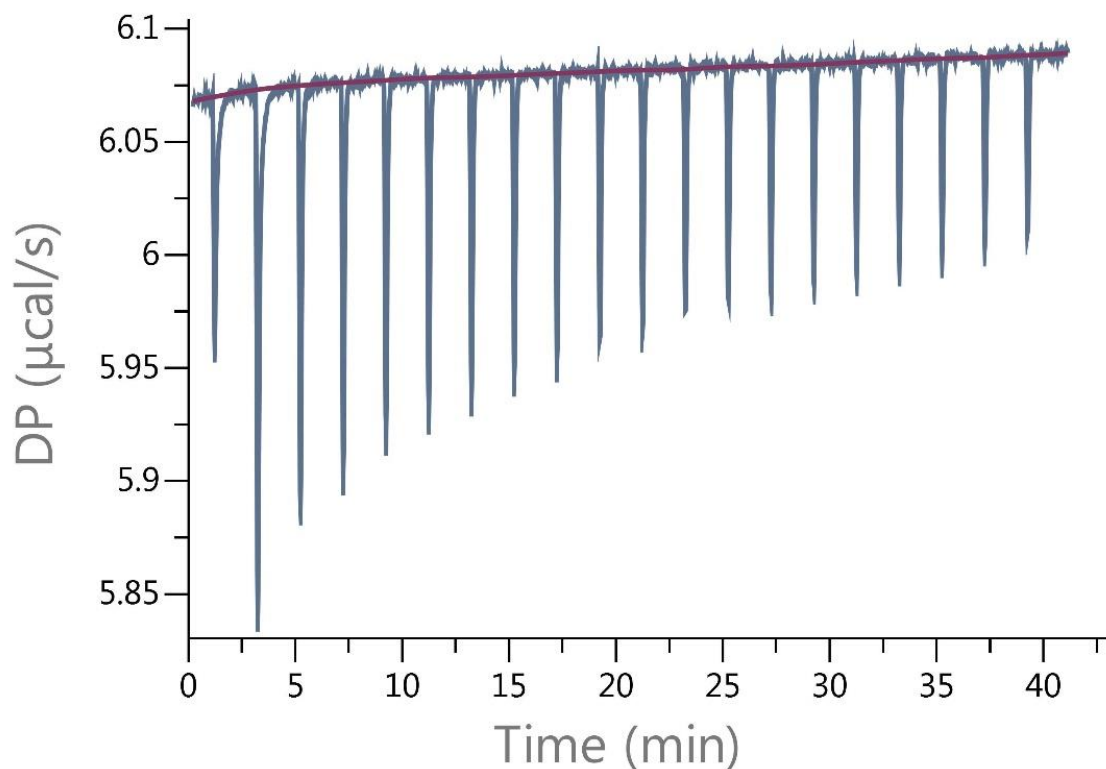
The values obtained from fixating n=1, has to be disregarded as the fit is not in line with the data points (systematic deviations).

Reduced $\chi^2$= 1.3x10$^{-2}$ Kcal/mol$^2$

## 10.10.7 ITC measurement – DβCD
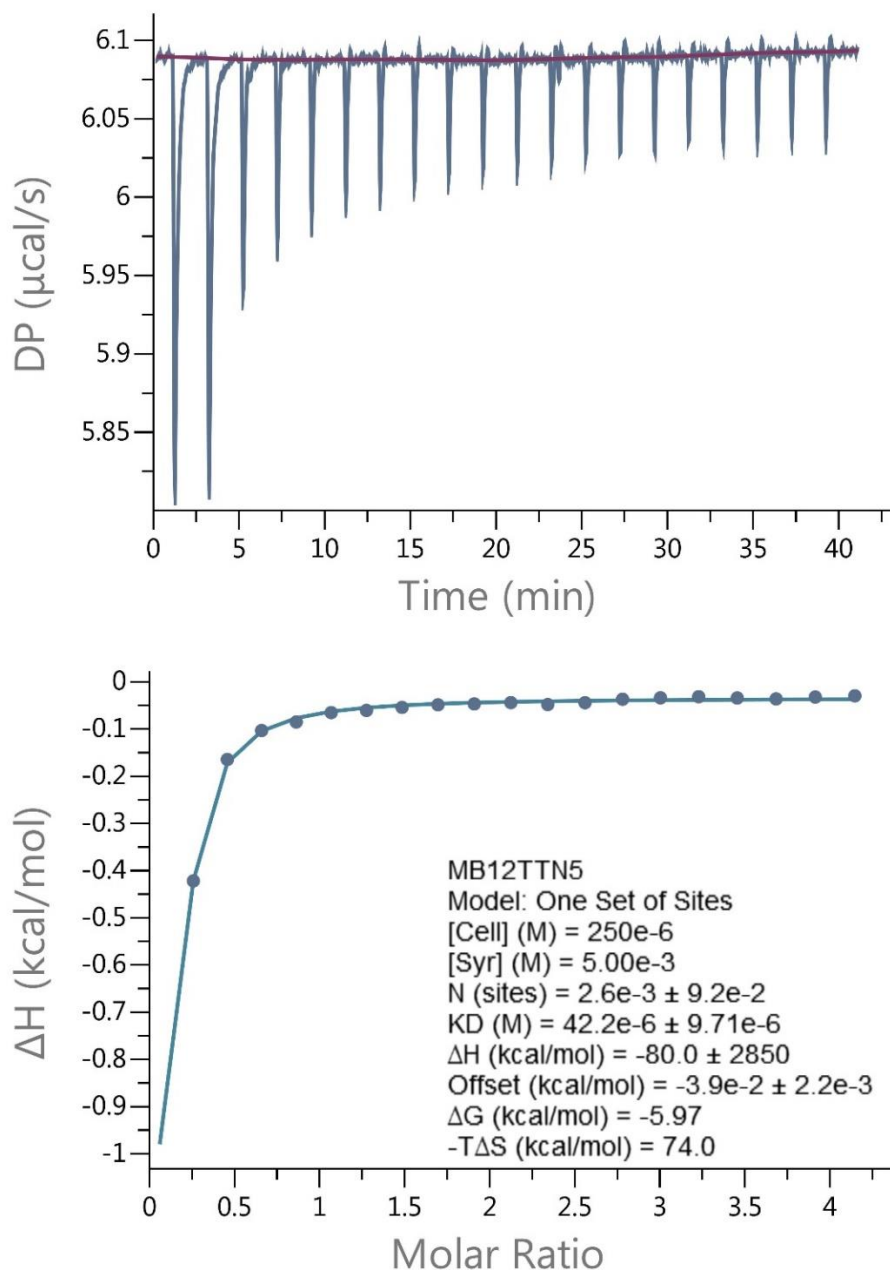
*At 5 mM*



Binding observed. However, the initial peak is higher than first measurement. The solution was saturated to fast and the values are therefore unreliable.

Values reported:

$K_D= 42.2 \times 10^{-6} \pm 9.71 \times 10^{-6}$ M

$K_A = 23670$ M$^{-1}$

$\Delta H = -80 \pm 2850$ Kcal/mol

$\Delta G = -5.97$ Kcal/mol

$-T\Delta S = 74.0$ Kcal/mol

Reduced $\chi^2 = 2.8 \times 10^{-5}$ Kcal/mol$^2$

MB12TTN5
Model: One Set of Sites
[Cell] (M) = 250e-6
[Syr] (M) = 5.00e-3
N (sites) = 1.00
KD (M) = 93.3e-6 ± 187e-6
ΔH (kcal/mol) = −0.340 ± 0.274
Offset (kcal/mol) = 8.7e-5 ± 4.4e-2
ΔG (kcal/mol) = −5.50
−TΔS (kcal/mol) = −5.16

The values obtained from fixating n=1, has to be disregarded as the fit is not in line with the data points (systematic deviations).

Reduced $\chi^2$= 5.3x10$^{-3}$ Kcal/mol$^2$

MB12TTN2
Model: One Set of Sites
[Cell] (M) = 250e-6
[Syr] (M) = 2.00e-3
N (sites) = 2.5e-3 ± 3.1e-2
KD (M) = 20.0e-6 ± 4.00e-6
ΔH (kcal/mol) = –80.0 ± 1000
Offset (kcal/mol) = –7.9e-3 ± 4.5e-3
ΔG (kcal/mol) = –6.41
–TΔS (kcal/mol) = 73.6

Binding observed. However, the initial peak is higher than first measurement. The solution was saturated to fast and the values are therefore unreliable.

Values reported:
$K_D$= 20.0x10$^{-6}$ ±4.00x10$^{-6}$ M
$K_A$=50000 M$^{-1}$
ΔH= -80 ± 1000 Kcal/mol
ΔG= -6.41 Kcal/mol
-TΔS= 73.6 Kcal/mol
Reduced $\chi^2$= 1.1x10$^{-4}$ Kcal/mol$^2$

MB12TTN2
Model: One Set of Sites
[Cell] (M) = 250e-6
[Syr] (M) = 2.00e-3
N (sites) = 1.00
KD (M) = 436e-6 ± 8.40e-3
ΔH (kcal/mol) = -2.14 ± 34.1
Offset (kcal/mol) = 0.385 ± 2.80
ΔG (kcal/mol) = -4.58
-TΔS (kcal/mol) = -2.44

The values obtained from fixating n=1, has to be disregarded as the fit is not in line with the data points (systematic deviations).

Reduced $\chi^2$= 2.5x10$^{-2}$ Kcal/mol$^2$

*At 1 mM*



MB12TTN1
Model: One Set of Sites
[Cell] (M) = 251e-6
[Syr] (M) = 1.00e-3
N (sites) = 2.6e-3 ± 8.4e-2
KD (M) = 16.5e-6 ± 16.7e-6
ΔH (kcal/mol) = –80.0 ± 2650
Offset (kcal/mol) = 8.7e-2 ± 4.8e-2
ΔG (kcal/mol) = –6.52
-TΔS (kcal/mol) = 73.5

Values reported:
$K_D$= 16.5x10$^{-6}$ ±16.7x10$^{-6}$ M
$K_A$=60606 M$^{-1}$
Reduced $\chi^2$=9.1x10$^{-3}$ Kcal/mol$^2$

Values reported:

ΔH= -80 ± 2650 Kcal/mol

ΔG= -6.52 Kcal/mol

-TΔS= 73.5 Kcal/mol

MB12TTN1
Model: One Set of Sites
[Cell] (M) = 251e-6
[Syr] (M) = 1.00e-3
N (sites) = 1.00
KD (M) = 703e-6 ± 49.6e-3
$\Delta$H (kcal/mol) = –8.04 ± 492
Offset (kcal/mol) = 1.47 ± 19.5
$\Delta$G (kcal/mol) = –4.30
–T$\Delta$S (kcal/mol) = 3.74

The values obtained from fixating n=1, has to be disregarded as the fit is not in line with the data points (systematic deviations).

Reduced $\chi^2$= 7.4x10$^{-2}$ Kcal/mol$^2$

## 11.11 4-N-3′-O-Bis(tert-Butoxycarbonyl) Gemcitabine (11)

### 11.11.1 From Gemcitabine (Na₂CO₃ as a base).
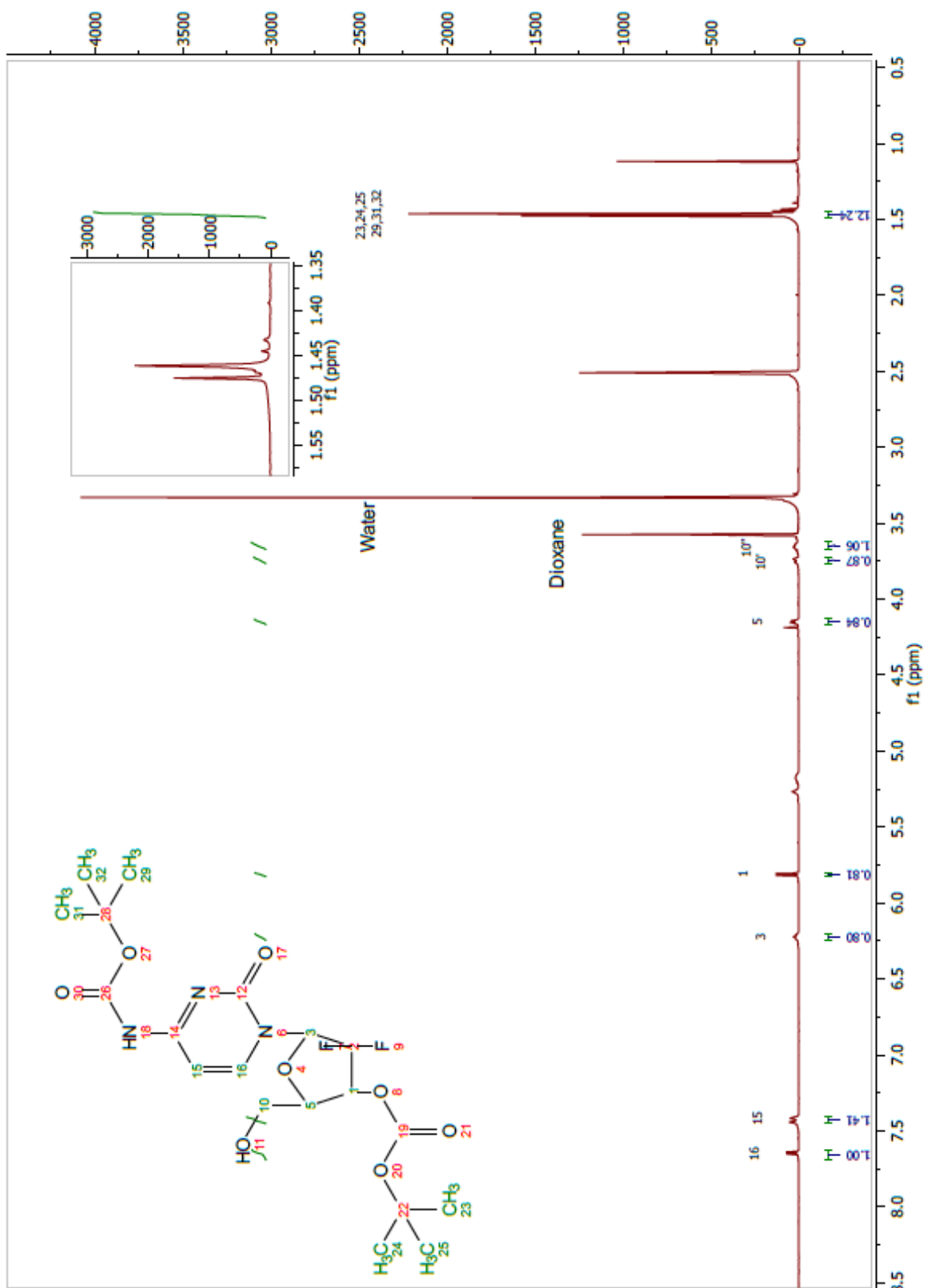


$^1$H NMR ((CD$_3$)SO$_2$): δ 7.64 (1H, d, J=7.54Hz), 7.43 (1H, d, J=14.16Hz), 6.22 (1H, t, J=9.0 Hz), 5.80 (1H, d, J=7.38), 4.15 (1H, m) 3.75 (1H, m) 3.65 (1H, m), 1.46 (9H, m).

$^1$H NMR ((CD$_3$)SO$_2$): δ 8.10 (1H, d, *J*=7.59 Hz), 7.08 (1H, d, *J*=7.79 Hz), 6.25 (1H, t, *J*=8.6 Hz), 5.31 (1H, d, *J*=5.81 Hz), 4.23 (1H, m) 3.76 (1H, dt, *J*=3.66, 12.45) 3.66 (1H, m), 1.45 (9H, s).

## 11.12 ((2R,3R,5R)-5-(4-((*tert*-butoxycarbonyl)amino)-2-oxopyrimidin-1(2H)-yl)-3-((*tert*-butoxycarbonyl)oxy)-4,4-difluoro-5-methyltetrahydrofuran-2-yl)methyl ((3R,5R,7R)-adamentane-1-carbonyl)glycinate (13)

### 11.12.1 Before Purification
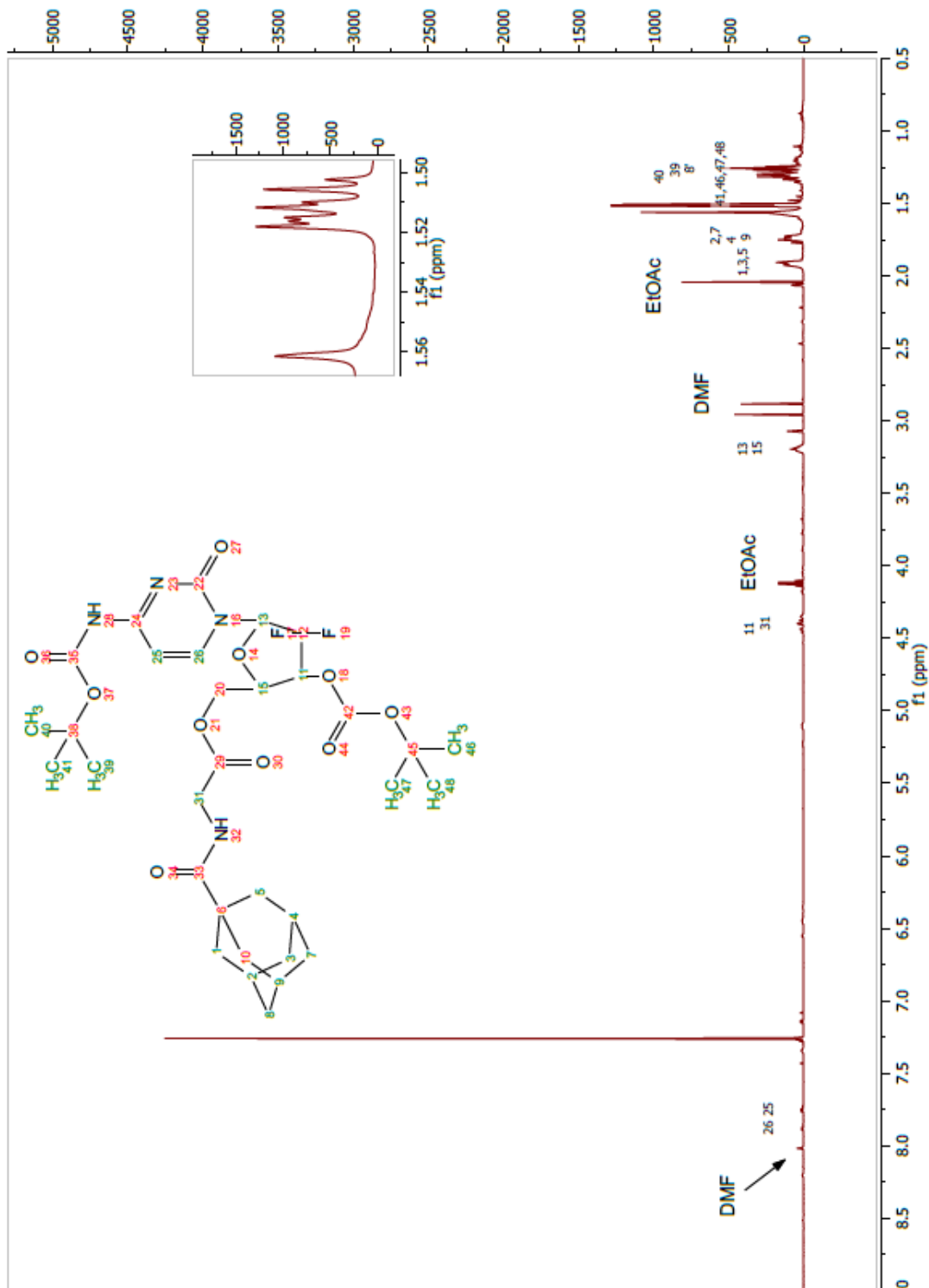


$^1$H NMR (CDCl$_3$): δ 7.88 (m), 7.75 (m), 4.47-4.42 (m) 4.40 (m), 4.38 (m), 4.36-4.34 (m), 1.92 (m), 1.74 (m), 1.35-1.22 (m).

## 11.12.2 Purification

**REVELERIS® PREP**

**Method Name:**
Run Name: MFB/2017-05-05_07-17-47 mbl3
Run Date: 2017-05-05 07:27

Column: Reveleris® Silica 40g
Flow Rate: 40 mL/min
Equilibration: 7.1 min
Run Length: 25.0 min
Mode: Flash Liquid

Solvent A: Methylene chloride
Solvent B: Methanol
Solvent C: Empty
Solvent D: Empty
Slope Detection: Off

UV Threshold: 0.05 AU
UV Sensitivity: Low
UV1 Wavelength: 254 nm
UV2 Wavelength: 265 nm
UV3 Wavelength: 280 nm

ELSD Threshold: 20 mV
ELSD Sensitivity: Low
Collection: Collect Peaks
Per-Vial Volume: 8.5 mL
Non-Peak Volume: 8.5 mL
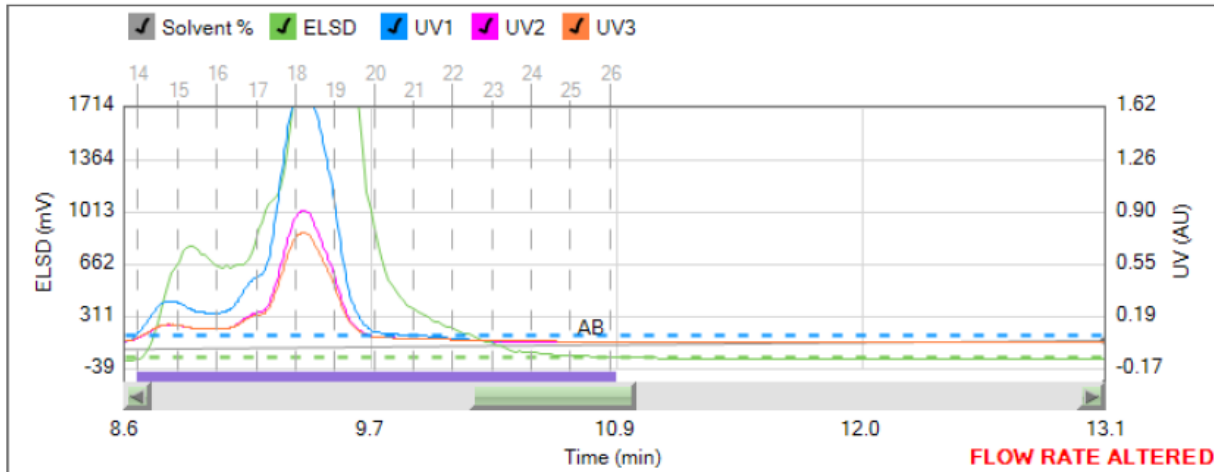


1 - 2F2A
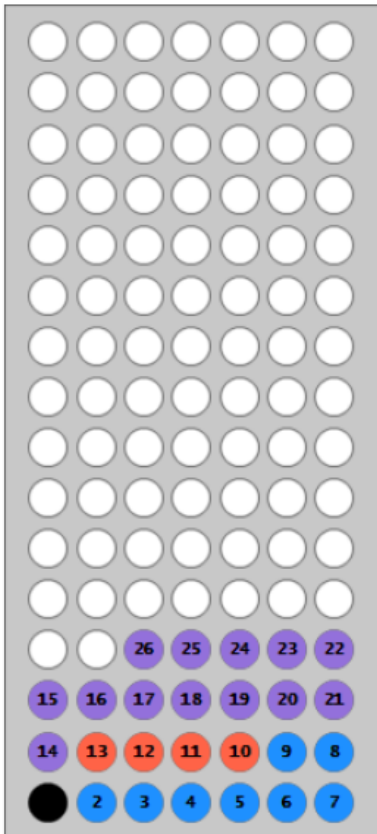


### Gradient Table

| | Min | Solvents | % 2nd |
|---|---|---|---|
| 1 | 0.0 | AB | 0 |
| 2 | 20.0 | AB | 10 |
| 3 | 0.0 | AB | 10 |
| 4 | 5.0 | AB | 20 |

### Vial Mapping Table

| Peak # | Start Tray:Vial | End Tray:Vial |
|---|---|---|
| 1 | 1:2 | 1:9 |
| 2 | 1:10 | 1:13 |
| 3 | 1:14 | 1:26 |

*¹H NMR fraction 2-9*
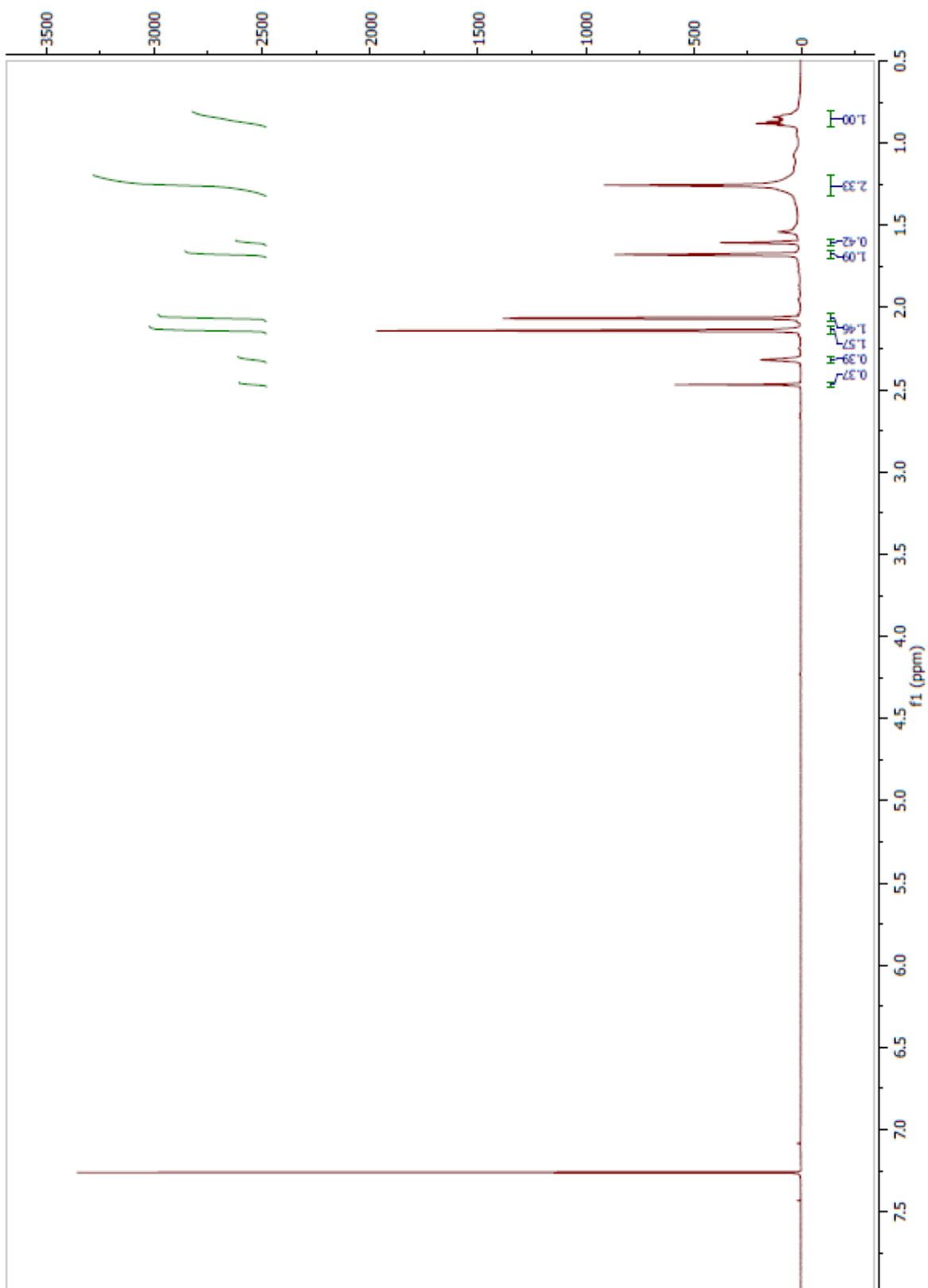


¹H NMR (CDCl₃): δ 2.47 (1H, m), 2.32 (1H, p, *J*=2.54 Hz), 2.14 (3H, m), 2.06 (3H, d, *J*=2.94 Hz), 1.68 (2H, m), 1.61 (1H, t, *J*=3.19 Hz), 1.25 (4H, m), 0.85 (2H, m).

$^1$H NMR (CDCl$_3$): δ8.79 (1H, m), 8.52 (1H, s), 4.61 (2H, s), 4.32 (1H, tt, *J*=12.40, 3.50 Hz), 3.71 (1H, m), 2.06 (1H, d, *J*=2.92 Hz), 1.94 (3H, m), 1.86 (3H, dt, *J*=12.91, 2.92 Hz), 1.71 (4H, m), 1.54 (9H, m), 1.39 (3H, m), 1.25 (3H, m), 0.86 (2H, m).
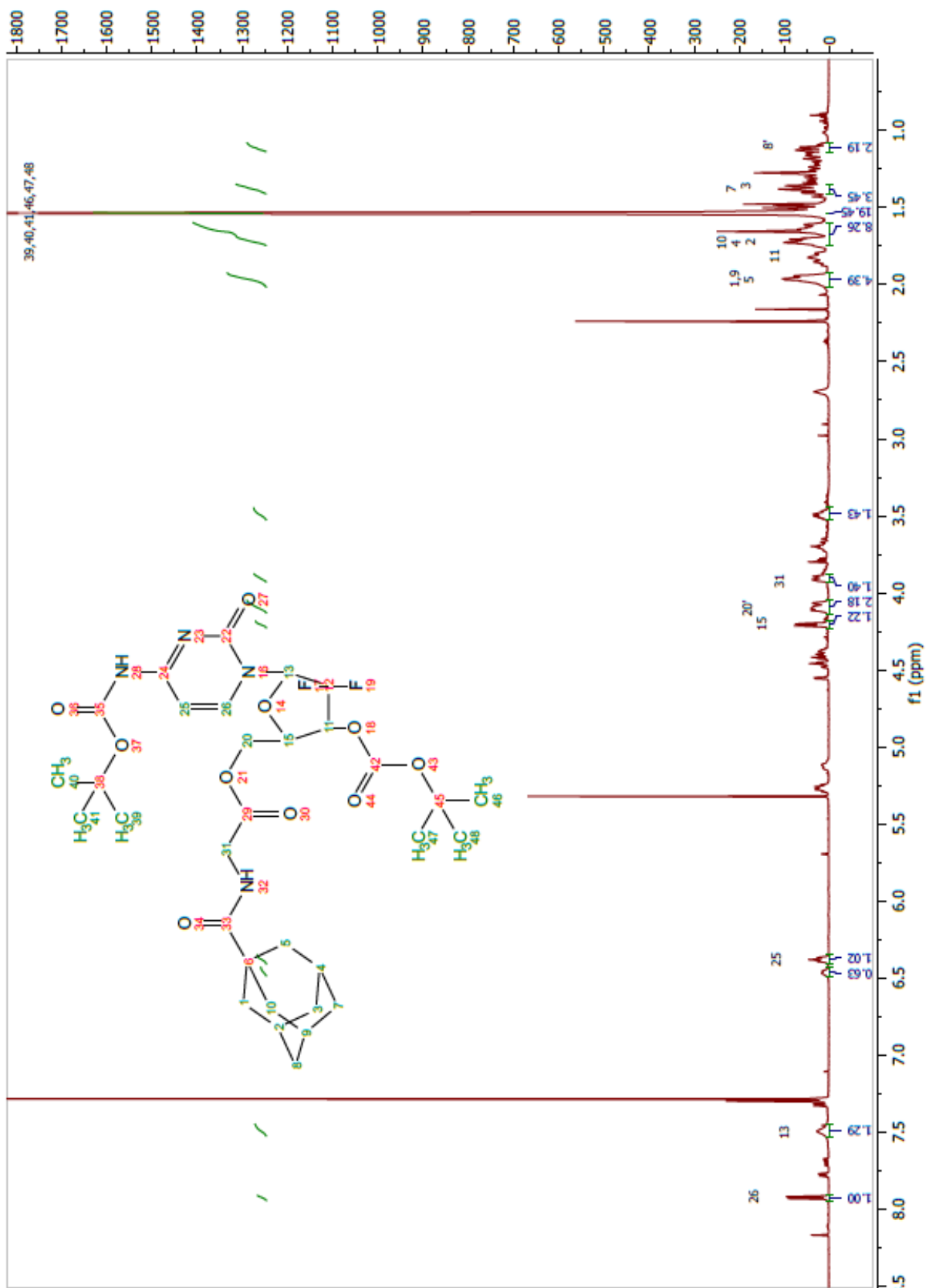
$^{1}$H NMR (CDCl$_3$): δ 7.93 (1H, d, *J*=7.68 Hz), 7.49 (1H, m), 4.21 (1H, m), 4.09 (2H, m), 3.91 (2H, m), 1.97 (5H, m), 1.71 (4H, m), 1.54 (18H, m) 1.37 (4H, m), 1.12 (2H, m).
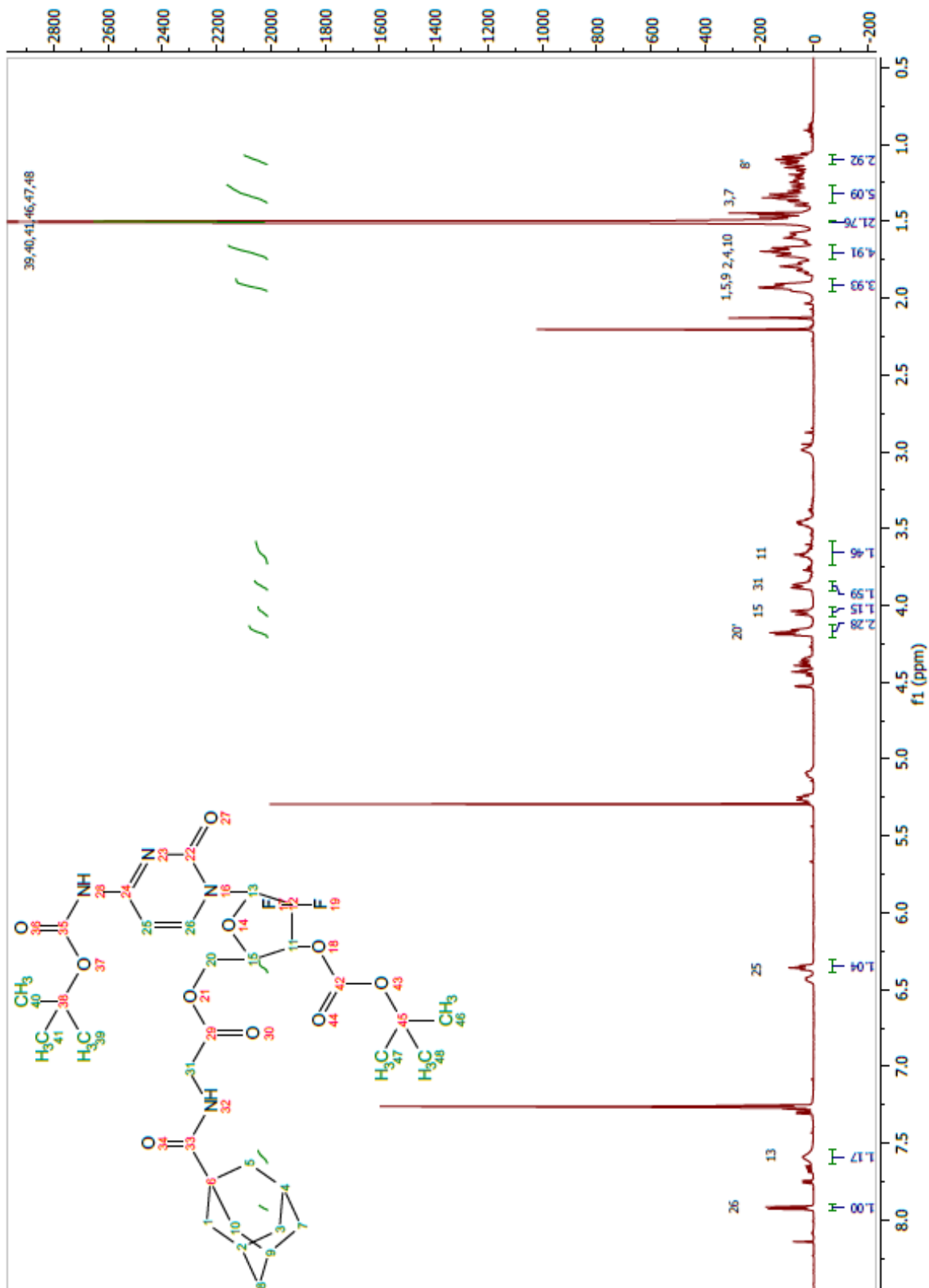
$^1$H NMR (CDCl$_3$): δ 7.92 (1H, d, *J*=7.51 Hz), 7.58 (1H, m), 6.36 (1H, t, *J*=7.76 Hz) 4.18 (2H, m), 4.05 (2H, d, *J*=12.22 Hz), 3.87 (2H, d, *J*=12.22 Hz), 1.93 (5H, m), 1.71 (4H, tt, *J*=13.86, 3.75 Hz), 1.51 (18H, m) 1.32 (4H, m), 1.11 (2H, m).

## 11.13 ((2R,3R,5R)-5-(4-amino-2-oxopyrimidin-1(2H)-yl)-4,4,-difluoro-3-3hydroxy-5-methyltetrahydrofuran-2-carbonyl)glycinate (5)

### 11.13.1 ^{1}H NMR
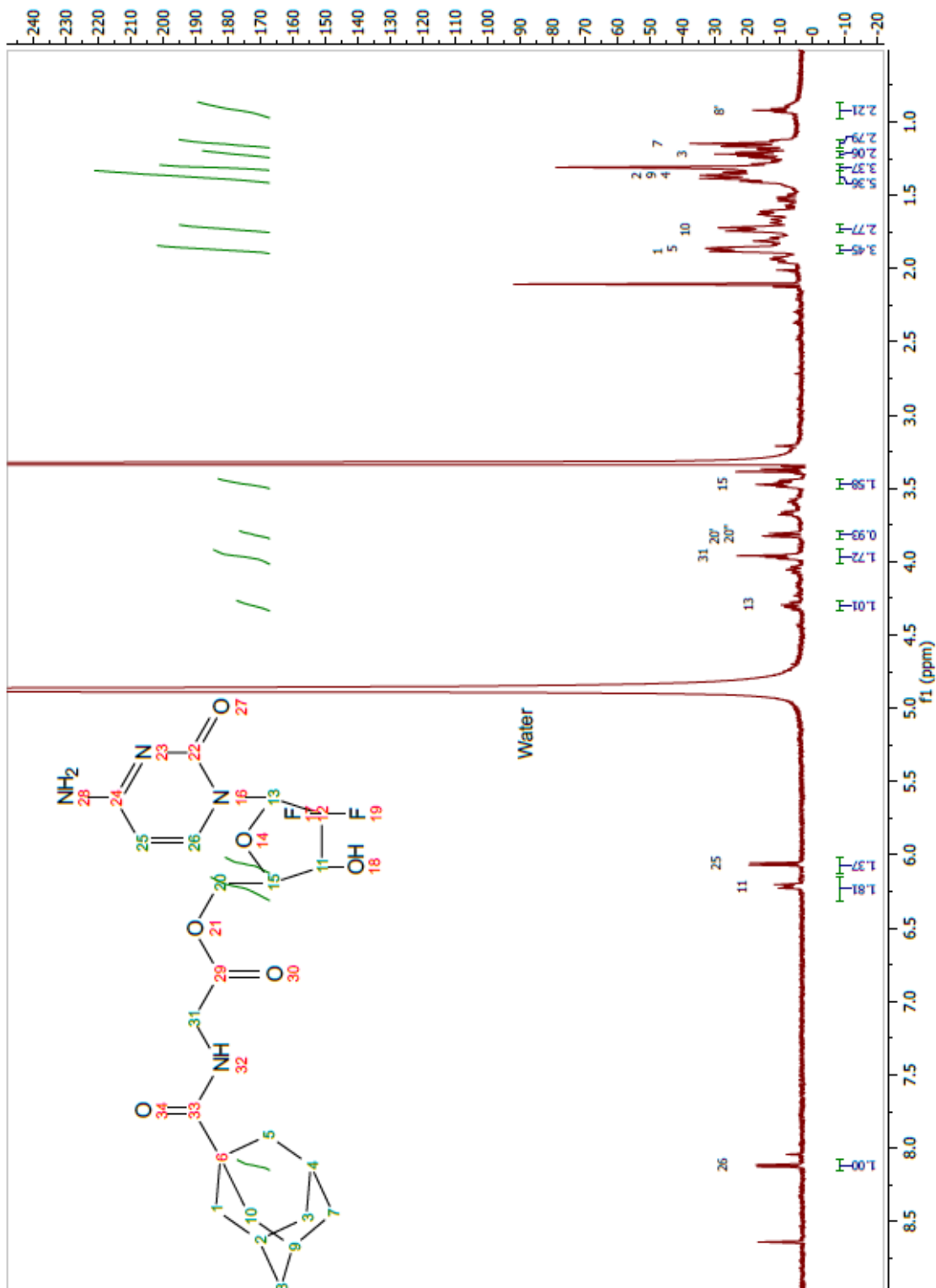


^{1}H NMR (CD$_3$OD): δ 8.12 (1H, d, J=8.13 Hz), 6.21 (1H, m), 6.06 (1H, d, J=8.12 Hz), 4.30 (1H, m), 3.96 (2H, m), 3.81 (2H, dd, J=9.56, 3.20 Hz), 3.47 (1H, m), 1.87 (4H, dd, J=9.91, 3.30 Hz), 1.73 (1H, dt, J=13.89, 4.02 Hz) 1.37 (3H, m), 1.21 (2H, m), 1.14 (2H, m), 0.92 (2H, t, J=7.52 Hz).

214

## 11.13.2 LC-MS
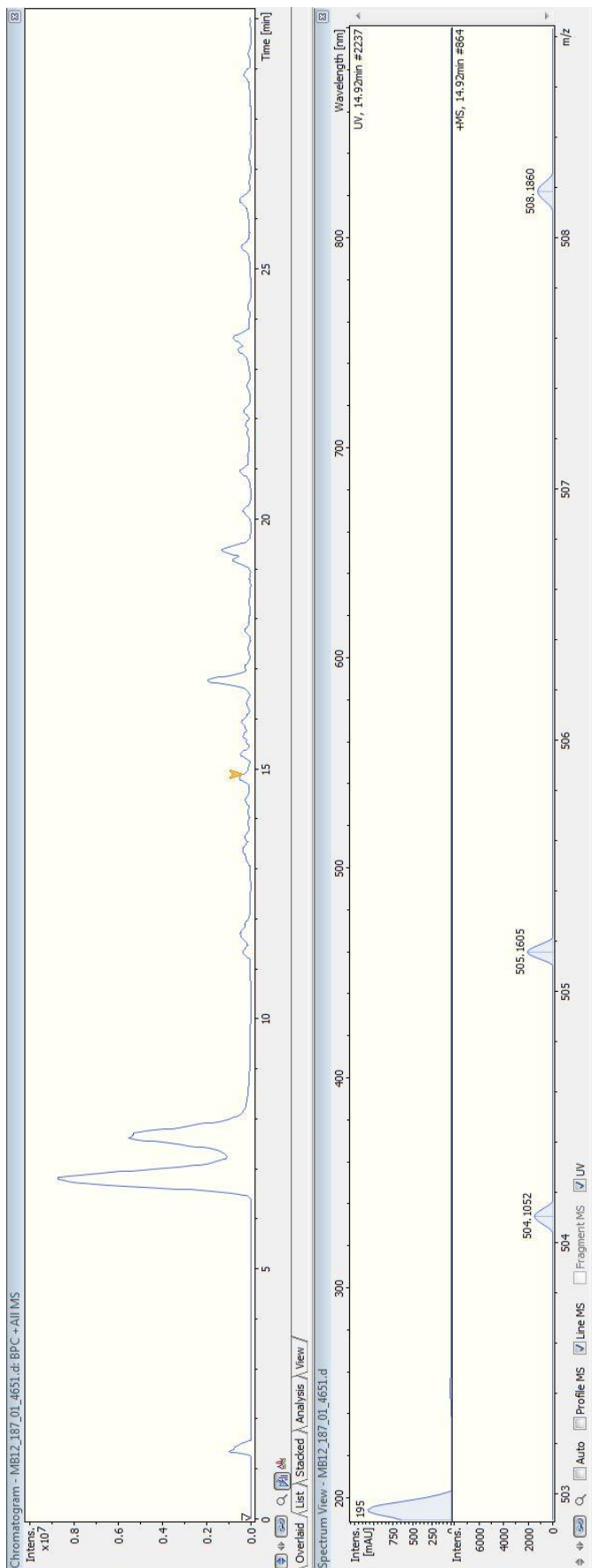


LC-MS: m/z = 505.1605 [M+Na$^+$], calc. for. (C$_{22}$H$_{28}$F$_2$N$_4$O$_6$ Na$^+$): m/z: 505.1869

Deviation of 0.0264 Da.